Design of a Bifurcated Stent Graft, With its Accompanying Delivery System.

Candidates Name:

Liam Morris

Award:

MSc by Research (Mode A)

Institution:

Galway & Mayo Institute of Technology

Supervisor:

Dr. Patrick Delassus

"Submitted to the National Council for Education Awards, July 2000"

Abstract

Abdominal Aortic Aneurysms (AAA) haemorrhaging is a life-threatening disease An aneurysm is a permanent swelling of an artery due to a weakness in its wall

Current surgical repair involves opening the chest or abdomen, gaining temporary vascular control of the aorta and suturing a prosthetic graft to the healthy aorta within the aneurysm itself The outcome of this surgical approach is not perfect, and the quality of life after this repair is impaired by postoperative pain, sexual dysfunction, and a lengthy hospital stay resulting in high health costs All these negative effects are related to the large incision and extensive tissue dissection

Endovascular grafting is an alternative to the standard surgical method This treatment is a less invasive method of treating aortic aneurysms It involves a surgical exposure of the common femoral arteries where the stent graft can be inserted through by an over-the-wire technique All manipulations are controlled from a remote place by the use of a catheter and this technique avoids the need to directly expose the diseased artery through a large incision or an extensive dissection

The proposed design method outlined in this project is to develop the endovascular approach The main aim is to design an unitary bifurcated stent graft (i e bifurcated graft as a single component) to treat these Abdominal Aortic Aneurysms This includes the delivery system and deployment mechanism necessary to first accurately position the stent graft across the aneurysm sac and also across the iliac bifurcation, and secondly fix the stent graft in position by using expandable metal stents Thus excluding the aneurysm from the circulation and therefore preventing rupture Miniaturisation is a critical aspect of this design, as the smaller the crimped stent graft the easier to guide through the vascular system to the desired location

Biocompatibility is an important aspect The preferred materials for this prosthesis are to use Shape Memory Alloys for the stent and a multifilament fabric for the graft A taper design is applied for the geometry as this gives a favourable flow characteristic and reduced wave reflections

Adequate testing of the stent graft to prove its durability and the ease of the method of deployment is a prerequisite A bench test facility has being designed and build to replicate the cardiovascular system and the disease in question aortic aneurysms at the iliac bifurcation The testing here shows the feasibility of the proposed delivery system and the durability of the stent graft across the aneurysm sac

Finally, these endovascular treatments offer the economic advantage of short hospital stays or even treatment as an outpatient, as well as elimination of the need for postoperative intensive care The risk of developing an aneurysm increases with age, that is one of the main reasons to look for less invasive ways of treating aneurysms Consequently, there is enormous pressure to develop and use these devices rapidly

Table Of Contents.

Chapter		Page
Acknowledgements		i
1.0	**Introduction**	1
1 1	What are Aneurysms?	2
1 2	How are Aneurysms Treated?	4
1 2 1	Traditional Surgical Technique	4
1 2 2	Stent Graft Technique	5
1 3	Endovascular Design Problems	7
1 4	Aims & Objectives	8
2.0	**Overall Design of the Cardiovascular System**	9
2 1	Introduction	9
2 2	Velocity Profile in Pulsatile Flow	11
2 2 1	Impedance Methods	13
2 3	The Heart	16
2 3 1	The Cardiac Output	16
2 4	The Vascular System	16
2 5	Wave Reflections	19
2 6	Types of Flow	20
2 7	General Properties of Blood	23
2 8	Summary	23

Chapter			Page
3.0	**Development of Study Protocol**		24
	3 1	Introduction	24
	3 2	Simulation of the behaviour of the blood flow through the Aortic Bifurcation	26
		3 2 1 Design Procedure	27
		3 2 2 Design of Piston Pump	27
		3 2 3 Piston Pump Characteristics	29
	3 3	Regulation of the test system temperature	34
	3 4	Replica of the Abdominal Aortic Aneurysm at the Bifurcation	34
		3 4 1 Manufacturing of the Female Casts	36
		3 4 2 Creating the Male Wax Models	41
		3 4 3 Creating the Silicon Models	41
		3 4 4 Comparison of Model Aneurysm to Aortic Aneurysms	42
	3 5	Simulation of the Pulsatile Pressure in the Aorta	43
	3 6	The Blood	46
	3 7	Modeling of the Systematic Circuitry	47
		3 7 1 Description of the Test System Circuit	48
3 8	Conclusion		48
4.0	**Attachment Systems**		50
	4 1	Introduction	50
	4 2	Characteristics of Stents	50
	4 3	Biocompatability of Stent Materials	51
	4 4	Stent Materials	52
		4 4 1 Stainless Steel	52
		4 4 2 Platinum	53
		4 4 3 Nitinol Alloys	53
	4 5	Stent Designs	54
	4 6	Longitudinal force required to dislodge the stent	55
		4 6 1 Commercially available stents	55

Chapter **Page**

4 6 2 Comparison of the effects of adding Hooks & Barbs 57

4 6 3 Comparison of the effects of Arterial Characteristics 58

4 7 Comparison of Stent Designs 59

4 8 Problems with Stent Designs 60

4 9 Stent Material Characteristics 60

4 9 1 Shape Memory Alloys 62

4 9 2 Alloy and Transformation Temperature 64

4 9 3 Superelastic Behaviour 65

4 10 Disadvantages of SMAs 66

4 11 Conclusion 67

5.0 Medical Textiles 68

5 1 Introduction 68

5 2 Characteristics of Graft Materials 68

5 3 Types of Biomedical Materials Used 70

5 3 1 Nylon 70

5 3 2 Polyethylene Terephthalate (PET) or Polyester 70

5 3 3 Polytetrafluoroethaylene (PTFE) 71

5 3 4 Expandable PTFE 71

5 3 5 Polyurethane 71

5 3 6 Silicon Rubber 72

5 4 Classification of Textiles 72

5 4 1 Fibres 73

5 4 2 Yarns 73

5 4 3 Fabric Structure 74

5 5 Characteristics of Fabric Structure 77

5 6 Conclusion 80

Chapter **Page**

6.0 Prosthesis Design 81

6 1 Introduction 81

6 2 Graft Geometry 81

6 2 1 Wave Reflection Analysis 82

6 2 2 Differential Equations for Transient Flow 83

6 2 3 General Wave Equations 84

6 2 4 Reflection and Transmission of Waves at Junctions 86

6 2 5 Graft Design 90

6 2 6 Geometry Conclusion 93

6 3 Graft Material 94

6 3 1 Design of Fabric 94

6 3 2 Bursting Strength 96

6 3 3 Testing of The Woven Fabrics 97

6 3 4 Fabric Summary 99

6 4 Forces on Bifurcated Graft 100

6 4 1 Calculation of the Forces on the Bifurcated Graft 100

6 5 Stent Geometry 109

6 6 Choice of Stent Type & Material 110

6 7 Manufacturing of the Z-Stent 111

6 7 1 Procedure for Manufacturing the Z-Shaped Stent 111

6 8 Combination of Stent and Graft 114

6 9 Conclusion 116

Chapter **Page**

7.0 Delivery System Design 117

7 1 Introduction 117

7 2 Selection Criteria for Stent Graft Placement 117

7 3 Catheters and Guidewires 118

7 3 1 Guidewires 118

7 3 2 Catheters 119

7 3 3 Placement of Catheters 120

7 3 4 Failure of Catheters 122

7 4 Arterial Access 131

7 4 1 Open Arterial Access of the Femoral Artery 131

7 5 Graft Systems 133

7 6 Miniaturisation 134

7 6 1 Folding of the graft material 135

7 6 2 Procedure for Crimping Stent & Graft 137

7 7 Methods of Deployment 139

7 7 1 Difficulties of Unitary Approach 139

7 7 2 Attachment Mechanisms 140

7 7 3 Deployment Methods 144

7 8 Comments & Further Options for Delivery Methods 148

7 9 Joining of Catheter Parts 150

7 10 Procedure for Proposed Delivery System 151

7 11 Conclusion 156

8.0 Prototype Testing 157

8 1 Introduction 157

8 2 Method of Deployment 157

8 2 1 Procedural Testing 158

8 2 2 Comments 163

8 3 Durability of Stent Graft 163

Chapter **Page**

8 3 1 Radical Stiffness of Z-Shaped Stent 164
8 3 2 Forces Required to Dislodge Stent 165
8 3 3 Stent Graft with Proximal & Iliac Stents 167
8 4 Clinical Follow Up 171
8 5 Conclusion 172

9.0 Conclusion 173

10.0 References 179

Appendix A Fourier Series Representation of Pressure & Flow 183

Appendix B Plans for Bench Test 185

Appendix C Calculation of Displacement, Velocity & Acceleration of Plunger 207

Appendix D Mechanical Properties of Fibres & Tested Woven Fabrics 210

Appendix E Calculation of Resulstant Force on Bifurcated Graft 217

Appendix F Plans for Prosthesis & Delivery System 234

Appendix G Calculation of Resulstant Force on Tip of Catheters 242

Acknowledgements

I am greatly indebted to many people for their help and contribution throughout this project

I owe my warmest thanks to my supervisor Dr Patrick Delassus, who provided me with the opportunity to complete my masters in biomedical research Also, I would like to thank him for his encouragement, valuable advice and criticism throughout the last 21 months

I would like to thank Mr John Kelly & Mr Barry Dolan of AVE/Medtronic who willingly provided their time and knowledge so as to advise me in the biomedical aspects of this project I would also like to thank Mr Gerald O'Donnell for his guidance and support throughout the duration of this project

Special thanks are due to the staff of the Workshop & Motorshop facilities (G M I T) especially Gabriel Costello for his assistance with the CNC milling machine and John Noone, Johnny Murray & John Mitchell for their assistance with the practical aspects of this project

Finally, I would like to thank my parents for their encouragement and financial support during my entire college life

Chapter 1

Introduction

1.0 Introduction.

This project deals with the design and development of a stent graft prosthesis with its accompanying delivery system, that is capable of preventing Abdominal Aortic Aneurysms (AAA) haemorrhaging, that is the swelling of an artery The purpose of this project is therefore threefold

- Review of the issues involved that is the design procedures and methods that would be acceptable from a biomedical point of view
- Designing and testing the proposed methods in an adequate bench test facility capable of simulating the cardiovascular system and the disease in question (aortic aneurysms at the iliac bifurcation)
- Commenting on the successes or failures of the proposed methods and if at all possible improving the design

It is important to understand the disease in question and a brief comparison of the traditional surgical method as opposed to the endovascular procedure (stent graft method) will be presented here This should give the reader a clearer understanding and appreciation of the advantages associated with the endovascular method So I would like to continue with this introduction by briefly commenting on aortic aneurysms, the traditional surgical method, the endovascular method and finally my methods of proposing a stent graft system with its' accompanying delivery system

1.1 What are Aneurysms?

An aneurysm is a permanent swelling of an artery due to a weakness in its wall Aneurysms can form anywhere, but the most common and troublesome sites are the arteries of the brain, and the aorta, [which is] the large major artery through which the heart pumps blood to the rest of the body, shown in Figure 1-1 [1] The gravest threat an aneurysm poses is that it will burst and cause a life-threatening haemorrhage But even if it doesn't rupture, a large aneurysm can impeded circulation and promote unwanted blood-clot formation The mean age of patients with aneurysms is 67 years and males are affected more than women is a ratio of 4 1 About 1 in 250 individuals greater than 50 years of age will die of a ruptured abdominal aortic aneurysm [2]

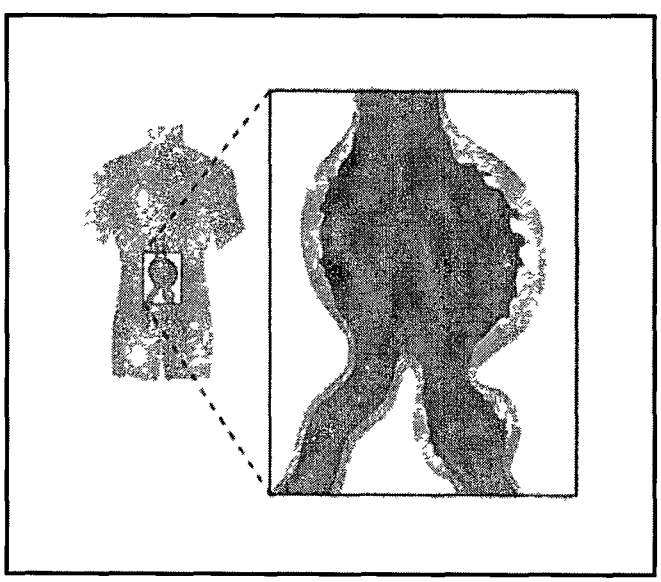

Figure 1-1: Aneurysm forming in the aorta.

There are, basically, three reasons why an aneurysm might develop in one of your arteries

1. There are three layers of tissue in your arterial walls The supportive strength of your arteries is supplied by the muscular middle layer, and this layer may be congenitally defective ["Congenitally" means "present at birth "] The normal pressure of blood in the affected artery causes a balloon-like swelling, which is called a saccular aneurysm, to develop at that point Aneurysms due to congenital defects are nearly always found in arteries at the base of the brain Because of

their shape and because several of them are often clustered together, they are known as "berry" aneurysms

2. Inflammation, whatever the cause, may weaken an arterial wall Most arterial inflammation is caused by disorders such as polyarteritis nodosa [poly = many, arter = of the artery, itis = inflammation or swelling], or bacterial endocarditis [endo = outer layer, card = heart, itis = inflammation or swelling]
3. A portion of the muscular middle layer of an arterial wall may slowly degenerate as the result of a chronic condition such as atherosclerosis or high blood pressure An aneurysm that is caused by atherosclerosis is likely to be a sausage-shaped swelling called a fusiform aneurysm that runs along a short length of the artery A similar type of swelling may be caused by high blood pressure Increased pressure of blood in an artery, however, can stretch the wall in many different ways It can even split the layers, and force blood between them This is called a dissecting aneurysm [1]

Conclusion :

Because of the random aspect in the causes of the disease, it is very difficult to forecast the development of an aneurysm Even the detection of an aneurysm is not obvious, since there is no major external symptom Consequently, medical prevention cannot be applied in this case of disease

On the other hand, the deterioration of the muscular layer cells cannot be reversed by a chemical treatment and therefore, the only issue to treat an aneurysm is to resort to a surgical repair

1.2. How are Aneurysms treated?

1.2.1. Traditional Surgical Technique.

Current surgical repair involves opening the chest or abdomen, gaining temporary vascular control of the aorta and below the lesion, opening the aneurysmal sac and suturing a prosthetic graft to healthy aorta within the aneurysm itself The sac of the aneurysm is then sutured over the graft thus excluding the dacron form direct contact with bowel and other viscera

Figure 1 2 illustrates the procedure for this surgical repair

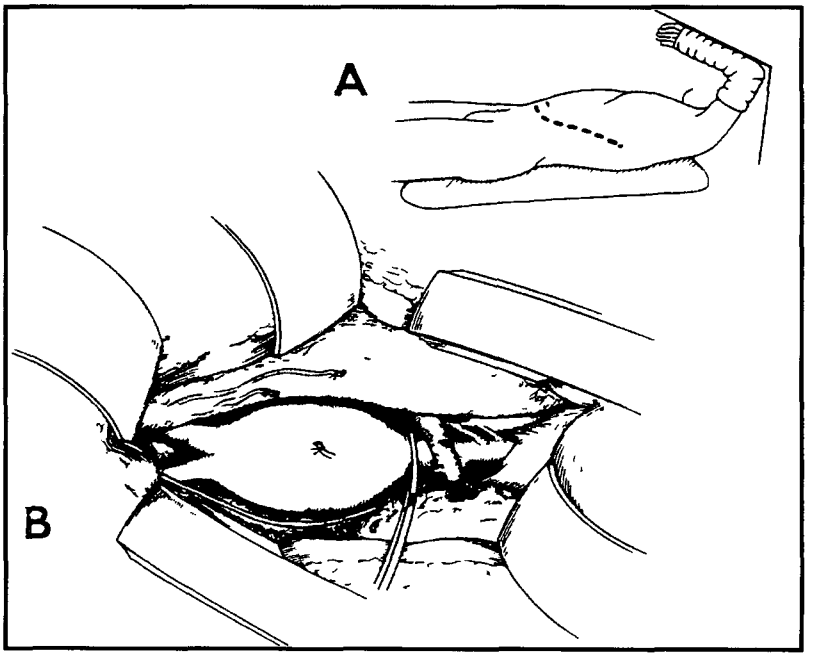

Figure 1.2 : Retroperitoneal repair of an AAA.
A) Curvilinear incision; B) Medial retraction of peritoneum.
(adapted from Calligoro et al ref 3)

The outcome of standard surgical Abdominal Aortic Aneurysm (AAA) repair has proven to be excellent, with mortality rates in the range of 3% to 5% However, standard AAA repair is not perfect, and the quality of life after this repair is impaired by postoperative pain, sexual dysfunction, and a lengthy hospital stay resulting in high health costs All these negative effects are related to the large incision and extensive tissue dissection Mortality and morbidity increase with the presence of associated

diseases, and a mortality rate of 60% has been reported for high-risk patients. The standard repair is also extremely difficult in patients with multiple abdominal operations with extensive scarring and infection [3].

1.2.2. Stent Graft Technique.

Endovascular grafting is an alternative treatment to standard open aneurysm repair. This treatment involves a surgical exposure of the common femoral arteries where the endovascular graft can be inserted through by an over-the-wire technique. All the manipulations are controlled from a remote place by the use of a catheter and therefore this technique avoids the need to directly expose the diseased artery through a large incision or an extensive dissection [3].

Figure 1.3 shows an example of stent graft installation and Figure 1.4 illustrates the device to introduce the graft through the femoral artery.

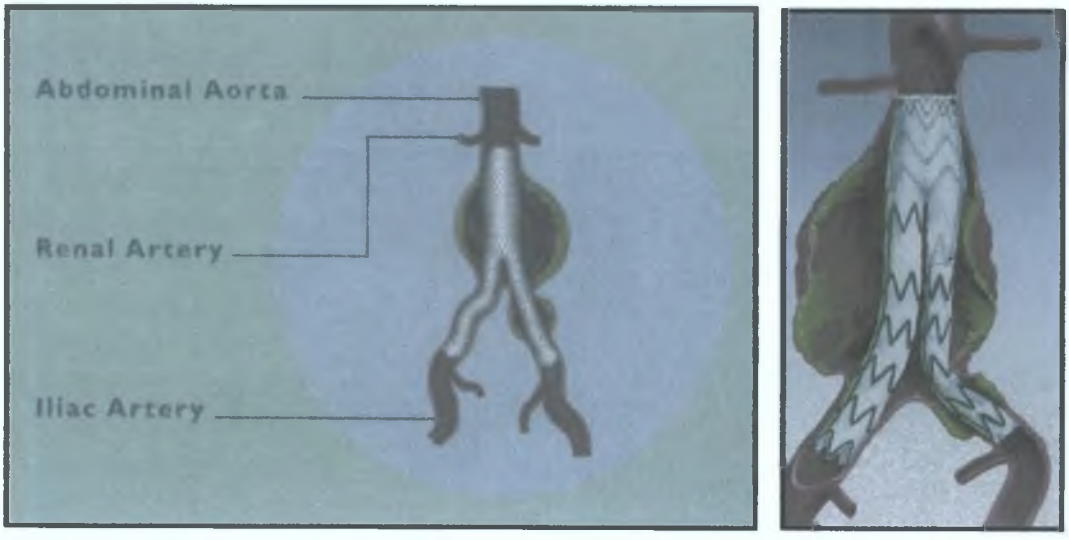

Figure 1.3 : Example of Stent Graft covering the aneurysm at the bifurcation.

(adapted from World Medical Talent Stent Graft ™)

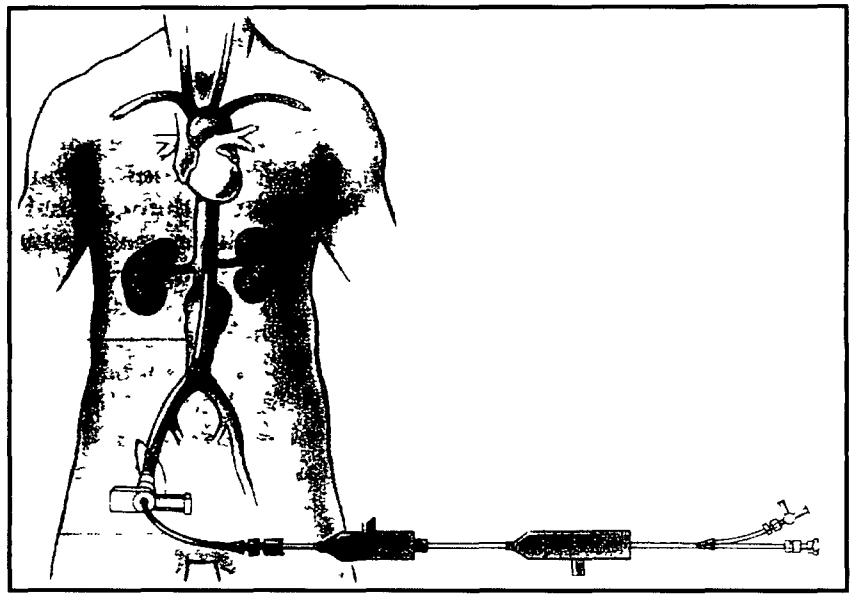

Figure 1.4 : Introduction of the Endovascular Grafting System®.

(adapted from Hopkinson et al ref 4)

Endovascular aortic aneurysm repair has increased in popularity since Parodi et al demonstrated its technical feasibility in a patient in 1991 Despite improvements in peri-operative management, the morbidity and mortality following conventional aortic aneurysm surgery remains considerable

It is feasible to place prosthetic grafts within the arterial tree by inserting them via a remote site, guiding them intraluminally to the appropriate location, and fixing them there with attachment systems, such as a variety of expandable stents Accordingly, there is a potential for these transluminally placed endovascular grafts to provide improved treatment for a variety of arterial lesions, including aortic and aortoiliac aneurysms, thereby avoiding major surgery and the dramatic consequences that it can lead to (heart attack, kidney failure or even death) [4]

Such endovascular treatments offer the economic advantages of short hospital stays or even treatment as an outpatient, as well as elimination of the need for postoperative intensive care and are, therefore, extremely attractive to both patients and physicians The risk of developing an aneurysm increases with age without any question, that is

one of the main reasons to look for less invasive ways of treating aneurysms Consequently, there is enormous pressure to develop and use these devices rapidly [5]

1.3. Endovascular Design Problem:

Now that we understand the disease and the advantages associated with the endovascular procedure, our proposed methods must solve the following

- The Aneurysm has to be stopped from expanding any further This is done by placing a Stent Graft at the bifurcation as shown in figure 5
- The Stent attaches the Graft against the wall of the Aorta below the Renal arteries
- The bifurcated Graft (which is placed between the Renal and internal (hypogastic) arteries) blocks off the aneurysm sac from the flow of blood thus preventing it from expanding any further

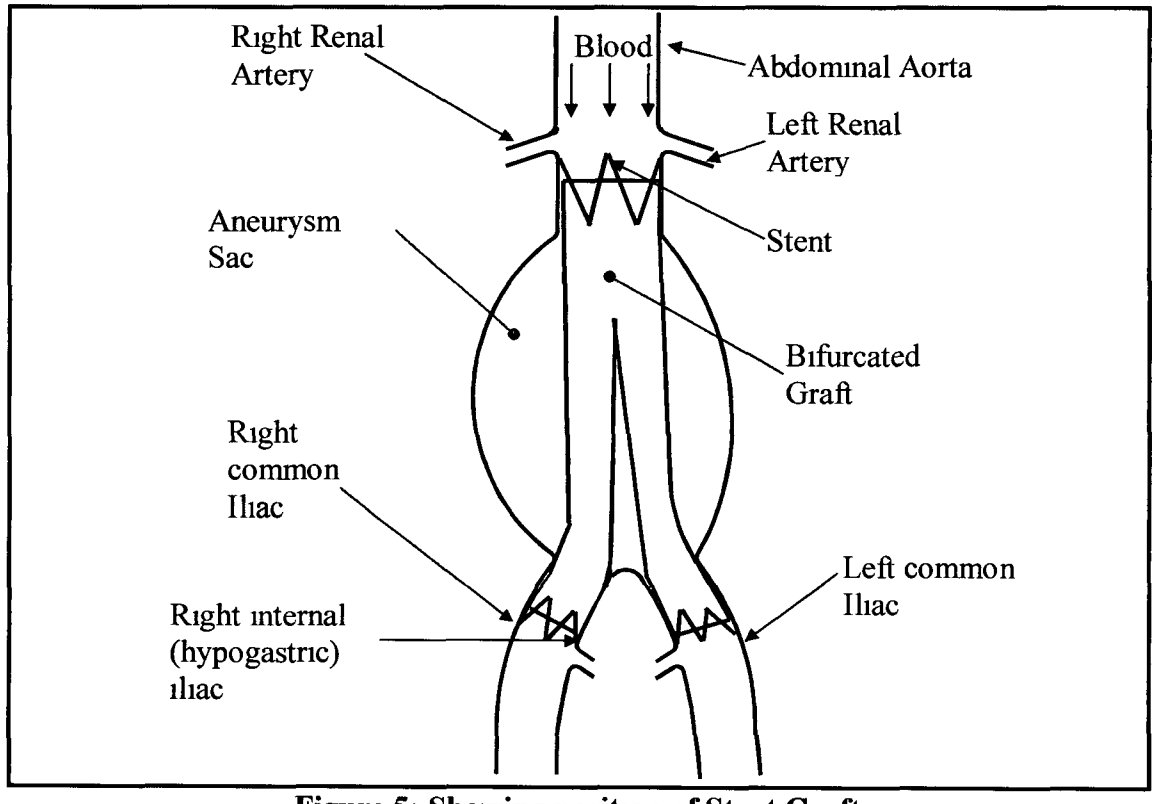

Figure 5: Showing position of Stent Graft.

(Labelling for AAA adapted from Vander ref 6)

1.4. Aims & Objectives.

The main aim is to design a Unitary bifurcated graft stent (i e bifurcated graft as a single component) to treat Abdominal Aortic Aneurysms First we will design a straight graft with both ends anchored to the infrarenal aorta and then the bifurcated graft The insertion of a bifurcated graft is technically more demanding than that of a straight graft The first experimental use of a bifurcated (Y-shaped) graft was by Chuter TAM in 1993 and the first clinical experience was by Scott RAP in 1994 As you can see this is a relatively new technology in the field of endovascular surgery and a lot of design issues and novel methods need to be addressed so as to improve the durability and simplify the delivery of these devices So the aims and objectives of this project is

- To design a Unitary bifurcated graft stent to treat Aortic Aneurysms at the Iliac Bifurcation
- To investigate the types of materials available for the stents, graft, catheters, guidewires etc The choice of material is critical for the delivery and overall durability of the prostheses
- To design the bifurcated Stent and Graft This would include the final expanded shape and crimping of the stent and the folding and unfolding of the graft
- To design the delivery system and deployment mechanism for the stent graft, with miniaturisation of the stent and graft in mind
- To design and construct an in vitro bench test capable of replicating the Cardiovascular System and the disease in question Aortic Aneurysms at the iliac bifurcation This includes simulating pulsatile flow and pressure, constructing mock silicon arteries to replicate Aortic Aneurysms at the iliac bifurcation etc
- To build the protocol, which comprises of the stent, graft, catheters etc
- To test the following on the simulated working conditions of the bench test
    - Delivery system - Method of deployment
    - Attachment system
    - And its durability
- Commenting on the successes or failures of the protocol after physical testing and improving procedure if at all possible

Chapter 2

Overall Design of the Cardiovascular System

2.0. Overall Design of the Cardiovascular System.

2.1. Introduction.

For this project we need to know the critical areas of the cardiovascular system, that is of interest to us for both the design of a suitable bench test facility and for the design of the overall stent graft and delivery system

As discovered by the British physiologist William Harvey in 1628, the cardiovascular system forms a circle, so that blood pumped out of the heart through one set of vessels returns to the heart via a different set Described in its simplest form, the circulation consists' of a pump, the heart, which forces blood periodically and rhythmically into a branching system of elastic tubes The pulsations so generated travel centrifugally and are partially reflected at points of discontinuity to travel backwards again, while pulsations themselves are damped by the time they reach the smallest branches, the capillaries, which are in intimate contact with the cells of tissues The blood then returns in a more or less steady stream to the heart with secondary pulsations imposed in veins by skeletal muscular activity and by the heart itself Figure 2 1 shows how blood is pumped via one circuit (the pulmonary circulation) from the right ventricle through the lungs and then to the left atrium It is then pumped through the systemic circulation, from the left ventricle through all the tissues of the body except the lungs and then to the right atrium Thus, it is this ventricle (the left one) that should be our center of interest [6]

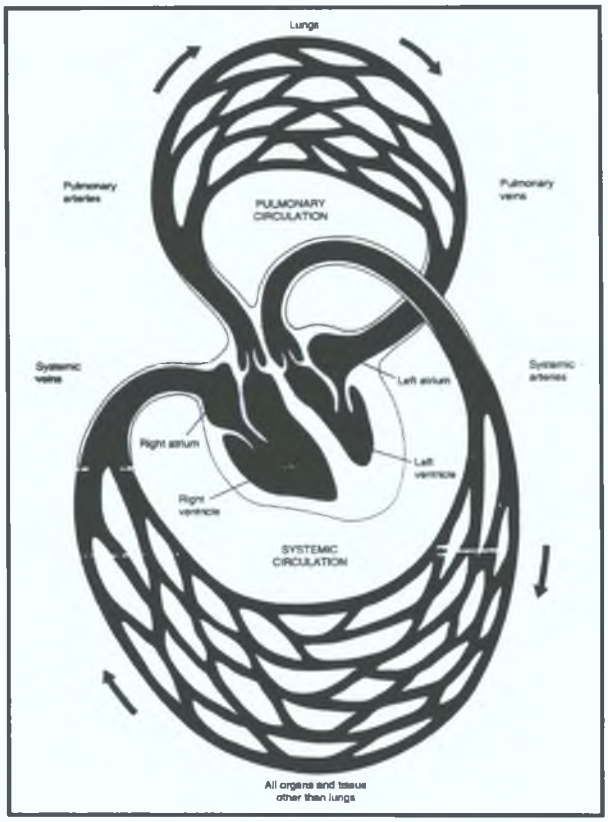

Figure 2.1: The systemic and pulmonary circulations.

(Adapted from Vander ref6)

The typical distribution of the blood pumped by the left ventricle in an adult at rest is given in Table 2.1.

Organ	Rest (ml/min)
Brain	750 (13%)
Heart	250 (4%)
Muscle	1200 (20%)
Skin	500 (9%)
Kidney	1100 (20%)
Abdominal organs	1400 (24%)
Other	600 (10%)
Total	***5800***

Table 2.1: Distribution of systemic blood flow to the various organs and tissues of the body at rest *(Adapted from Chapman and Mitchell).*

2.2. Velocity Profile In Pulsatile Flow.

As blood flow in arteries is not steady, thus it is to be anticipated that the velocity profile will not be of the same parabolic form that is found in steady laminar flow The equation of motion is based on the Navier-Strokes equations The Navier-Stokes equations have applications to blood flow when the non-Newtonian features of blood can be ignored and when the blood vessel diameter is much larger than the dimensions of individual blood cells These equations are not accurate enough for flow in the neighborhood of a stagnation point or flow in a capillary blood vessels, or flow with blood clots Since the full solution to the Navier-Strokes equations are impossible to solve mathematically, some assumptions are used to solve these equations The assumptions are that blood is an incompressible, laminar, axially symmetric Newtonian fluid, with no tangential velocity components Neglecting also body forces such as gravity forces, local convective acceleration since this term can be neglected when compared to the transient acceleration This is approximately satisfied in large arteries in which $\frac{vr}{c}$ is about 0 25 (where c is the wave velocity) and also neglecting second order terms The equation of motion for pulsatile flow in polar co-ordinates is [7,8]

$$\frac{\partial v}{\partial t} = -\frac{1}{\rho}\frac{\partial p}{\partial z} + \nu\left(\frac{\partial^2 v}{\partial r^2} + \frac{1}{r}\frac{\partial v}{\partial r}\right) \qquad (2.1)$$

Where

$\frac{\partial v}{\partial t}$ = partial deviate of velocity with respect to time

r = radius of artery

ν = kinematic viscosity

ρ = density of blood

$\frac{\partial p}{\partial z}$ = partial deviate of pressure with respect to axial distance

Now for a pressure gradient = $\frac{\partial p}{\partial z} = A^* e^{i\omega t}$ *Womersley (1958)* showed that a solution to equation 2 1 is

$$\text{Velocity} = v = \frac{A^* r^2}{i\mu\alpha^2}\left(1 - \frac{J_0\left(\alpha y i^{3/2}\right)}{J_0\left(\alpha i^{3/2}\right)}\right)e^{i\omega t} \qquad (2.2)$$

where

A^* = complex conjugate of A

μ = coefficient of viscosity

α = womersley number = $r\left(\frac{\omega}{\nu}\right)^{1/2}$

ω = angular velocity = 2*π*frequency(in Hz)

J_0 = Bessel function of order zero

Equation 2 2 gives the velocity of motion of the lamina of liquid at a fraction of the radius y, from the axis of the tube The solution of this equation is concerned with complex quantities and may be made by separation into the real and imaginary parts The real and imaginary parts of Bessel function of the first kind of zero order

Greenfield and Fry (1965a) made a detailed comparison between flow measured in the thoracic aorta with an electromagnetic flowmeter The predicted flow showed close agreement with Womersleys equation These equations can be used when the Reynolds number and womersley numbers are >>1 Womersley equation cannot be rigorously applied to arteries, nevertheless, it is almost certainly as close, or closer, a practical approximation as Poiseuille's is for steady flow in arteries [8]

2.2.1. Impedance Methods.

Due to the difficulty in solving the Navier Strokes equations, fluid oscillations in systems may be analyzed conveniently by the use of procedures borrowed from linear vibration theory and electrical transmission-line theory These methods are used to describe a relationship between the ratio of blood pressure and flow at any given point on the arterial tree Once this ratio is known which is called the effective or input impedance, other pressure and flow relationships can be easily found in other parts of the arterial tree The input impedance of the human arterial tree can be obtained by analyzing the measured pressure and velocity waves at a given site and with the use of a Fourier series to describe the pressure and flow waves in terms of complex valued harmonics [6,7] By applying the Fourier series to both the pressure and flow waveforms, one can fit a trigonometric series as an approximation to the actual function This is achieved by taking a number of readings of equally spaced points that can accurately describe the waveform and apply a numerical Fourier series to the data Mathematica Version 3 0 (*Wolfram)* which is a computerized mathematical package has its own build in numerical trigonometric package that is capable of representing readings over one periodic function of the waveform in question Figure 2a & 3a shows typical pressure and flow waves found in the aorta and Figure 2b & 3b shows the represented Fourier series calculated by Mathematica The trigonometric series for these waveforms are given in Appendix A

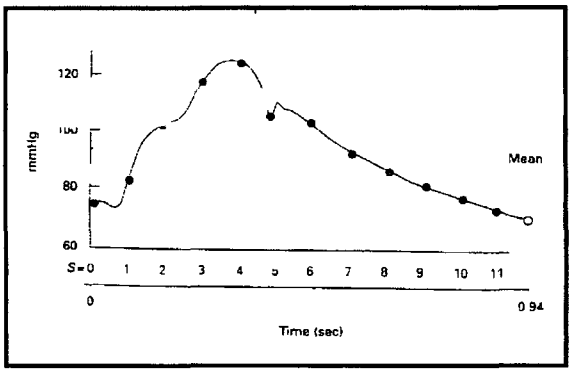

Figure 2.2a: Typical arterial pressure wave recorded in the aorta, *(Adapted from McDonald ref 8)*

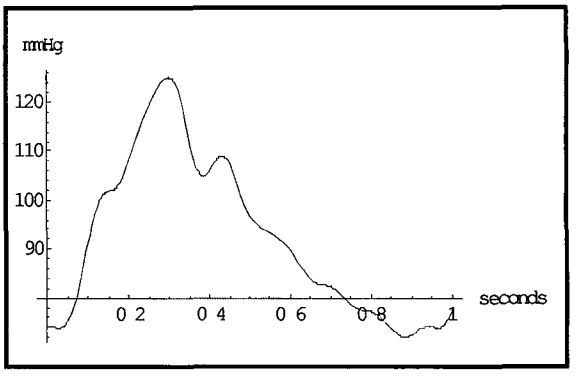

Figure 2.2b: Fourier series representation of the pressure waveform.

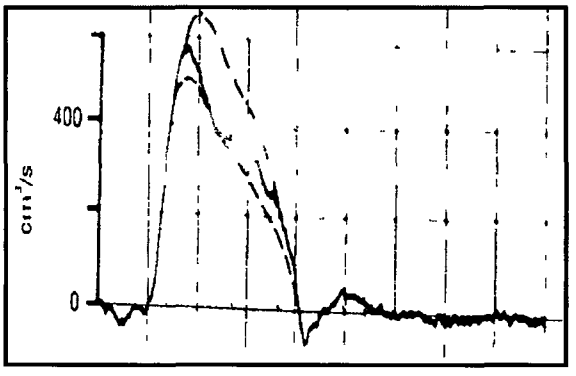

Figure 2.3b: Typical flow waves recorded in three normotensive subjects, aged 28,52 & 68 years. *(Adapted from McDonald ref 8)*

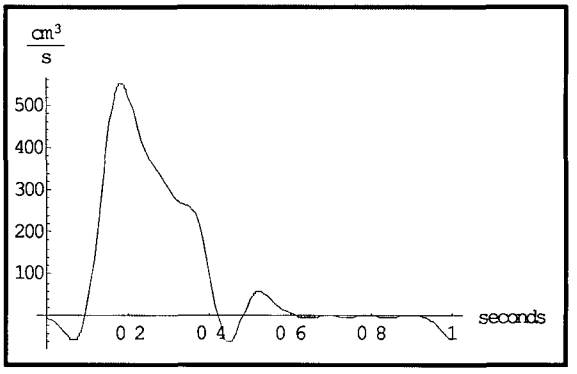

Figure 2.3b: Fourier series representation of the flow waveform for the 68 years subject.

Figure 2 4 shows the two most representative characteristics of each area of the cardiovascular system, that is, the pressure and the velocity

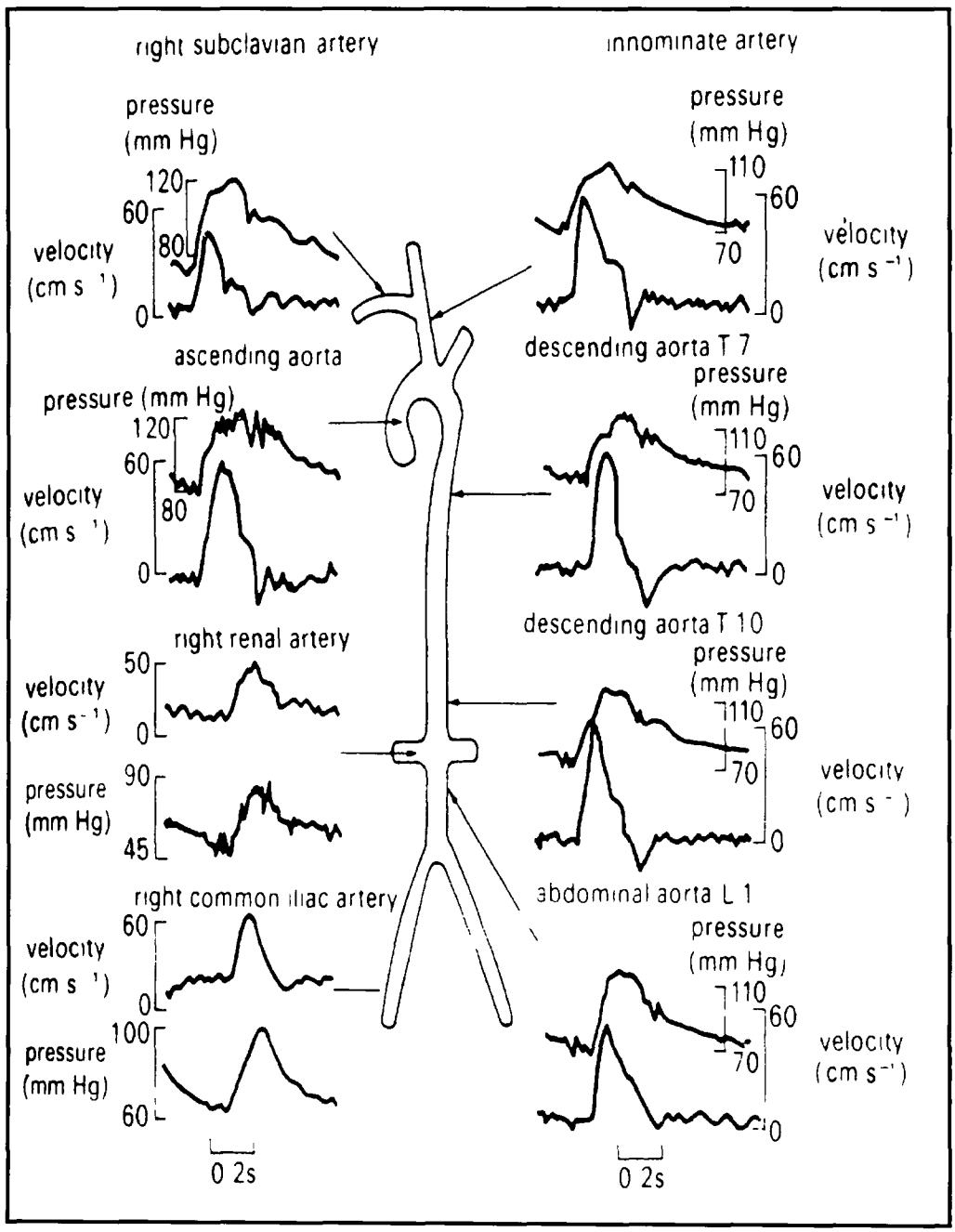

Figure 2.4 : Pressure and flow waves in human arterial tree.

(Adapted from Y.C Fung ref 7)

2.3. The Heart.

The Heart is the prime mover of blood By periodic stimulation of its muscles it contracts periodically and pumps blood throughout the body The cardiac cycle is divided into two major phases, the period of ventricular contraction and blood ejection, systole, followed by the period of ventricular relaxation and blood filling, diastole At an average heart rate of 72 beats/min, each cardiac cycle lasts approximately 0 8s, with 0 3s in systole and 0 5 s in diastole [6]

2.3.1. The Cardiac Output.

The volume of blood pumped by each ventricle per minute is called the cardiac output (CO), usually expressed as litres per minute It is also the volume of blood flowing through either the systemic or the pulmonary circuit per minute

The cardiac output is determined by multiplying the heart rate (HR) - the number of beats per minute - and the stroke volume (SV), the blood volume ejected by each ventricle with each beat

$$CO = HR \times SV$$

Thus, if each ventricle has a rate of 72 beats/min and ejects 70 ml of blood with each beat, the cardiac output is [6]

$$CO = 72 beats / \min \times 0\,07 L / beat = 5\,0 L / \min$$

2.4. The Vascular System.

The aorta and other systemic arteries have thick walls containing large quantities of elastic tissue Arteries are tough on the outside and smooth on the inside An artery actually has three layers an outer layer of tissue, a muscular middle, and an inner layer of epithelial cells The muscle in the middle is elastic and very strong The inner layer is very smooth so that the blood can flow easily with no obstacles in its path

When the ventricles eject blood into the pulmonary and systemic arteries during systole as shown in figure 2 5, a volume of blood equal to only about one-third the

stroke volume leaves the arteries during systole. The rest of the stroke volume remains in the arteries during systole, distending them and raising the arterial pressure. When the ventricular contraction ends, the stretched arterial walls recoil passively, like a stretched rubber band being released, and blood continues to be driven into the arterioles during diastole. As blood leaves the arteries, the arterial volume and therefore the arterial pressure slowly falls, but the next ventricular contraction occurs while there is still adequate blood in the arteries to stretch them partially. Therefore, the arterial pressure does not fall to zero. Arteries can be viewed most conveniently as elastic tubes which increase in diameter as the internal pressure increases [6,9].

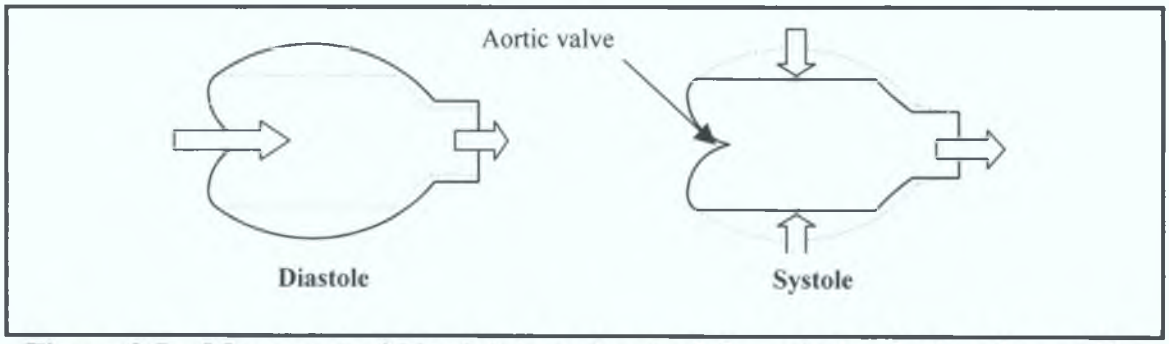

Figure 2.5: Movement of blood into and out of the arteries during the cardiac cycle. The lengths of the arrows denote relative quantities flowing into and out of the arteries and remaining in the arteries during systole.

Figure 2.6(A) shows the aortic pressure pattern of a typical pressure change that occurs in all the large systemic arteries. It is this rhythm between the heart and the artery results in an efficient circulation system. Figure 2.6(B) shows how the arterial pressure changes with age [9].

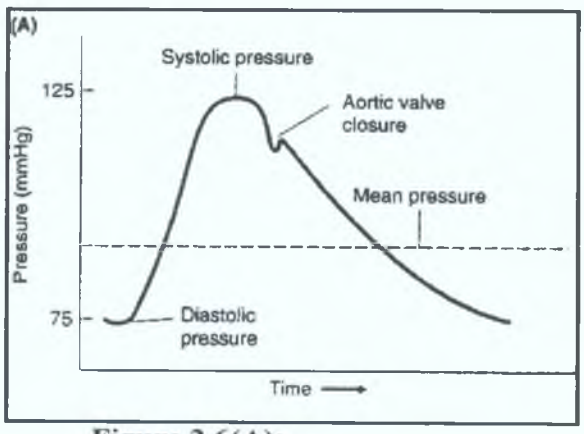

Figure 2.6(A):

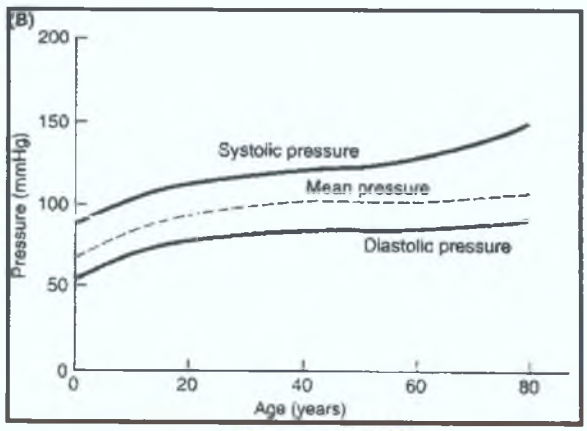

Figure 2.6(B)

(Adapted form Guyton ref 9)

The two most important factors determining the magnitude of the pulse pressure is

1. Stroke volume, the greater the volume of blood ejected the higher the pressure
2. Arterial compliance, this is a relationship between the increase in pressure due to an increase in volume and therefore shows how easily an artery can be stretched It is termed by the following relationship

$$\text{Compliance} = \frac{\Delta\text{volume}}{\Delta\text{pressure}}$$

The higher the compliance the more easily it can be stretched

The mechanical properties for the abdominal aorta are shown in Table 2 2

Mechanical Properties	Values
Young's Modulus	Varies between 2 0 – 8 0 * 10^6 dyne/cm^2 or 2 0 – 8 0 * 10^5 N/m^2
Bulk modulus	Varies between 2 2 * 10^6 – 8 0 * 10^6 dyne/cm^2 or 2 2 – 8 0 * 10^5 N/m^2
Poisson ratio	Close to 0 5
Average Aortic wall thickness	1 1mm during diastole 0 9mm at end systole
Density	1060 – 1066 kg/m^3
Radical pulsation	± 5 – 6%
Pulse wave velocity	Varies with age from 500cm/s to 1500cm/s

Table 2.2: Mechanical Properties of the Abdominal aorta.

(Adapted from McDonald ref 8)

2.5. Wave Reflections

The arterial tree is made up of a system of distensible tubes along which pressure and flow waves are generated by the heart and are transmitted and reflected A traveling wave such as the pressure or flow wave will be reflected to some extent wherever there is a discontinuity in the system Possible reflecting sites include branching points, areas of alteration in arterial distensibility, and high-resistance arterioles A discontinuity may be a change in caliber, as at a point of branching, or merely a change in the elastic properties of the arterial wall The existence of wave reflections are observed by the shapes of the pressure and flow waves measured, e g during ventricular ejection the aortic pressure often continues to increase while the flow is decreasing as shown in figure 2 7 This secondary rise in pressure must be due to wave reflections Wave reflections are the major cause of increasing systolic blood pressure and decreasing ventricular ejection with age The amplitude of a propagated wave diminishes exponentially as it travels Therefore, even with complete reflection, the reflected wave will always be smaller than the incident wave in amplitude (with the exception of the point of reflection where they will be the same) This discrepancy will increase as the distance between measuring site and reflection site increases Therefore there can never be a complete cancellation of the two waves and a standing wave cannot be achieved Due to wave reflections, pressure and flow waves do not have similar profiles At any given time, the pressure and flow at a given site are the sums of the newly arrived waves and the retarded waves of reflection from earlier fluctuations This means that the pressure-flow relationship is frequency dependent Multiple Reflections occur due to further branching beyond the iliac bifurcation, multiple reflections occur which makes wave reflection calculations more complex Multiple reflections are important as they affect both pressure and flow [6,7,8,9]

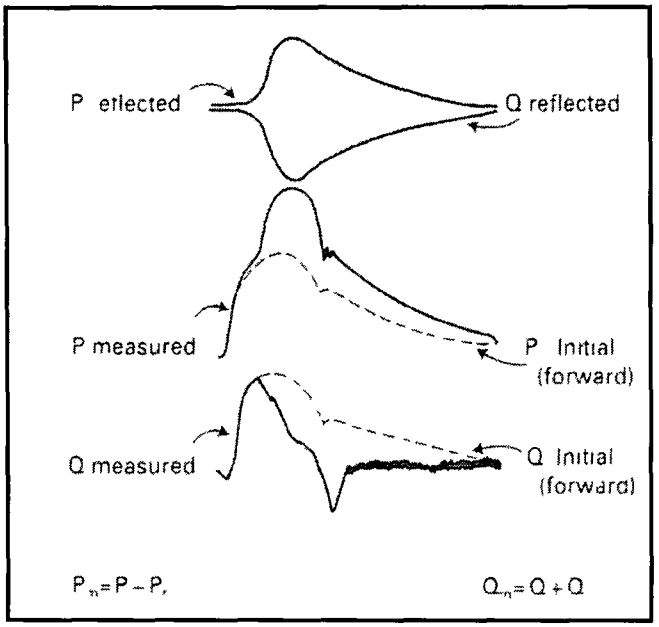

Figure 2.7: The Influence of the pulse wave reflections on the aortic pressure (P) & Flow (F) ***(Adapted from Guyton ref 9)***

2.6. Types of Flow.

There are two types of flow that pulsatile flow could be, that is either laminar or turbulent In laminar flow the fluid viscosity is dominant and causes the fluid particles to move in straight lines while in turbulent flow the flow becomes fluctuating and agitated The velocity profile is generally more flatter in turbulent flow while in laminar flow it is parabolic It turns out that the effect of rough walls is negligible for laminar pipe flow, and all the laminar formulas are valid for rough pipe walls also But turbulent flow is strongly affected by roughness Reynolds number which is in dimensionless form is the ratio of the inertia forces to viscous forces and is given by the following formula

$$\text{Reynolds number} = Re = \frac{\rho v d}{\mu}$$

Where

d = diameter of tube

ρ = density

μ = viscosity of fluid

v = velocity of fluid

When this number is around 2,000 the transition from laminar to turbulent flow occurs For pulsatile blood flow in arteries the flow velocity changes with time The Reynolds number is based on the instantaneous velocity of flow averaged over the cross-section, which varies with time Figure 2 8 shows a record of velocity of flow versus time In a period of rising velocity the Reynolds number increases slowly until it reaches a level marked by the dotted line (Re = 2,300), at which the flow could be expected to become turbulent if it were steady But an accelerating flow is more stable than a steady flow, because turbulence cannot develop instantaneously So, when the turbulence finally sets in, the velocity and Reynolds number are much higher than the dotted line level On the other hand, in a period of decreasing velocity the disappearance of turbulence occurs at a level of velocity considerably below the dotted line This is partly because decelerating flow is inherently less stable than steady flow, and partly because existing eddies take a finite time to decay

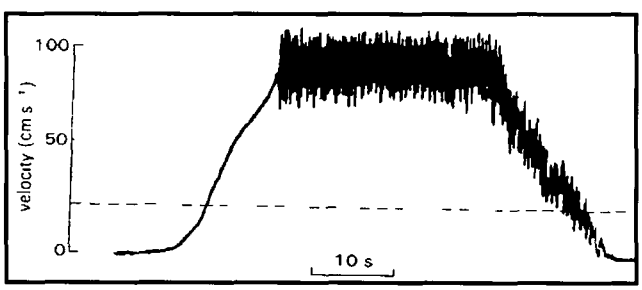

Figure 2.8: A Turbulent flow velocity-versus-time record.
(Adapted from Y.C Fung ref 7)

Thus, the critical Reynolds number of laminar-turbulent transition depends on the rate of change of velocity, as well as on the eddies upstream and the roughness of the pipe wall For pulsatile flow in a tube, when the Womersley number is large, the oscillatory inertia force dominates and the effect of the viscosity of the fluid does not propagate very far from the wall The Womersley number is in dimensionless form, which is the ratio of transient inertia force to shear force as is given by the following formula

$$\text{Womersley number} = \alpha = \frac{d}{2}\sqrt{\frac{\rho\omega}{\mu}}$$

where

ω = frequency of oscillation

In the central portion of the tube the transient flow is determined by the balance of the inertial forces and pressure forces as if the fluid were non-viscous We therefore expect that when the Womersley number is large the velocity profile in a pulsatile flow will be relatively blunt, in contrast to the parabolic profile of the Poiseuillean flow, which is determined by the balance of viscous and pressure forces That is indeed the case as seen from figure 2 9 In figure 2 9, it can be seen that the velocity profile is quite blunt in the central portion of the aorta So we can conclude that pulastile flow is indeed turbulent [7,8]

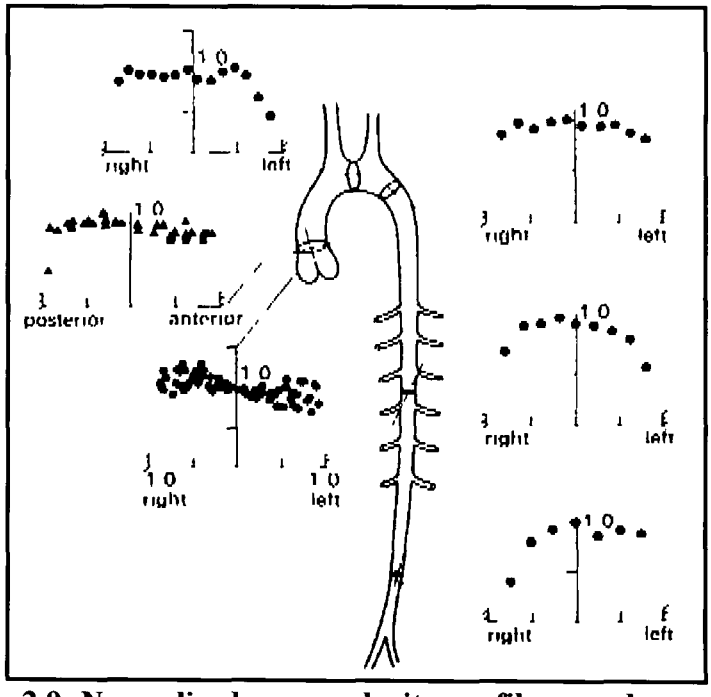

Figure 2.9: Normalized mean velocity profiles in a dog aorta.

(Adapted from Y.C Fung ref 7)

2.7. General Properties of Blood.

Eighty per cent of blood is water Despite the fact that chemical substances and cellular elements are constantly entering and leaving the bloodstream, its general composition is relatively uniform in the higher-order animals This results from a number of regulatory mechanisms acting in conjunction with a rapid circulation which ensures that any potentially large variations in blood composition, initiated by tissue metabolic processes, are reduced by virtue of the relatively large volume of blood flowing through the organs concerned The specific gravity of whole blood ranges from 1 055 to 1 065

Due to the presence of red cells at the normal haematocrit value of 45% (percentage of red cells in whole blood), the viscosity of blood is three to four times that of water (μ_{water} = 0 01 $g \times s^{-1} \times cm^{-1}$) A 'Newtonian' fluid such as water accurately obeys Newton's equation, while blood, on the other hand, only approximates to a Newtonian fluid Under most physiological conditions, however, the hematocrit and, hence, viscosity of blood is relatively constant and we can assume blood to be Newtonian [10]

2.8. Summary.

Now we are in a better position to design our bench test and stent graft This chapter was only intended to be a brief introduction to the cardiovascular system We will of coarse be referring in more detail to other aspects of the cardiovascular system where it is appropriate from the point of view of our final design Comparisons will be made between our bench test and the cardiovascular system, so that the reader can assess the validity of the bench test and the final prosthesis design

Chapter 3

Development of Study Protocol

3.0. Development of Study Protocol.

3.1. Introduction

The following general guidelines are recommended for preclinical and clinical testing before the devices are brought into widespread usage.

1) ***Bench Testing:*** A test model to test,

- **Graft portion:** Physical properties such as strength, durability, porosity, kink resistance, suture holding, flexibility, longitudinal and radial strength.
- **Stent portion or attachment system:** Inertness in blood, lack of toxicity, absence of metal fatigue, flexibility, compression resistance and other physical properties that contribute to a leak-proof seal and secure fixation at junction points with arteries.
- **Delivery system:** To demonstrate appropriate maneuverability, kink resistance, radiopacity, marker visibility [4].

2) ***Animal Testing:***

- Ability to visualise and deploy the device
- Firm fixation.
- Acceptable freedom from leakage, migration, vessel wall erosion, thrombosis, excessive intimal hyperplasia (growth of tissue), lumen narrowing, distal embolization.
- At least six months trials before clinical testing [4].

3) ***Clinical Testing:*** Clinical testing must demonstrate the safety, efficacy, and effectiveness of stent grafts in the treatment of human arterial diseases.

- **Feasibility testing:** This should demonstrate that the insertion of the stent graft device is possible in a given disease sate in a given location and that the device functions safely and effectively for at least six months. These tests must include comparative preprocedural and postprocedural noninvasive measurements of the distal circulation and

in the case of aneurysms, their size before and three and six months after stent graft placement

- **Comparative performance testing:** This phase of evaluation is designed to show that the stent graft device will perform essentially equivalent to or significantly better than standard treatment Studies should include an adequate number of patients to be monitored after the procedure to allow statistically valid comparisons after 1 – 2 years with other similar patients that used the standard procedure [4]

In designing a Stent Graft with its delivery system, the first stage was to build a bench test capable of replicating the Cardiovascular System and the disease in question Aortic Aneurysms at the Iliac bifurcation The design of the test system requires the following units

1. ***Simulation of the behavior of the blood flow through the aortic bifurcation*** This unit will include the design procedure of a piston pump, capable of simulating pulsatile flow

2. ***Simulation of the pulsatile pressure in the Aorta*** The Aorta in the test system has to be pressurised similar to that in the body A pressure valve with an adjustable spring deflection and hence capable of reproducing normal blood pressure and the reduced blood pressure as required during the endovascualr procedure will be positioned after the aorta to provide this pulsatile pressure

3. ***Regulation of the test system temperature*** The normal body temperature is around 37°C So a temperature controller will be needed

4. ***Replica of the Abdominal Aortic Aneurysm at the Iliac bifurcation*** This is the making of a mock silicon Abdominal Aortic Aneurysm at the Iliac bifurcation

5. ***Comparison of using water instead of blood:*** For our test system we will use water as this is a safe fluid to use for our bench test as no corrosion will occur in the piston pump Both we will compare the characteristics of blood with that of water and we should see that water is a safe compromise

6. ***Modeling of the systemic circuitry*** This is where the tanks are connected to the piston pump and where there is a recycling loop for the flowing liquid

3.2 Simulation of the behavior of the blood flow through the Aortic Bifurcation

The heart is a pump, which delivers blood by periodic waves If we analyse the working cycle of the heart, which comprises of the blood filling period (called diastole) followed by a blood ejection period (called systole) We can easily notice the resemblance to the working of a vacuum pump, where the liquid to pump is consecutively sucked and then delivered within one cycle The most easily realisable kind of vacuum pump is the reciprocating pump The characteristics of this type of pump to model the flow of blood output from the heart is not readily available on the consumer market Either the pulsating pump is motorised but its capacity is too large or it is manual with the right capacity but then its behavior is fluctuating with time So I had to manufacture my own Piston Pump, which is capable of reproducing pulsatile flow and pressure The Piston Pump is an axial pump, which gives a sinusoidal output as shown in Figure 3-1

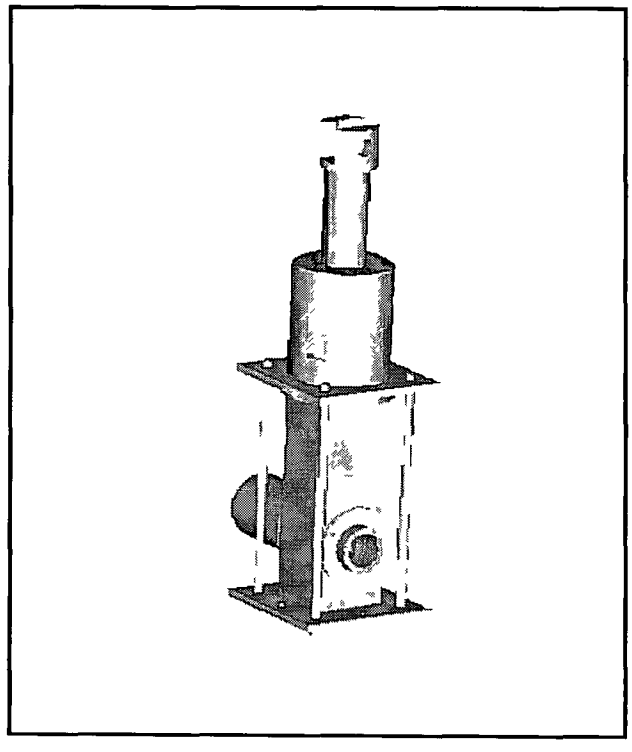

Figure 3-1 Piston Pump

3.2.1. Design Procedure:

The body's mean pulsation rate is 72 beats/min with a cycle time of therefore 0 8 sec One cycle of the heart includes ventricular contraction and blood ejection (systole) of 0 3sec and ventricular relaxation and blood filling (diastole) of 0 5 sec a ratio of 5 3 So the problem is how to get the suction time different from the delivery time? The solution is to shift the axis position of the crankshaft away from the axis position of the cylinder thus obtaining the linkage called general or offset slider crank mechanism The problem with such a design is that a very long connecting rod would be needed to turn the crank shaft without getting jammed

The difference between the times of the forward and backward strokes is superfluous So an easier design which can work is an axial pump which gives a sinusoidal output

So the essential characteristics to simulate are

- pulsating flow (at whatever speed),
- quantity of blood flowing through the abdominal aorta (i e the pump output),
- blood flow velocity in the abdominal aorta,

3.2.2. Design of Piston Pump.

This design is based on the construction of power pumps, which are particular reciprocating machines All pieces were designed to be easily manufactured in a typical workshop, that is without CNC machines This explains the mere cylindrical shapes of the different parts The design of the piston pump consists of a liquid end, power end and a prime mover

Liquid End: This consists of the following

> ***Cylinder*** This is where the pressure is developed It consists of a cavity, which must be linked to outside by three orifices one for suction manifold, the second for the discharge manifold and the last one for the plunger
>
> ***Plunger or piston.*** The plunger transmits the force that develops the pressure
>
> ***Stuffing box:*** This houses the lower and upper bushings, the hydraulic seal and a spring which holds the seal and bushings in an axial position This arrangement eliminates overtightening and allows uniform break in of seal

Valves and manifolds: The valves are typical one-way valves and are easily found in the consumer market. The connections specially made for these valves were slightly modified in order to assume a good junction between the valves and the cyclinder.

Figure 3.2 shows the assembly procedure of the liquid end and the previous diagram figure 3.2. For further details, I invite the reader to look at the plans presented in Appendix B.

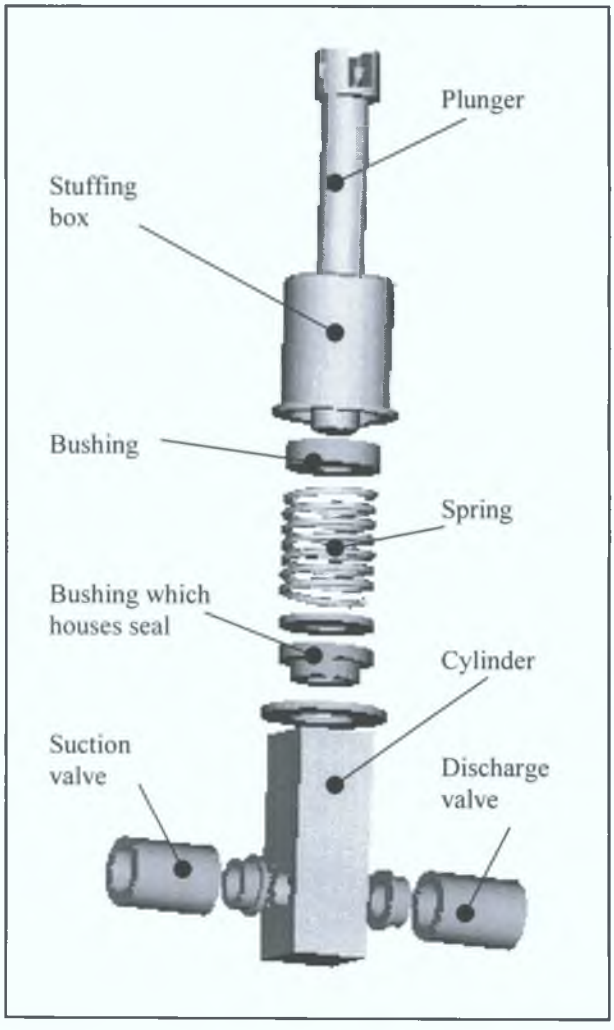

Figure 3.2: Disassemble of Piston Pump

Power End: This consists of the crankshaft, connecting rod crosshead, and bearings. In most of the reciprocating pumps, the manufacturing of the power end is a critical parameter for the working life of the pump, since it is the birthplace of the main vibrations. Nevertheless, because our pump is not working very fast (only 72 rpm),

this was not my greatest preoccupation Therefore, the crankshaft is a mere disk made out of steel The connecting rod transfers the rotating force of the crank pin to an oscillating force on the wrist pin The connection between the connecting rod and the crankshaft is achieved by a bolt-nut assembly, where the bolt carries the crank pin The connection between the connecting rod and the crosshead manufactured in the plunger is managed by a wrist pin, which is held in place by using circlips on both sides

Prime Mover: The prime mover is the element of the pump that gives the power needed to move the mechanism In our case, it is an electric DC motor This kind of motor is very easy to set up, because its connection to the electrical supply is simple and also its rotational speed is proportional to the voltage applied Therefore, the motion of the crank (72 rpm) can be adjusted by using a transformer The motor, whose axle carries all the components of the power end, is held in position by the use of a specially designed stand which prevents vibrations otherwise caused by the power end

3.2.3. Piston Pump Characteristics.

Stroke volume: As shown in Figure 3 3 is the kinematics of the piston pump The pump output or stroke volume is the quantity of liquid that is flowing through the Abdominal Aorta and this has a value of 2r, which is the stroke length

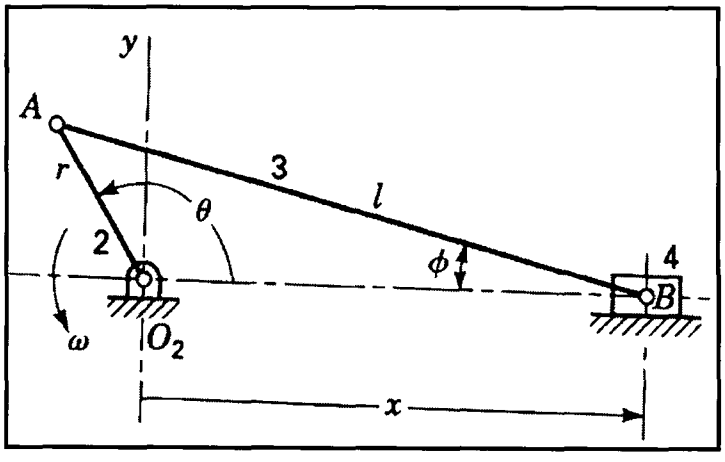

Figure 3.3: Kinematics of Axial Piston Pump

(Adapted from Shigley & Uicker ref 11)

The stroke volume of our piston pump is

$$\text{Stroke volume} = \frac{\pi}{4} d^2 \times \text{Stroke length}$$

The blood flow through the Abdominal Aorta varies between 3.2 ~ 3.7 l/min. The normal pulse rate is 72 beats/min for men and 80 beats/min for women. It is quite normal for men to vary between 60 and 80 beats/min and for women to vary between 68 and 90 beats/min. As we get older our mean pulse rate is around 80 beats/min. Since older people are is most likely to get this disease we will choose a pulse rate of around 80 beats/min, and a flow rate of 3.5l/min. For these conditions, we obtain the following for the stroke volume.

$$\text{Stroke volume} = \frac{\text{Flow rate}}{\text{rpm}} = \frac{3.5\text{L/min}}{80\text{rpm}} = 0.043\text{Litres} = 43\text{ml} = 43\times10^3\,\text{mm}^3$$

$$\text{Stroke volume} = \frac{\pi}{4} \text{d}^2 \times \text{Stroke length} = 43\times10^3\,\text{mm}^3$$

To find a suitable stroke length we need to keep the maximum value of ϕ as small as possible (see Figure 3.3) because if this angle ϕ is large jamming will occur. Since our connecting rod is of a standard size of 100mm a recommended ratio of connecting rod length *l* to radius of crankshaft r for an axial pump design is in the range of 3:1 to 6:1 [12]. Since the higher ratio would result in a large and uneconomical power frame, we will choose the 3:1 ratio. So therefore our crankshaft radius is 100/3 ≅ 33.33mm. We will choose say 30mm for the crankshaft radius, which corresponds to a stroke length of 60mm. This gives a diameter of the piston rod to be

$$\text{Diameter of piston} = \text{d} = 30.2\text{mm}$$

Velocity: Appendix C includes the equations and diagrams showing the position of the ram (or plunger), its velocity and finally its acceleration. To get these results a computerised mathematical package (Mathematica version 3.0 Wolfram) was used. Starting with the equation of displacement, Mathematica differentiated first with

respect to time to get the velocity and differentiate a second time with respect to time to get the acceleration Then we used the graphics function to plot these three transient parameters (position, velocity and acceleration)

To find the maximum velocity of the fluid through the Aorta and compare it to figure 2 4 in chapter 2 We can use the following relationship neglecting the effects of friction for the maximum velocity in the aorta

$$\text{Maximum velocity} = \frac{\text{Cross sectional area of piston}}{\text{Cross sectional area of Aorta}} \times (\text{Max velocity of piston})$$

$$\text{Velocity in Aorta} = \frac{(\text{d piston})^2}{(\text{d aorta})^2} \times \text{velocity of piston}$$

For comparison purposes with Figure 2 4, we let the diameter of aorta be 22mm Figure 3 4 shows the velocity obtained from our piston pump if it is feeding into an artery of 22mm As we can see from Figure 3 4 for the maximum velocity is around 50cm/s, which is comparable to the average maximum velocity in the aorta

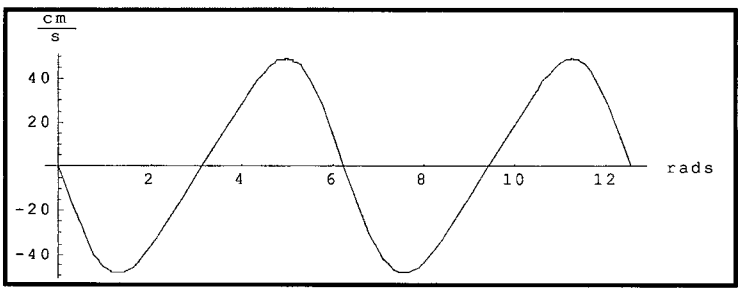

Figure 3.4: Pulsating velocity

Figure 3 5 A & B shows the manufactured piston pump with it prime mover supported by the motor support The full plans for the motor support is also given in AppendixB

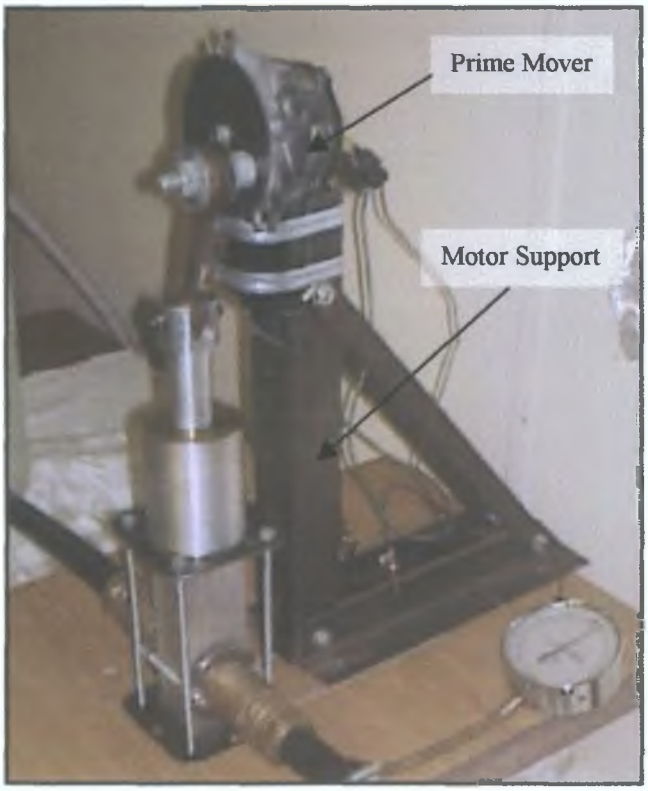

Figure 3.5A

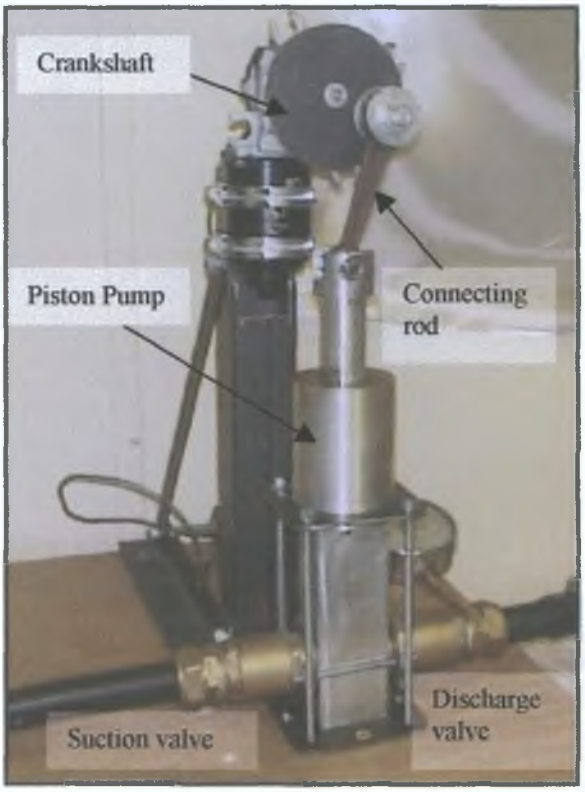

Figure 3.5B

Table 3.1 compares the Piston Pump to the various values in the Abdominal Aorta rather than the Heart itself as this test system depends on the characteristics in the Aorta.

	Abdominal Aorta	**Piston Pump**
Mean pulsation at rest 72beats/min cycle time 60/72 ≈ 0 8sec blood ejection (systole) 0 3sec blood filling (diastole) 0 5sec	72beats/min (same as the heart) 80 beats/min for older people [6,9]	varies between 20 to 100 rpm Output gives a sinusoidal output
Max blood pressure during systole	116 - 150 mmHg normal Reduced to 60 to 70mmHg during Endovascular operation using nitroglycerin solution [3]	Can be adjusted to suit by adjusting spring stiffness of pressure valve (to be explained latter on in this chapter)
Velocity	0 - 60cm/s [7,8]	0 - 55 cm/s at pump outlet
Blood Flow (cardiac output) 5 litres/min	Between 3 2 ~ 3 7 litres/min approx at abdominal aorta [6]	3 2 ~ 3 7 litres/min at 75 ~ 87 rpm

Table 3-1: Comparison between Piston Pump Characteristics and Abdominal Aorta

3.3. Regulation of the Test System Temperature.

Body temperature is around 37°C. To achieve a temperature close to this valve a Thermostatic of Proportional temperature controller could be used. Thermostatic controllers are less expensive than Proportional controllers but not as accurate. Since a temperature around this valve is required, Thermostatic controllers can be set up to do the job.

3.4. Replica of the Abdominal Aortic Aneurysm at the Bifurcation.

The Aortic bifurcation of a healthy person has a typical straight-Y shape. Obviously this is not the case for aortic bifurcation with aneurysms, as represented in Figure 3.5.

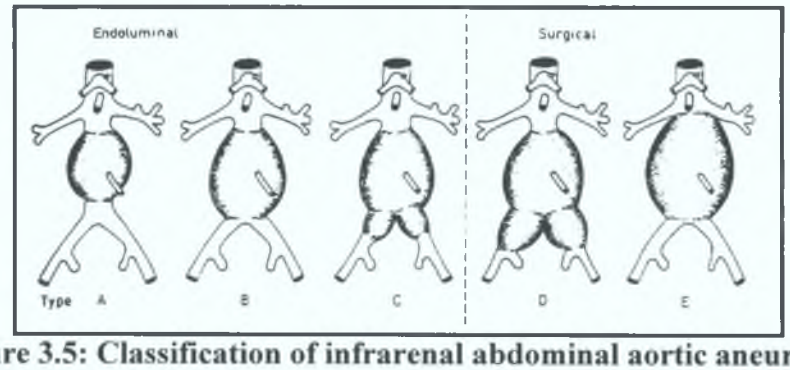

Figure 3.5: Classification of infrarenal abdominal aortic aneurysm.

(Adapted from Hopkinson, Yursuf, Whitaker & Veith ref 4)

This figure shows us that aneurysms can develop at random locations with many different shapes and sizes. When the area covered by the disease is too big, then it is not possible to treat it by endovascular repair.

For tests to be carried out in vivo, mock Abdominal Aortic Aneurysms at the Iliac bifurcation will have to be replicated using either latex or silicon rubber. Silicon rubber is preferred to latex rubber as it is transparent and this aids in visualising the delivery of the stent graft. The technique used to manufacture this Aortic Aneurysm is the lost wax process. CNC technology is used to manufacture the female casts made from aluminium as shown in Figure 3.6(A). This female cast is used to make the male wax cast. Silicon rubber or Latex can be painted in layers on the male wax cast. When

Aneurysm as shown in Figure 3.6(B). Figure 3.6(C) shows the manufactured female casts and the mock silicon & latex arteries.

Figure 3.6A:
Aluminium cast of Aortic Aneurysm

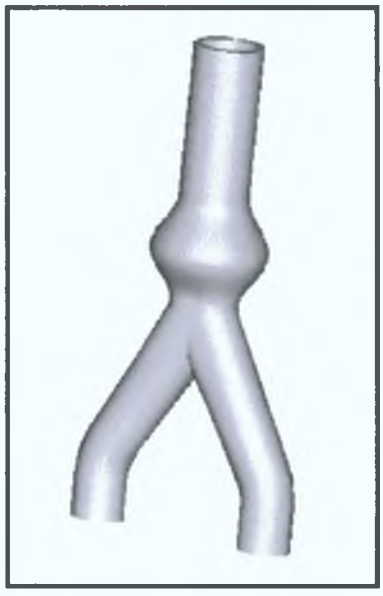

Figure 3.6B:
Model of Aortic Aneurysm

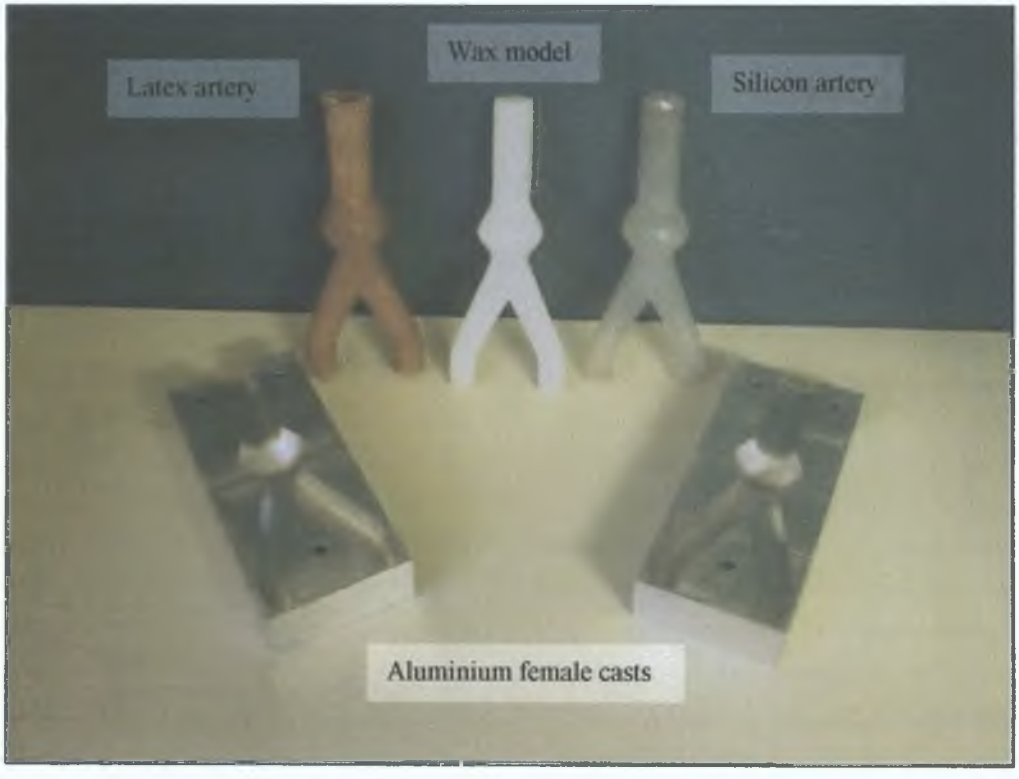

Figure 3.6C: Manufactured Mock Silicon Arteries

3.4.1 Manufacturing of The Female Cast.

Pro-Manufacture will create the data necessary to drive the NC machine tool to machine the Pro-Engineer part. It does this by creating the ASCII cutter location (CL) data files necessary to be processed into NC machine data. The general procedure is illustrated in Figure 3.7 below.

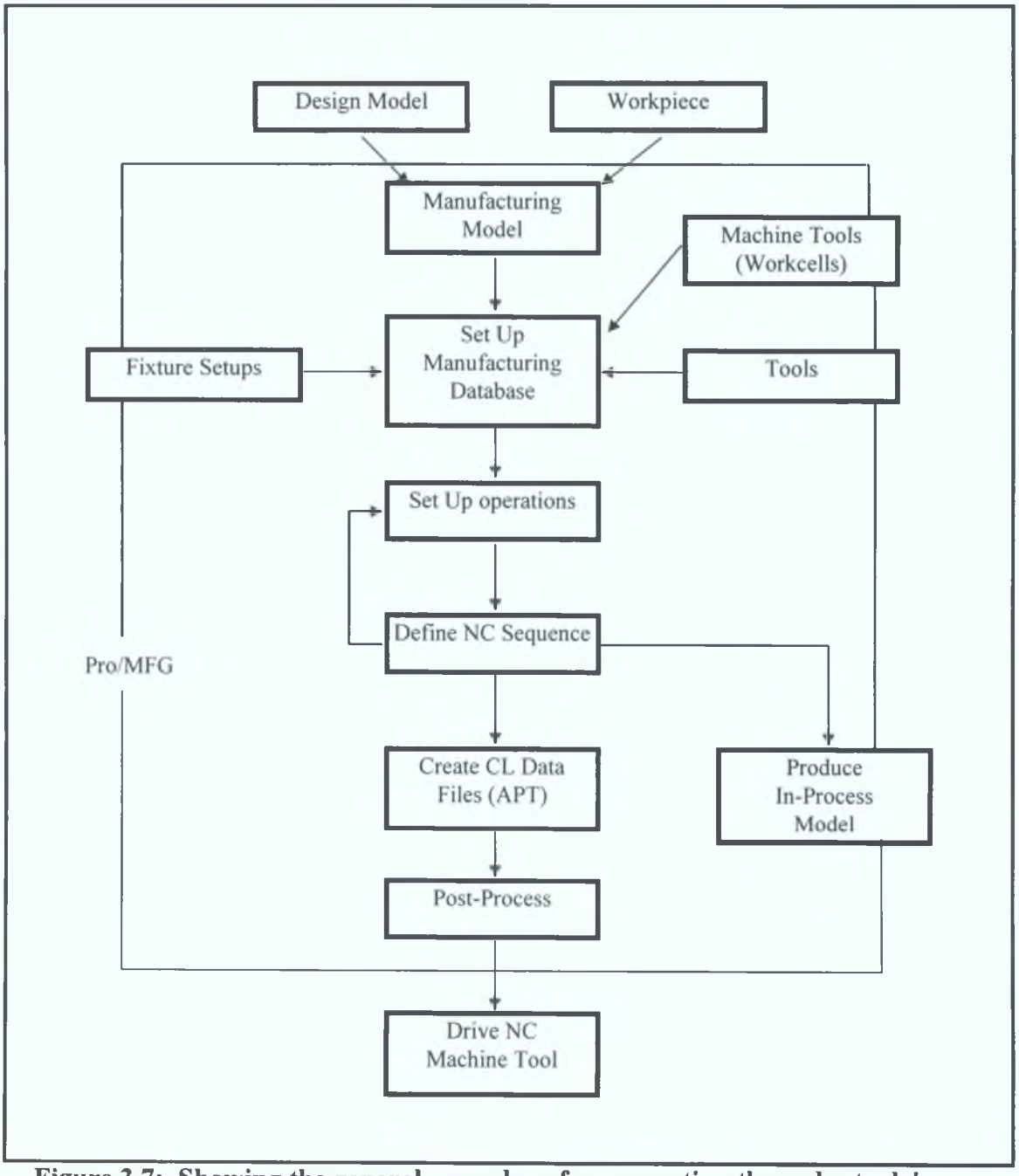

Figure 3.7: Showing the general procedure for generating the codes to drive an NC machine tool.

The steps to manufacturing the mock silicon arteries is as follows

1. Pro-Engineer which is a solid modeller is used to generate the 3-D drawing of the female casts made from aluminium as shown in Figure 3 6(A)
2. This 3-D drawing is then imported into Pro-Manufacturing which is a family of optional modules for Pro-Engineer that provides the tools to simulate computer numerical control of the manufacturing processes needed to manufacture the female cast Pro-Manufacture also creates the data files necessary to generate the CNC codes which can be downloaded to the CNC machine to manufacture the part The sequence of events needed to generate the CNC codes are as follows
    - Create or retrieve the manufacturing model
    - Check units of measurement and time
    - Set-up the manufacturing database
        - Create the workpiece around the manufacturing model
        - Define the operations An operation is a series of NC sequences performed at a particular workpiece and using a particular co-ordinate system to be used as the origin (0,0,0) for cutter location, which is defined for cutter location (CL) data output Pro/MFG NC sequence co-ordinate systems should be oriented so that the positive Z-axis points away from the holding fixtures of the machine How you orient the X-axis and Y-axis will affect the CL data file By default, NC sequences tend to orient themselves in the direction of the X-axis, therefore in milling the cut directions will be parallel to the X-axis Operations must be set up before creating NC sequences The 3 axis milling machine is selected here The various tools used can be defined here also The Bridgeport CNC machine has a maximum of 12 tool holders
        - Define the Machining and NC sequences An NC sequence is a workpiece feature that represents a single tool path such as cut motions which can be defined or automatically generated by the system, depending on which milling option you use such as face, volume, contour surface, profile etc The machining processes and

the tools necessary are selected here The manufacturing parameters such as cut feed, spindle speed etc must be defined for each NC sequence

- Create the retraction plane for each tool You offset the retraction plane a safe distance from the workpiece The same retraction plane can be used for each tool
- Select or create a co-ordinate system to define the orientation of the workpiece on the machine
- For each NC sequence a surface or volume to be machined or drilled must be selected As each NC sequence is being created, you have an option to display and modify the tool paths generated by the system
- The NC check and Playpath will alert you of any problems and display the cutter path and a simulation of the tool and material removal prior to completing the NC sequence You can now verify the tool path and make a visual cheeks for interference with fixtures and model features
- For the manufacturing of the female cast these are the recommended NC sequences that are shown in Figure 3 8
    - Face Mill the top surface of the workpiece using a ∅60mm flat face milling cutter
    - Volume Rough cut the desired shape using a ∅8mm ball nose milling cutter
    - Contour line milling Finish mill the desired shape using a ∅8mm ball nose cutter The contour cut line option will first mimic the shape of the edge or entity specified as the cut line and then gradually change shape as necessary to accommodate different surface topology The direction of the milling cutter passes are shown in Figure 3 8.
    - Holemaking Centre drill the three holes

- Holemaking: Drill the three ∅8mm holes.

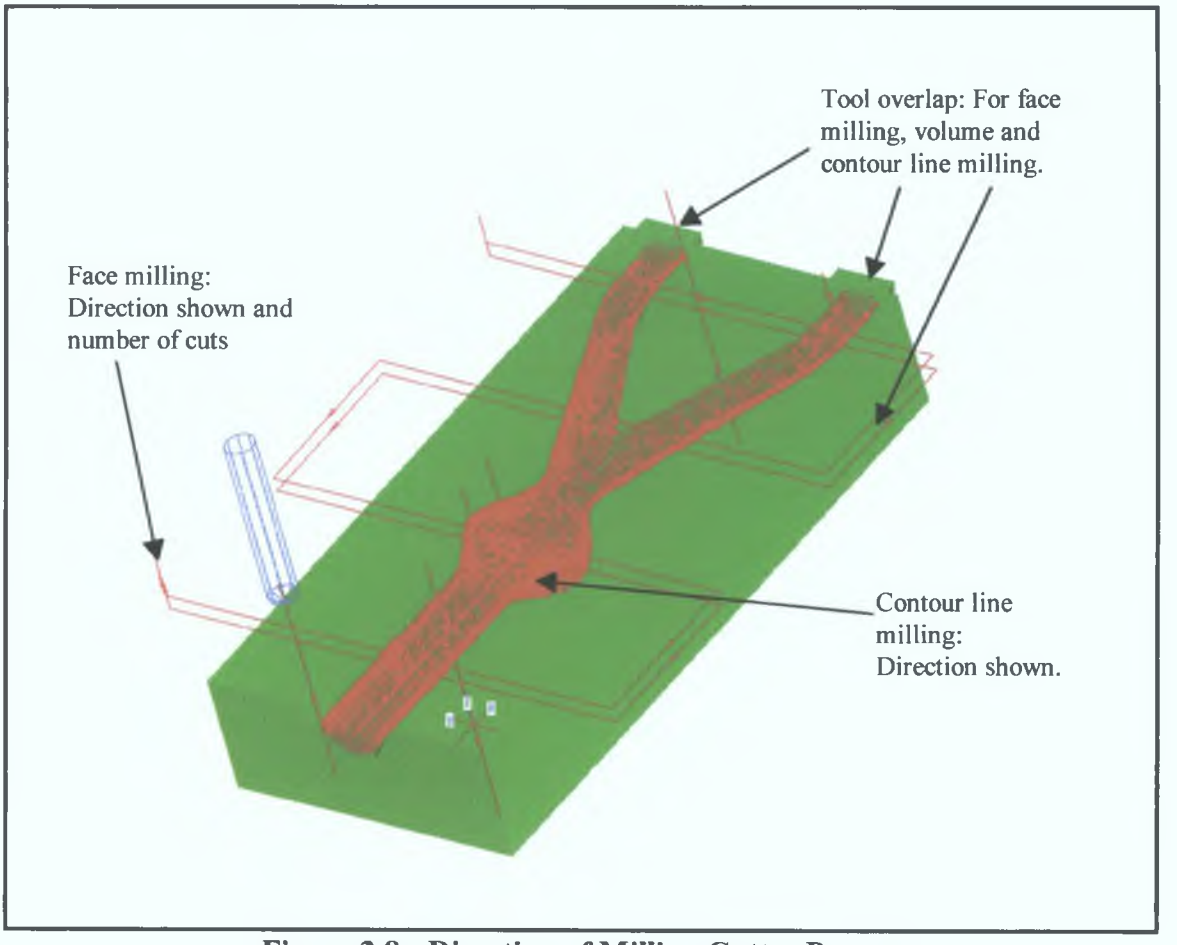

Figure 3.8: Direction of Milling Cutter Passes.

3. Post-Processing. The cutter location (CL) data file is created for the particular operation, which comprises of all the NC sequences. Pro/MFG generates the cutter location (CL) data files in an ASCII format that needs to be post-processed to create machine control data (MCD) files before any machining operations occurs. NC post-processors can be developed using the optional module Pro/NC POST. A full representation of a NC machine and its controller are created using the QUEST facility. QUEST stores this information in a database, which can be used by GENER. GENER uses this information about the NC machine to convert the points and vectors of a cutter location (CL) file into the joint location and machine codes of the NC

machine. This file generates the g-code file that is necessary to operate the Bridgeport Interact 412 3-axis milling machine. Figure 3.9 shows the verbose window that contains some general statistics of the GENER process as well as the APT Input and the NC control code output. This MCD file can now be downloaded to the Bridgeport milling machine, thus creating the female casts.

Figure 3.9: Verbose window.

3.4.2 Creating the Male Wax Models.

1. Clean the surface of the female casts and make sure it is free of loose material
2. Blot the two female casts together
3. Wax is then heated and poured into the female casts
4. The wax is then left to cool and harden for one hour
5. Open female casts and you can remove the wax model

3.4.3 Creating the Silicon Models.

1. The silicon rubber used is SILASTIC T-4 supplied by Dow Corning which is a high strength transparent rubber SILASTIC T-4 is a two component material consisting of SILASTIC T-4 Base, which is mixed with SILASTIC T-4 O Curing Agent, which cures at room temperature
2. Weigh 100 parts of SILASTIC T-4 Base and 10 parts of Curing Agent in a clean container
3. Mix the two together until the curing agent is completely dispersed in the base Hand or mechanical mixing can be used, but do not mix for an extended period of time or allow the temperature to exceed 35°C The working time at 23°C is 90 minutes Mix sufficiently small quantities to ensure thorough mixing of base and curing agent Air entrapment is minimised when mixing small quantities
4. Clean the surface of the wax model
5. Paint an even layer of the mixed base and curing agent onto the wax model using a brush
6. Allow 12 hours for the silicon layer to cure at room temperature (22-24°C) Heat acceleration the cure is possible but not recommended as you could melt the wax model
7. Every 12 hours keep painting an extra layer of the mixed base and curing agent until sufficient thickness is achieved It usually takes 15 to 20 coats to achieve a thickness of 1 5 to 2 mm
8. When sufficient thickness is achieved the wax can be melted away using boiling water, leaving you with the silicon mock artery as shown in figure 3.6(C).

3.4.4 Comparison of Model Aneurysm to Aortic Aneurysm

A comparison of our model aneurysm is given in Table 3 2 with typical sizes of AAA

	Range for Patients	**Model Aneurysm**
Proximal Aortic Neck diameter	22mm – 36 mm [16]	28mm
Aneurysm Max diameter	40mm to 75mm [4]	50mm
Aneurysm length	can vary up to 60 to 90mm[4]	55mm
Proximal Aortic Neck length	15mm (min value for stent placement) to 35mm [17]	Can vary position of Renal Arteries
Angle at bifurcation	Can vary considerable from 5° to 90° with sometimes a lot of tortuosity in Iliac artery [3,4]	30°
Iliac diameter	10mm – 20mm [16]	20mm
Wall thickness	1 1mm diastole 0 9mm systole [8]	1 5mm
Radical compliance	5% - 7% [8]	5% - 10%

Table 3.2 Comparison between model aneurysm and range for patients.

3.5: Simulation of the Pulsatile Pressure in the Aorta.

To keep the Aorta pressurised similar to that in the body A pressure valve will be positioned after the aortic bifurcation capable of varying the pressure This can be achieved by compressing or deflecting a spring connected to a plate (which can be of any type such as a ball, flat, plug, slurry etc) which is fitted on a seat It is by twisting a second plate in or out that is used to adjust the deflection of the spring and hence increase or decrease the pressure required to push the plate and therefore open the valve Figure 3 10 shows the principal of the operation

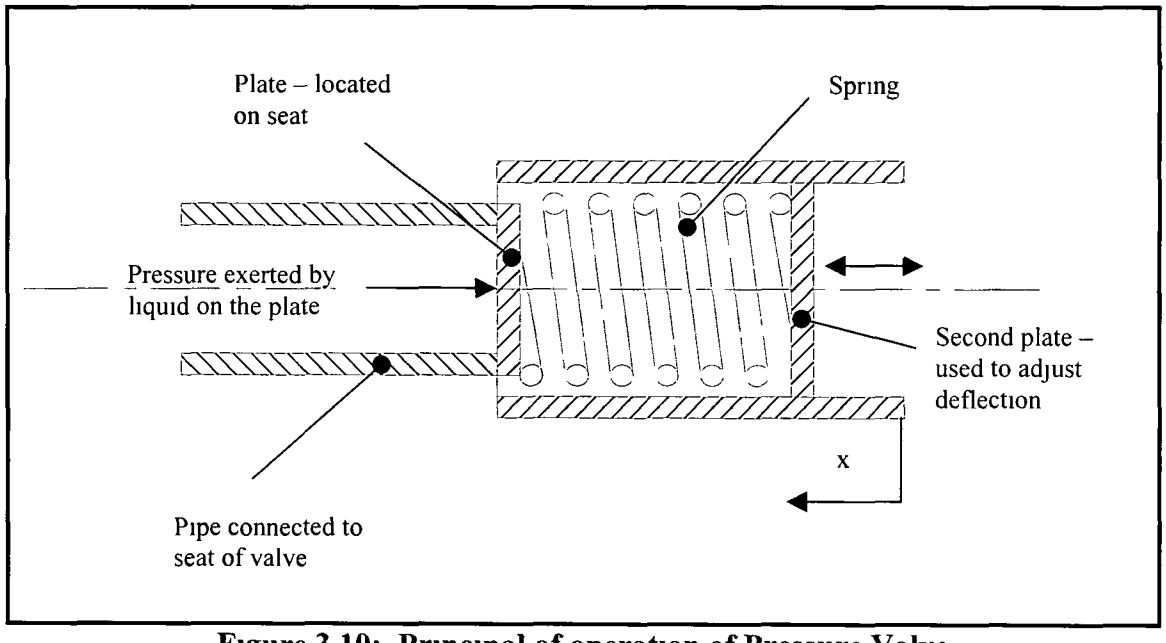

Figure 3.10: Principal of operation of Pressure Valve

Table 3 3 shows the force needed to compress the spring in the x direction and hence we are able to calculate the pressure needed to open the plate of the valve for whatever deflection you apply by the second plate These results were obtained experimentally, by place placing known weights on the conical spring and measuring the deflection of the spring

Force(N)	Compression(mm)	Pressure(N/m^2)
0	0	0
0 14715	0 5	2927 456234
0 2943	1 2	5854 912469
0 4905	3 2	9758 187448
0 5886	3 9	11709 82494
0 6867	4 35	13661 46243
0 7848	4 75	15613 09992
0 981	6 1	19516 3749
1 4715	8 7	29274 56234
1 962	11 1	39032 74979
2 4525	13 15	48790 93724
2 943	15 3	58549 12469

Table 3.3. Showing the compression necessary to adjust Pressure.

To measure the pressure we use the following simple relationship,

$$\text{Pressure} = P = \frac{Force}{Cross-sectional-area-of-seat} = \frac{4F}{\pi d^2}$$

Where d= diameter of seat is 8mm

Figure 3 11 shows the graph of pressure verses compression

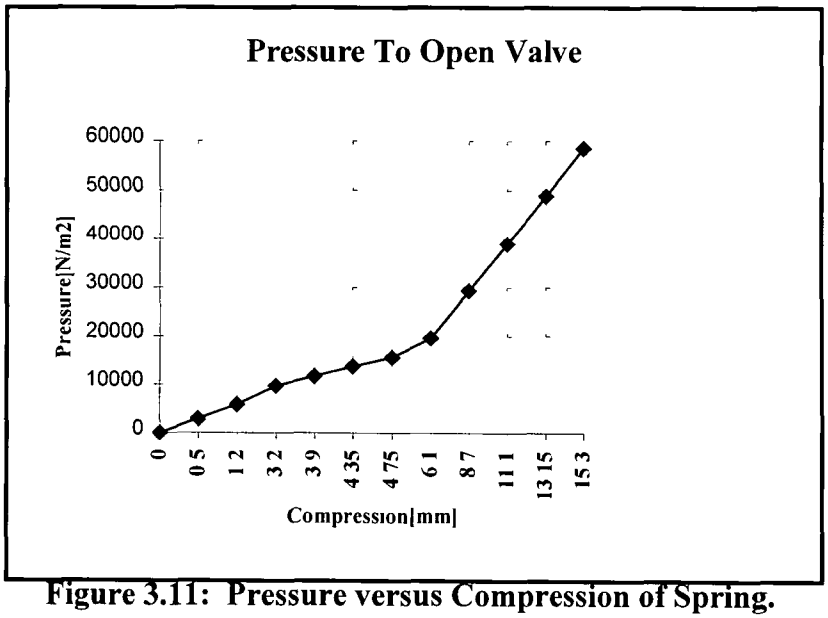

Figure 3.11: Pressure versus Compression of Spring.

This is a typical curve expected for a conical spring We are only interested in three values that is the normal blood pressure which is 16,000N/m^2 which corresponds to 120mmHg As shown in figure 2 6(B), as you get older your blood pressure increases to 150mmHg which is 20,000N/m^2 The reduced blood pressure during the endovascular procedure is 9340N/m^2 which corresponds to 70mmHg So to find the deflection which corresponds to these values we will find the spring stiffness of the conical spring As you will probably notice that the slope of the curve is approximately linear between 0N/ m^2 and 20000N/ m^2 which is within our range of the blood pressure needed So to find the slope or spring stiffness of the curve for this range we interpolate two points that are on this straight line and calculate the slope using the following formula,

$$\text{Spring stiffness} = k = \frac{19516\,4 - 0\,0}{0\,0061 - 0\,0} = 163\,9\frac{N}{m}$$

$$\text{So force needed to open valve } F = \frac{\pi d^2 P}{4} = kx$$

Where F = force in Newtons

P = pressure in N/m^2

d = diameter of seat = 8mm = 0 008m

x = deflection of deformation of spring in meters

k = spring stiffness = 163 9N/m

$$\text{So deflection needed} = x = \frac{\pi d^2 P}{4k}$$

So for 150mmHg or 20000N/ m^2 of pressure, deflection needed x = 6 13mm

So for 120mmHg or 16000N/m^2 of pressure, deflection needed x = 4 91mm

So for 70mmHg or 9340N/m^2 of pressure, deflection needed x = 2 86mm

3.6. The Blood.

As we will probably use water to test the delivery system, we should compare the characteristics of blood with the ones of water so that we are in a better position to evaluate our design Table 3 4 shows a comparison between water and blood

	Water	**Blood**
Incompressible	✓	✓
Specific gravity	1	1 055 to 1 065
Viscosity	0 01 $g \times s^{-1} \times cm^{-1}$	0 04 $g \times s^{-1} \times cm^{-1}$

Table 3.4: Comparison between water and blood.[8,10]

So, blood is a fluid very close to water Only the viscosity differs but this difference is an advantage for the design of the test system and especially for the working of the delivery system

As a conclusion, we can say that the approximation of the calculation where we use water instead of blood will be precise and safe enough

3.7 Modeling of the Systemic Circuitry.

Here all the parts are connected together so that the test can be carried out as shown in Figure 3.12.

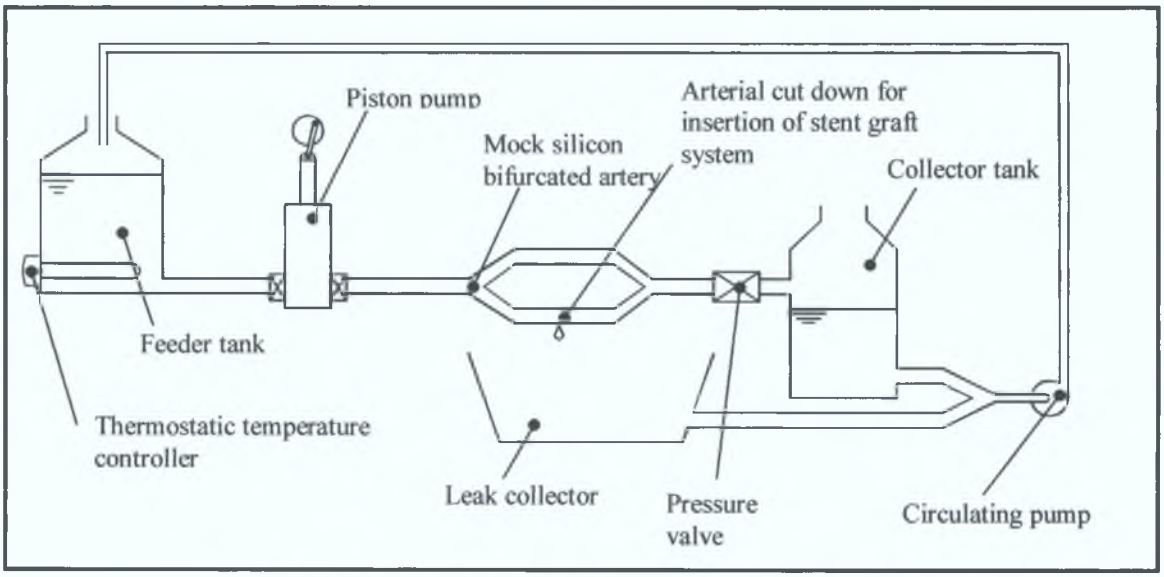

Figure 3.12: Description of the test system.

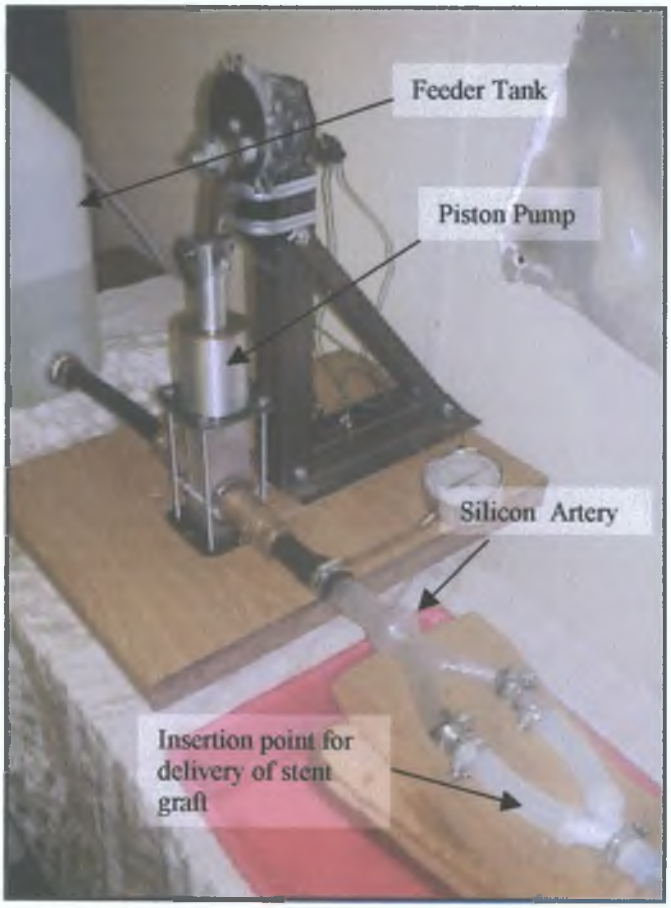

Figure 3.13: Manufactured Bench Test

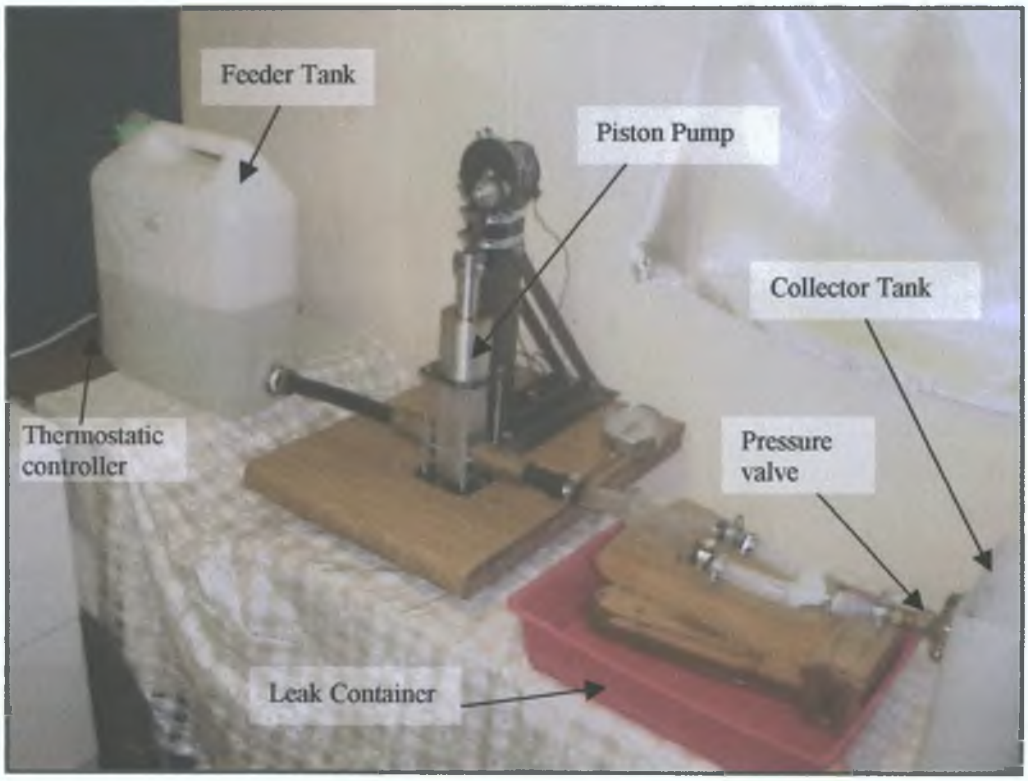

Figure 3.14: Manufactured Bench Test.

3.7.1 Description of the Test System Circuit.

As can be seen in Figure 3.12, 3.13 & 3.14, the piston pump is fed by the feeder tank. An important requirement that should be spotted here is the output of this reservoir, this is limited to the pipe connecting it to the suction manifold of the main pump. The pipe must therefore be wide enough to allow a good filling of the main pump during the suction stroke. Indeed, if the inside diameter of these components is too small, then the feeding flow of liquid won't be sufficient, because the inertia of the liquid (starting from rest in the tank) limits the average velocity of this flow.

Directly after the piston pump, the flow of liquid is now pulsating through the mock silicon artery.

This artificial bifurcated artery is held in place above a basin: the leak collector. As the name tells it, this basin is used to collect the liquid that will inexorably leak out of the bifurcation during the manipulation of the stent graft delivery system.

The pressure valve as mentioned before is placed after the artificial bifurcation This is needed to keep the mock silicon artery pressurised

All the liquid coming from the piston pump output is either collected in the collector tank or leak collector and connections are then made via a Y-piece to the circulating pump

The building of the test system circuitry could be stopped right here, the main pump feeder tank being refilled by a tap connected to the water mains and the main collector tank being discharged into a sink But if the liquid used for the graft stent delivery tests is water improved with some additives, then the circuitry should include a recycling loop for the flowing liquid This task is completed by a circulating pump that pumps the liquid from the main collector tank to the main pump feeder tank The great advantage of a circulating pump is that you don't need to adjust its capacity according to the input flow It is automatically regulated

3.8. Conclusion.

Designing a bench test that is capable of replicating the cardiovascular system and the disease in question Aortic Aneurysms at the iliac bifurcation are a prerequisite for adequate testing of the stent graft system Simulating the pulsatile flow of the heart was achieved by a piston pump The advantage of a piston pump is that the kinematics of the pump has been designed to give the same stroke volume, pulse rate (rpm) and fluid velocity as given in the Abdominal aorta (see table 3 1) Mock abdominal Mock abdominal aortic aneurysms at the iliac bifurcation were replicated using transparent silicon rubber by the lost wax process with the aid of CNC technology, which could be designed to the same geometry and compliance of typical abdominal aortic aneurysms (see table 3 2) To keep the aorta pressurised similar to that in the body A pressure valve is positioned after the mock silicon artery The pressure can be varied by compressing or deflecting a spring connected to a plate that is fitted on a seat inside the pressure valve A recycling loop is achieved by the test system circuitry This bench test is capable of testing the durability and delivery of the stent graft for the first stage of testing

Chapter 4

Attachment System

4.0 Attachment Systems.

4.1 Introduction.

Attachment systems are used to fix a prosthetic vascular graft in position across the aneurysm sac from within using expandable metal stents Thus excluding the aneurysm from the circulation and therefore preventing rupture This chapter is concerned with the issues involved for the attachment system such as stent types, biocompatibility, mechanical characteristics, types of stents available etc

4.2 Characteristics of Stents.

Stents are round, spring like devices with a mesh structure that provides a mechanical support for the graft against the wall of the artery This is achieved by producing a radical force onto the arterial wall Stents are relatively rigid structures made of steel, which are delivered in a compact form to a desired vessel Stents have an open lattice configuration to allow the endothelium (a layer of flat cells, which lines the blood vessels) to spread and eventually cover the stent This is one of the reasons that the stent has so much open surface without compromising the structural integrity of the stent The open wall configuration also keeps the thrombogenicity of the metal surface at a minimum [18] Some of the main characteristics are as follows

1. ***High Expandability:*** a high expandability ratio is desirable i e , a small device can expand to a large diameter
2. ***Minimal Foreign Body Content:*** a well designed stent should minimise surface area and wall thickness in order to diminish the ratio of thrombus deposition
3. ***High Tensile Strength:*** the stent must possess an outward force greater than the imposed hoop stress caused by the vessel wall Over expansion has been related to intimal hyperplasia and thrombosis (compliance mismatch) Longitudinal flexible is also critical for tortuous vessels Improper bedding of the stent will cause thrombus to be deposited in a continuous layer over the entire stent

4. ***Radiopacity:*** placement must be confirmed and rechecked periodically by non-invasive and inexpensive means [18,19].

4.3 Biocompatablity of Stent Materials:

The first issue in selecting a stent material is the biocompatability of the material. All stent materials must be rigorously tested to prove their patency and use in the body.

Vascular stents are more or less embedded into the vessel wall at the time of deployment. This endovascular manipulations during stent placement causes unavoidable endothelial damage. This exposes subendothelial tissues, which are thrombogenic, to the bloodstream. The result is activation of the coagulation system and concurrent thrombus formation. The biological effects of metallic stents, which influences stent thrombogenicity are as follows:

1. ***Surface texture*** - the smoother the stent the less thrombogenic it is, and vice versa.
2. ***Electrical surface charge*** - Intravascular surfaces (endothelium) usually have an electronegative charge, as is also true for cells and proteins in the blood. Because of their similar charge, repelling forces exist that keep blood cells and proteins away form the endothelium to a certain degree. Most metals and alloys used for stents have a positive surface charge. When exposed to blood, they do not repel but attract negatively charged proteins and cells, causing thromboses
3. ***Free surface energy:*** This is another physicochemical property influencing the biological behaviour of stents. It is related to unsatisfied intermolecular bonds at the material surface, and largely determines how well a fluid is spread over the material (its 'wetability'). It may be measured as critical surface tension (in dyne/cm). If this is above 20-30 dyne/cm the material is thrombogenic [20].
4. ***Surface Characteristics:*** The finishing process during manufacturing has a direct effect on the biocompatability of the device. Electropolishing which is used on the 300-series stainless steels, removes most of the elements from the surface of the metal and leaves a high concentration of chromium. Once the stent has been exposed to air and sterilisation, a layer of chromium oxide forms [18].

5. ***Degree of stent expansion:*** With ideal expansion, the metal struts of a stent should be pressed into the vessel wall Next to the struts, depressions in the vascular wall result These will fill with thrombus, covering the corresponding stent surface In between the struts, tissue moulds protrude towards the vessel lumen If these retain their endothelium, this can be the origin of multicentre re-endothelialezation [20]

4.4 Stent Materials.

The biocompatability and general characteristics of the stent materials are important Some stents are balloon dilated and others are self-expanding Table 4 1 gives a summary of the stent materials available and the method of expansion

Material	**Delivery/Expansion method**
316L stainless steel	Balloon
304 stainless steel	Balloon
Nitinol (nickel & titanium)	Self (shape memory effect)
Nitinol (nickel & titanium)	Self (superelastic effect)
Tantalum	Balloon
Eligiloy (cobalt-based alloy)	Self
Platinum/iridium	Balloon

Table 4.1 Summary of Stent Material & Corresponding Delivery Method

(Adapted from Pepine et al ref21)

Here is a summary of the materials available

4.4.1 Stainless steel is a highly thrombogenic material due to the release of mainly nickel and chromium ions It is well known from literature that the stainless steel 316 L used as implants release free chromium and nickel ions which are able to destroy or damage enzymes and proteins Furthermore it is known that these chromium and nickel ions can aggravate allergies Some type of surface coating is necessary to set up a barrier against the heavy metal ions diffusion of nickel and chromium ions into the surrounding tissue and the blood stream The diamond-like coated surface of the Phytis

stent is an example of such a coating [22] Other methods of reducing thrombosis is to use polymer-coated stents which are impregnated with drugs Platelet-targeted fibrinolytic agents can be passively bound to polymer-coated stents and are well retained even after prolonged continuous perfusion These agents may thus reduce stent-related thrombosis and require further *in vivo* evaluation [23]

4.4.2 Platinum has been used in human implants over a long period of time and is known to be extremely biocompatible In fact platinum is one of the least thrombogenic metals known Platinum is a flexible metal and can be used in tortuous arteries It is also radiopaque [24]

4.4.3 Nitinol alloys contain more nickel than stainless steel However, Nitinol is an intermetallic compound and not an alloy in the metallurgical sense, the bonding force of nickel to titanium is much stronger in Nitinol than to the alloy components in stainless steel As Nitinol oxidises after proper surface treatment, if forms a TiO2 layer with no nickel present at the surface making Nitinol very biocompatible and with high corrosion resistance Polarisation testing in Hank's solution has repeatedly shown that Nitinol is chemically more stable and less corrosive than stainless steel Nitinol produces a fluoroscopic image that is comparable to stainless steel Nitinol's extraordinary compliance makes it the most mechanically similar to biologic materials unlike stainless steel and titanium, which are very strong and stiff Self-expanding Nitinol stents will always expand to their pre-set diameters with no recoil (spring back) Nitinol stents will grow with the vessel and adapt to the shape more than the plastically deformed stainless steel devices Thus exerting a more favourable effect on vascular remodelling with less neointimal formation than a balloon expandable designs Small Nitinol wires and tubes will pass through tortuous paths in the body and remain straight and torqueable [25]

4.5 Stent Designs.

The suitability of a specific stent for fixing an aortic graft in position depends on a number of factors relating to the aorta and the stent graft, the shape and size of the proximal neck, the construction of the aortic wall, the presence of thrombus, the shape and size of the stent graft, the area of the stent-graft in contact with the aortic wall, the flexibility or resistance to radical force, the ability of the stent to provide a radial spring force and any other specific features such as hooks or barbs, balloon or self-expanding stents [26,27] These features are different for each type of stent The combined effect of all these individual variables can be compared to assess the security of fixation for each type of stent This can be simply done by measuring the distraction forces required to dislodge stents of comparable sizes from aorta of a specific internal diameter [26]

Numerous *in vitro* experiments have been done in this area, to assess the fixation strength of commercial available stents, with or without hooks and barbs and the longitudinal force required to dislodge a stent when variables such as aortic diameter, aneurysm neck length and degree of mural calcification are taken into account

The results of these experiments can be analysed and compared and this should give us a good indication of the characteristics involved in stent design from the point of view of *in vitro* experiments that would otherwise be unattainable and possibly overlooked

4.6 Longitudinal Force Required to Dislodge the Stent.

4.6.1 Commercially available stents:

S M Andrews et al analysed five commercially available stent designs that were dimensional suitable for aortic stenting in abattoir acquired porcine aortas Figure 4 1 shows the various types of stents that are available and they investigated the suitability of these stents for endovascular graft fixation [26]

Figure 4.1a Gianturco-Z stent

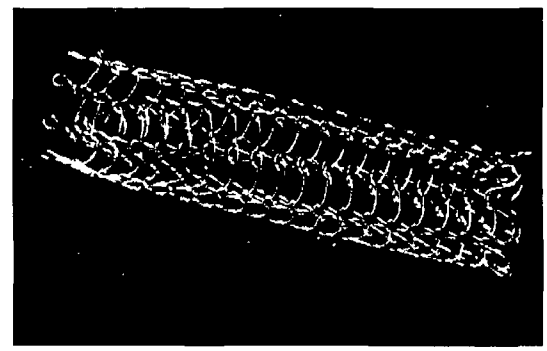

Figure 4.2b Strecker stent

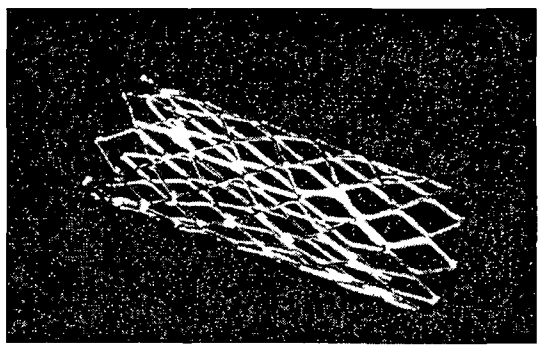

Figure 4.1c Palmaz stent

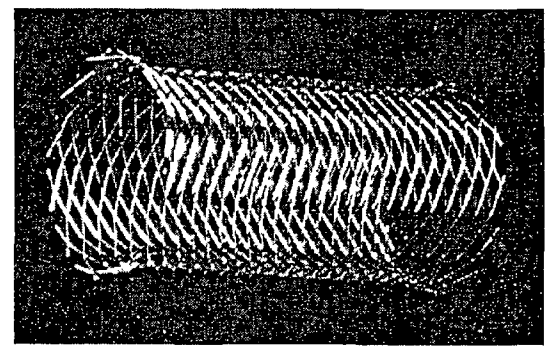

Figure 4.1d Wallstent

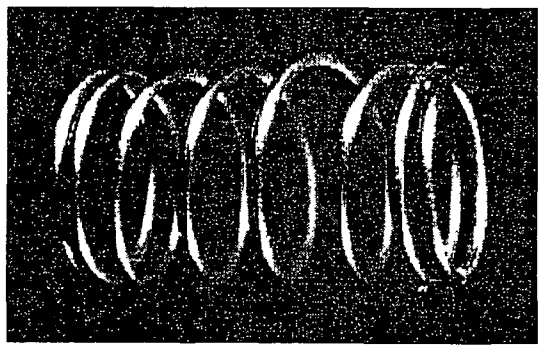

Figure 4.1d Nitinol coil

A summary of the stent shown in Figure 4-1 are:

Gianturco-Z stent: A self-expanding stainless steel stent.

Strecker stent: A flexible, balloon-expandable, fine tantalum knit stent.

Palmaz stent: Balloon-expandable mesh consisting of crossed stainless-steel struts.

Wallstent: A flexible, self-expandable mesh consisting of fine interwoven, stainless-steel struts.

Nitinol coil: Uses the shape memory effect of Nitinol so that it can be introduced as a single diameter wire and will transform into a rigid coiled shape stent.

Two simple *in vitro* experiments were performed on each type of stent.

1. A tensiometer was used to measure the distraction force necessary to dislodge the stent by more than 5mm.
2. A pulsatile flow circuit of 60 beats/min with a systolic pressure of 100mmHg was used to see the flow rate required to cause migration of the stent graft by more than 5mm. The stent graft comprised of a stent sutured to a 30mm long 10mm external diameter thin walled PTFE graft. The stent just overlapped the inside of the graft.

For standardising the experiments each type of stent was designed to expand to an external diameter of 11mm and each stent was introduced into lengths of abattoir-acquired porcine aorta with an internal diameter of 10mm [26].

Table 4.2 shows the values of the results.

Stent Type	**Ex1: Mean distraction force(N)**	**Ex2: Flow rate**
Palmaz stent.	2.13	> 8 l/min
Gianturco-Z	1.75	> 8 l/min
Wallstent	0.29	mean 2.9 l/min
Nitinol coil	2.55	> 8 l/min
Strecker stent	Force could not be measured	Flow rate could not be measured

Table 4.2 ***(Adapted from Andrews et al ref26)***

4.6.2 Comparison of the effects of adding hooks and barbs.

Malina et al tested stents in human cadaver aortas with and without hooks and bards Longitudinal traction then was applied to the distal end of the grafts and measured by a tensiometer The traction was increased gradually by steps of 0 5N until the stent-grafts were dislodged from the aorta These tests used dacron grafts with diameters of 16, 20, and 24mm that were sutured to self-expandable Gianturco Z-stents with a few millimetres of the stents protruding from the grafts proximally The stents were 2 5 cm long and 4 5 cm wide in their uncompressed state and consisted of 10 bends of stainless steel wire [28]

Four different modifications of the Gianturco stents were examined

1. Smooth stents without any anchoring appendages
2. Stents equipped with 4 weak hooks and barbs (5mm long and 0 25 mm thick)
3. Stents with 8 stronger hooks and barbs (10mm long and 0 3mm thick)
4. 8 reinforced hooks but no barbs

All barbs protruded out from the graft at an angle of about 30°

Stent Type:	Mean force required to dislodge stent
Smooth stent	2 5 N (IQR 2 0 to 3 4 N)
4 weak hooks and barbs	7 8 N (IQR 7 4 to 10 8 N)
8 strong hooks and barbs	22 5 N (IQR 17 1 to 27 9 N)
8 strong hooks and no barbs	11 8 N (IQR 10 4 to 13 0 N)

Table 4.3. Force required to dislodge the Z-stents with the different modifications from cadaveric aortas. IQR stands for interquartile range. ***(Adapted from Malina et al ref28)***

4.6.3 Comparison of the effects of arterial characteristics.

A W Lambert et al investigated a stent-graft comprising a 9cm long, 24mm diameter shape memory alloy nitinol stent inside a dacron graft The longitudinal force required to cause migration of the stent-graft from human cadaveric infrarenal aortas was measured The aim of this analyses was to determine which of the measured explanatory variables, aortic diameter, degree of calcification, aneurysm neck length affect the load needed to remove the deployed stent-graft from the test aorta The statistical technique used in selection of the model and significant effects was an analysis of variance (ANOVA) The results show that the aneurysm neck length was highly significant (p<0 00001) The aortic diameter effect and the calcification was significant with p values of 0 002 and 0 047 respective [27]

Loads were then applied to produce a dislodgement of the aortic/ stent-graft interface by 5 mm The aneurysm neck length used were 20mm, 15mm and 10mm Also the internal diameter of the "neck" was measured Table 4 4 shows the results of the mean pull required depending on the neck length and aortic diameter [27]

Category	**Mean Pull (N)**	**Source**	**Test statistic (g)**	***p* value**
Neck length (mm)		Aortic diameter	9 92	0 002
10	2 2 (1 2-3 3)	Aortic calcification	3 34	0 047
15	2 8 (1 4-4 1)	"Aneurysm neck" length	207 47	<0 00001
20	4 2 (2 0-4 8)			
Aortic diameter				
<20	3 3			
>20	3 0			

Table 4.4: Results showing mean pull required to dislodge stent depending on the neck length and aortic diameter. ***(Adapted from Lambert et al ref27)***

4.7 Comparison of Stent Designs.

- As demonstrated by *Andrews et al* the Wallstent has an inferior resistance to distraction compared to the Palmaz, Nitinol coil and Gianturco-Z stent. This can be attributed to the flexibility of the stent, which allows less resistance to the radical forces, which are reduced as tension is placed on the stent. A more physiological model, as provided by the second experiment demonstrated that the Nitinol coils, Gianturco-Z stents and the Palmaz stents all have fixation characteristics such that they resist migration at high flow rates, when used to hold endovascular grafts in porcine aorta *in vitro.* The Strecker stent could not be assessed, as it was not possible to attach the graft without deforming the fine tantalum strands and thus precludes its use for the fixation of endovascular grafts.
- *Malina et al* showed that hooks and barbs are capable of improving the fixation of endovascular grafts tenfold as shown by their experiments. Both the hooks and barbs improved attachment. Short hooks and barbs (5mm) engaged the thickened aortic intima only; the fragility of the intima then seemed to limit the force required to displace the stents. Therefore, the stents with longer and stronger barbs, which penetrated the entire aortic wall, provided a firmer fixation. Rather than being pushed into the aortic wall by the radial force of the stent, the hooks and barbs engage the aortic wall when the stent-graft is pulled distally by the bloodstream. The angle between the stent and its hooks and barbs is important for this action. Oversizing the graft diameter increased slightly the displacement force but only for stents without hooks and barbs. Stents with hooks and barbs retained their strength of fixation even when the grafts were undersized by 1 to 2mm. Smooth stents had marginally stronger fixation in increasingly atherosclerotic aortas, while the displacement force for stents with hooks and barbs was unaffected by the aortic calcification.
- *A.W Lambert et al* showed that the most significant factor was found to be the length of the aneurysm neck in all analyses. It was to be expected that the longer the aneurysm neck, the greater would be the weight required to produce migration. It is of relevance that even with only 10mm neck length, a mean weight of 215g was required to produce migration of the stent-graft and this is comparable with the

results obtained for the Palmaz, Gianturco and Nitinol coil stents as described by *Andrews et al.* The predictive effect of the degree of calcification and aortic diameter was less obvious and it would appear from these experiments to have only a small effect and should be viewed cautiously.

4.8 Problems with stent design.

- Attempts to improve endovascular graft anchoring by excessive oversizing of smooth stents might be futile, especially because stents may cause pressure ulcers and perforations of the vessel walls [28].
- The dangers of hooks and barbs that pierce the aortic wall is that they might penetrate to juxta-aortic structures, such as the duodenum and the renal vein and the long term risks have not been assessed.
- Placing additional hooks and barbs on each stent will increase the volume of the devices and make them more difficult to introduce through slim sheaths [28].
- Due to the stiffness of metallic stents, the mechanical properties of the vessel at the implantation site are greatly influenced, thus reducing the pulsatile diameter of the stented vessel and causing greater pressure wave reflections and pulsatile mechanical stress at the interface between the stented and non-stented portion [28].

4.9 Stent Material Characteristics.

As mentioned previously, one of the main problems is the influence of the stent on the pulsatile diameter of the host vessel. Self-expanding stents reduces most of the risk of this problem as compared to balloon expandable stents. Balloon expandable stents have to be over-expanded to achieve a certain diameter (because of plastic recoil after balloon deflation), unlike self-expanding stents which always expand to their present diameters with no recoil (spring back) and will continue to push outward on the vessel after deployment. Should the vessel grow in diameter or if the shape is slightly oblong or irregular to begin with, these stents will grow with the vessel and adapt to the shape more than the plastically deformed stents. One of the best self-expanding stent

materials are shape memory alloys, also known as Nitinol and has the following advantages over other stent materials [25]

1. Device materials such as stainless steel and titanium are very strong and stiff, yielding little in response to pressure from surrounding tissue Nitinol's extraordinary compliance makes it the most mechanically similar to biologic materials
2. NiTi alloys have a shape memory strain of up to 8% Nitinol's increased elasticity allows it to be bent more significantly than stainless steel without taking a set Small Nitinol wires and tubes will pass through tortuous paths in the body and remain straight and torqueable
3. Nitinol's elasticity or "springback" is some 10 times greater than stainless steel This allows for the design of formed components and devices that can be held in a delivery system then return to the original shape when deployed
4. Excellent corrosion resistance [25]
5. It can be shown that the spring rate of stainless steel is approximately twice that of NiTi alloys and NiTi would produce a lower and more continuous force on the artery than would stainless stain [25,29]
6. Shape memory alloys is repeatable and the shape memory effect can be used in cyclic devices where it must exhibit the shape recovery many times [30]
7. Nitinol produces a fluoroscopic image that is comparable to stainless steel [29]
8. Wire drawing is probably the most widely used of the techniques, and excellent surface properties and sizes as small as 0 05mm (0 002in) are made routinely [31]
9. The materials respond well to abrasive removal, such as grinding, and shearing or punching can be done if thicknesses are kept small [30]

Before we go any further a brief summary of shape memory alloys is presented next It is important to get an appreciation of these materials and their amazing characteristics Due to the ease of forming these materials into any shape, we will use Nitinol for out stent design as described in chapter 6

4.9.1 Shape Memory Alloys.

Shape Memory Alloys (SMA's) are novel materials, which have the ability to return to a predetermined shape when heated The first SMA to be discovered was Nitinol The name Nitinol comes from the chemical symbol of its two components metals nickel (Ni) and titanium (Ti) and the laboratory where it was discovered, Naval Ordinance Laboratory (NOL) [32] When a SMA is cold, or below its transformation temperature, it has a very low yield strength and can be deformed quite easily into any new shape which it will retain However, when the material is heated above its transformation temperature it undergoes a change in crystal structure, which causes it to return to its original shape If the SMA encounters any resistance during this transformation, it can generate large forces [33,34]

The key to the shape memory effect is a change in the crystalline structure of the material as they are cooled or heated through their characteristic transformation temperature Above its transition temperature it is an ordered cubic structure known as Austenite (which exists at higher temperatures) Below the transition temperature it is in a monoclinic phase called Martensite (which exists at lower temperatures) The martensite is easily deformed to several percent strain at quite a low stress, whereas the austenite (high temperature phase) has much higher yield and flow stresses as shown in Figure 4 2 When the material is tested slightly above its transformation temperature, martensite can stress-induced It then immediately strains and exhibits the increasing strain at constant stress level Upon unloading, the material reverts to austenite at a lower stress and the shape recover occurs, not upon the application of heat but upon a reduction of stress This effect, which causes the material to be extremely elastic, is known as pseudoelasticity

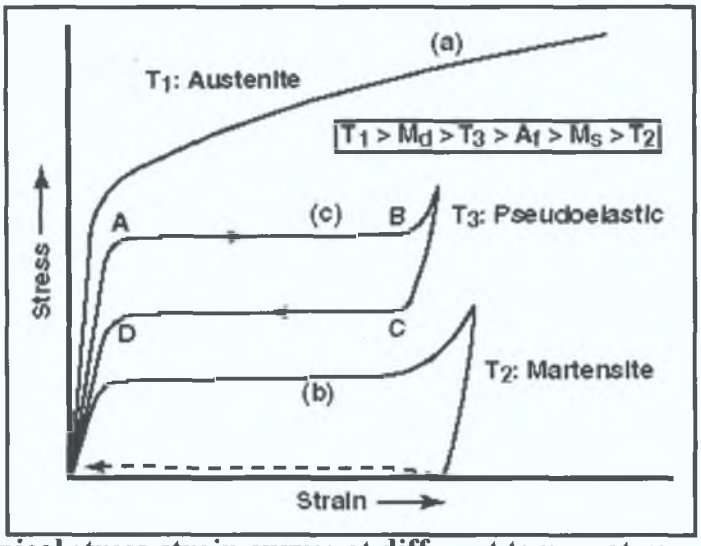

Figure 4.2 Typical stress-strain curves at different temperatures relative to the transformation. ***(ref36)***

The crystals in the monoclinic phase are tilted in opposing bands so that the structure appears as a "squashed" cubic structure. When it is deformed, the material does not act like a normal metal, rather than deform through dislocation movement, the crystal bands bend and align themselves in one direction or the other. When the crystalline structure is heated beyond its transition temperature the "squashed" monoclinic crystals expand back into the ordered cubic state, thereby reversing any deformation done in the martensitic state. The changes in the crystal form and the resulting shape changes are shown in a simplified form in Figure 4.3 [35,36].

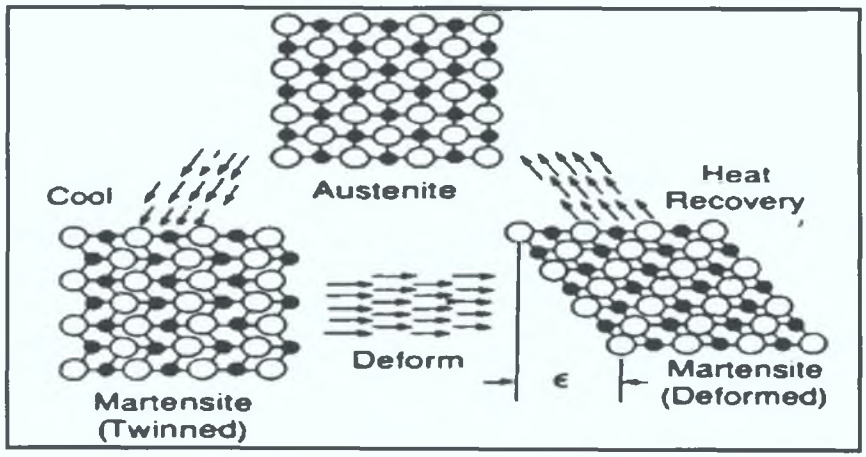

Figure 4.3: Representation of the changes in the crystal form of shape memory alloys which lead to the shape memory effect. ***(Adapted from Hodgson ref30)***

The properties of the NiTi alloys, particularly, indicate their probable greater use in biomedical applications. The material is extremely corrosion resistant, demonstrates excellent biocompatibility, can be fabricated into the very small sizes and has properties of elasticity and force delivery that allows uses not possible any other way [31].

4.9.2 Alloy and Transformation Temperature.

Adjustments in ratio of the two elements nickel and titanium can make a large difference in the properties of the NiTi alloy, particularly its transformation temperatures. The temperature most frequently specified for the finished product is the Active Austenite Finish (Active A_f) Temperature, which is generally determined by a bend free recovery test. Typical tolerances are +/- 3 to 5°C. For superelastic materials the Active A_f must be below the use temperature of the material.

The choice of alloy depends upon the requirements of the application. Most applications are designed to take advantage of either the shape memory effect or the superelastic effect. A sampling of the different categories of alloys available from SMA and is given in Table 4.5 below [36].

Alloy Code	**Typical Active A_f**	**Composition (% by weight)**	**Typical Uses**
S	10 to 20 deg.C	~55.8 Ni, bal. Ti	Orthopaedic Devices, Surgical Tools, Cellular Telephone Antennas.
N	0 to 20 deg.C	~56.0 Ni, bal. Ti	Guidewires, Mandrels
C	0 to 10 deg.C	~55.8 Ni 0.25 Cr, bal. Ti	Stents, Braided Wire, Fine Wire.
B	20 to 40 deg.C	~55.6, bal. Ti	Body Temp. Activated Devices, Sents, Filters
M	45 to 95 deg.C	~55.1-55.5 Ni, bal Ti	Actuators, Toys, Demo Springs
H	95 to 115 deg.C	<55.0 Ni, bal. Ti	Actuators

Table 4.5 Alloy Composition and Transformation Temperature. ***(ref36)***

Note: Alloys S, N, and C are typically used for their superelastic properties Alloys M and H are typically used for their shape memory properties Alloy B is commonly used for either shape memory or body temperature superelasticity

Also the transformation temperature is also influenced by any applied stress If a stress sufficient to deform the martensite in a sample is still imposed while the sample is heated, then shape recovery which would normally occur at the transformation temperature can only occur after enough extra heat energy to move the sample against the imposed stress is applied This means that the observed shape recovery temperature goes up In NiTi, this effect moves the transformation temperature up about 1°C for each 6,895kPa of imposed stress Similarly, if the stress is imposed while the material is cooled toward the transformation temperature, the material can change to martensite above its normal temperature [30]

4.9.3 Superelastic Behaviour.

An alloy of NiTi can behave superelastically if its Active A_f temperature is just below the use temperature A superelastic material will not be superelastic at all temperatures, but will exhibit good superelastic properties in a temperature, which is about 50°C above Active A_f Also if the applied stress is sufficient to raise the martensite formation temperature above the normal shape recovery (austenite formation) temperature, the superelastic effect occurs With the application of stress, the alloy will strain due to stress induced martensite but as soon as the stress is reduced the material reverts to unstrained austenite The resulting stress-strain curve is shown in Figure 4 4 and one can see that the supper elastic effect yields an extremely springy material which can be deformed to large strains at fairly constant stress and can exert uniform recovery forces over large amounts of springback [30,36]

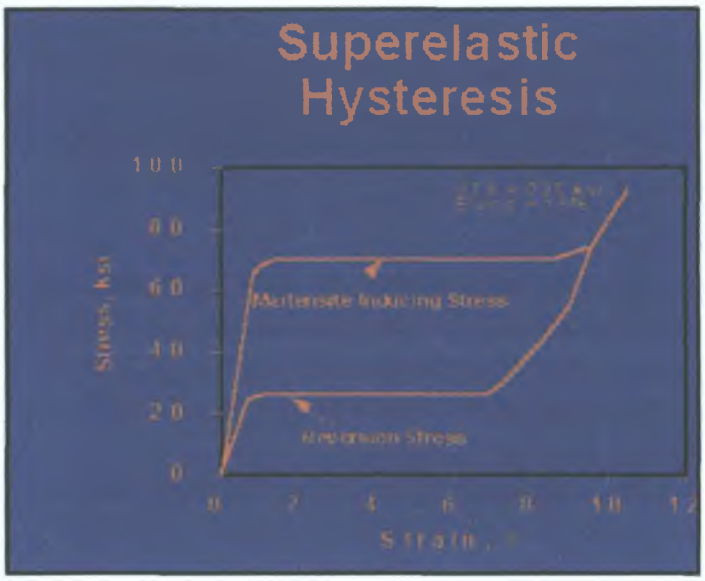

Figure 4.4 Superelastic Stress-Strain Curve.

4.10 Disadvantages of SMAs.

As with any exotic material there will always be disadvantages, which must be taken in account when using these materials. Most of the disadvantages are due to the machining, joining and coating of these materials. The following disadvantages are as follows:

- Attempt to machine results in very rapid strain hardening of the material.
- SMAs are difficult to fasten into an assembly. They are not easily joined. Welding is not effective. Welding SMAs to other materials results in brittle welds, and brazing or soldering is also very difficult. Welding the material to itself can be done if one is careful. Welds with a molten zone, such as lazer, E-beam or TIG welds, are brittle unless worked and reannealed to recrystallize the cast structure. Resistance or friction welds without a molten zone are quite strong and satisfactory if care is taken to keep oxides out of the weld zone. The most effective method is to clamp the material into place or constrain their position with some sort of restraint [30].
- Due to the reactivity of the titanium in NiTi, all melting of them must be done in a vacuum or an inert atmosphere. Methods such as plasma-arc melting, electron-beam melting, and vacuum-induction melting are all used commercially [31].

- NiTi alloys cost several hundred dollars per pound or more, depending on the fabricated shape [30].
- Whereas stainless steel can be coated with gold and other radiopaque materials to enhance radiopacity, coating Nitinol with these materials might negatively influence the superelastic performance of Nitinol. More work needs to be done in this area [25].

You have to be careful when choosing to use shape memory alloys for any application due to the cost of development and the cost of the SMA material. SMAs can prove to be more expensive than the cost of the existing product using established technology. But on the other hand the advantages to using SMA as a stent material could prove desirable compared to the other materials if proper methods for manufacturing these stents are used as will be explained in chapter 6.

4.11 Conclusion

Stent structures have the ability to be initially stretched out to reach a small profile, which facilitates a safe insertion and delivery of both stent and graft. When released, stents can position the graft against the wall of the artery and thus excluding the aneursymal sac from the blood flow. Self-expanding stents are more compliant to the pulsating artery than balloon expandable stents. Shape memory alloys and especially the nickel-titanium compositions offer a number of engineering properties that is not available in any other material. These stents will grow with the vessel and adapt to the shape more than plastically deformed stents. The fixation characteristics are an important issue in stent design so as to prevent stent migration. The most significant factor for the longitudinal force required to cause stent migration, is that of the neck length. The Palmaz, Nitinol coil and the Gianturco-Z stent all have similar fixation characteristics unlike that of the Wallstent. Adding hooks and barbs increases the longitudinal force by a factor of 8 to 10. Care should be taken when designing stents and such issues as biocompatibility, structure and ease of manufacturing should be taken into account when designing and manufacturing stents.

Chapter 5

Medical Textiles

5.0 Medical Textiles

5.1 Introduction

The propose of a textile is to exclude the aneurysm from the blood flow. Textile materials are a form of graft material, which is either woven or non-woven. Textile structures in implantation are identified by structure, material composition, and the behaviour of fibre surface and degradation. A major concern with artificial implants is the reaction the body will have towards the implant. A biotextile when implanted must meet the physical and mechanical requirements (such as strength, elasticity, durability, etc) and must also be biocompatible.

5.2 Characteristics of Graft Materials.

Vascular grafts must have specific characteristics. Textile structures are usually used however they do not always meet all the requirements. These are the typical characteristics.

1. Must be chemically inert, non-toxic and not to incite an inflammatory or foreign cell response in the tissues. The biomaterial must not damage blood cells or cause formation of destructive blood clots. This refers to both the fiber polymer and the fabrication techniques.
2. Have a low cost of fabrication.
3. To be sterilised without altering any of its characteristics.
4. Easily compressible without deformation of graft.
5. Easily expandable and readily adapt to the vessel in which they have been inserted [19].
6. The grafts must adhere firmly and permanently to a stent and must not interfere with the attachment of the stent to the arterial wall.
7. Graft surface roughness and surface wettability, which increases surface tension and therefore aids for platelet adhesion. In order to lower these adverse reactions, the

graft's surfaces can be coated with hydrophilic polymers, or heparinized or anticogulant chemicals to prevent thrombus formation [37]

8. Fibre diameter, in general, should be smaller than the cells for their adherence Although human tissue is capable of encapsulating objects much larger than fibres, it can better encapsulate the small circular fibres than large irregular cross-sectional fibres [38]
9. Radiopaque markers must be easily placed along the graft
10. Could use porous material (6μm) so as to lead to tissue growth and prevent clotting [19]
11. Grafts should be compliant to stimulate the ingrowing tissue and form a new elastic component of the arterial wall Mismatch in compliance between the artery and the grafts results in high shear stress and turbulence of the blood flow with local stagnation The relatively high graft stiffness determines a high impedance in the pulsatile, arterial velocities of pressure as well as flow waves are all increased by stiff graft walls Such increases do not occur with identical proportions, so reflected waves from pressure and flow, respectively are at different phases that increase the risk of turbulence, and unstable regions of flow at low Reynolds's number [39]
12. Biodegradability is an important property that enables the patient's cells to replace the graft by natural tissues These are materials that are absorbed by the body two to three months (or longer) after implantation Bioadsorbable implant materials should maintain their mechanical properties and functions until the biotissues are completely cured After complete healing of biotissues, the implanted materials should be degraded and absorbed quickly to minimize their side effects Such materials that are biodegradable are polyamides, some polyurethane's, collagen and alginate Although cotton and viscose rayon are biodegradable, they are not used as implants Materials such as polyester, polypropylene, polytetrafluoroethylene (PTFE) are considered non-biodegradable [38]

5.3 Types of Biomedical Materials used.

Synthetic materials can either be woven or knitted from mono or multi filament yarn It can also be non-woven These materials can then be formed into a tubular fashion to form a fabric that is suitable for a vascular prosthesis The various polymer materials used are as follows

5.3.1 Nylon.

"Nylon" is a generic term that designates a group of related chemical components classified as polyamides Nylon was one of the first materials used as a vascular graft It has a low moisture absorption capacity, good physical properties of strength and resilience and excellent chemical properties Nylon can be heat set Nylon can be produced in both regular and high tenacity strengths Nylon has the highest resistance to abrasion of any fibre It can take a tremendous amount of rubbing, scraping, bending and twisting without breaking down [40,41]

5.3.2 Polyethylene terephthalate (PET) or Polyester

Polyester has good mechanical and chemical properties It is minimally porous which allows for healing of the graft-artery interface It has a low moisture absorption which gives it good resistance to fast deterioration These fibres have high wet and dry tensile strengths It resists wrinkling when wet or dry They can be heat set to give exceptional dimensional stability to the yarn or fabric Polyester fabrics have good abrasion resistance, low creep and good wearability Following implantation, polyester grafts form a fibrin layer over their flow surfaces As healing proceeds, fibroblasts incorporate within the interstices of the graft and the inner layer may become quite organised within days Polyester can be sterilised by all methods Polyester is commonly used because it is available in a wide range of linear densities To give more elasticity to the graft, elastomeric yarn can be blended with the polyester Dacron is a typical polyester material

5.3.3 Polytetrafluoroethaylene (PTFE).

PTFE is a polymer composed of repeating units of carbon and fluorine $(CF_2\ CF2)_n$ in a linear chain arrangement Because the peripheral fluorine atoms are much larger than the centrally located carbon atoms, fluorine atom overcrowding results in a fluorine sheath completely covering the carbon chain This sheath provides the well known chemical inertness and stability and a low coefficient of friction [42]

During manufacturing process, PTFE depends on the melting temperature and cooling rate of the bulk material, which in turn affects the crystallinity and thus the mechanical properties such as strain under stress and creep In general, the higher the crystalline content the harder the material [42]

Typical PTFE materials used are Gore-Tex graft and Impragraft

5.3.4 Expandable PTFE

Expanded Teflon (ePTFE) is a nontextile material produced by mechanical stretching that is utilised for vascular grafts Expandable PTFE grafts are rendered porous by expanding sintered particles of Teflon [42,43]

5.3.5 Polyurethane

Polyurethane has come into use as a synthetic graft Although it is relatively nonthrombogenic, earlier forms of this material were found to degrade over time Aneurysmal dilation was frequently reported and required the addition of external grafts to repair these lesions Medical grade polyurethane has undergone molecular alteration which resulted in a better stability and improved resistance to biologic oxidation The material is composed of soft polyester and hard urethane-urea groups Biocompatibility may be increased by augmenting the proportion of urea groups It is especially used for its elasticity [19]

5.3.6 Silicon Rubber:

Silicon rubber polymer has been used successfully for a wide range of in vivo (internal) applications It has thermal and oxidative stability, good flexibility and elasticity, tissue and blood compatibility and is inert and relatively non-toxic It has been used successfully for tubing and shunts, vascular applications and catheters [39]

5.4 Classification of Textiles.

Textiles are fibres, which are either filament (a fibre of continuous length) or stable (filaments joined together) which are either spun, twisted or compressed into yarns Yarns are then either woven , knitted or otherwise into a fabric Various finishes can be added to the fabric to improve desired characteristics Figure 5 1 shows the steps in producing a fabric [41]

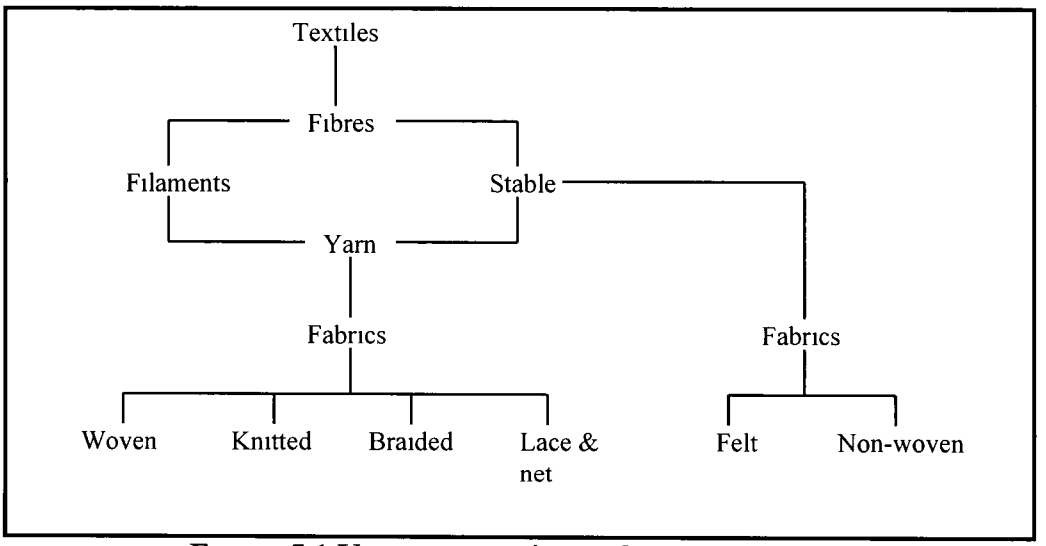

Figure 5.1 Various steps in producing a Fabric.
(Adapted from Miller ref41)

5.4.1 Fibres

Textile fibres are solids with distinct shapes In its simplest form, fibre manufacturing processes consists of liquefying a solid polymer, transforming it into the shape of a fibre by forcing the liquid polymer through orifices in an extremely fine die called a spinneret, and then resolidifying the liquid by either liquid (wet process) or by air Fibres can be either continuous filament yarns or stable yarns Filament yarns are better for graft materials because they are thin, smooth and have better uniformity unlike stable yarns that are thicker fibrous and have a rough finish

5.4.2 Yarns.

The character of a yarn are determined by the following

1. Kind and quality of fibre
2. Amount of processing necessary to produce fineness
3. Amount of twist, which increases tensile strength of the finished yarn
    - The idea of twisting fibres into a yarn is to force fibre surfaces into contact and thus set up frictional forces which bond the fibres together and produce a yarn which will withstand tension along its' length, i e the lower the twist the softer and weaker the yarn and visa versa Fine yarns require more twist than coarse yarns

The amount of twist also depends upon the type of fabric to be woven and depends on the following

1. Yarns intended for soft-surfaced fabrics are given only a slack twist They are called soft-twisted yarns
2. Yarns intended for smooth-surfaced fabrics are given many twists This contributes strength, smoothness, elasticity, and some wrinkle resistance to fabrics
3. Yarns intended for crepe fabrics (with rough, pebbly or crinkled surfaces) are given a maximum amount of twist, which adds wrinkle resistance

If a twist is prolonged past the maximum yarn strength the yarn becomes harder but not stronger because the stresses set up by continued twisting causes the fibres to weaken

Stretching of yarns can be achieved by special mechanical heat-setting treatments to thermoplastic filament fibres such as nylon or polyester The filament yarn can be tightly twisted and then heat-set at 120°C for an hour and thus setting crimp into the yarn to give a spring like condition to the yarn Other methods of stretching yarns are those made of biconstituent fibres, such as two different polymers produced as a single filament [40,41]

5.4.3 Fabric Structure

A fabric may be defined as a planar assembly of fibres, yarns or a combination of these Individual yarns may be quite limp and weak, but when a number of them have been combined into an appropriate structure a strong resilient fabric can be produced [39] The most commonly used fabric forming methods for graft structures for medical grafts fabrics are as follows

1. Interlacing

- **Weaving:** This is the interlacing of a lengthwise yarn system (warp) and a widthwise yarn system (filling or weft) at 90° to one another with fabric flowing from the machine in the warp direction as shown in Figure 5 2a So a simple woven fabric is one that is composed of two series of yarns (warp and weft) interlaced at right-angles Figure 5 3 shows the effect on the possible closeness of yarns in a fabric The closer the interlacing as shown in 'A' the firmer the fabric As the interlaces becomes less frequent as shown from 'B' to 'D' the fabric losses its firmness and will rapidly decline and lateral movement of yarns will become increasingly easier as the fabric loses stability Warp and weft yarns do not interlace exactly because the warp yarns are under heavy tension and tend to lie straighter than the weft

yarns which are not under such tension Fabrics are therefore usually more extensible in the weft direction than in the warp [40,41]

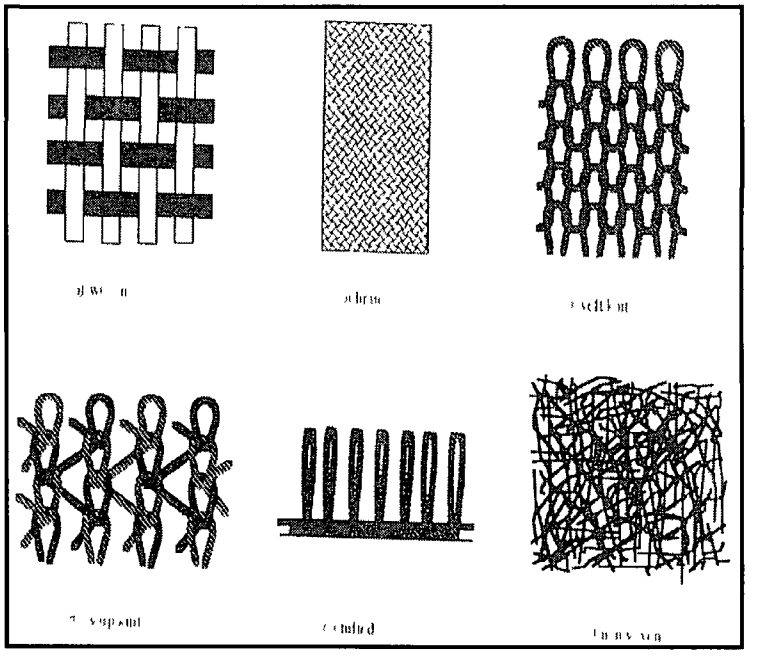

Figure 5.2: Types of Fabric Structure.
(Adapted from Miller ref41)

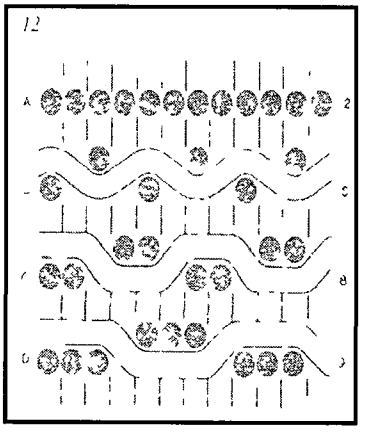

Figure 5.3 Closeness of Yarns in Fabric.
(Adapted from Miller ref41)

- **Braiding:** This is the interlacing of two yarn systems such that the paths of the yarns are diagonal to the fabric delivery direction forming either a flat or tubular structure as shown in Figure 5 2b Not normally used for medical graft fabrics due to it been too rigid

2. Interlooping (Weft and Warp Knitting)

- **Knitting:** Knitted fabrics are constructed with a single yarn that is formed by interlocking loops by the use of hooked needles When the interlocking loops run lengthwise, each row is called a wale A wale corresponds to the direction of the wrap in woven fabric Each row is called a coarse, which corresponds to the filling or weft The interlocking loops of the knitted construction permit the fabric to stretch in any direction, even if low-grade yarn having little elasticity or yarn that lacks natural elasticity is used The fabric that has more courses in it will be more rigid and stable in length The fabric that has more wales and more coarses per area will also have better recovery from stretching than one with fewer wales and courses per area, whereas, the fabric with less wales and courses per area will be less rigid, stretch more easily but will have poorer recover ability [40,41]

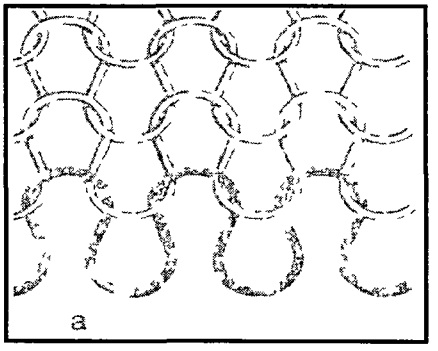

Figure 5 4a

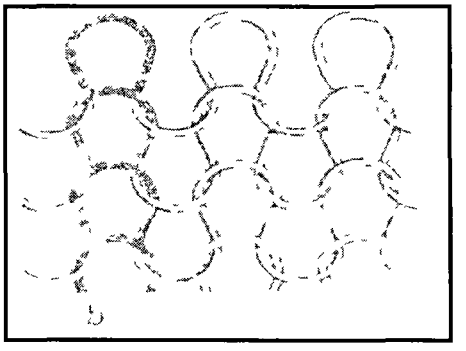

Figure 5.4b ***(ref40***

3. Bonding (Nonwovens)

- Nonwoven fabrics are the bonding or the interlocking of fibers or both, accomplished by mechanical, chemical, thermal or solvent means

5.5 Characteritics of Fabric Structure.

1. **Porosity:** A graft should be microporous to provide a stable anchorage for vascular cells and stimulate cell ingrowth Grafts which are impermeable to blood after the time of implantation do not permit the subsequent ingrowth of cells which is necessary for uniform and satisfactory bonding of the internal lining of the prosthesis [42] This can be achieved by using woven or knitted fabrics Special mechanical stretching methods must be applied to non-wovens to give them porosity Woven graft structures are typically less porous than knitted structures which diminishes blood leakage through the interstices but at the same time can hinder growth Porosity depends on the kind of fibre in the fabric (some fibres such as nylon, polyester, PTFE are hydrophobic - that is they don't readily absorb water Other fibres such as cotton and rayon absorb water readily), the tightness of the yarn twist, the compactness of the construction of the fabric and the finishing process used Knitted vascular grafts are more porous which allows tissue growth but leakage may be a concern Typical water permeability's of woven grafts are 50-550 cc/cm^2/min and of knitted grafts are 1,000 - 2,000 cc/ cm^2/min [40,41]
2. **Mechanical Requirements:** Plain woven fabrics have a high bursting strength, a good fatigue resistance and can have a low permeability to water (or blood) which reduces bleeding Woven prostheses have the strongest construction but lack compliance and consequently they may be too stiff Knitted prostheses have better flexibility and compliance But stretch can be obtained in woven fabrics by weaving the fabric extra wide and then reducing in width during scouring or heat-setting This can then be stretched out again, later returning to the heat-set width when released owing to its memory of the heat-set state Also the use of blended yarn in either the warp or weft direction can increase compliance and flexibility of woven fabrics Knitted prostheses are not well suited for large diameter vessel or locations of high stress because they have a weak construction and are not very dimensionally stable compared to woven prostheses [41,42] Knitted fabrics generally crease or wrinkle less than woven fabrics since the loops act as hinges Fibres can be heat treated and mechanically drawn to convert it from a weak, heavy, amorphous filament into a strong, tough, textile filament By proper manipulation

of temperature, tension, strain (elongation), and relaxation, the fibre can, with certain limits, incorporate desired strength, elongation, and thermal shrinkage properties in the hot stretched yarn [39]

3. **Dilation and the effects on Graft material.** Certain polymers such as PTFE and ePTFE can be radically expandable with coaxial balloons at inflation pressures within the working pressure of most angioplasty catheters When stent grafts are deployed they are dilated and the material surrounding the stent is dilated [43] *McClurken et al* found that the radial elongation of vascular PTFE exceeded 600% before failure With approximately 23% elastic recoil this can ensure adequate fixation of the graft material to the stent by frictional force [44] However, when used as a free-standing vascular conduit, the dilation of the PTFE material must compensate for the loss of diameter by elastic recoil otherwise the inherent recoil of the ePTFE will decrease the lumen diameter and subsequently alter blood flow characteristics within the implant, possibly leading to the ultimate failure of the device With increased dilation there is reduced porosity This is probably related to crowding of the fibrils, caused by the wall thinning resulting in the decrease of the radial internodal distance This will ultimately result in the loss of cellular ingrowth and will change the healing characteristics of the material, especially on the luminal surface For larger balloon dilations fibres would break apart and this would result in the weakening of the material and thus in the decreased tensile strength and the ultimate failure of the endovascular stent graft [43]
4. **Durability of Fabric:** This depends on the following
   - i. The kind and quality of the fibre
   - ii. The tensile strength of the yarn
   - iii. The amount of twist in the yarn
   - iv. The use of ply yarns as compared with singles
     - Yarns may be twisted around each other or plied to obtain greater strength, when two or more strands or yarns are twisted together they are called ply yarns
   - v. The use of monofilaments or multifilaments

- Monofilaments yarns are not effective where flexibility is required, they produce a rather stiff wire gauze effect which produces a rather glassy and rigid fabric structure Monofilaments are susceptible to creasing due their high resistance to bending and lack of elasticity when stretched as compared to multifilaments
- Multifilaments yarns give more flexibility to a fabric The more finer and numerous the filaments are in the yarn the more flexible and less likely to crease is the fabric The individual filaments are vulnerable to abrasion

vi. The use of uniform yarns rather than novelty yarns

vii. The compactness of the construction

- A compacted fabric (a more closely woven fabric) has a larger quantity of yarns than a loosely woven one and is therefore more serviceable

5. **Crimping:** Crimping can be used to overcome the limited longitudinal stretch of vascular prostheses Crimped geometry improves the graft's bending ability without kinking Crimping is achieved when either nylon or polyester fabrics are pleated or creased at temperatures above 100°C The internal structure of the fibre is 'locked' in the fibres A 'set' imposed by heat will remain so long as the temperature of setting is not approached or exceeded in use So we are safe at the body's temperature of 37°C [41]
6. **Finishing Requirements:** Finishing methods are used to give certain desired qualities to the fabric The types of finishing methods are
   - **Absorbency Finishes:** Certain processes such as Fantessa, applied to polyester fabrics render the fibres adsorptive Nylonizing is used for nylon 6 to make it more absorptive by treating them with a solution of nylon 8
   - **Resins:** Coatings such as thermoplastic type resins or rubber can be added to a fabric to make them stronger and give a smoother surface
   - **Water Repellency & Soil Repellency:** Durable finishes such as silicon compounds are excellent water repellents Application of this finish to the fabric results in coating the individual fibres of the yarn A group of fluorochemical finishes which act as water repellents also act as soil repellents [40,41]

- **Thrombus Repellency:** In order to prevent thrombus the fabrics surfaces can be coated with hydrophilic polymers, or heparinized or anticogulant chemicals to prevent thrombus formation [37]
- **Singeing:** Fibres that protrude from the fabric are burned away to give the fabric a smoother surface [39]

5.6 Conclusion.

Textile fabrics are truly engineering structures, which can be designed to suit vascular graft prostheses With the availability of various polymers, yarn construction (either mono or multi-filament, biconsitituent fibres), weaving methods, finishing methods etc, a graft of acceptable elasticity, mechanical strength, creep resistance, flexibility (resistance to creasing) and most importantly biocompatibility can now be achieved Although recent advances in tissue engineering, has already been able to produce several types of biocompatible tissues, it is only recently that major steps in vascular tissue engineering was made It could be many years yet before a FDA approved vascular graft from this technology could be achieved So for the meantime and the near future, methods used for manufacturing textile fabrics seems like an ideal compromise

Chapter 6

Prosthesis Design

6.0 Prosthesis Design.

6.1 Introduction.

When a stent graft is positioned inside the Aorta across the iliac bifurcation, certain undesirable flow characteristics can be attributed to the prosthesis. One major problem associated in the arterial tree is wave reflections as explained in section 2.5 chapter 2. Graft designs can intensify further the effects of wave reflections. Wave reflections have the adverse effect of increasing systole blood pressure and reducing ventricular ejection. Also vorticity creation and increased turbulence which affects the flow patterns gives rise to wall shear stresses that causes blood cell damage which erodes the endothelial lining, exposing positively charged cells which attract flow born cells that causes thrombosis. Compliance mismatch due to the fact that the elasticity of the vascular substitute is different from that of the host artery is a recognised major cause of late graft failures. Creasing of graft can be a problem during unfolding. When designing the prosthesis we must try to minimise these effects by carefully choosing the right materials and geometry for our design. It must be emphasised that it is impossible to eliminate these problems but with careful design methods we can minimise these effects [8,45].

6.2 Graft Geometry.

There are two types of bifurcated grafts.

- ***Unitary construction:*** Bifurcated graft as a single component.
- ***Modular construction:*** Comes in two separate parts. The main part comprises of the proximal end and one leg which is positioned first in the aorta. Then the other leg is attached from within the aorta.

From a hemodynamic point of view the unitary construction would give a better durability and flow characteristic since there is no joints along its construction unlike the modular design. The junction of the modular construction is a potential site for leakage. For these reasons we will be improving the unitary construction.

6.2.1 Wave Reflection Analysis.

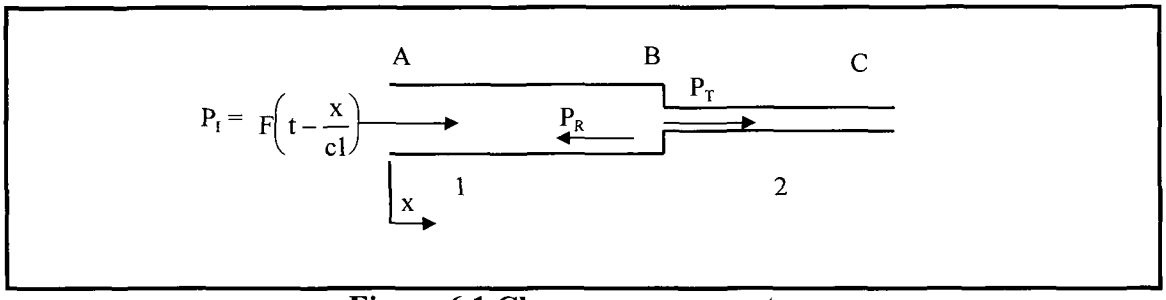

Figure 6.1 Change in cross-section

A good starting point in designing the geometry of the graft is to use the principals of water-hammer analysis These methods can be used to minimise the effects caused by wave reflections Wave reflections occur where a tube changes in cross-sectional area or branches into two daughters

A tube that changes in cross-sectional area is analysed first, as shown in Figure 6 1 Then a bifurcation is studied in which the principals of analysis are exactly the same P_I denotes the oscillatory pressure associated with the incident wave and is represented by the function $F\left(t - \frac{x}{c1}\right)$ This is a pressure head that denotes a one-dimensional wave of constant profile, moving with a constant wave velocity c1 and constant periodic motion in the +x direction Similarly P_R is the oscillatory pressure associated with the reflected wave and is represented by the function $f\left(t + \frac{x}{c1}\right)$ This denotes the same wave moving in the –x direction The amplitude of P_R is $\Re F\left(t - \frac{x}{c1}\right)$ $\Re$ is the reflection coefficient and is defined as the ratio of the incident pressure head to the reflected pressure head P_T represents the amplitude of the transmitted wave which is $\Im F\left(t - \frac{x}{c1}\right)$ $\Im$ is the transmission coefficient

6.2.2 Differential Equations for Transient Flow.

In order to analyse unsteady flow we start with the equation of motion (or momentum) and an equation of continuity Their solution leads to equations for pulse wave propagation of disturbances in flow and pressure throughout piping systems as used in water hammer analysis The name "impedance methods" has been given to the steady oscillatory studies Fluid oscillations in systems may be analysed conveniently by use of procedures borrowed from linear vibration theory and electrical transmission-line theory These methods are not useful for general transient conditions as it presumes the existence of a periodic oscillatory motion in the fluid system Any initial transients that may have been generated during the initiation of the oscillatory motion are assumed to have died out A frequency response analysis based upon steady oscillatory forced vibrations is used The differential equations are taken in simplified form, average flow relations are removed, the friction term is linearised, and the equations are solved for a harmonic oscillation of common frequency throughout the system When boundary conditions, such as valves, pumps, pipeline junctions etc, are included, solutions for typical fluid systems are possible [46,47,48]

Starting with the equation of motion (equation 6 1) and the continuity equation (equation 6 2) valves for both the reflection and transmission coefficients can be found The continuity equation here *(see ref 46 & 47 for a full derivation)* takes into account the effects of the distensibility of the tube and the bulk modulus of the liquid with the wave velocity term c

$$\frac{\partial h}{\partial x}+\frac{v}{g}\frac{\partial v}{\partial x}+\frac{1}{g}\frac{\partial v}{\partial t}+\frac{2fv|v|}{gd}=0 \qquad \textit{(6.1)}$$

$$\frac{\partial h}{\partial t}+v\frac{\partial h}{\partial x}+\frac{c^2}{g}\frac{\partial v}{\partial x}=0 \qquad \textit{(6.2)}$$

Where

$\frac{\partial h}{\partial x}$ = partial differentiation of head with respect to axial length

$\frac{\partial v}{\partial x}$ = partial differentiation of velocity with respect to axial length

$\frac{\partial v}{\partial t}$ = partial differentiation of velocity with respect to time

f = friction factor

v = velocity

g = 9 81m/s^2

d = diameter of tube

c is the magnitude of the wavespeed which depends on the bulk modulus of the fluid and on the distensibility of the tube It can be shown that *(see ref 46, 47 & 48 for a full derivation)*

$$\text{wavespeed} = c = \frac{1}{\sqrt{\rho\left(\frac{1}{K} + \frac{da}{tE}\right)}} \qquad \textit{(6.3a)}$$

For incompressible flow as is a reasonable assumption in heamodynamic analysis, the wave speed c reduces to

$$c = \frac{1}{\sqrt{\rho\left(\frac{da}{tE}\right)}} = \sqrt{\frac{tE}{\rho da}} \qquad \textit{(6.3b)}$$

Where
ρ = Density of tube
K = Bulk modulus of liquid
d = diameter
t = thickness
E = young modulus
a depends on the end conditions

If anchored at one end $a = 1 - \frac{\nu}{2}$, If anchored at both ends $a = 1 - \nu^2$

ν = Poisson's ratio

6.2.3 General Wave Equations.

Equation 6 1 and equation 6 2 are now solved simultaneously It is initially assumed that in equation 6 1 that the term $v\frac{\partial v}{\partial x}$ is small when compared with $\frac{\partial v}{\partial t}$, and in equation 6 2 the term $v\frac{\partial h}{\partial x}$ is small when compared with $\frac{\partial h}{\partial t}$ Since the ratio of v/c

through the graft is usually of the order or 1/100 or less With the friction term neglected, both equations 6 1 & 6 2 are now written in the following form

$$\frac{\partial h}{\partial x}+\frac{1}{g}\frac{\partial v}{\partial t}=0 \qquad \textit{(6.4)} \qquad \frac{\partial h}{\partial t}+\frac{c^2}{g}\frac{\partial v}{\partial x}=0 \qquad \textit{(6.5)}$$

By taking the partial derivative of equation 6 4 with respect to t and equation 6 5 with respect to x, one may eliminate v and h, which yields

$$\frac{\partial^2 h}{\partial t^2}=c^2\frac{\partial h^2}{\partial x^2} \qquad \textit{(6.6)} \qquad \frac{\partial^2 v}{\partial t^2}=c^2\frac{\partial^2 v}{\partial x^2} \qquad \textit{(6.7)}$$

Now the general solution to these equations which is used to find the reflection and transmission coefficients is

$$\textit{Head rise} = H - H_o = F\left(t-\frac{x}{c}\right)+f\left(t+\frac{x}{c}\right) \qquad \textit{(6.8)}$$

Equation 6 8 implies that at time t at a point in the tube with co-ordinate x, the head rise is equal to the sum of the travelling pressure heights or waves comprising of $F\left(t-\frac{x}{c}\right)$ and $f\left(t+\frac{x}{c}\right)$ These waves are propagated in opposite directions in the tube with a velocity of c metres per second

$$\textit{Velocity change} = V - V_o = -\frac{g}{c}\left[F\left(t-\frac{x}{c}\right)-f\left(t+\frac{x}{c}\right)\right] \qquad \textit{(6.9)}$$

This equation is a relation between the magnitude of the pressure heights $F\left(t-\frac{x}{c}\right)$ and $f\left(t+\frac{x}{c}\right)$ and the change in velocity, which occurs at a section of moving column of fluid

Note: H_o and V_o are the values of H and V when time is zero

6.2.4 Reflection and Transmission of Waves at Junctions.

1. For a change in cross-sectional area

Referring to Figure 6 1 & applying both equations 6 8 & 6 9

$$H_{(AB)t} - H_{(AB)o} = F\left(t - \frac{x}{c1}\right) + f\left(t + \frac{x}{c1}\right) = P_I + P_R$$

$$V_{(AB)t} - V_{(AB)o} = -\frac{g}{c1}\left[F\left(t - \frac{x}{c1}\right) - f\left(t + \frac{x}{c1}\right)\right] = -\frac{g}{c1}(P_I - P_R)$$

$$H_{(BC)t} - H_{(BC)o} = \Im F\left(t - \frac{x}{c2}\right) = P_T,$$

$$V_{(BC)t} - V_{(BC)o} = -\frac{g}{c2}\Im F\left(t - \frac{x}{c2}\right) = -\frac{g}{c2}P_T,$$

The condition of continuity at junction B is

$$\text{Area1}\, V_{(AB)t} = \text{Area2}\, V_{(BC)t}$$

The pressure at junction B is the same

$$P_I + P_R = P_T$$

After neglecting the initial velocity head at time zero in the two pipe sections

$$V_{(AB)t} = -\frac{g}{c1}(P_I - P_R),$$

$$V_{(BC)t} = -\frac{g}{c2}P_T$$

2. *Calculation of the reflection coefficient*

$$\text{Area1}\, V_{(AB)t} = \text{Area2}\, V_{(BC)t}$$

$$\frac{A1}{c1} P_I - \frac{A1}{c1} P_R = \frac{A2}{c2} P_T = \frac{A2}{c2}(P_I + P_R)$$

$$\left(\frac{A1}{c1} - \frac{A2}{c2}\right) P_I = \left(\frac{A1}{c1} + \frac{A2}{c2}\right) P_R$$

$$\left(\frac{\frac{A1}{c1} - \frac{A2}{c2}}{\frac{A1}{c1} + \frac{A2}{c2}}\right) P_I = \Re P_I = P_R$$

$$\text{Reflection coefficient} = \Re = \left(\frac{\frac{A1}{c1} - \frac{A2}{c2}}{\frac{A1}{c1} + \frac{A2}{c2}}\right) \qquad \textit{(6.10)}$$

3. *Calculation of the transmission coefficient*

$$\text{Area1}\, V_{(AB)t} = \text{Area2}\, V_{(BC)t}$$

$$\frac{A1}{c1} P_I - \frac{A1}{c1} P_R = \frac{A2}{c2} P_T$$

$$P_R = P_T - P_I$$

$$\frac{A1}{c1} P_I - \frac{A1}{c1}(P_T - P_I) = \frac{A2}{c2} P_T$$

$$\frac{2A1}{c1} P_I = \frac{A1}{c1} + \frac{A2}{c2} P_T$$

$$\frac{\frac{2A1}{c1}}{\frac{A1}{c1} + \frac{A2}{c2}} P_I = \Im P_I = P_T$$

$$\text{Transmission coefficient} = \Im = \frac{\frac{2A1}{c1}}{\frac{A1}{c1} + \frac{A2}{c2}} \qquad \textit{(6.11)}$$

$\Im - \Re = 1$

4. Calculation of the Reflection & Transmission coefficients for a Bifurcation.

Referring to Figure 6 2

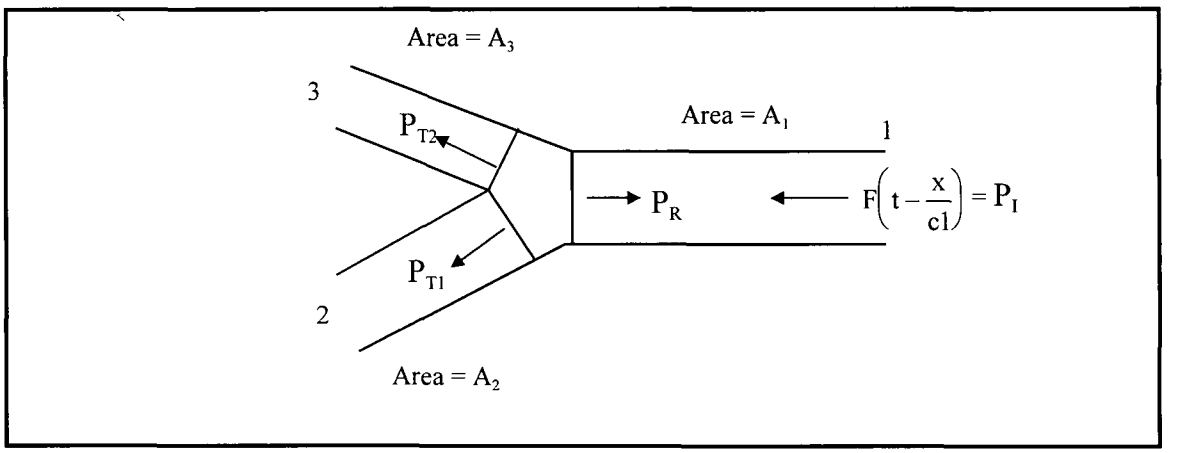

Figure 6.2: Bifurcated Junction

For an oscillatory pressure wave in a bifurcation

$P_I + P_R = P_{T1} = P_{T2}$

For volume flow rate we have

$Q_I - Q_R = Q_{T1} + Q_{T2}$

Transmitted pressure wave $= P_{T2} = P_{T1} = \Im F\left(t-\frac{x}{c1}\right)$

Reflected pressure wave $= P_R = \Re f\left(t+\frac{x}{c1}\right)$

In a similar manner for a change in cross-sectional area it can be shown that

$$\text{Transmission coefficient} = \Im = \frac{2A_1/c_1}{A_1/c_1 + A_2/c_2 + A_3/c_3} \qquad \textit{(6.12)}$$

$$\text{Reflection coefficient} = \Re = \frac{A_1/c_1 - A_2/c_c - A_3/c_3}{A_1/c_1 + A_2/c_c + A_3/c_3} \qquad \textit{(6.13)}$$

$\Im - \Re = 1$

Note: These equations for the bifurcation show that the pressure transmitted to the two branches are equal irrespective of their cross-sectional areas

The results for the transmission and reflection coefficients show us, that these factors depend upon the cross-sectional area and wave velocity of the two sections of the tube We want to keep the reflection co-efficient as small as possible Therefore the area ratio of Area1 with respect to Area2 + Area3 should be as close to unity as possible This gives a total transmission of the incident wave and no reflection at the junction Also the wave velocity c should be as small as possible One variable we have control over for the wave velocity is the Young's modulus of the chosen material for the graft The Young's modulus varies accordingly to the material type and the weaving method chosen i e either mono or multi filament fabric This implies that there is always a wave reflection due to a change in the elastic properties of a graft or a mismatch in compliance between the host artery and the stent graft The wave reflection here cannot be totally eliminated but minimised by the choice of graft material and stent material that would reduce the different in mismatch in compliance

6.2.5 Graft Design.

The major energy losses, which cause increased turbulence of flow and wave reflections of a bifurcated graft, occur at the junction of the parent tube with the two daughters There are two options for these junctions as shown in Figure 6 3

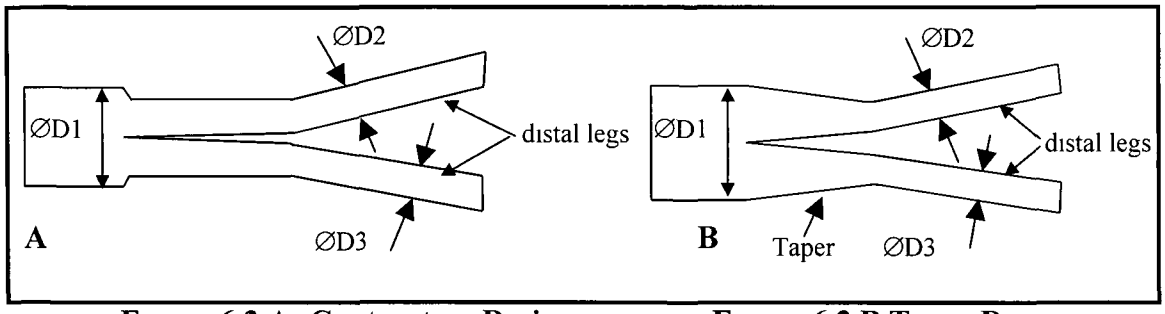

Figure 6.3 A: Contraction Design **Figure 6.3 B Taper Design**

In Figure 6 3A we can see how the proximal end of ØD1 goes directly to the two distal ends of ØD2 & ØD3 But in Figure 6 3 B a taper is used to join the proximal end to the final diameters of both distal ends The following advantages the taper design has

1. ***Energy losses:*** If we use an area ratio of less than one, we therefore are introducing a sudden contraction of the flow as shown in Figure 6 3A & Figure 6 4 As the fluid enters pipe 2 the steamlines tend to converge so that at B a maximum velocity and minimum pressure are found This will subsequently cause flow separation in the downstream pipe as the pressure increases due to a decrease in velocity from B to D At B the central stream is surrounded by fluid which is in a state of turbulence but has very little forward motion Between B and C the fluid is in a very disturbed condition because the stream expands and the velocity decreases while the pressure rises From C to D the flow is normal At the entry there is a loss of energy due to the increased turbulence and vortex motion The head loss associated at the entrance may be expressed as [49]

$$\text{Head loss} = h_c = k_c \frac{V^2}{2g}$$

where

V is the mean velocity of flow

k_c is the loss coefficient shown it Table 6 1

d2/d1	0 0	0 1	0 2	0 3	0 4	0 5	0 6	0 7	0 8	0 9	1 0
k_c	0 50	0 45	0 42	0 39	0 36	0 33	0 28	0 22	0 15	0 06	0 00

Table 6.1: Loss coefficients for Contraction of Flow. ***(ref 49)***

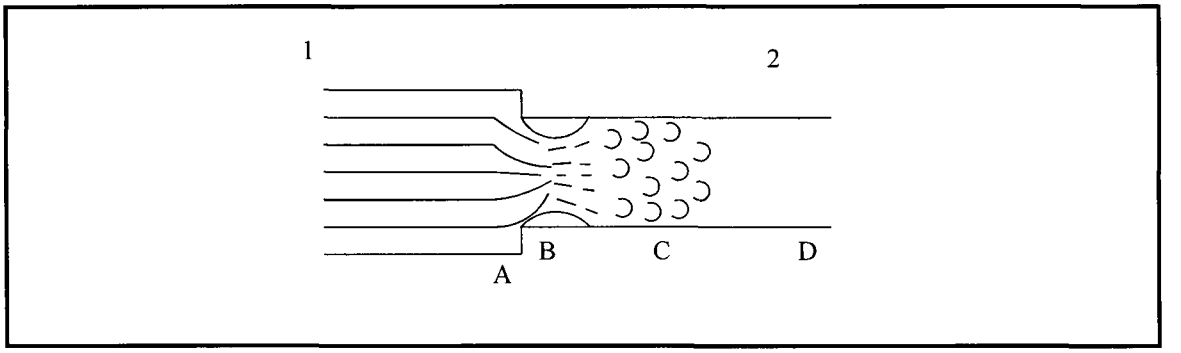

Figure 6.4. Showing Contraction of Flow. ***(ref 49)***

In order to reduce the foregoing losses, abrupt changes of cross-section should be avoided With a gradual contraction the loss coefficient can be reduced by employing a frustum of a cone i e the taper design as shown in Figure 6 3B Loss coefficients as small as 0 05 is possible Along the length of the taper a greater pressure difference exists which would prevent flow separation and a reduced vortex circulation This will give a reduced wall shear stress and consequently reduces the changes of blood cell damage Figure 6 5 & Figure 6 6 shows the flow pattern for a steady flow rate obtained by the Computational Fluid Dynamics software package Flotran A constant maximum blood velocity of 0 6m/s^2 was applied at the inlet and a fixed end pressure of 16,000N/m^2 was also given Indeed it can be seen that the contraction type of graft Figure 6 6 contracts the fluid flow more than the more uniform flow of the taper design of Figure 6 5

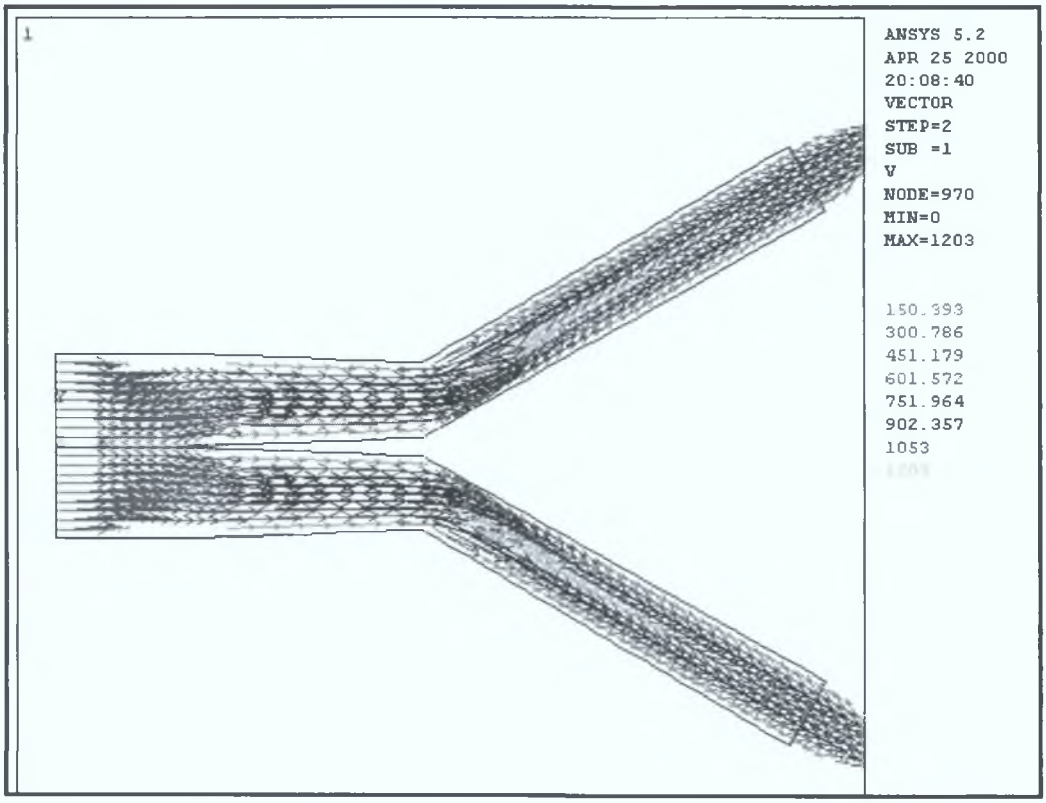

Figure 6.5. Taper Design – More uniform flow at junction.

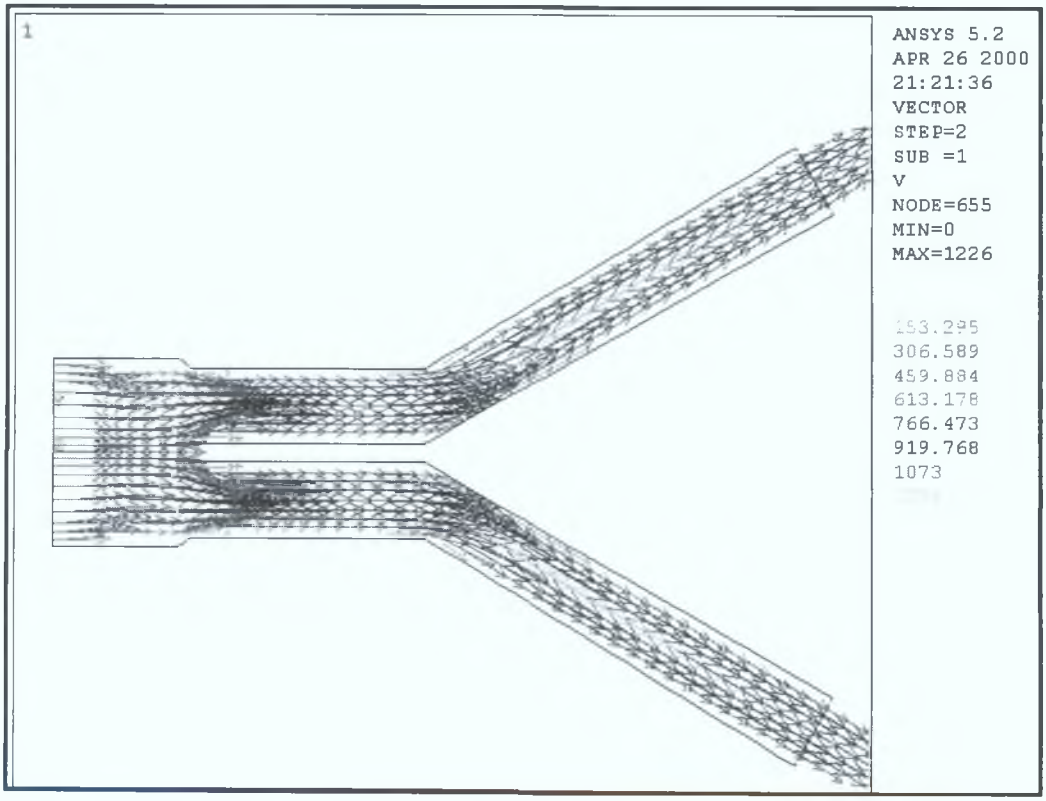

Figure 6.6. Contraction Design – Contraction of Flow at Junction.

2. ***Wave reflections:*** To reduce the effects of wave reflections we must decrease the reflection co-efficient and increase the transmission ratio (equation 6 12 & 6 13) If we look at the equations for the reflection and transmission co-efficient we can see that at the junction of the bifurcation shown in Figure 6 3A that A1 > A2 + A3 This indicates that there will always be a reflected wave at this bifurcated junction While in Figure 6 3B, the junction of this bifurcated taper graft has A1 = A2 + A3 indicating that there is no reflection but total transmission of the incident wave at the junction The reflection of the incident wave through the tapered graft is caused through the taper itself and not at the junction With a long taper the reflection co-efficient is minimal, but as we have already seen the energy losses for a taper is minimal

6.2.6 Geometry Conclusion.

The geometry of the bifurcated graft can have a drastic effect on the flow patterns and increased pressure in the aorta The taper design reduces the effects of wave reflections which in turn reduces the chances of increased proximal pressure With the contraction graft type more of the incident wave is reflected which increases the proximal pressure and hence the likelihood of further arterial dilation The cardiac output of the heart can be reduced due to an increase of wave reflections The taper design also gives more uniform flow unlike the contraction design in which flow separation is a problem

6.3 Graft Material.

Textile yarns and fabrics are normally used as a graft material, because they have a flexibility and moderate strength. As already discussed in chapter 5, we already know the options available for our graft material from a biomedical point of view. According to *Charlesworth (1988)* the long-term patency is not affected by the specific polymer or the method of construction of the textile (knitting or weaving) [50]. So what concerns us, is the mechanical properties of the fabric and how these can affect the wave velocity, turbulence of flow and how to reduce kinking or creasing of fabric after unfolding.

In deciding on what materials to use, we can look at some mechanical properties of the fibres that make up the yarn. The mechanical properties of fibres as given by *Adanur* [38] shown in Appendix D. It is difficult to choose a material for a fabric, since it is the weaving method that ultimately decides the final properties of the textile fabric. Fibres have a high tenacities but this is to be viewed cautiously as the corresponding strength of the textile fabric is disproportionately lowered, due to the inefficient translation of fibre strength into yarn strength and yarn strength into fabric strength. From a graft point of view we are only interest in the final fabric and how this effects the durability of the graft.

6.3.1 Design of Fabric.

- The fibre must be a filament (a fibre of continuous length) rather than a stable fibre (a filament joined together). Filament yarns are better for graft materials because they are thin, smooth and have a better uniformity unlike stable yarns that are thicker fibrous and have a rough finish.
- The yarn can be either mono-filament or multi-filament. Due to the problem of creasing, which is due to the fact that the bending stress-strain curves of man made fibres lay below the tensile curves and indicates that creasing is due to yielding on the compression side of the bend, rather than yielding in tension. This was accompanied by the development of kink-bands on the inside of the bend [51]. Mono-filaments have a large bending resistance unlike multi-filaments since a

number of thin multi-filaments are twisted in a helical form to form the yarn and the bending resistance is reduced dramatically so that creasing does not occur due to the following reasons

1. The stiffness of the textile fibre or any structural beam is directly proportional to its elastic modulus, and to the fourth power of its diameter So for a high modulus fibre, we must have a thin diameter For the same diameter yarn the mono-filament has a larger diameter than any of the individual fibres in the multi-filiament Since as much as 5 to 30 fibres can be twisted in a cylindrical helix fashion to form the yarn As shown in Appendix 4 Nylon 6 and Teflon have the lowest modulus and could be suitable for fabrics
2. Since the multi-filiament fibre is twisted in a helical form it can be easily compressed during folding of graft due to the fact that there is some slack in the fibre which can be easily stretched

- Care should be taken on the weaving methods of fabrics since tightly woven fabrics generally will restrict fibre movement When such fabrics are creased, the fibres in the yarns and the yarns in the fabric have insufficient space to enable them to move and slide relative to each other Instead, the fibres become permanently strained or elongated beyond their yield points, consequently impairing the fabric's wrinkle recovery ability Loosely woven fabrics allow more fibre redistribution and motion during creasing, and so less intrinsic fibre strain develops However, the geometric movement of fibres in yarns and yarns in fabric may be large, with no inherent ability for the fabric to recover, and so any wrinkle which does develop may be more permanent So a fine balance between the two should be sought for
- The yarns then are woven or knitted into the final fabric A woven fabric is preferred for the following reasons
    - From a mechanical point of view woven fabrics have a high bursting strength, good fatigue resistance and can have a low permeability to blood depending on the porosity of the graft Woven fabric lacks compliance but this may not be a problem since special heat setting or blending techniques can be achieved to give better compliance to a woven fabric Knitted fabrics

are not will suited to large diameter vessels because they have a weak construction

6.3.2 Bursting strength.

To be sure that woven fabrics will not dilate due to the pulsating blood pressure we must check the bursting strength of typical woven fabrics Even though fibres are non-Hookean, they obey hooks law up to 1 to 2% extension after this a proportion limit is reached and beyond this the fibre will creep under load The thickness of these fabrics vary between 0 1 and 0 25mm and since the ratio of the wall thickness of the fabric for both the proximal and distal legs to radius is < 0 1 We can use the following formulae for thin walled tubes to check if the bursting strength of the fabric is within the elastic limits of the fibres

Circumferential or hoop stress = $\sigma_{\theta\theta} = \frac{Pd}{2t}$,

Longitudinal stress = $\sigma_{XX} = \frac{Pd}{4t}$

The radical stress σ_{rr} is generally much smaller than the hoop stress for thin walled tubes and is assumed to be negligible

The circumferential strain $\varepsilon_{\theta\theta}$ is equal to the change of radius divided by the original radius

$$\varepsilon_{\theta\theta} = \left(\frac{1}{E}(\sigma_{\theta\theta} - \nu\sigma_{XX})\right),$$

Now incremental pipe radius = $\Delta R = \frac{R}{E}(\sigma_{\theta\theta} - \nu\sigma_{XX})$

where

P = blood pressure

E = young's modulus of fabric material

ν = Poisson's ratio

R = radius of graft

L = length

t = thickness

For a static failure we can use the Von Misses Criteria

Von Misses Stress = $\sigma_{von} = \sqrt{\sigma_\theta^2 + \sigma_\theta \sigma_X + \sigma_X^2} \leq$ yield strength of fabric

6.3.3 Testing of The Woven Fabrics.

To calculate the bursting strength of typical fabrics, I tested five different types of woven fabrics on an Instron Tensile Testing machine to obtain the mechanical properties of the fabrics The procedure I followed is as follows

Testing Procedure:

- The ravelled strip strength test method *(Adanur* ref38*)* was used This is where a rectangular section of a fabric is tested and the edge yarns in the longer direction are ravelled out and removed from the fabric A five mm fringe on either side should be sufficient
- Masking tape should be applied to the jaws to prevent jaw breaks Care should be taken to ensure that either jaw breaks or slippage do not occur
- The fabric is then clamped lengthwise in the flat jaws of the testing machine
- A typical strain rate given by *(Meredith* ref51*)* is $5\ 77 \times 10^{-3} \frac{\%Strain}{\sec}$ A rapid test requires a greater breaking load than a slow one
- Now testing can be done, and the mechanical properties of the fabrics can be ascertained

Note: The fringe is needed to prevent the edge yarns from popping out of the fabric Popped out yarns usually do not share the full burden of the load Ravelling permits you to line up the yarns parallel with the direction of pull on the testing machine

It must be noted that the mechanical properties are different in the weft or filling (widthwise direction) than in the warf (lengthwise direction) Fabrics are usually more extensible in the weft direction than in the warp

What we are interested is up to the yield point since beyond this point permanent deformation occurs which we do not what to happen Also failure by creep beyond the yield point is possible The results of the mechanical properties of the fabrics are

given in Appendix D. Table 6.2 shows the calculations of the wavespeed (equation 6.3b), circumferential strain and the von misses stress for one of the worst case scenarios that for a 30mm diameter aorta and a high blood pressure of 20,000N/m^2.

No	Material	Yarn/No of fibres	Direction	Wave-speed (m/s)	$\varepsilon_{\theta\theta}$	σvon misses (MPa)	Yield strength (MPa)
1	Polyester	Mono	Warf	76.4	2.3×10^{-3}	3.97	18.6
2	Polyester	Mono	Weft	68.5	2.8×10^{-3}	3.97	26.7
3	Polyester	Multi/<25	Warf	64.25	4.9×10^{-3}	1.42	14.3
4	Polyester	Multi/<25	Weft	44.5	0.01	1.42	6
5	Polyester	Multi/<30	Warf	58.6	6.67×10^{-3}	1.6	8.2
6	Polyester	Multi/<30	Weft	53.5	8×10^{-3}	1.6	5.6
7	Polyester	Multi/15	Warf	67.7	4.1×10^{-3}	2.65	24.44
8	Polyester	Multi/15	Weft	65	4.68×10^{-3}	2.65	21.7
9	Nylon	Multi/15	Waft	53.6	5.85×10^{-3}	3.31	58
10	Nylon	Multi/15	Weft	49.6	6.85×10^{-3}	3.31	38

Table 6.2.

Since our calculations were based on static failure and not fatigue failure, we must comment on the significance of this. In cumulate extension-cycling, this is where the slack is removed at the end of each cycle, experimental results for nylon show that at low imposed strains (2 to 5%) a limiting extension is reached. Whereas at high imposed strains the extension continues until break occurs. Since our strains are much lower than the circumferential strain and also the von misses stress is lower than the yield stress, we can safely assume that these fabrics will not continue to extend to failure. For fatigue failure of fibres, failure does not occur unless the imposed extension is very close to the usual breaking extension as is clearly not the case for our fabrics. At low imposed extensions, failure does not occur. Table 6.3 shows the number of cycles to break various yarns in cumulative-extension test.

Imposed Extension(%) / Fibre	5	7.5	10	12.5	15
Nylon		$>5\times10^5$	11000	220	12
Polyester	$>5\times10^5$	16000	18	7	

Table 6.3: Cycles to Failure for Selected Fibres. ***(Adapted from Morton ref51)***

As we can see serve extensions need to be achieved for failure to occur in the fibres

6.3.4 Fabric Summary.

As can been seen from the results, the mono filament has the highest initial modulus and this corresponds to the highest wave velocity With a high wave velocity this causes a higher reflection coefficient due to the initial modulus of the material A mono filament material as discussed already is susceptible to creep during the folding of the material Since static or fatigue failure of these fabrics are unlikely, any of the multi filament fabrics are best suited since creep during unfolding is unlikely

6.4 Forces on Bifurcated Graft.

To assess the suitability of the various stent types and designs available for graft fixation, it is essential to know the theoretical forces on the bifurcated graft due to the pulsating pressure Typical pressure & flow relationships found in the aorta as given in section 2 2 1, chapter 2 can be applied here To find the pulsatile forces acting on the bifurcated graft as shown in figure 6 8,

we will first use the continuity equation for a deformable body and then eulers equation of motion and finally apply the linear momentum equation for a deformable control volume

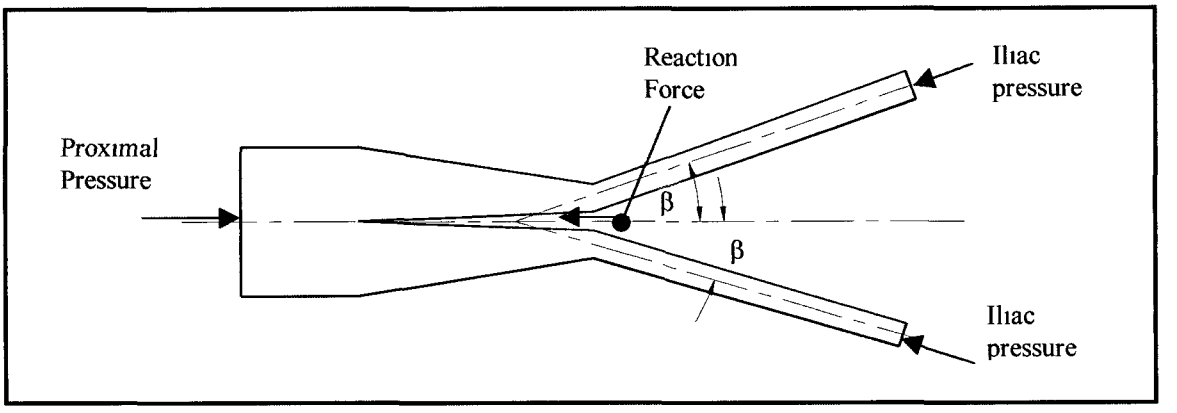

Figure 6.8

6.4.1 Calculation of the Forces on the bifurcated Graft:

As given in section 2 2 1, a Fourier series representation of a pressure and flow relationship will be applied here The continuity equation for a deformable body is applied first, to find the exit velocity through both distal legs The proximal end of the control volume will be a function of pressure but the rest of the graft will use a fixed control volume This is a reasonable assumption since the graft will not expand during the pulsating pressure Next application of eulers' equation of motion (which includs the associated energy losses), to find both distal pressures Finally the linear momentum equation for a deformable control volume will be used to obtain the forces acting on the bifurcated graft

1. ***To find exit velocity:***

To find the exit velocity, the continuity equation is developed from the general principle of conservation of mass for a deformable control volume

$$\frac{dm}{dt} = 0 = \frac{\partial}{\partial t}\int_{CV} \rho dV + \int_{CS} \rho \mathbf{V} \bullet \mathbf{n} dA \qquad (6.14)$$

where

ρ = density of blood = 1050kg/m^3

dV = elemental volume

V•n = represents the component of the velocity V normal to the elemental area dA of the control surface

$$\int_{CS} \rho \mathbf{V} \bullet \mathbf{n} dA = \sum_{1} (\rho_1 A_1 V_1)_{out} - \sum_{1} (\rho_1 A_1 V_1)_{in}$$

For a deformable control volume the volume is a function of the pulsating pressure The radial force of a compressed stent in a graft is around 0 5N Over the surface area of the proximal graft this would correspond to

$$\frac{\text{radical force}}{\text{surface area}} = \frac{\text{radical force}}{\pi \times d \times \text{length}} = \frac{0\ 5N}{\pi \times\ 028m \times\ 02m} = 284N/m^2$$

Where

d = proximal diameter = 28mm

length = length of the proximal end of the stent

Compared to the blood pressure we can neglect its effects on dilating the proximal end Due to the viscoelasticity of the artery there is a phase shift in its pressure diameter relationship that we are neglecting, but for the purposes of finding the pulsatile forces acting on the graft, this phase shift should not make much difference to the final result *Gow & Taylor (1968)* derived a formula that describes the increase of the arterial radius due to the increasing and decreasing blood pressure Typical radical compliance is around 5 - 7% *Gow & Taylor's* equation takes the following form

$$\text{Increase in radius} = \Delta R = \frac{\frac{2(1-\nu^2)\Delta P r_0}{E}\left(1-\frac{t}{r_0}\right)^2}{\left(1-\left(\frac{t}{r_0}\right)^2\right)}$$

Increase in proximal volume = ΔVol = circumference × length × $\Delta R = \pi dL\Delta R$

The rate of change of volume with respect to time must be calculated for the proximal end of the graft

$$\text{Total volume} = Vol_{Total} = Vol_{original} + \Delta Vol = \frac{\pi}{4}d^2L + \pi dL\Delta R$$

where

E = young's modulus of artery which is around $6 \sim 8 \times 10^5 \frac{N}{m^2}$

ν = Poisson's ratio which is 0 5

r_0 = original radius of graft

t = thickness of artery, which is around 1 1mm

ΔP = pressure change (systole blood pressure – diastole blood pressure)

d = original diameter of proximal end

L = length of proximal end of graft

From the equation of continuity for a deformable control volume with constant density we have

$$\rho\frac{\partial}{\partial t}Vol_{Total} + \sum_i(\rho_i A_i V_i)_{out} - \sum_i(\rho_i A_i V_i)_{in} = 0 \qquad \textit{(6.15)}$$

The term $\rho\frac{\partial}{\partial t}Vol_{Total}$ must be calculated for the proximal end only This term has a value of zero for the other sections of the graft since we have assumed a fixed control volume

2. *To calculate the distal pressures.*

To find the pressures acting on the control volume we can use Euler's equation of motion for unsteady, streamline and frictionless flow

$$\frac{1}{\rho}\frac{\partial p}{\partial x} + g\frac{\partial z}{\partial x} + v\frac{\partial v}{\partial x} + \frac{\partial v}{\partial t} = 0 \qquad \textit{(6.16)}$$

where

$\frac{\partial p}{\partial x}$ = partial differentiation of pressure with respect to axial length

$\frac{\partial z}{\partial x}$ = partial differentiation of piezometric head with respect to axial length

$\frac{\partial v}{\partial x}$ = partial differentiation of velocity with respect to axial length

$\frac{\partial v}{\partial t}$ = partial differentiation of velocity with respect to time which is the acceleration of the fluid

ρ = density

g = pull of gravity

Note that Eulers' equation is the same as the Navier Strokes equations if we will neglect the inviscid flow and shear stresses, the effects of gravity and all the body forces The energy losses can be taken into account if we use published experimental results based on empirical methods for pipe flows This is a simpler approach to this problem than trying to solve the full Navier Strokes equations which is very difficult to solve mathematically

When this equation is integrated from 1 to 2 for incompressible flow and if we take friction into account we get

$$\frac{p_1}{\rho g} + \frac{v_1^2}{2g} + z_1 = \frac{p_2}{\rho g} + \frac{v_2^2}{2g} + z_2 + \frac{1}{g}\int_1^2 \frac{\partial v}{\partial t}dx + h_f \qquad \textit{(6.17)}$$

Note: Since pulsatile flow is turbulent, we do not need to use the kinetic energy correction factor for the value of the velocity as this normally varies between 1 01 to 1 10 and usually can be neglected

The acceleration term $\frac{1}{g}\int_1^2 \frac{\partial v}{\partial t}dx$ must be calculated for each section separately and then added together

For each of the cylindrical shaped legs $\frac{1}{g}\int_1^2 \frac{\partial v}{\partial t}dx = \frac{L}{g}\frac{\partial v}{\partial t}$

But for each of the conical shape legs, $\frac{\partial v}{\partial t}$ is varying along its' length and is a function of the axial length x So we must relate the acceleration of the cone as a function of x

To find the acceleration of the fluid through the cone we will find the total velocity and then differentiate the total velocity with respect to time First we have to relate the change in radius of the taper as a function of the axial length x as shown in Figure 6 9

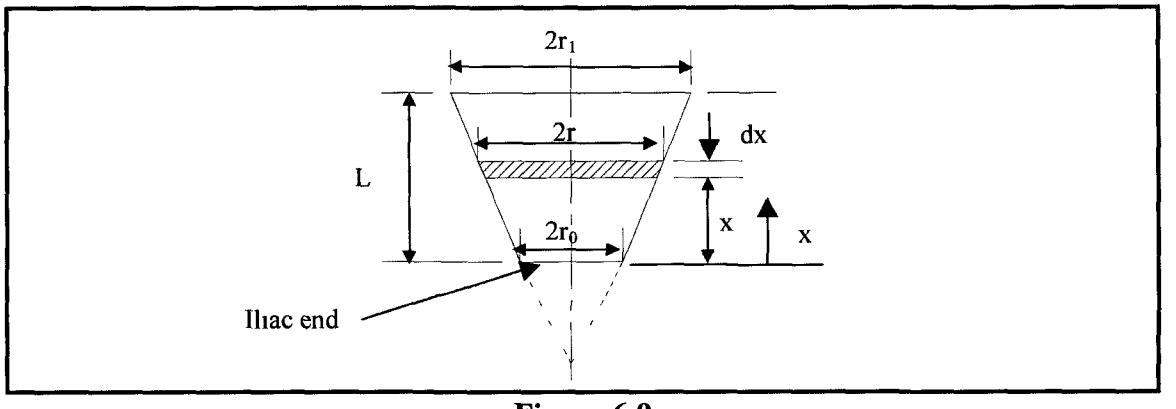

Figure 6.9

radius at any length $x = r = r_0 - (r_0 - r_1)\frac{x}{L}$

If A is the cross-sectional area of the iliac end as shown in figure 6 9, and v is the pulsatile velocity through the iliac end, then the total velocity for the fluid through the cone is

$$\text{Total velocity} \cong \sum_{X=0}^{X=L} \frac{Av}{A_{cone}} \delta x$$

$$\text{as } \delta x \rightarrow 0$$

$$\text{Total velocity of fluid through cone} = \int_0^L \frac{A\ v}{\pi(r)^2} dx$$

$$\text{Acceleration} = \frac{\partial vcone}{\partial t} = \frac{\partial}{dt} \int_0^L \frac{Av}{\pi(r_0 - (r_0 - r_1)\frac{x}{L})^2} dx$$

3. *Friction losses associated with the graft.*

To calculate the energy losses h_f associated from 1 to 2, it can be presumed that the head loss at any instant is equal to that of steady flow head loss for that flow rate at that instant Experimental evidence indicates that this presumption is reasonably valid for unsteady flow [52]

Since it was shown previously in section 2 6 Chapter 2, that pulsatile flow is turbulent, we have to rely totally on experimentation and semi-empirical methods These methods must be relied upon to approximate the friction losses for turbulent flow, as it is impossible to predict the losses theoretically unlike what can be done for laminar flow

There are two types of energy losses for turbulent flow, those associated with the roughness of the wall and those associated with minor losses such as converging or diverging sections, bends etc The total energy losses h_T is

$$h_T = h_f + \Sigma K = \frac{v^2}{2g}\left(\frac{fL}{d} + \sum K\right)$$

where

f = friction factor

h_f = Darcy's equation = $\frac{v^2}{2g}\frac{fL}{d}$

$\sum K$ = the sum of all the loss coefficients K

A lot of empirical work has been done in this area for turbulent flow through rough and smooth pipes Colebrook found the friction factor f in 1939 by combining the smooth wall equations developed by Prandtl and the fully rough wall formula developed by Nikuradse into an interpolation formula

$$\frac{1}{f^{1/2}} = -2.0\log\left(\frac{\varepsilon/d}{3.7} + \frac{2.51}{Re\,f^{1/2}}\right)$$

where

ε = roughness height

Re = Reynolds number

d = diameter of pipe

This is the accepted design formula for turbulent friction It was plotted in 1944 by Moody into what is now called the Moody chart for pipe friction It is accurate to ± 15% for design calculations It can be used for circular and noncircular cross-sections

We also have to rely upon experimentation to find the loss coefficients K for both bends and diverging sections Colebrooks formula and the theory for losses are reliable only for ducts of constant cross-section As soon as the section varies, we must rely principally upon experimentation to determine the flow properties For a gradual contraction the loss is very small as seen from the following experimental values [53]

Contraction cone angle 2θ deg	30	45	60
K for gradual contraction	0.02	0.04	0.07

Table 6.3: Experimental Values for gradual contraction.
(Adapted from White ref53)

A bend or curve in a pipe, always induces a loss larger than the simple Moody friction loss, due to flow separation at the walls and a swirling secondary flow arising from the centripetal acceleration The Moody loss due to axial length of the bend must be computed separately i e , the bend length should be added to the pipe length [53]

We will use an average friction factor for the proximal end of our graft We will estimate a value of 0 1mm for ε the roughness height of the woven graft This is a reasonable since the yarns woven together have their thickness around this value The Reynolds number for an average velocity of 0 6m/s for diameters ranging from 32mm to 18mm ranges from 6240 to 2880 Also pulsating flow is turbulent and a friction factor f of 0 044 is obtained from Moodys diagram This friction factor is suitable for this range of diameters A friction factor of 0 046 is suitable for the iliac legs and a loss coefficient value of 0 02 is suitable for the taper These values will all be substituted into Eulers equation by their respective energy loss equations

4. Forces acting on the Bifurcated graft.

The linear momentum equation for a deformable control volume is

$$\frac{d}{dt}(mV)_{syst} = \sum \mathbf{F} = \frac{d}{dt}\left(\int_{cv} V\rho dV\right) + \int_{cs} \rho \mathbf{V}(\mathbf{V}\bullet\mathbf{n})dA \qquad (6.18)$$

In words, the resultant force acting on a control volume is equal to the time rate of increase of linear momentum within the control volume plus the net efflux of linear momentum from the control volume

Where

V is the fluid velocity relative to an inertial (nonaccelerating) co-ordinate system The control volume approach uses the Eulerian method of analysis, which observes flow from a reference system fixed relative to the control volume

$\mathbf{V}\bullet\mathbf{n}$ Represents VCosθ, which is the component of the velocity V normal to the area element dA of the control surface Where θ is the angle between the velocity V and the unit outward normal to the elemental area dA

$\sum \mathbf{F}$ is the vector sum of all the forces acting on the control volume

m = mass of fluid

ρ = density of fluid

dA = elemental cross-sectional area

$$\int_{CS} \rho \mathbf{V} \bullet \mathbf{n} dA = \sum_{i} (\rho_i A_i V_i)_{out} - \sum_{i} (\rho_i A_i V_i)_{in}$$

For a deformable control volume the time derivative must be applied after the integration since the control volume changes with time For a deformable control volume, the velocity that is entering and leaving the control surface is now a function of both time and the increasing cross-sectional area of the deformable inlet and outlets Also the velocity through out the control volume is a function of both time and the increasing cross-sectional area of deformable control volume In our case the volume of the proximal end will be treated as a deformable volume while all other sections of the graft will have a fixed control volume The formulae for the deformable control volume of the proximal end is the same as that one used in the continuity equation The volume of the cone is given by

$$\text{Volume of cone} = \int_0^L \pi \left(r_0 - (r_0 - r_1)\frac{x}{L} \right)^2 dx$$

The first term in the linear momentum equation must be applied to each section of the graft separately and then summed together

Also when the graft is in the vertical position i e when the person is standing we must include the weight of the fluid for each section of the graft in the x-direction Since we have the same angle for each graft the y component of force is zero

Shown in Appendix E are the full calculations of the forces acting on the graft by using all of the previous formulae

6.5 Stent Geometry.

Migration of stent-grafts is a recognised complication of aortic endografting and many reports of late migrations have been reported As most migrations are diagnosed > 1 year, biological incorporation of endovascular grafts seems insufficient to resist the pulsatile forces present inside the aorta [28] We must therefore assess the possibility of stent graft migration and the anchoring systems available to prevent such migrations As calculated by the formulae in section 6 4, the maximum resultant force for several diameters of aortas as given in appendix E is shown in Table 6 4

Diameter mm	32	30	28	26	24	22	20	18
Max Force N	12	10	8 6	7 25	6	4 8	4	3 25

Table 6.4. Calculation of Maximum Force on Graft.

Table 6 5 shows a summary of the mean distraction forces for several types of stent designs as given in Chapter 4

Stent Type	**Mean Distraction Force (N)**
Plamaz	2 13
Wallstent	0 29
Nitinol Coil	2 55
Gianturco-Z smooth stent	2 5
Gianturco-Z with 4 weak hooks and barbs	7 8
Gianturco-Z with 8 strong hooks	11 8
Gianturco-Z with 8 strong hooks and barbs	22 5

Table 6.5: Mean Distraction Forces.)

We can note the following

1. Hooks and barbs are definitely needed, if there is only one stent on the proximal end But due to the problems of multiple wave reflections beyond the iliac bifurcation, stents on both iliac legs are needed These two iliac stents could provide the anchorage needed to support the graft
2. With no other mechanical support along the graft, buckling of fabric between the junction and the iliac stents is a possibility and thus stent migration is possible if smooth stents are used at the proximal end This situation can be tested in our bench test

3. As mentioned before stent graft migration are diagnosed after a year This could be due to further dilatation of the proximal or distal ends and thus there is no more anchorage of the distal or proximal stent Hooks thus can provide a stable anchorage without the worry of further dilation of the artery *Malina et al* has demonstrated that stents with hooks and barbs can retain their displacement force even if the graft is undersized by 1 to 2mm When hooks are used the limiting force is that of the wall of the aorta

6.6 Choice of Stent Type & Material.

As you will have noticed from Chapter 4, there is no major difference between the types of stents and their distraction forces We will therefore choose to manufacture the Z-type stent since this stent is the easiest shape to manufacture As explained already in Chapter 4, we will make this stent from shape memory alloy as this material proves to be the most suitable from a biocompatibity point of view The reasons for choosing this stent type and material is

1. ***For the Z-Stent:***
    - Easy to form into final shape
    - Easily crimped onto catheter
    - Can be sewn with little difficulty onto the graft
    - Has a dislodgement force comparable to other stent designs and can be improved greatly with the addition of hooks and barbs
2. ***Shape Memory Alloy:***
    - Setting the material into the final shape is achievable if correct steps are taken as will be explained next
    - Nitinol stents use either the shape memory or superelastic effect and does not need a balloon during delivery But Nitinol stents do require a sheath cover to prevent expanation during delivery This is no major disadvantage as the graft when folded needs a sheath cover during delivery

6.7 Manufacturing of the Z-Stent.

To make the Z-stent, the SMA's memory must be set The memory state of the material is established through training The end result of training is the freezing of the Austenite cubic phase, yielding a stable structure This is done by yielding the material to the desired shape (in our case the Z-shaped stent) and then restraining it in this stressed condition While it is stressed into position it is heated between 400°C and 800°C, for at least five minutes It can also be done as low as 300°C if sufficient time is allowed The time, temperature, and stress at which one trains the material determines its final properties The heat treatment is usually done in an air furnace, inert atmosphere furnace, molten salt bath, or fluidised bed

6.7.1 Procedure for Manufacturing the Z-shaped stent.

- A cylindrical mandrel made of steel or some other suitable material that would not melt at the required temperature is manufactured as shown in figure 6 10 The plans are given in Appendix F This mandrel is used to restrain the straight annealed shape memory alloy wire into the final stent shape The size and number of sides on the stent depends on the distance the treaded holes are apart and the number of holes taped around the sides of the mandrel
- Wind the SMA wire around the screw head on the cylindrical mandrel
- Fasten the wire to the mandrel, such by capturing them under the screw head
- Put them into the air furnace at around 500°C for 6 to 7 minutes
- Rapid cooling of some form is preferred via a water quench or rapid air cool, keeping the SMA wire held in position on the mandrel
- Unscrew and take out the newly formed SMA wire The wire should now be in the shape of the Z-stent as shown in figure 6 11 Figure 6 12 shows the manufactured mandrels and Z-shaped stents

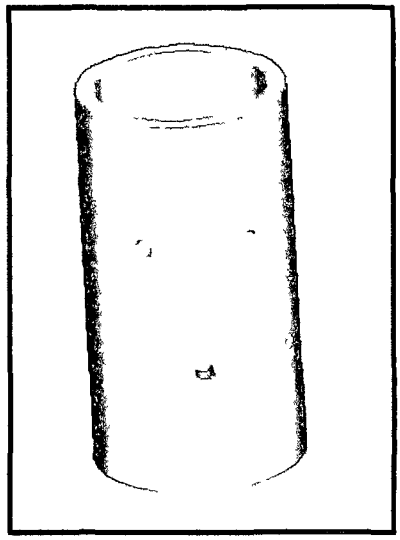

Figure 6.10: Cylindrical Mandrel

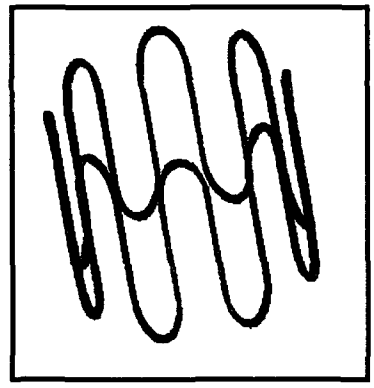

Figure 6.11: Z-Shaped Stent.

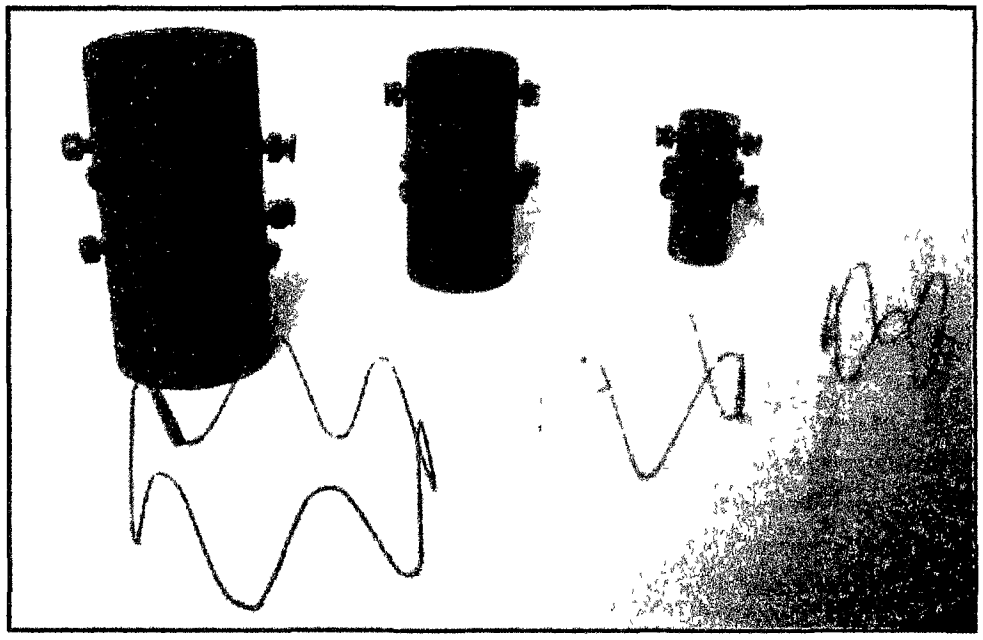

Figure 6.12: Various Size Mandrels & Z-Shaped Stents.

Warning:

- Higher heat treatment will increase the actuation temperature of the SMA wire and often gives a sharper thermal response, but there is usually a concurrent drop in peak force of the wire and in the ability to resist permanent deformation
- Heat treatment fixtures such as the mandrel used for our Z-shaped stent can be surprisingly sluggish in reaching the desired temperature in air or vacuum furnaces The desired stent properties are imparted largely by the time at the maximum temperature, so be careful that your stent actually reaches the desired temperature and time
    - Due to this problem the final shape of the stent may expand by 40% in the radical direction This is no major disadvantage, as the stent now has a higher radical force when compressed against the wall of the artery
- Trial and error is the best solution to get the required radical size Mandrels made of other materials could be tested and the temperature and duration varied, but as mentioned already the mechanical properties of the wire could be weakened by overheating for long durations in the air furnace

6.8 Combination of Stent and Graft.

The final part in designing the stent graft is the combination of both stent and graft The graft size is given in Appendix F The options available for improving the design are

- Radiopaque markers should be positioned along the graft for easy visualisation of the stent graft during delivery
- 1/3 of the stent should be left exposed to anchor the graft
- Thin clusters of polyester fuzz can be sewn to proximal and distal outside ends to promote tissue attachment and sealing
- Proximal end of graft is usually oversized by 1-2mm to ensure a tight fit
- Crimps can be added to iliac legs by heat setting the fabric, this offers more resistance to kinking or angulation caused by tortuosity of the common iliac and gives the graft more flexibility
- To reduce the chances of kinking and creasing of the fabric, a biocompatitle elastomeric material such as silicon, could be woven, sewn or glued as thin flat filaments to the graft fabric
- To add extra longditudal strength to the graft structure polymeric or metal struts may be glued or sewn between the proximal and distal stents This would be a better alternative to a fully stent graft structure as this would decrease the wave reflections due to a decreased stiffness of the structure Also the struts would be on the external side of the graft and would therefore not interfere with the flow pattern
- The stent should be sewn onto the graft when in the unfolded position Then crimp the stent and graft onto the catheter

Figure 6 12 shows the final shape of the bifurcated graft Figures 6 13 & 6 14 shows the sewn bifurcated stent and graft

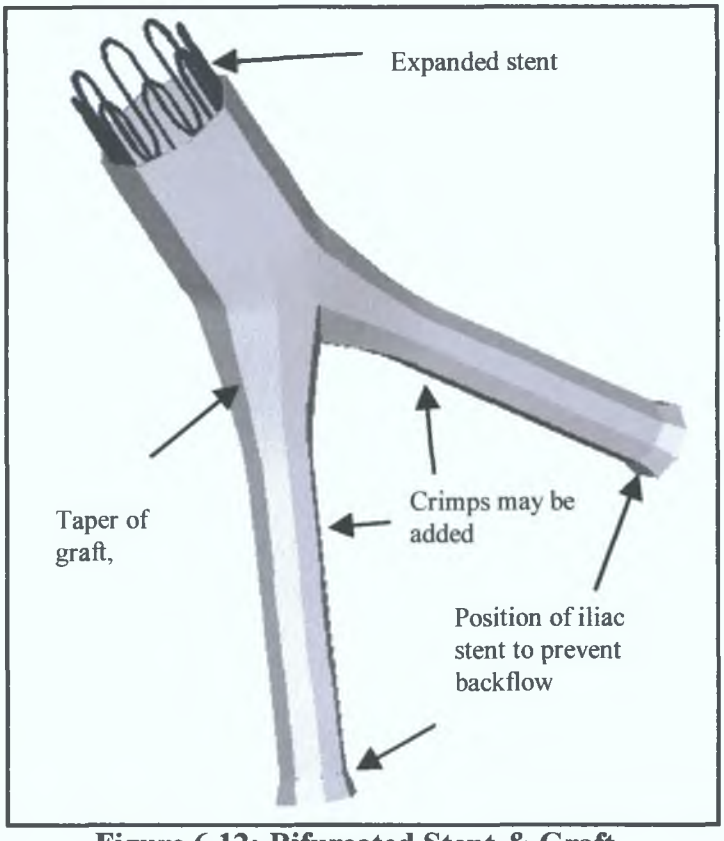

Figure 6.12: Bifurcated Stent & Graft.

Figure 6.13 A & B shows a close up of the Z-shaped stent sewn onto the polyester multifilament fabric.

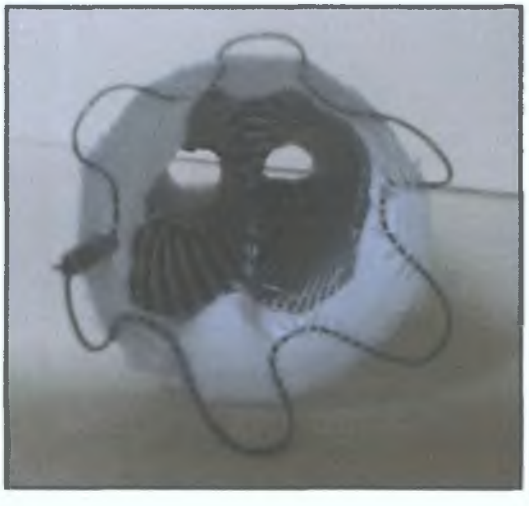

Figure 6.13 (A)

Figure 6.13 (B)

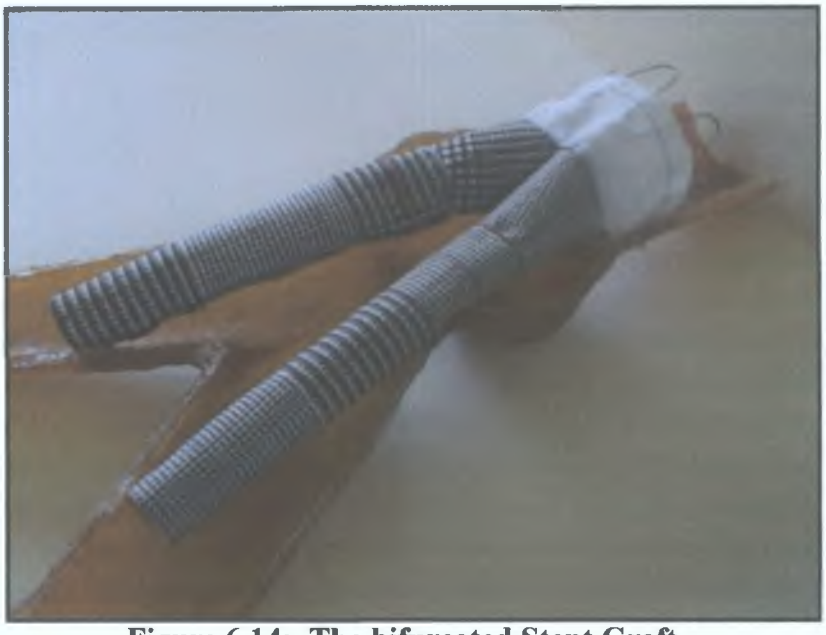

Figure 6.14: The bifurcated Stent Graft

6.9 Conclusion

Prosthesis design needs to be carefully analysed. Problems associated with both stent and graft needs to be addressed if at all possible. The most difficult part of prosthesis design is been aware of the problems caused by the stent graft while in the vascular system. As presented in this chapter, areas such as wave-reflections, stent migration, creasing of the graft etc, poses serious problems for the lifespan of the stent graft. The causes of these problems, needs to be minimised, as total elimination is virtually impossible. But of coarse one must realise that the benefits of inserting a stent graft across a life threatening disease such as aneurysms outweighs all the possible problems associated with this prosthesis.

Chapter 7

Delivery System Design

7.0 Delivery System Design.

7.1 Introduction.

For a successful endovascular procedure in which accurate placement of the stent graft across the aneurysm sac is to be achieved, requires a surgical exposure of the common femoral arteries where the endovascular graft can be inserted through by special over the-wire-techniques All the manipulations are controlled from a remote site by the use of guidewires and specially designed catheters This technique avoids the need to directly expose the diseased artery through a large incision or an extensive dissection, as is the case with current surgical repair This Chapter deals with the issues involved with stent graft placement and the methods that are possible for positioning of a unitary bifurcated stent graft

7.2 Selection Criteria for Stent Graft Placement.

The selection criteria for a safe delivery of the device, is an important issue as certain anatomic features and conditions must exist before attempting to deliver the Endovascular Grafts

1. The common and external iliac and femoral arteries must be of sufficient calibre to allow passage of the introducer sheath without damaging the vessel wall or must be amenable to balloon dilation or facilitate passage The common and external iliac arteries must be greater than 8mm, so as to advance delivery system
2. No angulated proximal neck (no more than 75° to the long axis of the aneurysm)
3. The femoral and iliac vessels must demonstrate limited tortuosity (twists, bends or turns) after arterial straightening manoeuvres are completed
4. Common femoral and/or iliac patency allowing endovascular access
5. Patients able to undergo local or epidural anesthesiz with sedation [3,4,19]

7.3 Catheters and Guidewires.

Guidewires and catheters are the basis of the delivery of endoprotheses during endovascular surgery They provide control and permits the delivery of the stent and graft to the vasculature

7.3.1 Guidewires.

The basic construction of each guidewire affects handling characteristics and makes each guidewire unique

Length: The guidewire length must be adequate to cover the cumulative distance required, both inside and outside the patient The guidewire length used for most procedures is 145 cm, but lengths up to 260 cm are available

Diameter: depends on how much support a specific catheter requires

0 014inch is used for small devices

0 035 - 0 038inch is used for large devices over 18F

Stiffness: Most guidewires have a tightly wound inner steel core that confers differing magnitudes of stiffness to the body of the guidewire A surrounding wrap of lighter, more flexible wire helps prevent fracture and fragmentation while the guidewire is in use

Coating: Coefficient of friction is reduced by coating the guidewire with a layer of Teflon or silicone

Tip Shape: The best use for a guidewire is determined by its tip shape

- An exchange wire is usually straight
- A curved guidewire is used for selective cannulation
- A floppy tip guidewire, which has no inner core in its tip is therefore flexible and reduces the potential for endoluminal injury by buckling when it encounters resistance

Special features: These include varying lengths of floppy tip, antithrombotic surfacing, steerability with a high torque 1 1 ratio between the shaft and the tip, and varying degrees of stiffness of the shaft [52]

7.3.2 Catheters

Catheters are used to position the stent and graft at the desired location and are guided over a guidewire Catheters differ with respect to construction material, diameter, length, head shape and special features Table 7 1 shows the types of materials and characteristics available for the design of catheters

Material	**Characteristics**
Polyethylene	• low co-efficient of friction
	• pliable i e easily bent without breaking - flexible
	• good shape memory
	• can be torqued
Polyurethane	• are softer and more pliable and follow guidewires more easily
	• have a higher co-efficient of friction
Nylon	• Stiffer and tolerate higher flow rates
PTFE (Teflon)	• is the stiffest material and used mainly for dilators and sheaths
	• have the lowest co-efficient of friction

Table 7.1 ***(Adapted from Schneider ref 52)***

The diameter of catheters should be as small as possible to accomplish the task at hand Catheter length must be adequate to reach the target site and still have enough length outside the patient for appropriate manipulations Most catheters range from 65 to 110 cm in length In general, use the shortest catheter that will perform the task The head shape of catheters as shown in figure 7 1 determines the function [52]

Some special features of catheters include various coatings, radiopaque tips, and graduated measurement markers

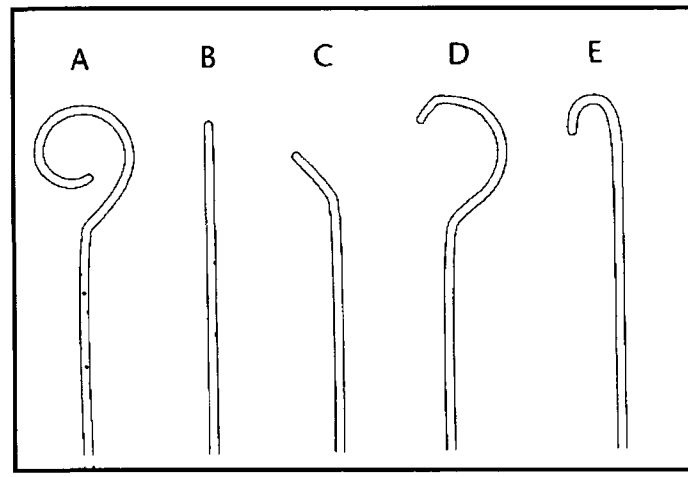

Figure 7.1: Various Catheter Head Shapes. A) Tennis racket catheter, B) Straight catheter, C) Berenstein catheter – general purposes, D) Cobra catheter – used for catheterization of branched vessels, E) Hook-shaped catheters – used for crossing the aortic bifurcation. ***(Adapted from Schneider ref 52)***

7.3.3 Placement of Catheters.

After placement of a guidewire across the arterial segment of interest, the next challenge is to pass the catheter into the correct location In general, the catheter will follow the guidewire as long as it is advanced incrementally and the guidewire is held in position so to ensure that it does not also advance There are several factors that can make delivery system insertion easier

1. Delivery system should be as small, smooth and tapered as possible Blunt or open-ended systems often need to be passed through a second sheath
2. To permit insertion of the loaded delivery system (sheath, central carrier and prosthesis) a tapered obturator can be present

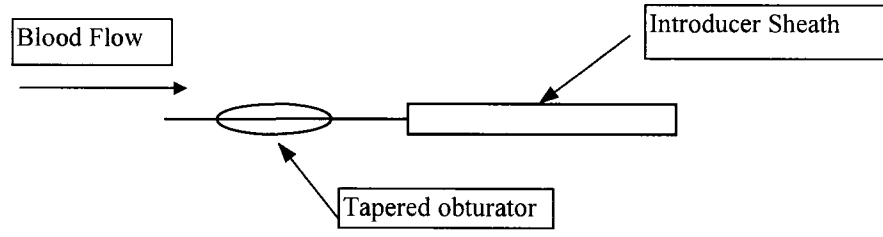

3. If advancing device through tortuous arteries, pressurisation of the flexible sheath can be performed using a tip balloon

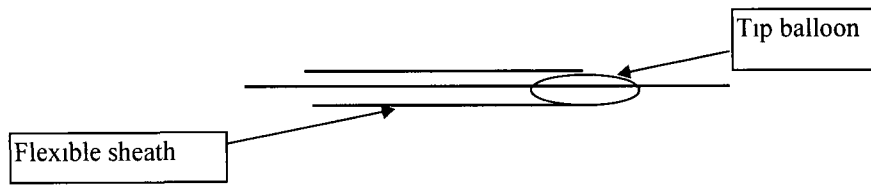

4. The mean blood pressure can be dropped using nitroglycerin solution Pressure is kept at 70mmHg
5. Delivery system should be inserted through the less tortuous iliac artery
6. Delivery systems should be inserted over a stiff guide wire e g Amplatz Superstiff (Meditech) or Amplatz Extastiff (Cook) Insertion of a stiff guidewire into tortuous vessels can be facilitated by transcatheter exchange e g Angulated radio-opaque catheters (cobra catheter) or soft-tipped slippery guidewires e g Glidewire (Tenumo)
7. For torturous iliac arteries you can introduce first an expandable sheath which is dilated by a dilator Then put the delivery system into this expandable sheath up through the tortuous vessels
8. The femoral artery should be supported by applying gentle traction during delivery system insertion Otherwise friction at the insertion site will tend to push the femoral artery beneath the inguinal figment, which increases the redundancy of the external iliac artery and further increases resistance to insertion
9. For iliac tortuosity a guidewire can be introduced from the brachial artery and recovered in the common femoral artery The guidewire can be kept taught while pulled from both sides
10. Due to aortic tortuosity (bends greater than 60°), indirect transabdominal pressure is sometimes able to straighten the aorta Also a stiff guidewire helps if the wire exits the body at two points
11. When the catheter cannot be advanced into position because of significant vessel tortuosity or because of the long distance between the catheter head and the entry site, a steady and gentle withdrawal of the guidewire while the catheter is advanced decreases friction at the level of the catheter head and usually accomplishes the requisite advancement

12. If the catheter and guidewire combination tends to buckle freely, you can choose to either insert a stiffer guidewire or attempt to advance both the catheter and guidewire simultaneously [3,4,19,52].

7.3.4 Failure Of Catheters.

When the catheter is inserted over the guidewire into the vascular system, compressive stresses are acting on the tip of the catheter due to the impact and pressure of the blood. The normal design procedure is for simple direct compressive stress but when the length to cross-section ratio begins to increase, then we have to examine the catheter for possible failure due to buckling. The importance of buckling is that failure happens suddenly and with very little warning even for ductile materials.

If the slenderness ratio C is greater than the transitional slenderness ratio Cc then failure is due to buckling

$$\text{Slenderness ratio} = C = \frac{\textit{Effective length}}{\textit{Radius of Gyration}} = \frac{\text{Le}}{\sqrt{\dfrac{\textit{Second moment of area}}{\textit{Cross - sectional area}}}}$$

$$\text{Transitional slenderness ratio} = Cc = \sqrt{2\pi^2 E / \sigma_y}$$

To check if failure by buckling will occur we will calculate for a nylon catheter over a stainless steel guidewire.

Material	**Young's modulus**	**Yield Strength**	**C**	**Cc**	**∅**	**Le**
Nylon	400MN/ m^2	464MN/m^2	1024	2.33	O.D 3mm I.D 2.5mm	1m
Stainless steel	200GN/m^2	1120MN/ m^2	4444	33.5	0.9mm	1m

Table 7.2

As can be seen, that in fact the slenderness ratio is greater than the transitional slenderness ratio indicating that failure will occur by buckling.

- ***Lateral Pressures acting on Tip of Catheter.***

Since pulsatile flow was shown to be turbulent, viscous effects caused by the boundary wall does not affect the flow pattern Also the velocity profile is blunt and therefore the effects of the boundary layer are negligible It is then possible to apply the formulae for flow past immersed bodies, as the boundary layer does not affect the flow pattern near the catheter when it is placed inside the aorta The forces acting on the catheter tip are due to the blood pressure and the kinetic energy of the blood, which is

$$\text{Force on catheter tip} = \int_S P\,\mathbf{n}\,dA + C_D \times 1/2 \times \rho \times V^2 \times A \qquad (7.1)$$

Where

$\int_S P\,\mathbf{n}\,dA$ is a surface integral of the normal component of the scalar field P acting on a defined curved surface

P = this is a scalar field which represents the blood pressure of 16000N/m^2 or the reduced blood pressure during endovascular surgery of 10000N/m^2

n = unit normal vector of the surface

dA = elemental area of surface

A = Frontal Area

C_D = drag coefficient = 1 for flat faced cylinder or 0 6 for a rounded faced cylinder

V = velocity of blood = 0 6m/s

ρ = Density of blood =1050kg/m^3

- ***Surface options for Tip of Catheter.***

The contour of the surface at the tip of the catheter can have an effect on the total resultant force, and hence buckling can occur To find the resultant force, we will use equation 7 1 and apply it to different surface options It will be seen how the choice of surface option for the catheter tip can drastically reduce the resultant force With a reduced catheter tip force a more flexible material can be used to guide the stent to the desired location

The contour of the tip of the catheter could have the following options

1. ***Flat faced:*** The forces acting on a flat faced catheter is

$$\text{Blood pressure} \times \text{Frontal area} + C_D \times 1/2 \times \rho \times V^2 \times \text{Frontal area}$$

Frontal area = $\frac{\pi}{4}\left(d_1^2 - d_2^2\right)$

d_1 = outer diameter

d_2 = inner diameter

C_D = 1 for a flat faced cylinder

2. ***Rounded ends:*** There are numerous ways to round the ends One way is to put a inner diameter hole through a sphere and the other is to round the ends like a half torus, with the diameter equal to the thickness of the catheter

a): ***Sphere with inner diameter hole through it:*** To find the resultant force acting on this rounded end, we must calculate the surface integral $\int_S P\,\mathbf{n}dA$ The surface of the sphere is represented in Cartesian form by the following S $x^2 + y^2 + z^2 = r^2$

Unit normal vector of the surface **n** is $\frac{\text{gradS}}{|\text{gradS}|} = \frac{1}{r}(x\mathbf{i} + y\mathbf{j} + z\mathbf{k})$

$$\int_S P\,\mathbf{n}dA = \int_A P\,\frac{1}{r}(x\mathbf{i} + y\mathbf{j} + z\mathbf{k})\,dA$$

To simply this calculation, we will convert to spherical polar co-ordinates

$$x = rCos\theta Cos\phi, \quad y = rCos\theta Sin\phi, \quad z = rSin\theta, \quad dA = r^2 Cos\theta d\theta d\phi$$

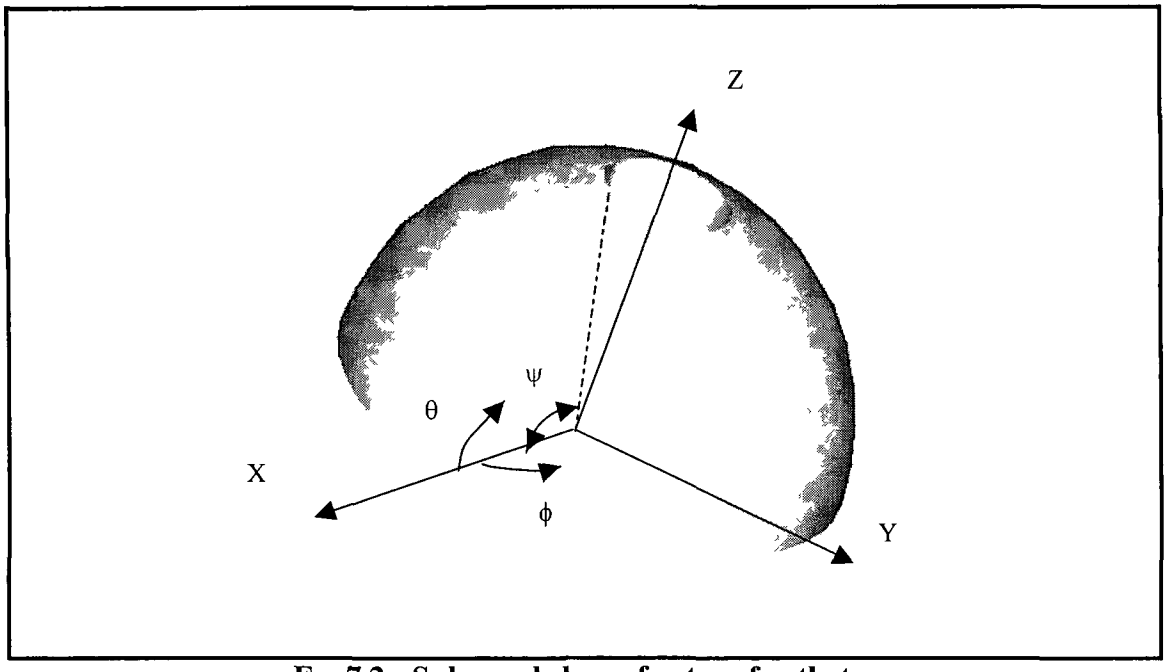

Fig 7.2: Spherical shape for tip of catheter

$$\int_S P\,\mathbf{n}dA = \frac{P}{r}\int_0^{2\pi}\int_0^{\psi} (r^3\cos^2\theta\cos\phi\mathbf{i} + r^3\cos^2\theta\sin\phi\mathbf{j} + r^3\sin\theta\cos\theta\mathbf{k})d\theta d\phi$$

φ represents the angle of the inner hole to the x-axis of the catheter as shown figure 7 2 As can be seen from figure 7 2 that the quadrant in question is facing the z direction, the z-direction is therefore the axis Hence, the forces summed in both the x and y directions will equal zero since their vector fields cancel each other out It is only necessary to integrate the z component of force

b): *Rounded ends in the form of a torus:* The calculation of the force acting on a torus is easily made by considering the parametric representation of a torus referring to figure 7 3

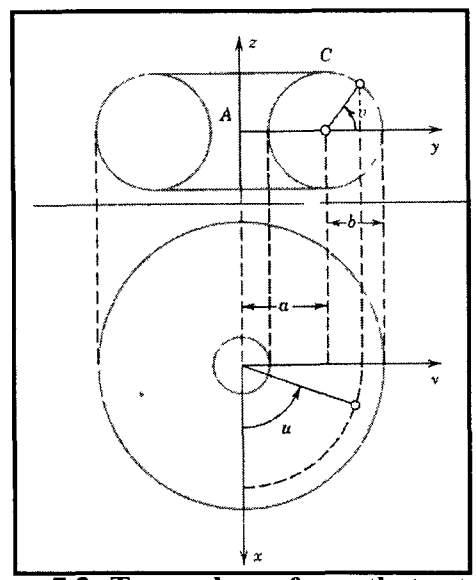

Figure 7.3: Torus shape for catheter tip.

$$S(u,v) = (a + b\cos(v))\cos(u)\mathbf{i} + (a + b\cos(v))\sin(u)\mathbf{j} + b\sin(v)\mathbf{k}$$

To find the unit normal vector, we must find the partial derivatives of both u and v and find their vector product

$$\mathbf{n} = \frac{S'(u) \times S'(v)}{|S'(u) \times S'(v)|} = \frac{b(a + b\cos(v))[\cos(u)\cos(v)\mathbf{i} + \sin(u)\cos(v)\mathbf{j} + \sin(v)\mathbf{k}]}{b(a + b\cos(v))}$$

We are only interested in the z component, since the sum of the forces in the other two directions are equal to zero Therefore the z component of force is,

$$\int_S P\,\mathbf{n}dA = P\int_0^{\pi}\int_0^{2\pi} b\big(a + b\cos(v)\big)\sin(v)\,dudv$$

3. ***Tapered ends:*** A taper can be applied to the ends of the catheter in the form of a cone shape To find the forces acting on the tapered tip, we follow the same procedure as for the rounded ends by calculate the surface integral $\int_S P\,\mathbf{n}dA$ The surface of a cone is represented in Cartesian form by S $x^2 + y^2 - c^2z^2 = 0$, where c is a constant that changes the shape of the taper

unit normal vector of the surface **n** is $\frac{\text{gradS}}{|\text{gradS}|} = \frac{1}{\sqrt{x^2 + y^2 + c^4z^2}}\left(x\mathbf{i} + y\mathbf{j} - c^2z\mathbf{k}\right)$

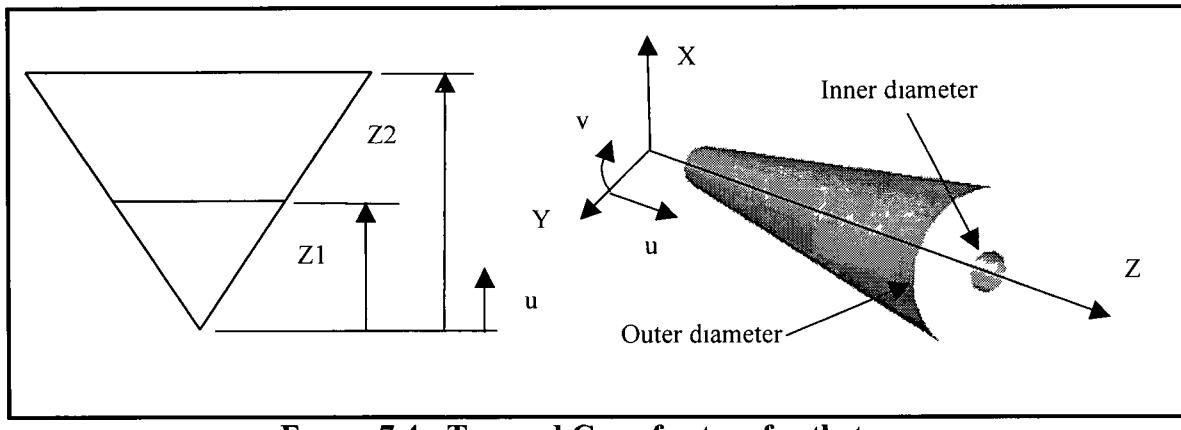

Figure 7.4: Tapered Cone for tip of catheter

In parametric form

x = ucosv, y = usinv, r = cu = variable radius of cone at height u,

$dA = u\sqrt{c^2 + 1}dudv$

We are only interested in the z component of force, since the sum of the forces in the other two directions are equal to zero Therefore the z component of force is,

$$\int_S P\,\mathbf{n}dA = P\int_0^{2\pi}\int_{z1}^{z2}\frac{c^2z}{\sqrt{x^2 + y^2 + c^4z^2}}\left(u\sqrt{c^2 + 1}\right)dudv$$

For each of these surface options the total force on the tip of the catheter is given by equation 7 1

$$\int_S P\,\mathbf{n}dA + C_D \times 1/2 \times \rho \times V^2 \times A \qquad (7.1)$$

C_D for rounded end is the shape of a sphere is = 0 4

C_D for a rounded end in the shape of a torus is = 0 6

C_D for a cone depends on the angle θ of the cone and is shown in table 7 3 The taper of catheter will have θ < 10°, therefore we take C_D = 0 3

θ	10°	20°	30°	40°	60°	75°	90°
C_D	0 30	0 40	0 55	0 65	0 80	1 05	1 15

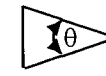

Table 7.3: Discharge co-efficients for cone. ***(Adapted from White ref 53)***

The critical axial force for both guidewire and catheter is given by Eulers equation for buckling

$$\text{Critical Load} = P_{cr} = \frac{\pi^2 EI}{4L^2}$$

L = The length of both guidewire and catheter (take as 500mm)

I_1 & I_2 = second moment of area for guidewire and catheter respectfully

E_1 & E_2 = Young's modulus for guidewire and catheter respectfully E for steel is 200Gpa, E for nylon is 2Gpa & E for PTFE is 0 2GPa

The calculated critical load for buckling is given in Table 7 4

∅ (mm)		Guidewire	Catheter(Nylon)	Catheter(PTFE)
Outer	Inner	P_{cr} (N)	P_{cr} (N)	P_{cr} (N)
3	1 5	0 064	0 0735	0 000735

Table 7.4.

For our proposed delivery system as will be explained in section 7 7 & 7 9, the end of the catheter is shown in figure 7 5 The end can have a rounded or flat faced tip as shown in figure 7 5A or a taper with a rounded tip as shown in figure 7 5B The rounded tip is needed in figure 7 5B to prevent endoluminal injury during delivery of the device

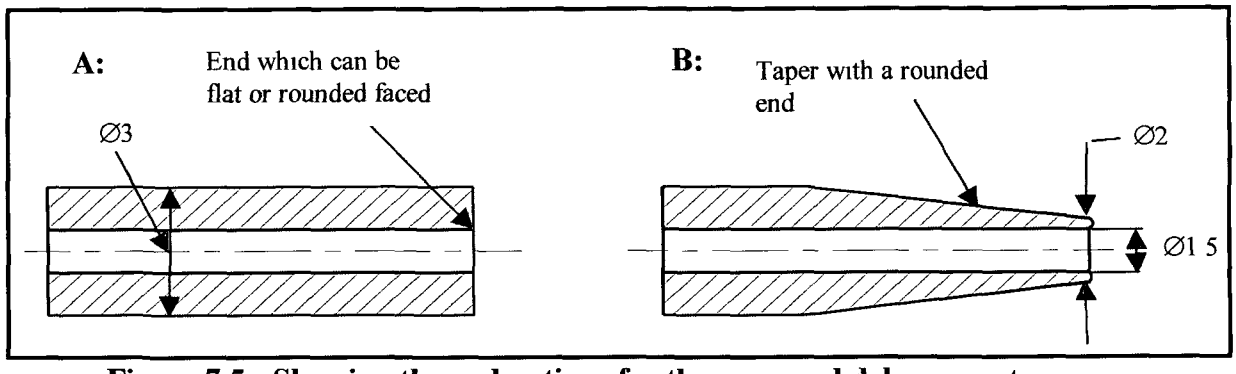

Figure 7.5: Showing the end options for the proposed delivery system

Mathematica is used to calculate the resultant force due to the blood pressure for each of the surface options and is given in Appendix G

∅ (mm)		Flat-faced			Rounded sphere			Rounded torus			Cone - Tapered tip + rounded end		
OD	ID	Force(N)			Force (N)			Force (N)			Force (N)		
		P	I	T	P	I	T	P	I	T	P	I	T
3	1 5	053	001	0540	053	0004	0534	053	0006	0536	014	0002	0142
3	1 5	085	001	0860	085	0004	0854	085	0006	0854	023	0002	0232

Table 7.5: Resultant Forces on Tip of Catheters,
First line corresponds to the reduced blood pressure of 10,000N/m^2
Second line corresponds to a normal blood pressure of 16,000N/m^2.
P is resultant force acting on the catheter tip due to blood pressure
I is the resultant force acting on the catheter tip due to the impact pressure
T is the total resultant force acting on the tip of the catheter = P + I

Note: For the cone – tapered tip a constant length of 50mm was used i e Z2 –Z1 = 50mm Therefore the outer radius = cZ2 and the inner radius = cZ1

As can be seen from table 7 5 that for each tip shape the impact force is considerable less than that of the pressure force for both blood pressures There is 3 to 4 times less force on the tip of the tapered end with a rounded tip than for any of the other types of tip heads The resultant force as calculated by equation 7 1 on the tapered tip is less than that of the critical Eulers load for buckling for both the reduced and normal blood pressures, unlike the other head options Therefore buckling of the catheter due to the blood pressure and impact of the blood on a tapered tip is unlikely For the other head options a stiffer catheter is needed to prevent buckling for the normal blood pressure The calculation was based on a taper length of 50mm A lower resultant force would occur if this length were longer But as can be seen 50mm is sufficient A more flexible catheter can be used with a tapered tip and this will give more flexibility and control around the vascular system

7.4 Arterial Access.

We must know the options available for a safe insertion of the stent graft system The goal of arterial access is the smallest incision that provides safe and effective entry Arterial access sheaths up to 10Fr (French is a scale used for the diameter of catheters, 1Fr = 0 33mm) can usually be placed safely using a percutaneous needle puncture approach For access devices larger than 10Fr, open access is advisable Since our delivery system size is in the range of 24 to 30Fr we must use the open access approach Open access of the femoral artery is usually used for stent graft delivery systems [52]

7.4.1 Open Arterial Access of the Femoral Artery.

Femoral artery exposure is performed in the usual manner with isolation of the common femoral artery and, if necessary, the deep femoral and superficial femoral arteries Figure 7 5 A & B shows the procedure for open access of the femoral artery

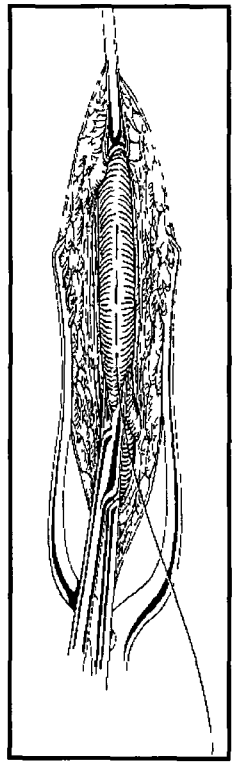

Figure 7.5A: Longitudinal incision of femoral artery ***(adapted from Hokinson ref 4)***

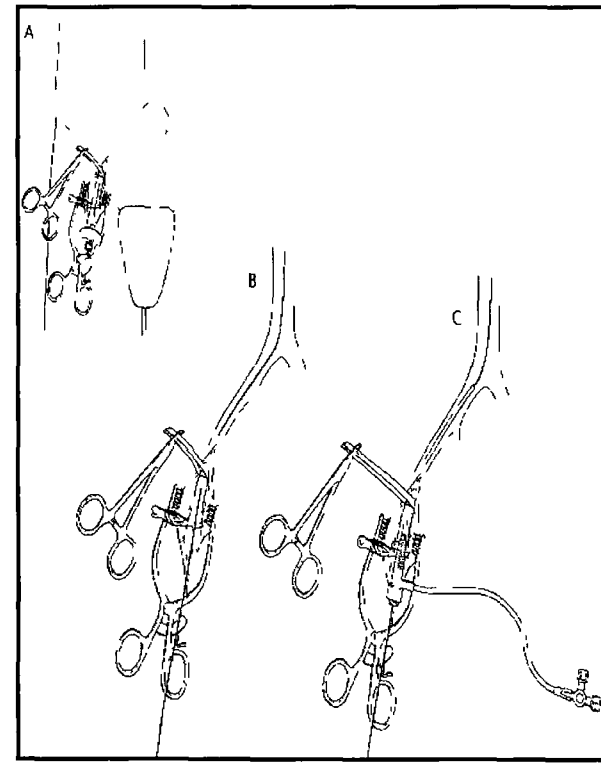

Figure 7.5B: Open access of femoral artery ***(adapted from Schneider ref52)***

A small incision is developed over the common femoral artery by a needle that is placed through the anterior wall of the artery at a 45-degree angle When pulsatile back bleeding is achieved, the guidewire is advanced through the needle The arteriotomy is dilated using progressively larger arterial dilators at increments of 2 or 3 Fr sizes until the appropriately sized sheath can be placed When the device exceeds 14Fr an arterial incision is required This can be done over the guidewire after it is in place Direct finger pressure at the site maintains hemostasis until the sheath can be advanced

Once the sheath is in place, leakage of blood around its shaft at the arteriotomy site is controlled by applying traction to the double-looped Penrose drain that encircles the proximal common femoral artery If traction alone is not adequate, a Kelly clamp is advanced to the level of the artery and the Penrose dram is pulled up tight and clamped

The delivery system can now be guided up through the femoral artery to the site of the aortic aneurysm

Note:

1. If common femoral artery in large and diseased, it should be opened longitudinally, following insertion of a guidewire through a needle puncture This minimises risk of an arterial dissection
2. Longitudinal arteriotomy (cut in artery) is preferred when delivery system is large
3. Transverse ateriotomy is more likely to extend circumferentially, especially if femoral artery is not supported during delivery system insertion
4. For the passage of large devices, exposure of the entire length of the common femoral artery and localisation of the medial and lateral iliac circumflex vessels is useful
5. Occasionally, when the iliac artery is tortuous or heavily diseased, or the endovascular devices for passage is particularly sizeable, the distal external iliac

artery is mobilized through the groin so that it can be straightened with caudad traction

6. Sheath size is limited by the diameter of the femoral artery rather than by the usual hemostatic limits of percutaneous puncture The initial sheath choice should be gauged according, using the largest anticipated sheath that will be required Once the arterial entry has been made, it is difficult to maintain hemostasis during sheath exchanges because the surrounding compressive tissue has been dissected away Therefore, the need for sheath exchanges should be minimized

7.5 Graft Systems.

There are two types of graft systems

Straight graft systems: Straight grafts are used for aneurysms below the renal arteries and above the iliac bifurcation There has to be sufficient proximal neck length between the renal arteries and the aneurysm and also sufficient distal neck length between the aneurysm and the iliac bifurcation for anchorage of both proximal and distal stents Straight graft systems are limited in their use as most aneurysms form at the junction of the Aorta and Iliac arteries, so bifurcated systems must be used instead

Bifurcated systems: Bifurcated systems are more complicated than straight graft systems Bifurcated systems are used when the aneurysms form at and below the junction of the Aorta and Iliac arteries There are two types of bifurcated grafts

- ***Unitary construction:*** Bifurcated graft as a single component
- ***Modular construction:*** One leg is attached in the Aorta

A summary of the two methods is given in Table 7 6

Modular	Unitary
Requires catheterization of the recipient site on the main graft	Requires insertion of cross-femoral catheter
Simple stent-graft components and delivery systems	More complex graft construction and delivery system
Nonidentical limbs easy to customise from stock components	Customization must be performed at the time of graft manufacture
Graft-graft junction created within the aneurysm, potential site for leakage	Bifurcation sewn, knitted, or woven into the graft, predictable durability
Easy to delivery in a fully stented form	Difficult to delivery fully stented, additional stents must be added as needed

Table 7.6

For our bifurcated system, we will try to improve the Unitary approach and propose ways of simplifying and improving the delivery system so that the problems in given in table 7 5 can be rectified It must be emphasised that for testing and design proposes we must start from the simple (straight graft systems) to the complex (unitary bifurcated systems) The design procedures solved and tested for straight systems can be directly applied to portions of the delivery system used for bifurcated systems

7.6 Miniaturisation.

This is the overall design consideration that is constantly been improved For a safer delivery, the device when crimped has to be as small as possible The following are the some of the important issues for miniaturisation of the Endovascular device

- For stent grafts - the smallest size of the crimped device is limited to the folding of the graft rather than the crimping of the stent
- Crimping of the stent graft is a crucial issue for the overall miniaturisation of the device The smallest diameter of the catheters depends on this limiting factor When trying to achieve the smallest device possible, a safer and an easier delivery system is achieved

7.6.1 Folding of the graft material.

To achieve the smallest profile possible we must crimp the graft as small as possible One method already exists and that is wrapping of the graft around the catheter and stent as shown in figure 7 6

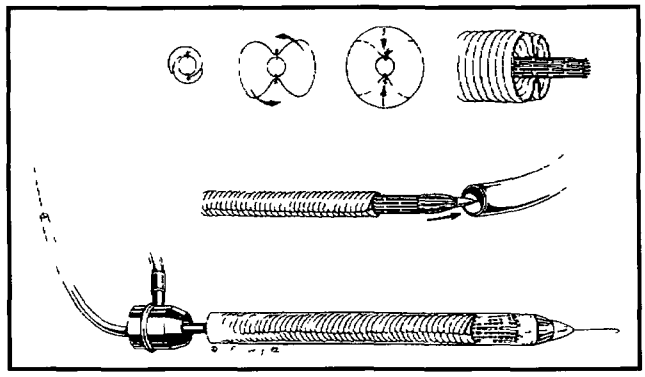

Figure 7.6: Method of wrapping graft around stent and catheter ***(adapted from Hokinson ref 4)***

Another method could be tried out as shown in figure 7 7 That is an eight sided shape been folded into a four sided shape

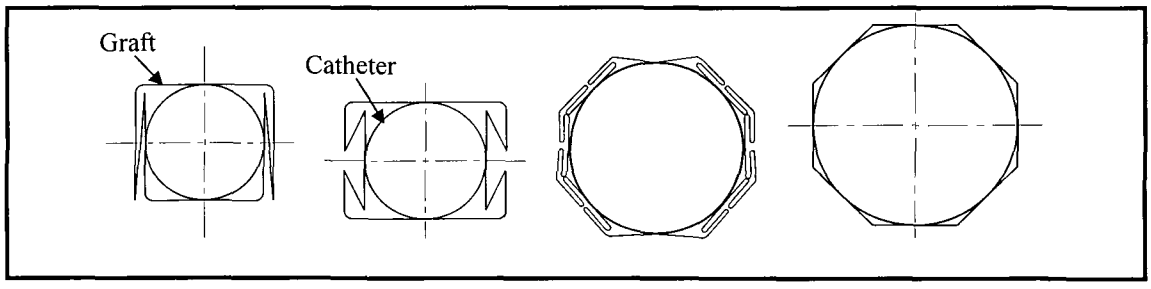

Figure 7.7A: **Figure 7.7B** **Figure 7.7C** **Figure 7.7D**

Figure 7 7A & Figure 7 7B shows how an eight sided shape can be folded into a four sided shape Figure 7 7C shows how a twenty sided shape can be folded into an eight sided shape Figure 7 7D shows an example of an unfolded eight sided shape

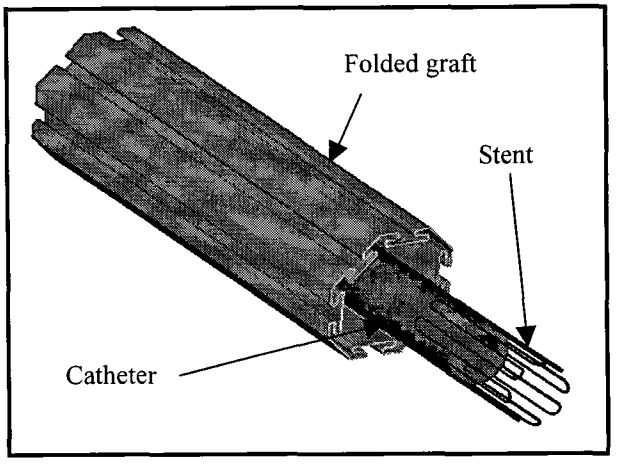

Figure 7.8: 3-D View of Disassembled Folded graft.

Table 7 6 shows the length of the diagonal of the folded shape for a eight sided shape folded into a four sided shape & a twenty sided shape folded into a eight sided shape

For a 8-sided shape folded into a 4 sided shape		**For a 20 sided shape folded into a 8 sided shape.**	
Diameter(mm)	**Length(mm)**	**Diameter(mm)**	**Length(mm)**
20	10 82	20	8 17
22	11 91	22	8 99
24	12 9	24	9 81
26	14	26	10 62
28	15 15	28	11 44
30	16 2	30	12 26

Table 7.6

When the Graft material is folded onto the stent and catheter the graft material can be squeezed tighter and compressed against the catheter and therefore this would reduce the diameter of the folded shape For example the 28mm diameter graft can be compressed into an 8mm-diameter sleeve

Figure 7 8 shows a 3-D view of a straight folding design for the disassembly of the folded graft and crimped Z-stent

Since the stent is sewn onto the graft while in the unfolded state, the actual folding method does not matter The graft material is a textile fabric, which can be easily squeezed or wrapped any way onto the catheter

7.6.2 Procedure for Crimping Stent & Graft.

When trying to compress a graft and placing it through a sleeve the following procedural method is advised

For a Straight Graft:

1. Sew Z-stent onto the unfolded graft at proximal and distal ends
2. Radically crimp the stent with your fingers and hold stent in final crimped position with either an elastic band or tie a bow knot around the stent
3. Wrap, fold and compress the graft material
4. Wrap a polyester or nylon fabric around the compressed graft material and hold the fabric in place using tape
5. Push the sleeve up through the wrapping fabric
6. Pull out the wrappings fabric and the restraints around the stent

For a Bifurcated Graft:

The same general procedure for the straight graft is used for the bifurcated graft but with a few extra procedures and precautions

1. For a unitary bifurcated graft, the two legs must be folded and squeezed separately and not wrapped around each other
2. Two separate fabrics are to be wrapped around each leg of the bifurcated graft
3. Two sleeves are then pushed up through each leg
4. The two fabrics are then removed
5. The stent and graft of the proximal end are crimped and compressed and a fabric wrapped around it, similar to the straight graft method
6. The main sleeve is than pushed up through the both legs and the proximal end
7. The fabric is then removed

Note: It is important for the delivery of a unitary bifurcated graft that the two folded or compressed legs act like a hinge at their bifurcation point So that each leg can be positioned into their respective iliac legs when they are in their compressed state

Figures 7.9- 7.11 shows the miniaturisation of the stent and bifurcated graft (see section 6.8, chapter 6 for the unfolded stent graft). The proximal diameter of this bifurcated graft is 30mm. When crimped, the stent and folded graft can be placed inside a ∅8mm sleeve. You can also see in figure 7.10 the bow knot holding the stent in place.

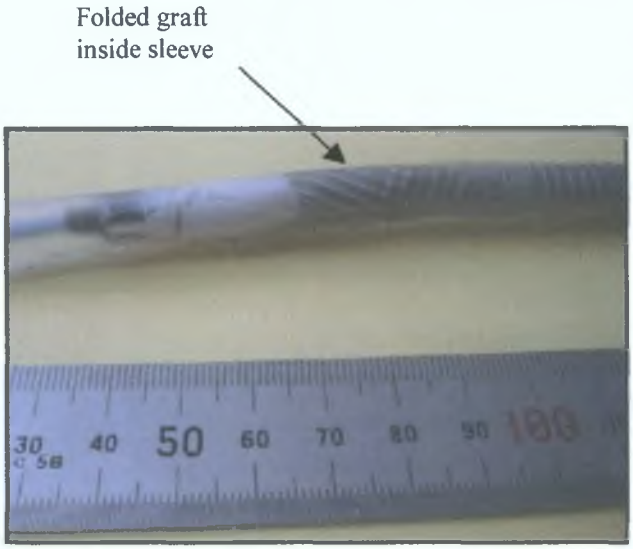

Figure 7.9: Crimped stent and folded sleeve inside the graft

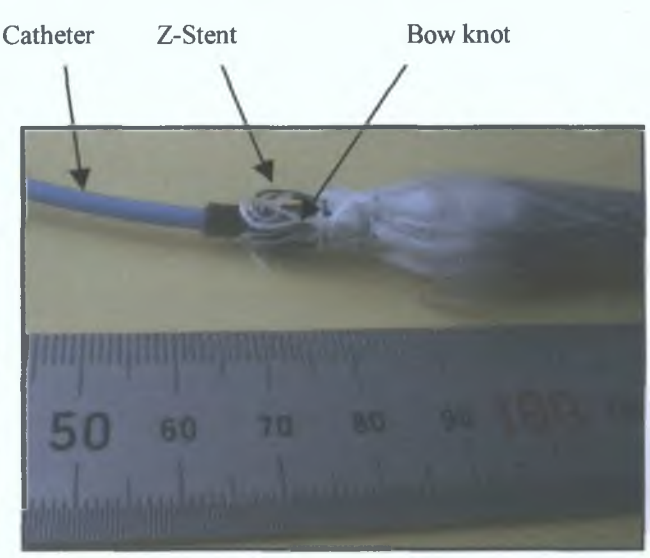

Figure 7.10: Part of sleeve pulled off, showing the bow knot around the stent.

Figure 7.11: Showing measurement of crimped stent and folded graft in mm.

7.7 Methods of Deployment.

This is one of the most important issues in endovascular surgery. There can be numerous methods available for a bifurcated system. The best method is one that is simple and yet effective. The more complicated the procedure, the more likely that problems will arise. The method of deployment must achieve the following goals:

- Accurate positioning of the stent graft between the renal and internal (hypogastric) iliac arteries.
- An attachment mechanism for the proximal and iliac stents that is capable of releasing the stents and thus attaching the graft against the wall of the aorta and also the walls of the both iliac arteries.
- A safe withdrawal of all guidewires, catheters, attachment mechanisms and sleeves.

Once these goals are achieved, the bifurcated graft will block off the aneurysm sac from the flow of blood and thus preventing it from expanding any further. As a result preventing rupture.

7.7.1 Difficulties in Unitary approach.

The basic difference between a modular construction and unitary construction is that in the modular design the proximal end and one leg are as one unit and are first positioned and then the other leg is then position and attached to at the bifurcation point. The unitary design has the whole graft as one unit. From a delivery point of view this causes a few extra problems which are not associated with the modular design.

1. The placement of an unitary graft is a complex matter since we have to position the other leg of the graft in the other iliac artery while the whole graft unit is in the vascular system.
2. Removal of the proximal stent posses a problem. Since in the modular construction the outer sleeve can easily be pulled down thus releasing the stent. But in the unitary construction the sleeve cannot be pulled down due to the position of both legs in the iliac artery which causes the graft to open in a Y-shape and thus blocks any form of sleeve from been pulled down over the entire graft.

The main advantage of the modular approach is that there is no need to attach the other leg at the bifurcation point. This can be a tricky operation due to the difficulty in accurate placement. The modular approach does not facilitate the taper design as described in Chapter 6, because accurate placement of the other leg needs to be done on a straight portion of graft.

7.7.2 Attachment Mechanisms.

Before we look at the method of deployment we should try to solve the problem of releasing the proximal stent. If we want to position the graft while in a folded state in the other iliac artery we must devise a method of releasing the proximal stent.

- ***Removal Cap Method:***

Since we cannot pull off a sleeve or cap downwards, this lead me to try to pull the cap upwards.

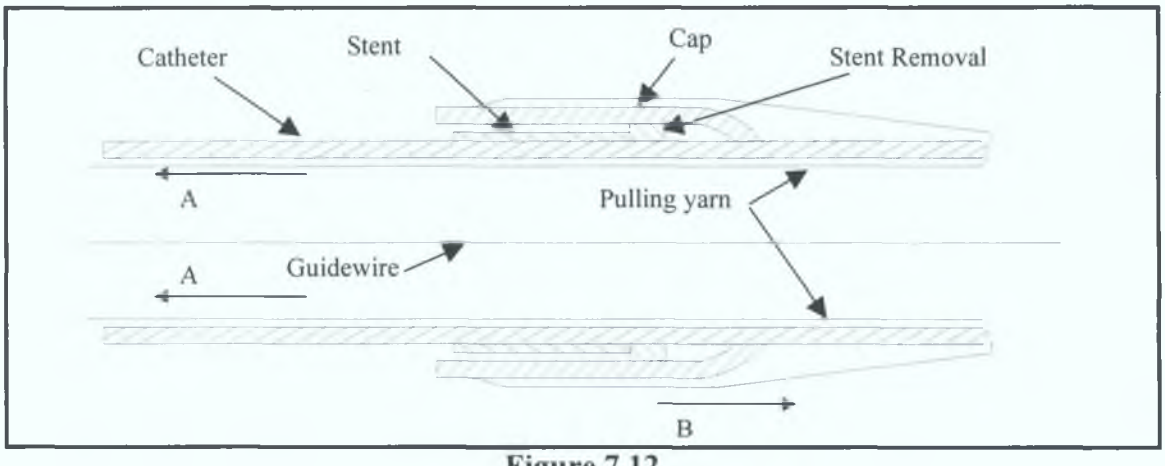

Figure 7.12

Referring to figure 7.12, which is a sectional view of the removal cap method. The procedure is as follows:

- The pulling yarn is pulled in the direction of arrows A.
- The yarn which is connected onto the cap pulls the cap in the direction of arrow B and thus releasing the stent.
- The stent removal is needed so as to prevent the stent from slipping up the catheter with the cap.

- The cap is then removed with the catheter through the unfolded graft and stent
- The yarn can be either be mono or multi filament

Problems with this design.

1. Due to a thickness of cap, which is needed to hold down the stent, this could cause damage to the interior wall of the artery Therefore the cap increases the stiffness of catheter
2. Frictional forces at tip of the catheter causes buckling of catheter This is mainly caused by the increased tension that is needed to pull the pulling yarn around the tip of the catheter

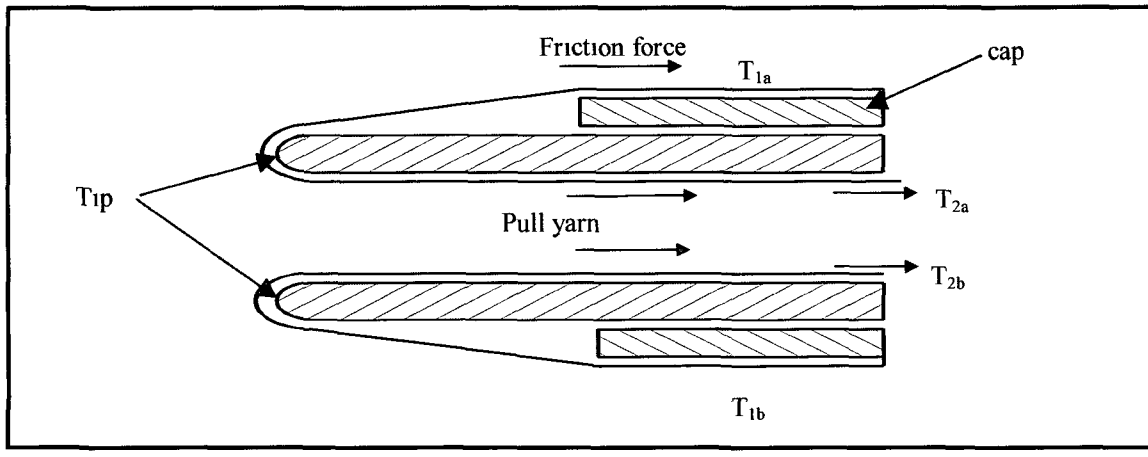

Figure 7.13

Referring to figure 7 13, when the cap is pulled off by the pull yarn, the radial force of the crimped stent is acting outward onto the cap This radial force causes a frictional force equal to $\mu \times$ radical force The value of the two incoming tensions added together is

$$T_{1a} + T_{1b} = \text{Frictional force} = \mu \times \text{radial force}$$

When the yarn is pulled around the top of the rounded cap the applied tension must be increased by an amount necessary to overcome the frictional resistance of the rounded tip. The increased tension is found by applying Amontons's law

$$\frac{T_2}{T_1} = e^{\mu\theta}$$

T_2 = leaving tension

T_1 = incoming tension

μ = coefficient of friction

θ = angle of friction in radians, which is equal to π

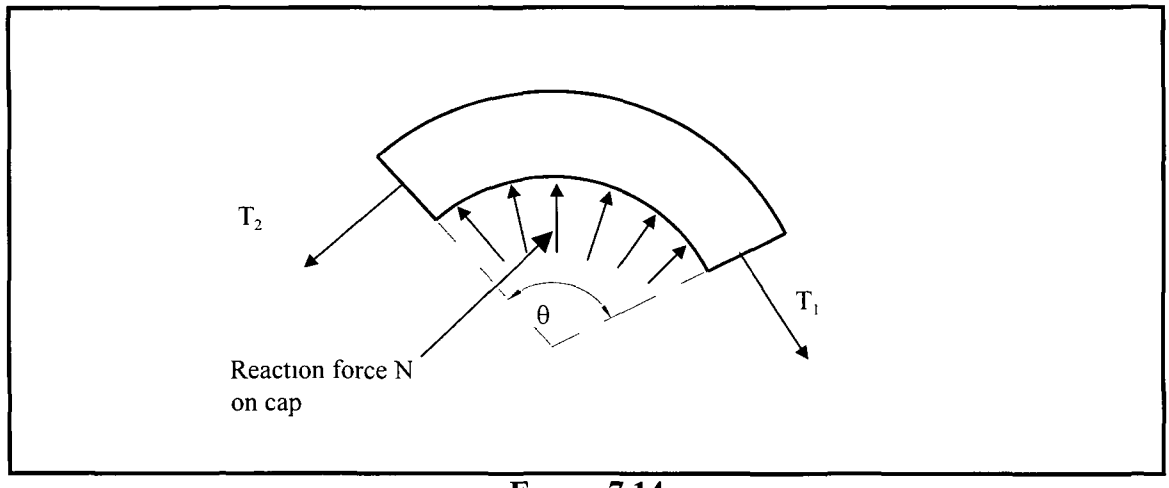

Figure 7.14

The total reaction force N in the x-direction on the cap from 0 radians to π is

$$\text{Reaction force in x-direction} = Nx = \frac{\int_0^{\pi} T_1 e^{\mu\theta} \cos\left(\frac{\theta}{2}\right) d\theta}{\mu}$$

Now the friction force is acting on both edges of the cap so the component of the reaction force in the y-direction will cancel each other out The total force in the x-direction will be 2Nx Axial loading can be assumed, since both forces are acting along the same distance from the axis, along their respective centroids Therefore, this eccentricity has cancelled each other out If 2Nx is greater than Pc, failure by buckling will occur

When this equation is integrated from π to 0 as given in Appendix G, the total resultant force acting on the tip of the catheter is 14 $134T_1$

So the total force acting on both catheter tips is

$$2Nx = 14\ 134(T_{1a} + T_{1b}) = 14\ 134(\mu \times \text{radial force})$$

As can be seen, the reaction force caused by the tip of the catheter is 14 times greater than if you pulled the cap off directly towards you as is done by the modular approach

3. Problems encountered during retrieval, as large cap could get jammed in graft

- ***Bow Knot Method:***

Instead of using a cap, a bow knot is used to release the proximal stent as shown in figure 7 15

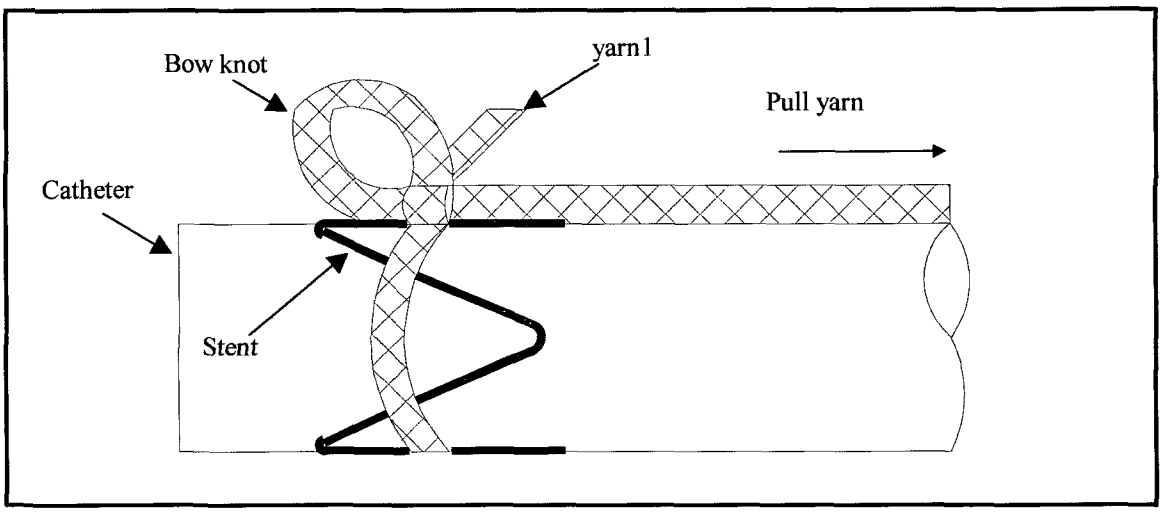

Figure 7.15

A monofilament or multifilament yarn is used to tie the bow knot A multifilament yarn is preferred because no creases will develop at the knot intersections unlike if a monofilament is used due to its greater bending resistance The procedure is

- When you pull the pull yarn in the direction of the arrow the bow part of the knot will reduce in size
- With continuing pulling, the knot will be opened and the stent will be released due to its radical force
- Yarn1 & the bow should be kept as small as possible Two bow knots could be used to hold the stent if so desired

- A stent removal similar to the cap method is also needed to prevent slippage of stent
- The friction force is comparable to that of the unitary approach of removing the stent by pulling the sleeve, unlike the previous removal cap method

Advantages of the Bow Knot.

1. There is a reduced thickness and size on the catheter, which leads to a reduced stiffness at the leading edge of the catheter This leads to a safer delivery with a reduced risk of arterial wall damage unlike with the cap method
2. Since the pull yarn of the bow knot can be pulled directly downwards without the need for pulling it around the top of the catheter this prevents an extra frictional force on the catheter tip
3. This method leads to a safe retrieval of the yarn

7.7.3 Deployment Methods.

This is the most important part of the delivery system design The method of deployment has to be simple in design The more complex your system, the higher the risk of failure and ultimately the consequences can be catastrophic for the patient

The steps of the delivery system design is

1. **The positioning of the graft into the other iliac artery.**

- ***Hinged Catheter:*** This is where a catheter longer than the length of the leg of the graft is hinged onto the main catheter see figure 7 16A The bifurcated graft is positioned onto the catheter and folded Once the legs of the graft are over the iliac bifurcation point there are a number of options for opening the hinge

  i: The hinged catheter could be opened and closed by a pull string mechanism as shown in figure7 16B As yarn A is pulled and yarn B is kept taught, the second catheter will open As yarn B is pulled and yarn A is kept taught, the second catheter will close The catheter then can be guided into the other iliac artery

ii: Two way memory shape memory alloy wire could be used as a hinge Current could be applied to the S M A wire and the heat generated would open the wire in the form of a hinge Removal of the current and the S M A wire would revert back to its' preset condition

iii: Instead of using a pull string mechanism, a snare catheter could be used as shown in figure 7 16C The snare catheter is inserted from the other iliac artery The loop is used to grab onto the hinged catheter and therefore you can pull this catheter into the other iliac artery

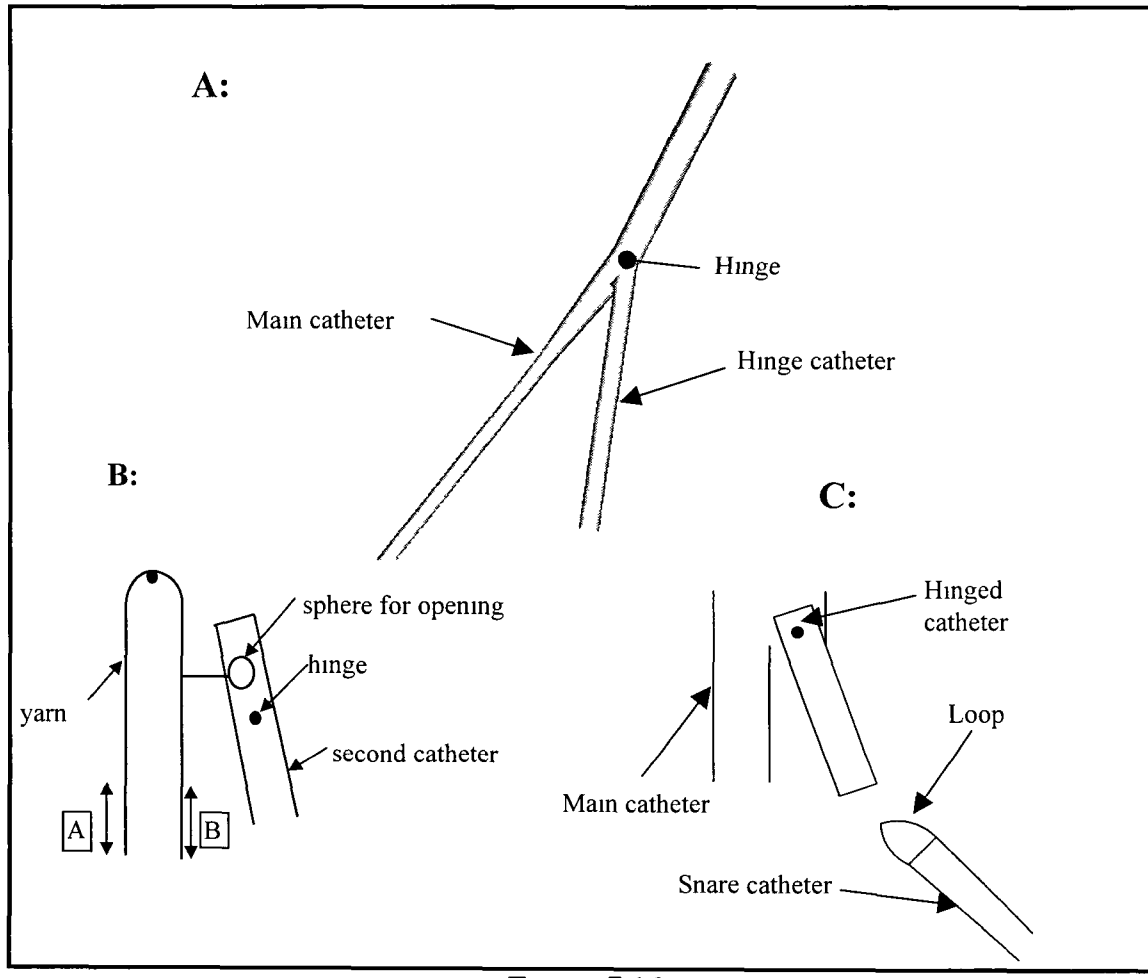

Figure 7.16

- ***Cross-femoral catheter:*** As shown in the figure 7 17 is a hooked shaped catheter which is inserted from the other iliac artery Guidewire 1 is pushed through this hooked catheter The hooked catheter guides guidewire 1 into the iliac artery where all the manipulations are done Guidewire 1 is then tied to guidewire 2 and pulled

back through the hooked catheter and thus pulling the other leg of the graft into its iliac artery. For clarity in drawing the main catheter system is not shown. There can be a hinge catheter but this is not needed as the graft material can act as a hinge.

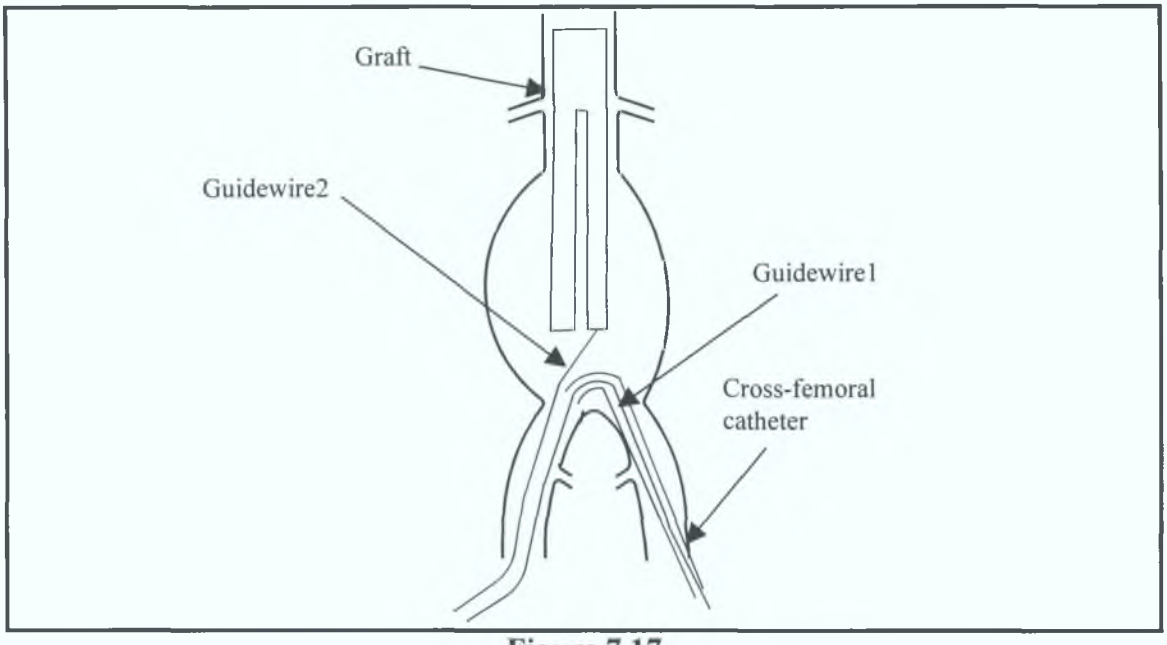

Figure 7.17

- ***Hinge graft:*** An easier catheter design is to have no hinged catheter and no catheter positioned into the other leg of the graft similar to that of the cross-femoral catheter. The proximal end of the graft and one of the legs are positioned onto the main catheter leaving the other leg free to rotate. The other leg is folded inside a sleeve. A snare catheter is used to pull the other graft leg into the iliac artery. This method uses the graft as a natural hinge. This is the preferred method to use for our delivery system.

2. **Releasing Distal Stent:** Due to the problem of wave reflections we need two distal stents positioned at the end of each leg. The distal stents are positioned at the end of each leg. The distal stent on the first leg can be released by a either a cap or bow knot where either can be pulled down towards you. The distal stent on the other leg is a more tricky stent to release. The options for such a design are:

   i: A sliding catheter would be a catheter capable of moving up and down through the main catheter and the second catheter as shown in figure

7 18A Figure 7 18B shows how a sliding catheter is capable of pulling off the second sheath and removal of this sheath up through the second leg of the graft Due to miniaturisation of the catheter system, failure due to buckling could be a problem

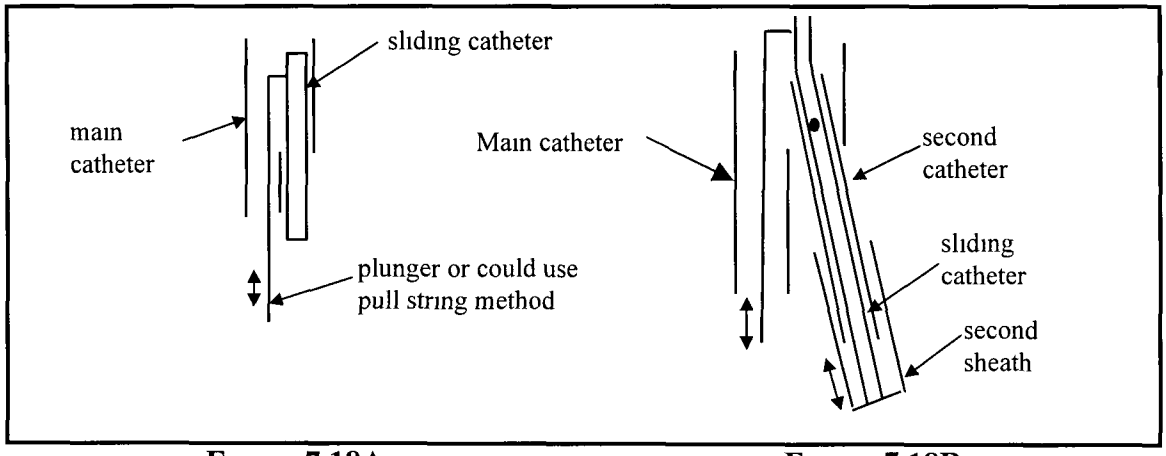

Figure 7.18A **Figure 7.18B**

ii: The distal stent which is sewn inside the folded graft leg would not need the support of a sliding catheter or any other catheter for that matter A sleeve or cap would be covering the distal stent A snare catheter could be inserted from the other iliac leg and thus capable of grabbing the sleeve and pulling it off and thus releasing the stent The cross-femoral method could also be used for this propose

iii: Instead of having the distal stents sewn onto the graft in the first place, you could position both or one of the distal stents after placement of the main bifurcated graft The main advantage of this would be customisation of the length of the graft Customisation could be achieved from stock components This will be further explained later in this chapter

7.8 Comments & Further Options For Delivery Methods.

Before I explain the final procedure for this proposed delivery system, some comments and further options will need to be explained first.

1. The snare hook method is the simplest and most widely used method for grabbing objects such as guidewires, catheters etc, in the arterial system in the body. The use of the snare hook method is the best for it cuts out the need for any snap on or hooking up mechanism which would be difficult and impractical to position in the aorta. It also prevents the use of a cross-femoral catheter which could cause damage at the junction of the iliac bifurcation.
2. The use of an occlusion balloon at the tip may be needed to reduce blood flow during the stent delivery. To falicate this multi-lumen tubing is needed. As shown in figure 7.19, there are a lot of options and different range of sizes available for multi-lumen designs.

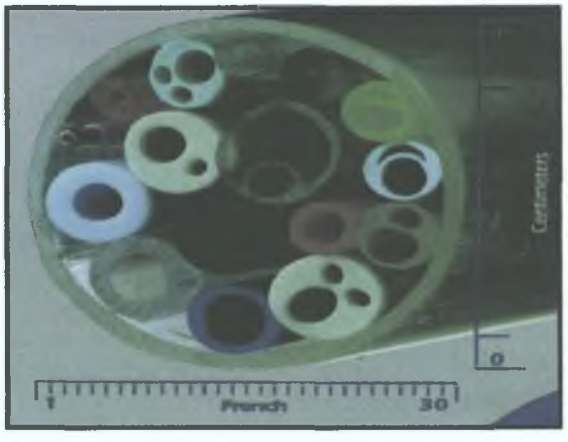

Figure 7.19. Multilumen tubing ***(Precision Extrusion, INC)***

3. A central balloon can be inserted latter for further fixation of stent against wall of the artery.
4. Bifurcated devices needs radiopaque markers at the proximal end and the two distal ends and throughout the graft material to allow for better visualisation of the system and correct positioning of the graft limbs during deployment.
5. The sheath should be made from Teflon (PTFE) since this material has the lowest co-efficient of friction.
6. There is no need for a pusher rod during the releasing of the stent due to the stent removal method.

7. Special hydrophilic coatings for catheters produce a surface, which becomes very lubricious when it is wetted with various body fluids These coatings can be applied by dipping or spraying on catheters, guidewires etc It is an effective way of making catheters biocompatible, antithrombogenic and antibiotic
8. Customisation can be achieved from stock components if distal stents are added after placement of main bifurcated graft The main sleeve (see figure 7 20) can have one or two slits depending if delivery catheter is inside or outside of graft If catheter is outside of the graft, then both iliac legs with their respective iliac caps can be easily obtained through both slits as shown in figure 7 20 and thus sized accordingly If the catheter is inside the graft, only one of the iliac legs can be obtained and sized through the slits of the main sleeve

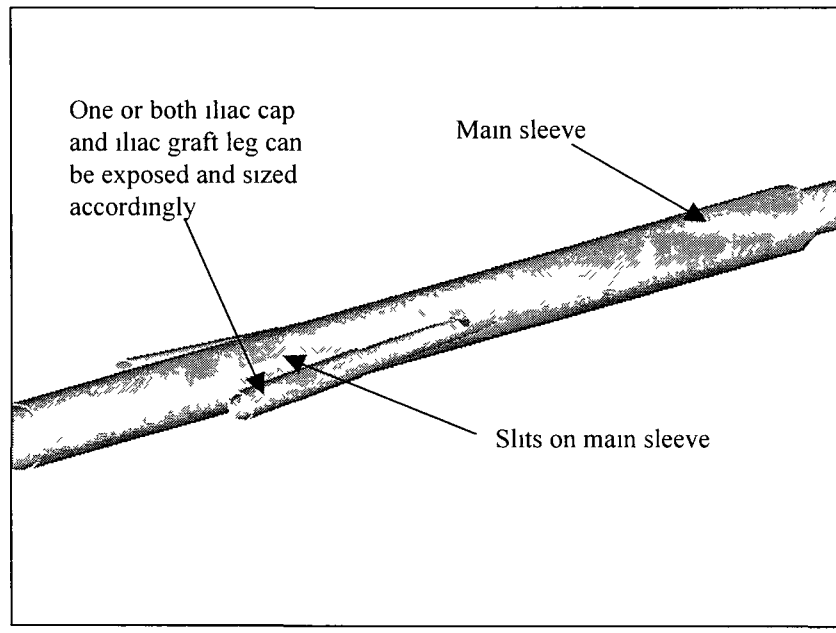

Figure 7.20: Customisation of Graft.

7.9 Joining of Catheter Parts.

The components for our delivery systems must be bonded together Several welding methods are suited for the bonding of plastic components from laser systems to ultrasonic or vibration technology Laser systems can produce flash-free joints and does not leave behind residue that might contaminate components, it is suited for bonding sensitive parts While most thermoplastics can be laser-welded, a successful bond is depended on one of the bonded parts being transparent and the other containing a heat-absorbent additive If, however, the bonded materials are characterised by a mismatch in the coefficient of thermal expansion, cooling rate, or modulus, or if there is poor molecular weight distribution, adhesives may be your best option Adhesives such as acrylic, epoxy, loctite, urethane, silicone, or UV-curing formulation is the most appropriate materials Epoxy technology for example is used to bond and coat endoscopes, catheters, pacemakers and related devices that require failure free performance [55]

7.10 Procedure for Proposed Delivery System.

The delivery of this stent graft system includes the positioning of the device using special over-the-wire techniques, an attachment mechanism which releases the stent and subsequent positioning of the stent graft against the wall of the artery

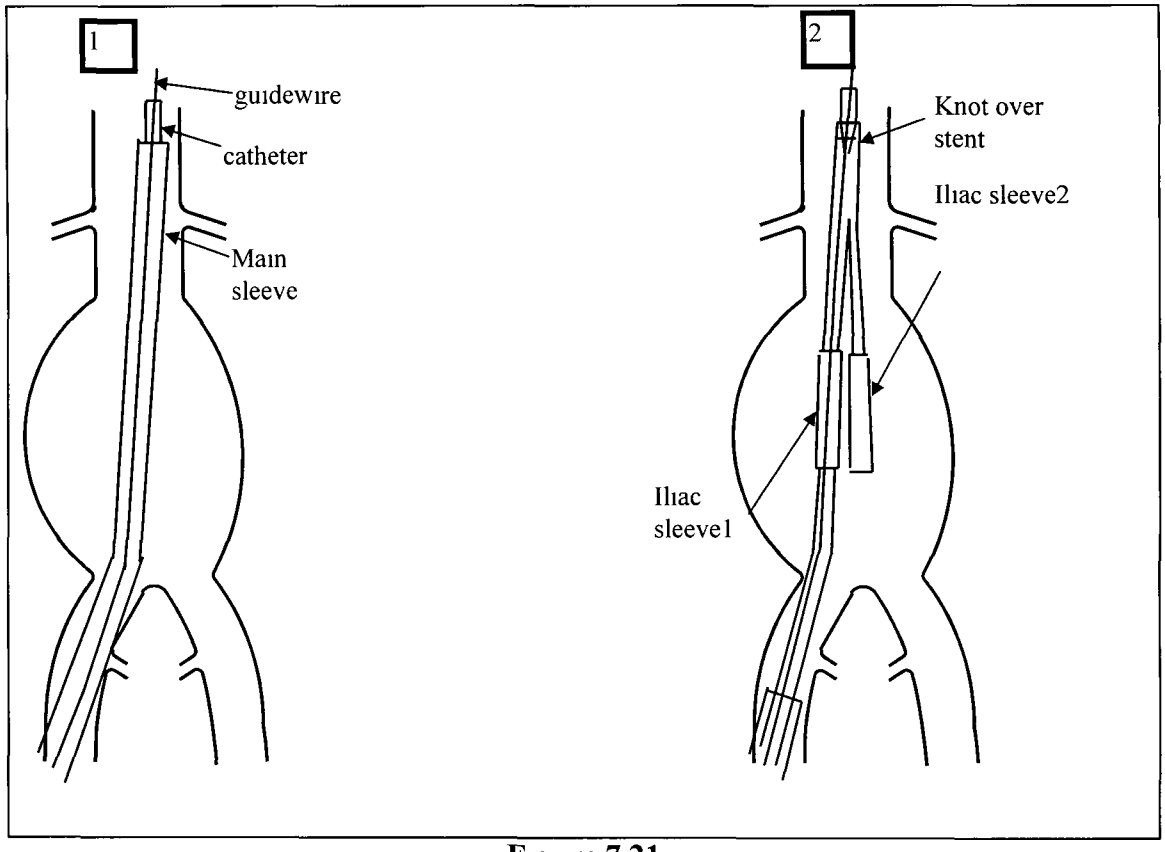

Figure 7.21

1. **a)** Introduce guidewire through femoral artery arteriotomy

   b) Push main catheter system over the guidewire, which contains the stent, graft, catheter, sleeve, attachment mechanism etc Push the catheter system until the end of the graft leg is over the bifurcation point of the artery A radiopaque mark on the sleeve should aid in placing this

2. Pull back the main sleeve while holding the main catheter stationary

Note: Two options are available

1. The main catheter can beside, over or under the compressed graft as shown in figure 7 22 This gives the option of customising both iliac legs
2. The main catheter can be through the compressed graft as shown in figure 7 23 This gives the option of customising one iliac leg

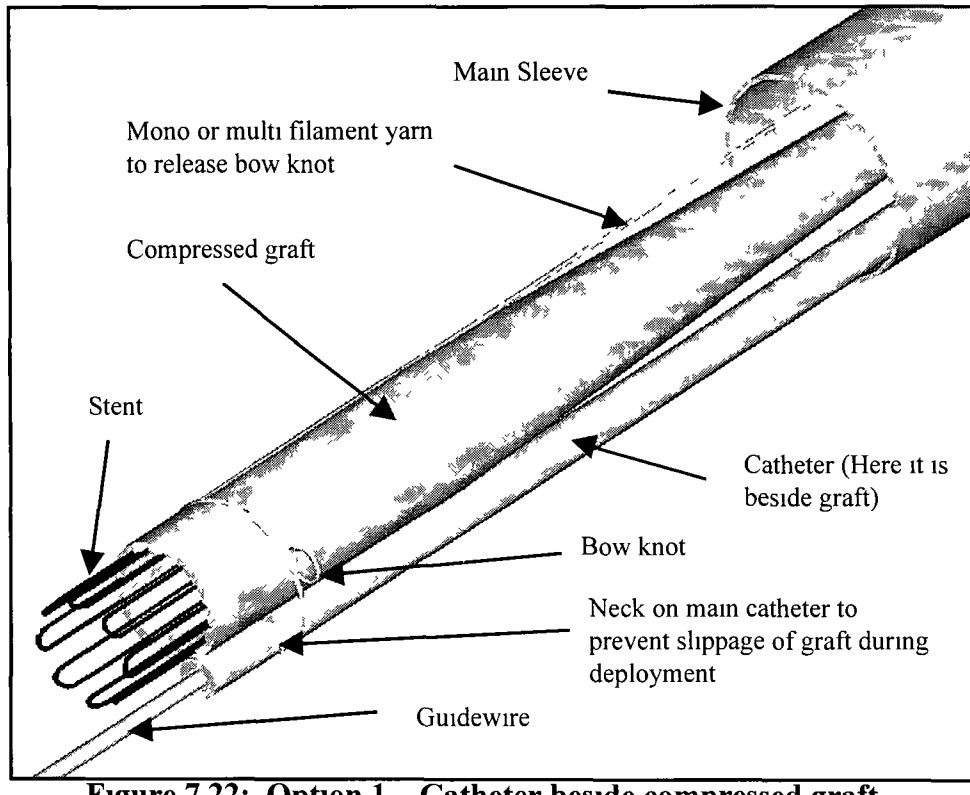

Figure 7.22: Option 1 – Catheter beside compressed graft.

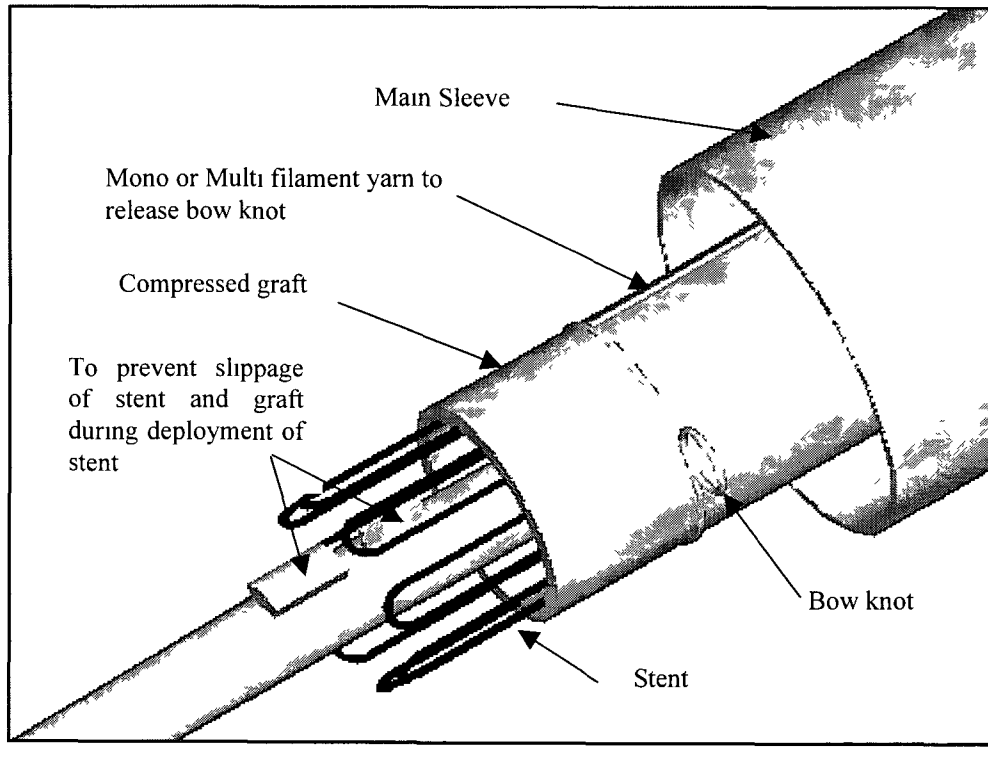

Figure 7.23: Option 2 – Catheter can be through compressed graft.

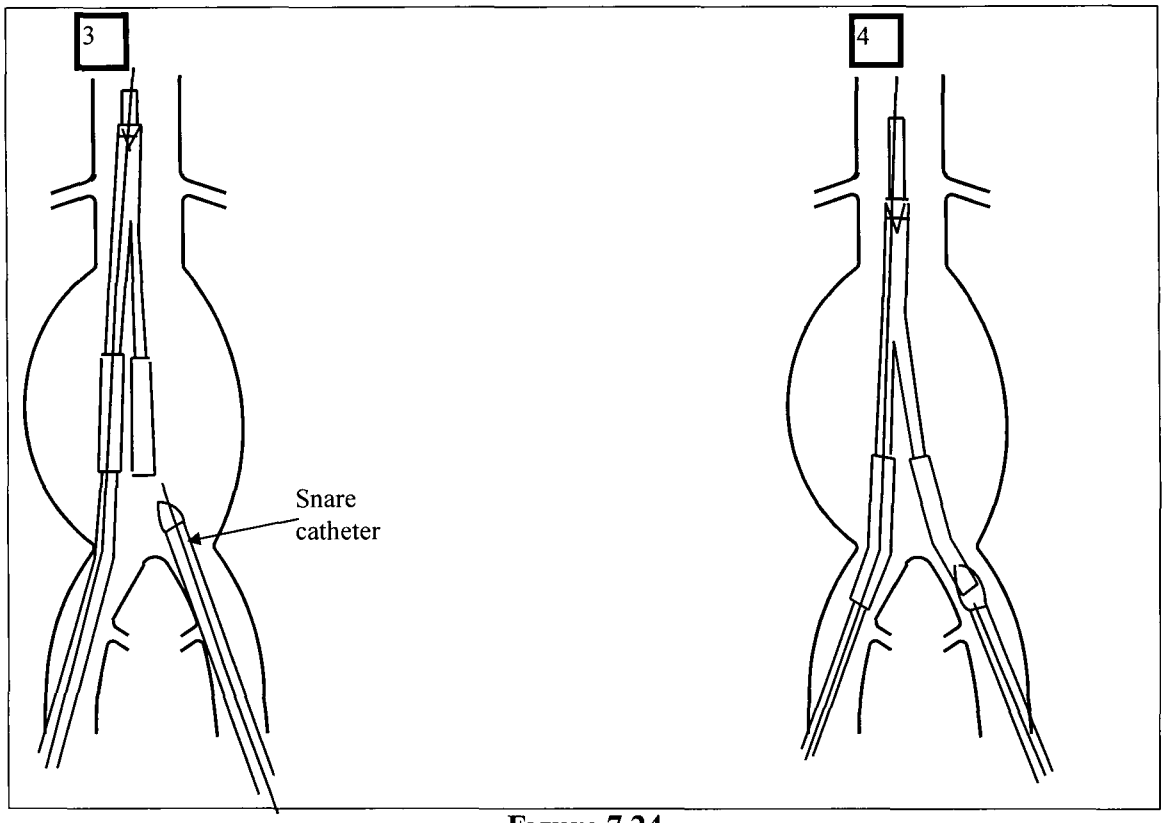

Figure 7.24

3. **a)** Insert a guidewire through the other femoral artery
   b) Guide a snare catheter with its' snare loop up through this guidewire to the iliac sleeve2 as shown in figure7 24 & 7 25
4. **a)** Loop the snare loop around the iliac sleeve2 and thus gripping the iliac sleeve2
   b) Pull both the main catheter and the snare catheter so that both iliac legs are positioned into their respective iliac arteries

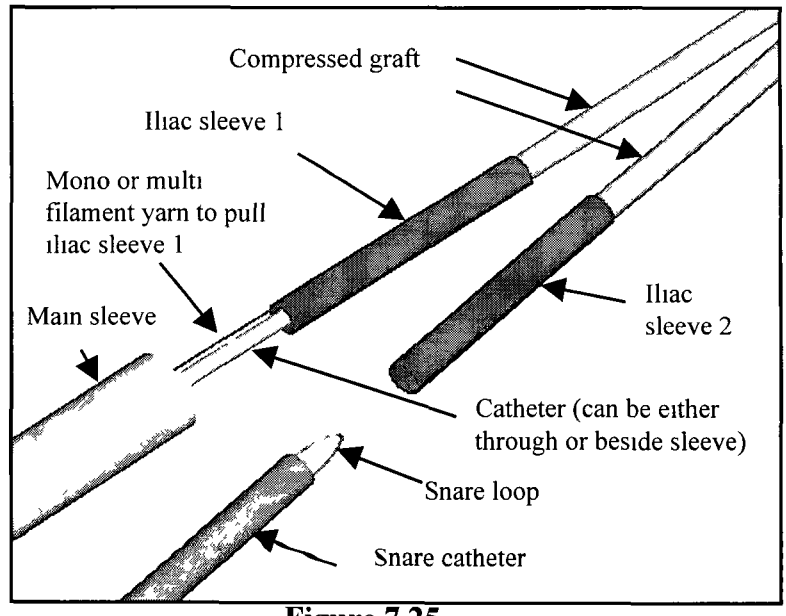

Figure 7.25

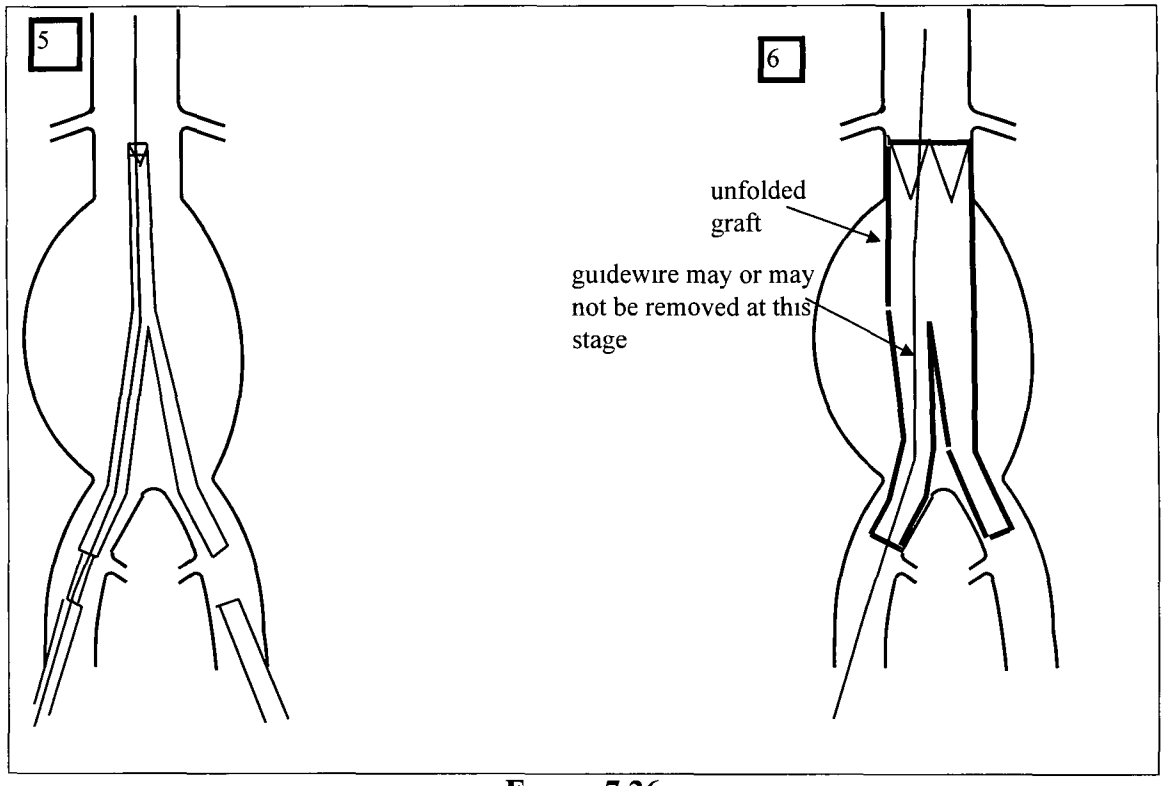

Figure 7.26

5. While holding the main catheter in place, pull off the two sleeves over each leg of graft Iliac sleeve 1 is removed by a mono or multi filament yarn which is attached to iliac sleeve 1 as shown in figure 7 26 The snare catheter is used to remove iliac sleeve 2
6. **a)** Pull the mono or muti filament yarn to release the knot and therefore releases the stent and main catheter Inflation of a balloon (which is positioned in front of the stent) is optional before releasing stent so as to reduce blood flow while positioning and final expansion of the stent

   b) The blood flow and pressure should unfold out the graft

   c) Remove the mam catheter and guidewire If the catheter is inside the graft there is no need to remove the guidewire at this stage But if the catheter is under or over the graft the guidewire has to be removed

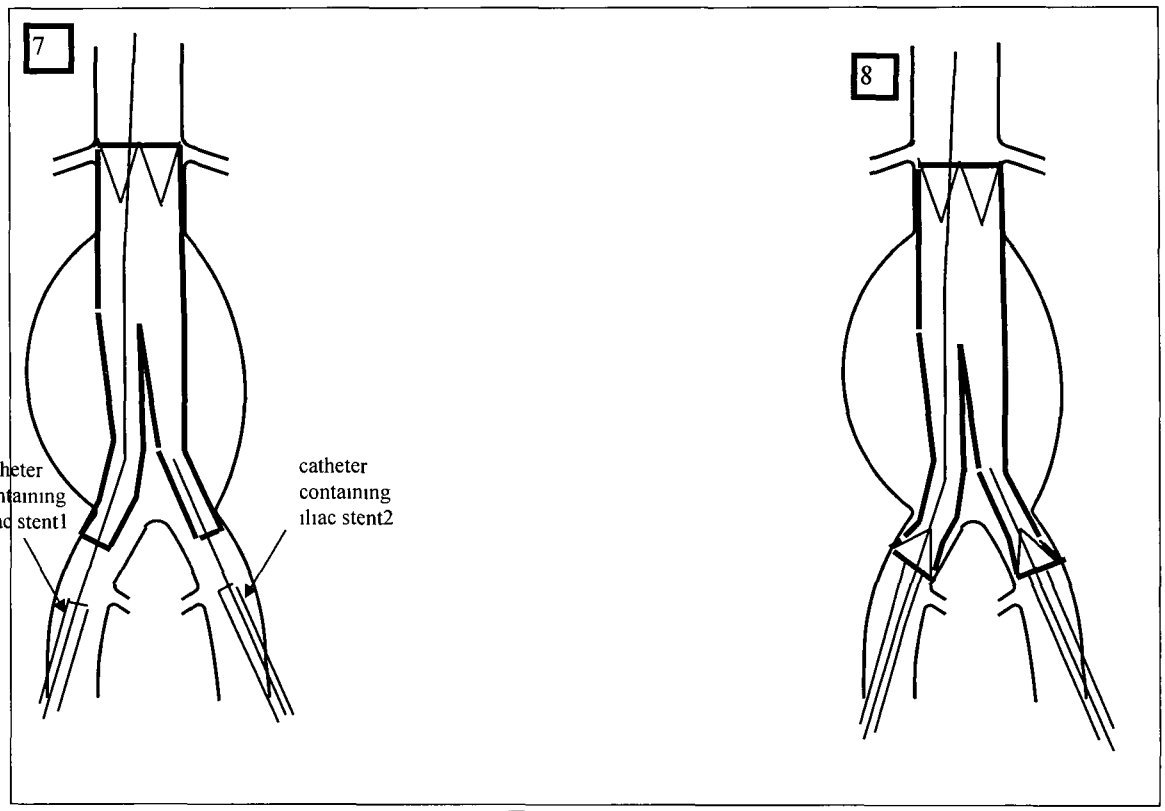

Figure 7.27

7. **a)** To prevent back flow up through the two iliac legs, a guidewire is guided through each leg of graft

   b) A stent with graft should now be positioned in one iliac leg first and then the other, over each guidewire

8. **a)** One distal stent is first deployed and then the other

   b) All catheters and guidewires must now be safely removed

7.11 Conclusion.

Accurate placement of the stent graft system across the aneurysmal sac is as important as the durability of the prosthesis Since if any complication occurs during the deployment procedure, open surgery must be reverted to This would be very traumatic for the patient in question and could prove to be life threatening

For a reduced risk of failure, the method of deployment must be simple in concept with no tricky procedure for any of its steps Miniaturisation of the device is critical, for a small profile is easier to manoeuvre around the vascular system The tip of the catheter should be as small, smooth and tapered as possible to reduce the chances of catheter buckling

The Unitary approach which we are improving is technically more difficult to position across the iliac bifurcation than the Modular approach The outlined procedure as given in this chapter has addressed the majority of options available for the Unitary approach In my opinion, the final preferred method as given in section 7 10 is as simple if not simpler to delivery than any of the Unitary delivery methods

One must remember that for this new area of endovascular surgery, improvements to ones design can be achieved One improvement to this proposed method is for accurate placement of the bifurcated stent graft with only one femoral artery exposed Also, the emphasis is very much on miniaturisation of the device, precutaneous needle puncture would be the optimum for the delivery of this prosthesis

Chapter 8

Prototype Testing

8.0 Prototype Testing

8.1 Introduction

To assess the successes or failures of the proposed stent graft and delivery system, physical testing in our bench test must be done The full prototype testing involves the following

- Method of deployment which comprises of the introduction and accurate placement of the crimped stent graft across the aortic aneurysm and iliac bifurcation
- The attachment system, which releases the stents using the bow knot technique
- Durability of the fully expanded stent graft

It must be emphasised that the artificial simulated conditions of the bench test does not fully replicate the conditions of the cardiovascular system Careful comparisons have to be made and the differences will be highlighted The results here are accurate only to the first stage of testing as given by this bench test As already discussed in chapter 3, animal and clinical testing must be done before any new device can be introduced for widespread usage

8.2 Method of Deployment.

The proposed procedure as outlined in section 7 9 will be demonstrated in the bench test The pressure valve is set to 10,000N/m^2 which corresponds to the reduced blood pressure of 70mmHg during the Endovascular procedure The piston pump is set to 72rpm, which is the average pulse rate for a person Each step of the procedure must be tested for any difficulties that could arise The success of the delivery system is dependent on all steps been successful If any problems arise, accurate placement of the stent graft could be put in jeopardy

8.2.1 Procedural Testing.

The procedure to be tested is as follows:

1. The silicon tube which represents the femoral artery is cut longitudinally. An introducer sheath is placed across the longitudinal slit in the silicone.
2. Introduce a flexible tip guidewire (∅0.035inch (∅0.9mm)) through the introducer sheath and up through the mock silicon artery.
3. Introduce the main catheter system (which contains the crimped stent graft, the main catheter, sleeve and the attachment mechanisms) over the guidewire through the introducer sheath as shown in figure 8.1.

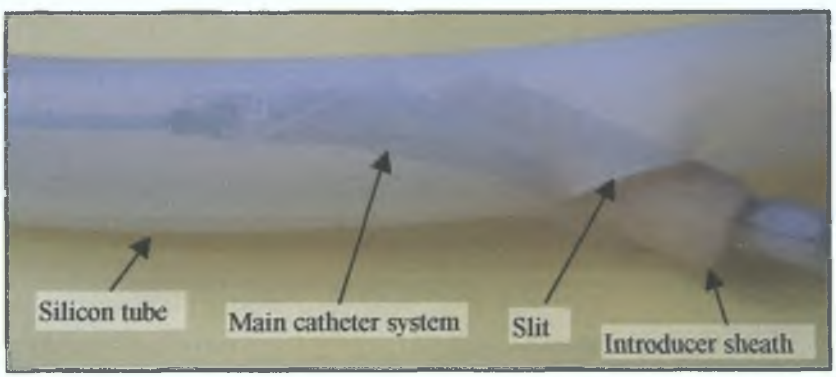

Figure 8.1: Introduction of Main Catheter System Through Longitudinal Slit in the Artery.

4. Push the main catheter system past the bifurcation point up through the simulated vascular system of the bench test as shown in figure 8.2.

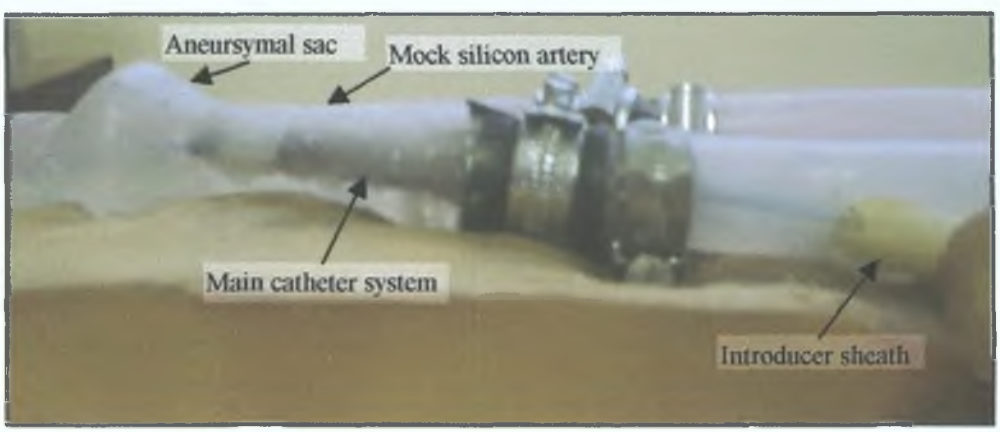

Figure 8.2: Introduction of Main Catheter System

5. Pull off the main sleeve while holding the main catheter stationary

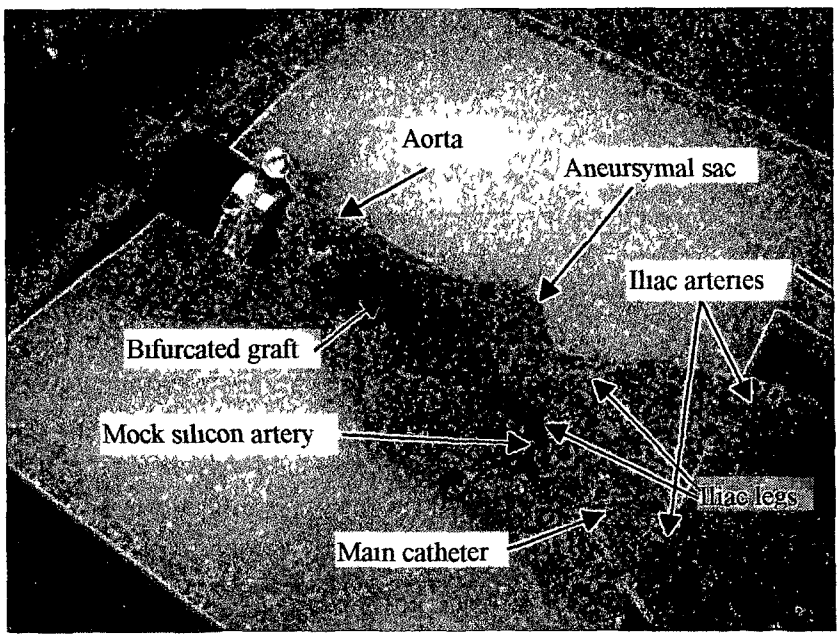

Figure 8.3: Removal of Main Sleeve.

6. Slit longidutally the other silicon artery which represents the other femoral artery Introduce a snare catheter (outer ∅4mm, inner ∅2mm) with its corresponding snare loop in the form of a nylon monofilament fibre
7. Guide the snare catheter up through its guidewire to the iliac sleeve 2
8. Loop the snare loop around the iliac sleeve2, thus gripping the sleeve Now pull the main catheter system and the snare catheter so that both iliac legs are positioned into their respective iliac arteries as shown in figure 8 4

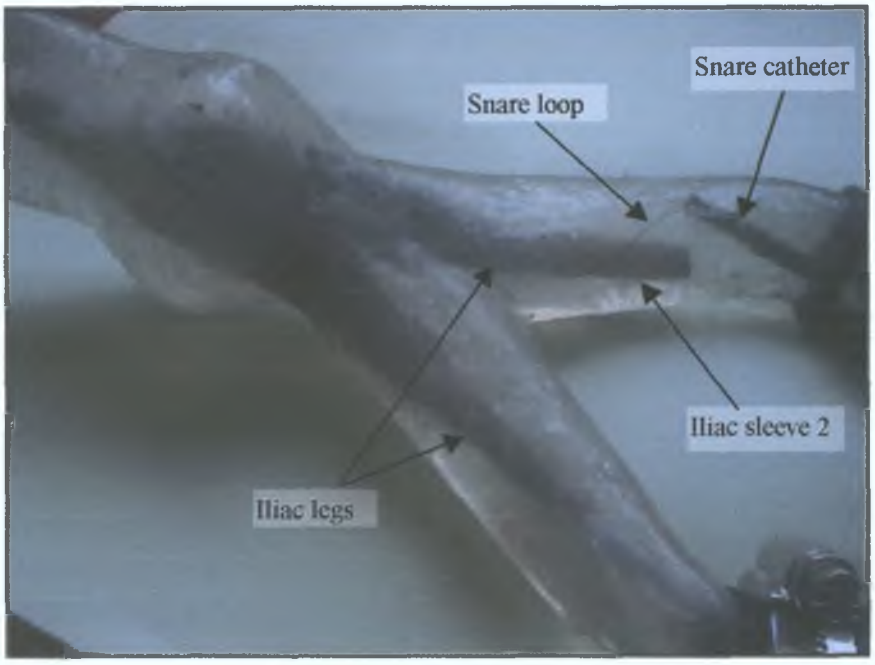

Figure 8.4: Positioning of Iliac Sleeve using Snare Catheter Method.

9. While holding the main catheter in place, pull off the two sleeves over each leg of the graft. One sleeve is pulled off by the snare loop while the other is pulled off by the fibres connected onto the iliac sleeve through the main catheter system.

Figure 8.5: Removal of Iliac Sleeves.

10. Position accurately the proximal end of the stent. Release the stent pulling the multifilament yarn to release the bow knot. The proximal end of the stent graft is fixed up against the wall of mock silicon artery.

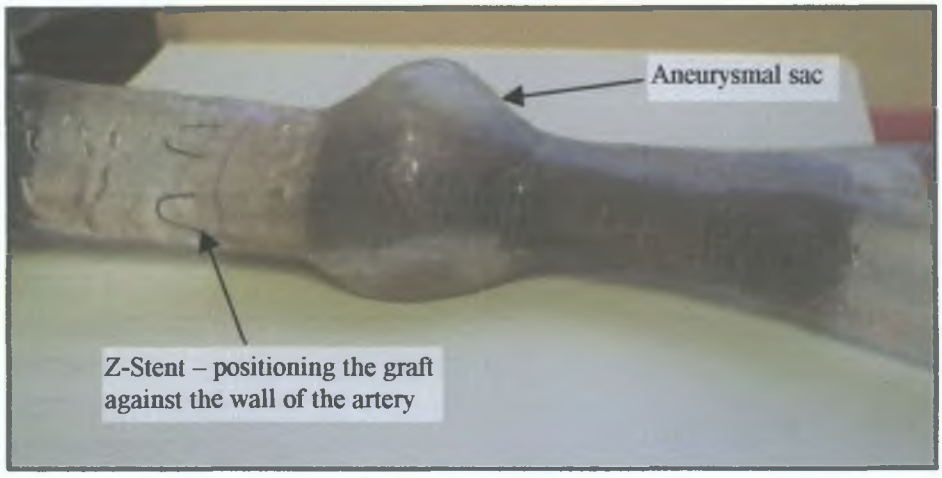

Figure 8.6: Fixation of Proximal Stent.

Figure 8.7: Fixation of Proximal Stent.

11. Remove the main catheter system and snare catheter.

Note: The two iliac stents can now be positioned or could have been part of the complete stent graft. For this case, the proximal stent would have to have been released before removal of the iliac sleeves. Then removal of both iliac sleeves would release both iliac stents.

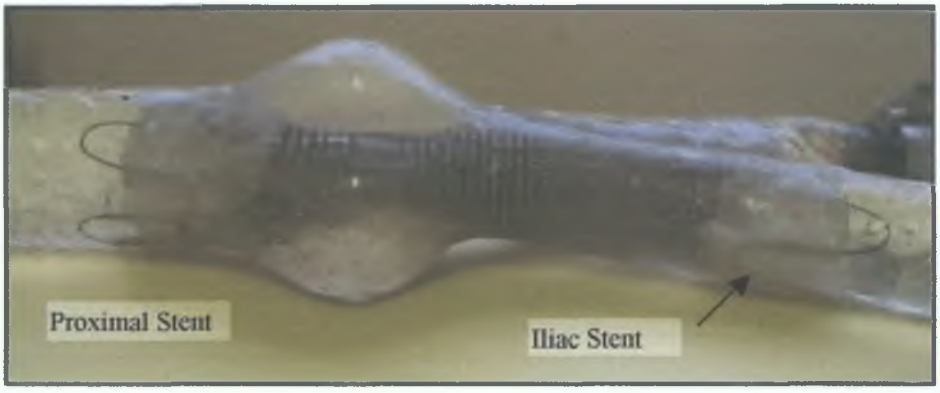

Figure 8.8: Fixation of Proximal & Iliac Stents.

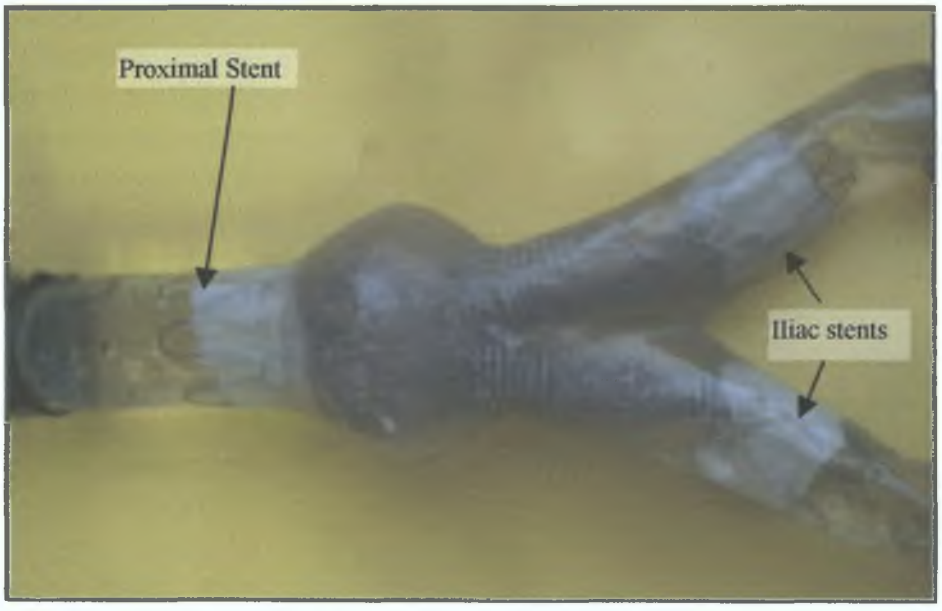

Figure 8.9: Fixation of Proximal & Iliac Stents

8.2.2 Comments.

- There was no difficulty in controlling or manoeuvring the catheter system through the simulated conditions of the vascular system.
- During the delivery, the pressure valve is set to 10,000N/m^2. But since the silicon tube was slit, the pressurised system was exposed to the atmosphere as happens during the endovascular procedure, (where there is a lot of blood loss ranging from 100ml to 1,000ml (mean 300ml) [57]. This decreases the overall pressure in the aorta, which reduces the chances of catheter buckling.
- The snare catheter method is one of the most used procedures for grasping objects in the vascular system. This method avoids the need for a cross-femoral catheter. It would be advised that radiopaque markers be placed on each iliac sleeve and on the tip of the snare catheter so that accurate visualisation can be achieved.

8.3 Durability of Stent Graft.

The derived formulae of section 6.4 are applied to find the theoretical forces acting on the bifurcated graft as generated by our bench test. The same formulae are applied with a few simplifying assumptions. What we can find is the velocity of the water through the proximal end and the set pressure at both ends of the iliac legs. Since we do not know the proximal pressure, we have to use a fixed control volume throughout all the graft so as to simplify the calculation. We can neglect the effects of any frictional losses from the pump outlet to the proximal end of the graft and throughout the graft itself since these frictional losses are negligible. Now the simulated vascular system is positioned horizontally and so the weight of the fluid is ignored. The result of this calculation will be compared to the results obtained in section 6.4 for a typical impedance valve of pressure to flow relationship.

To assess the suitability of the stent I manufactured from shape memory alloy as explained in section 6.7. The radial stiffness of our Z-shaped stent and the force required to dislodge our stent graft as generated by the bench test with only the support

of the proximal stent will be found and compared to commercially manufactured stents tested in real arteries.

8.3.1 Radial stiffness of Z-shaped stent.

To find the radial stiffness of our stent, known weights are placed radially on top of the stent. The sides of the stent are supported against lateral buckling. The deflection is measured and the radical stiffness of our stent is shown in figure 8.10a. Figure 8.10b shows the radical stiffness of typical commercial intervascular stent as tested by *Lambert et al*. *Lambert et al* tested these stents (as described in section 4.6.3) with a % deflection of 30% & 17%. Table 8.1 summaries the results of that test.

Category	Mean Pull (N)
Neck length(mm) 30% deflection	
10	2.14
15	2.7
20	4.0
Aortic Diameter	
<20	3.0
>20 (16% deflection)	2.86

Table 8.1: Mean distraction force needed to dislodge stent. ***(Adapted from Lambert et al, ref27)***

As can been observed from these results the aortic neck length is the most significant factor. The aortic diameter has only a minor effect on the distraction force. For a comparison to be made between our stent and the stent tested by *Lambert et al*, the radial stiffness of both stents must be compared. The outer diameter of our Z-stent is 48mm and the aortic diameter is 28mm. This corresponds to a % deflection of 42%. Referring to figure 8.10a, a radial load of 62g is needed to produce this deflection. The stent tested by Lambert et al had a % deflection of 30% & 16%. This corresponds to a radial load of 110g & 60g respectfully. The radial stiffness of 16% deflection gives a

radial force similar to our Z-stent The distraction for this stent as given in table 8 1 was 2 86N, which is similar to the values obtained in section 4 61 & 4 62 for both the smooth Gianturco-Z stent and Palmaz stent This dislodgement force can now be compared to the force required to dislodge our Z-shaped stent, which is sewn onto the bifurcated stent graft

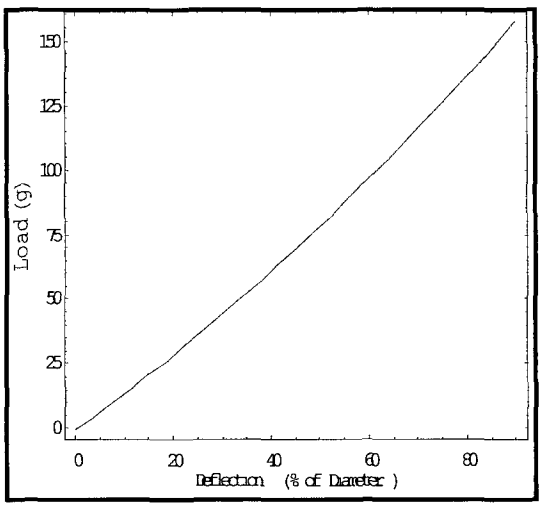

Figure 8.10a: Load required to radially deform the manufactured Z-shaped stent.

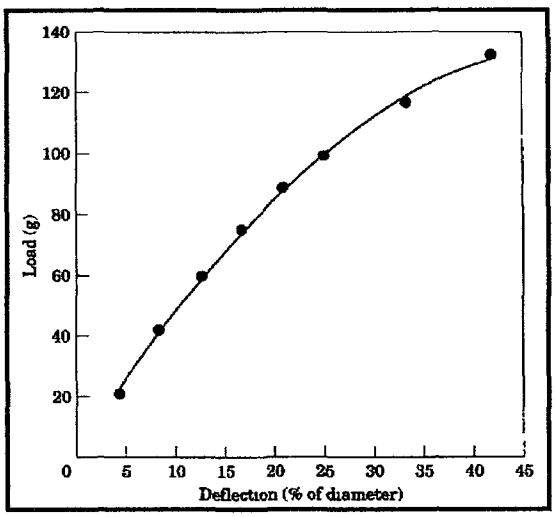

Figure 8.10b: Load required to radially deform a comerically available stent *(adapted from Lambert et al ref27)*

8.3.2 Forces required to Dislodge Stent.

The stent graft is positioned with only one stent at the proximal end The pump is set to 72rpm The pressure in the system is increased by the pressure valve until the stent graft is dislodged and pushed into the aneurysmal sac The recorded deflection of the spring, which caused the stent graft to be dislodged was 2 1mm

To find the force needed to open the valve we use the following formula

$$\text{Force} = F = kx$$

Where

k = spring stiffness = 163 9N/m

x = deflection = 2 1mm = 0021m

$$\text{Force needed} = (163\ 9\text{N/m})(\ 0021\text{m}) = 0\ 3442\text{N}$$

$$\text{Pressure} = \frac{\text{Force}}{\text{Cross sectional area of seat}} = \frac{4F}{\pi d^2}$$

Where d is the diameter of the seat = 8mm

$$\text{Pressure} = 6848\text{N/m}^2$$

This is the pressure at both iliac legs The force required to dislodge the stent is calculated by the continuity, euler and momentum equations and is given in Appendix E Figure 8 11 shows the pressure at the proximal end and figure 8 12 shows the resultant force necessary to dislodge the stent graft

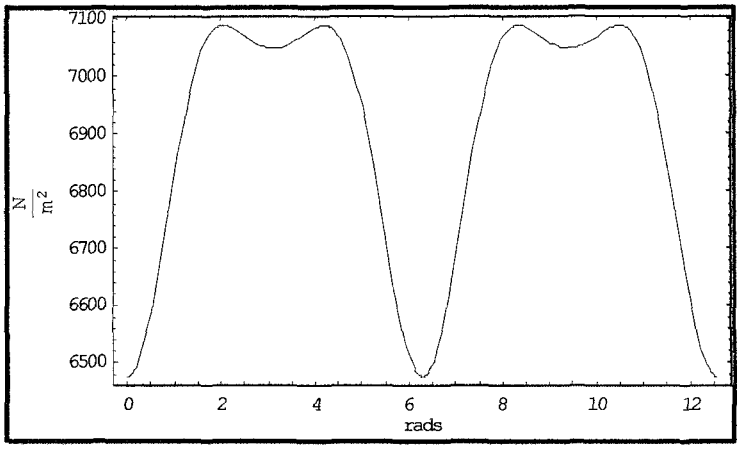

Figure 8.11: Proximal Pressure

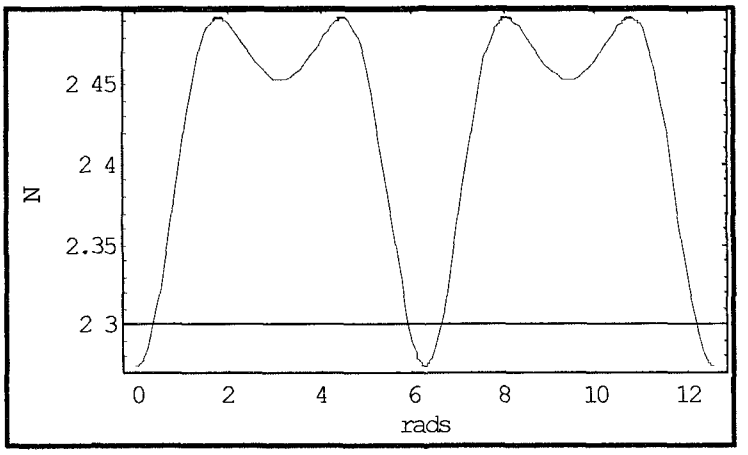

Figure 8.12: Resultant Force necessary to dislodge stent graft.

The conditions simulated in the bench test for stent graft migration is less than the conditions of the vascular system The resultant force of nearly 2 5N as given in figure 8 12 and is comparable to that obtained by *Lambert et al,* the smooth Gianturco-Z stent and Palmaz stent This test clearly demonstrates that the radical force of smooth stents is not capable of preventing stent graft migration

8.3.3 Stent graft with proximal and iliac stents.

Due to the problem of wave reflections two iliac stents are needed This stent graft was tested in the bench test and it was found that the same conditions needed to dislodge the stent graft with only one proximal stent, also dislodged this proximal stent into the aneurysmal sac The two iliac stent remained in position but buckling of the multifilament fabric (Nylon or polyester) between the proximal and iliac stent was the main cause of this failure This lead me to try out using two Ø0 4mm steel struts which were sewn onto the graft and positioned between the proximal stent and the two iliac stents as shown in figure 8 13

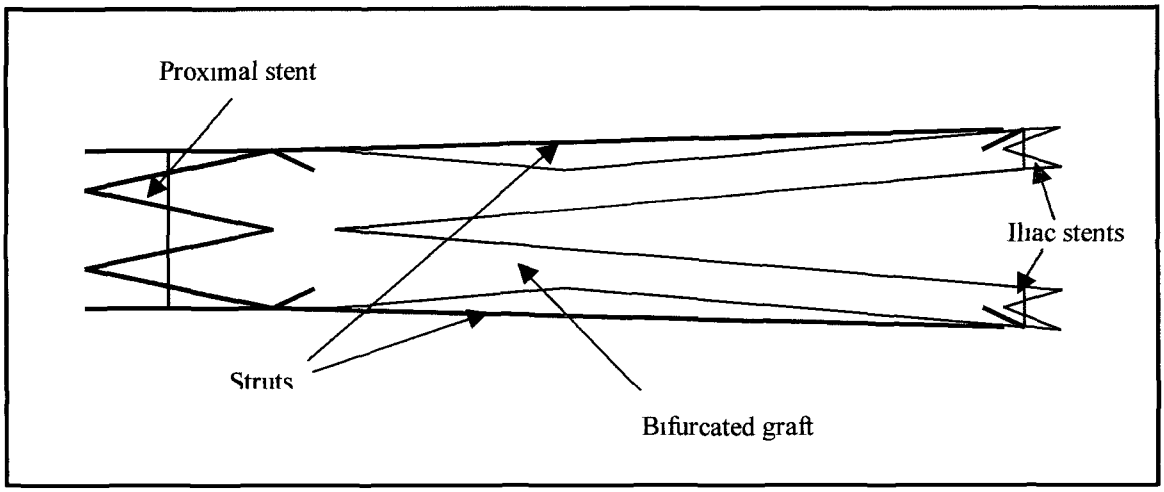

Figure 8.13: Placement of Two Struts between Proximal & Iliac Stents.

The stent graft now could withstand a spring deflection of 6 8mm This corresponds to an iliac pressure of 22,173N/m^2 The proximal pressure is shown in figure 8 14 The calculated proximal pressure and resultant force is given in Appendix E This pressure is in excess of the average blood pressure of 16,000N/m^2 and 20,000N/m^2 for older people. The pump was set to 90rpm which again is above the average pulse rate of 72 and the pulse rate for older people of 80 beats per min

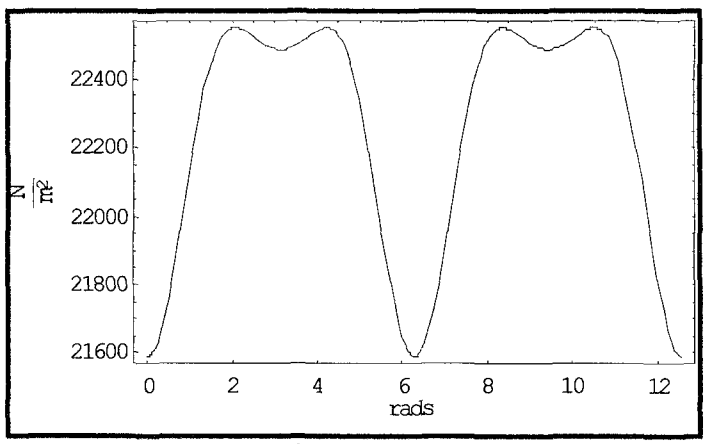

Figure 8.14: Proximal Pressure

This test shows that the stent graft with a proximal stent, two iliac stents and two struts forms a structure that is quite stable and will remain in position for a condition that is as severe as would be experienced in the vascular system Figure 8 15 shows a comparison of the resultant force calculated for the bench test conditions and those for a typical pressure & flow relationship as given in chapter 6, section6 4 There seems to be no need for a completely stented structure as the two struts can adequately hold the graft in position Using struts instead of a fully stented graft reduces the stiffness of the prostheses and hence a reduced wave velocity For safety reasons more struts could be positioned to strengthen the structure

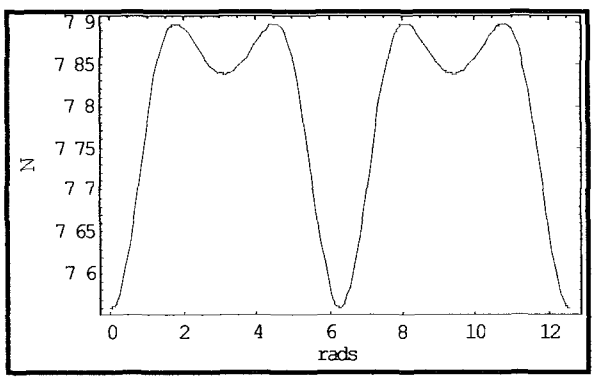

Figure 8.15a: Resultant force for stent graft with two struts as tested in the bench test.

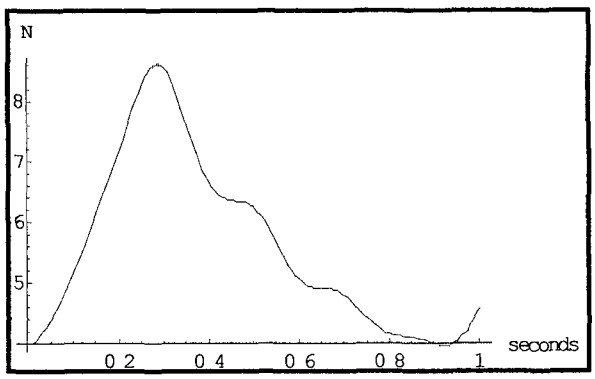

Figure 8.15b: Resultant force for typical pressure and flow relationship as given in Appendix E.

Reasons why the Resultant force, calculationed from a typical pressure flow relationship is larger than those obtained from the Bench Test.

- Since we only know the velocity at the proximal end and the fixed pressure at the iliac legs in our bench test It was not possible to apply the *Gow & Taylor (1968)* equation for the radial pulsation of the proximal end of the artery For the radial pulsation of the proximal end is a function of the unknown proximal pressure In neglecting this, the actual force is larger since we neglected the increase in area of the proximal end
- Since the mock silicon artery is lying horizontal the weight of the water is ignored
- The density of blood is slightly higher than that of water

Note

It was observed that the aneursymal sac was still expanding, the reasons for this are

- Stents are embedded into the vessel wall of the vascular system, which promotes a layer of flat cells, which line the blood vessels to spread and cover the stent The human tissue of the vessel wall is capable of encapsulating the fibres of the graft for the cells to adhere to this leads to tissue growth and can simulate ingrowing tissue and thus form a new elastic component of the arterial wall Following implantation a polyester graft forms a fibrin layer over its flow surfaces As healing proceeds fibroblasts incorporate within the interstices of the graft and the inner layer may become quite organised within days [18,38,42] As can be seen in the vascular system the portion of the stent graft in contact with the wall of the artery forms a seal which can prevent blood leaks into the aneurymsal sac This cannot happen in our bench test as we are using mock silicone rubber arteries and a perfect seal will not happen as the stent cannot be embeded into the rubber as is possible with tissue Using water which is four times less viscous than blood will seep through the silicone and stent graft joint more easily than would blood
- The sewing of the bifurcated graft was done by hand and leakage is possible
- Also it can be noticed that the polyester or nylon mutifilament fabric unfolds with no creases
- As noticed in the test was a reduced level of flow activity inside the aneurysmal pouch This was also noticed by *Lieber et al* who placed porous tubular-shaped stents across an aneuryeurysmal pouch This reduced the streakline rotation rate within the aneurysmal pouch, thus inducing flow stagnation that may aid in the formation of a stable thrombus in the pouch and lead to permanent occlusion of the aneurysm [58]

8.4 Clinical follow up

As with any new technology and especially with endovascular surgery, clinical follow up most be maintained so as to access the success and failures of the device which might otherwise be unpredictable The m-follow up reports showed the following

After Stent Graft Placement

- Transverse diameter of the AAA diminished progressively with time usually within 6-12 months after implantation has been proved in several cases
- Rarely encontered Problem

  Main risk associated lies with potential vessel rupture resulting from graft or balloon oversizing Over expansion - leads to aortic wall injury Under expansion - leads to leakage of blood and device migration
- Leaks which cause further expansion of the aneurysm can be caused at

  Proximal end

  either leg

  middle of bifurcation [57]

During Delivery Procedure

- Should supply a set of instructions rather than a method that obliged users to assemble their one device
- Leaks could be caused by tear in PTFE material during manipulation
- In an attempt to occude the descending aorta with the tip balloon, after deploying the graft, the balloon can move downward and the system becomes unstable and can drop inside the aneurysm lumen
- When using the distal balloon at the tip of the delivery catheter for partial occulusion of the abdominal aorta so as to reduce the flow within the aorta and making the actual delivery of the graft easier If attempts are made to totally occlude to aorta, the system becomes unstable with a tendency to move downstream

- A Central balloon is inflated at several levels along the iliac segments to unravel wrinkles in the graft material and to model the spring stents into the iliac vessel wall [57]

8.5 Conclusion

As shown by the experiments in the bench test, the proposed delivery method and stent graft system is acceptable Testing has shown us, that the radial force of the proximal stent is not sufficient to hold the bifurcated graft in place Hooks and barbs are definitely needed to provide a secure fixation Another alternative is to use struts Struts are connected from the proximal stent to both iliac stents to prevent dislodgement of the stent graft

Struts are a better alternative than fully a fully stented graft, as these metal or polymeric rods can be placed on the outside of the graft thus excluding them from direct contact with the blood flow

It must be emphasised that this design is only acceptable from this first stage of testing and that animal and clinical testing must be achieved The main differences between the bench test and the cardiovascular system is due to the reaction of the blood and the arterial tissues to the stent graft, which cannot be simulated in our bench test But is saying all of this, the protocol has the potential to be taken to the next stage of testing

Chapter 9

Conclusion

9.0 Conclusion

Completing this project has given me a great insight into how to research analysis and apply data to a design problem.

Analysing the design difficulties associated with treating aortic aneurysms intraluminally has developed my engineering skills and my perception about design. In fact, design ideas are developed through perspiration, which generates inspiration, unlike what I thought previously. Through researching, one can find the various problems associated with stent graft placement and a design method that is acceptable from an engineering and biomedical point of view.

In designing a stent graft with its accompanying delivery system the first stage was to build a bench test capable of replicating the cardiovascular system and the disease in question aortic aneurysms at the iliac bifurcation. This stage is necessary for valid testing of the stent graft and delivery system and is recommended as the first stage of testing before animal & clinical testing can be achieved. The bench test comprises of a piston pump capable of simulating pulsatile flow similar to the heart, which delivers blood by periodic waves. The kinematics of the piston pump has been designed to give the same stroke volume, pulse rate (rpm) and fluid velocity as is given in the abdominal aorta. Mock abdominal aortic aneurysms at the iliac bifurcation were replicated using transparent silicon rubber, which is designed to the same geometry and compliance of typical abdominal aortic aneurysms. The method used to make these mock silicon aneurysms was the lost wax process. The female casts were made with the aid of CNC technology. Silicon rubber was painted in layers on the male wax casts and when sufficient thickness is achieved the wax is melted away. To keep the silicon aorta pressurised similar to that in the body. A pressure valve is positioned after the mock silicon artery. The pressure can be varied by compressing or deflecting a spring connected to a plate that is fitted on a seat inside the pressure valve. The pressure can be varied from $0N/m^2$ to $60000N/m^2$, which is within the range of the normal blood

pressure of 16000N/m^2 and the reduced blood pressure during endovascular surgery of 9000N/m^2 A thermostatic controller is needed to keep the temperature at 37°C The test system circuit also consists of a feeder tank, leak container, collector tank and a circulating pump with forms a recycling loop

From a hemodynamic point of view we decided to improve the unitary approach This design gives a better durability and flow characteristics since there is no joints along its construction unlike the modular design The geometry of the bifurcated stent graft can have a drastic effect on the flow patterns across the graft As given by the reflection and transmission coefficients of waves at junctions, a taper design minimises the wave reflections and associated energy losses Since the area ratio at the junction is equal to unity, unlike the contraction type which is less than unity A taper from the proximal leg to the distal leg reduces the chances of vorticity creation and increased turbulence The unitary bifurcated graft facilitates the taper design unlike the modular graft since a straight portion of graft is needed for the attachment of the second stented leg

Attachment systems are needed to fix the bifurcated graft against the wall of the artery Self-expanding stents are more compliant to the pulsating artery than balloon expandable stents Self-expanding stents will always expand to their present diameters with no recoil and will continue to push outward on the vessel wall These stents will grow with the vessel and adapt to the shape more than plastically deformed stents Nitinol is one of the best self-expanding stent materials and is most mechanically similar to biological materials unlike stainless steel and titanium, which are very strong and stiff Nitinol exerts a more favourable effect on vascular remodelling with less neointimal formation than balloon expandable stents The Z-shaped stent has fixation characteristics that are comparable to other types of stent designs We therefore choose this design due to its ease of manufacturing The memory state of Nitinol into the Z-shaped stent is done through training This is done by yielding the material to the desired shape (in our case the Z-shaped stent) and then restraining it in the stressed condition for a period of 5-7 minutes at 500°C The final properties and the ease of setting the memory state of Nitinol, makes it superior to any other type of stent materials available

Textile fabrics are used to exclude the aneurysm from the blood flow Woven fabrics have higher bursting strength and good fatigue resistance unlike knitted fabrics But woven prostheses lack compliance and consequently may be too stiff Stretch can be obtained in woven fabrics by weaving the fabric extra wide and then reducing in width during scouring or heat-setting, also the use of blended yarn in either the warp or weft directions can increase compliance and flexibility of woven fabrics Biocompatible materials such as Nylon, Polyester & PTFE can all be used as a graft material As tested by the Instron tensile testing machine, multifilament woven fabrics have a much lower young's modulus than monofilament woven fabrics Therefore multifilament fabrics do not suffer from creasing and a fully stent graft structure is not needed to hold this type of fabric opened Due to the lower young's modulus there is a lower wave speed and hence wave reflections are also lower and consequently lower backpressure

Stent graft migration poses a serious problem for the lifetime of the stent graft and is a recognised complication of aortic endografting To assess the possibility of stent migration, the resultant force on the bifurcated stent graft was calculated A Fourier series representation of a typical pressure and flow relationship as found the aorta was applied With the use of the continuity equation for a deformable body, Eulers equation of motion and the linear momentum equation for a deformable body, the pulsating resultant force acting on the bifurcated graft can be obtained For aortic diameters varying from 18mm to 32mm the maximum resultant force varies from 3 25N to 12N respectfully The mean distraction force of a smooth stent such as the Gianturco Z stent, Palmaz stent and Nitinol coil as tested by *Andrews et al & Malina et al* is around 2 5N As demonstrated in our bench test the conditions required to dislodge our manufactured proximal Nitinol Z-stent with no other stenting along the bifurcated graft was a proximal pressure of 7100 N/m^2 at 72rpm When these values were substituted into the modified formulae a resultant force of 2 5N is obtained This resultant force for our Z stent is comparable to the tests obtained by *Andrews et al & Malina et al* Thus the radial force of any smooth proximal stent is not an adequate anchoring system for a bifurcated stent graft Due to the problems of multiple wave reflections beyond the iliac bifurcation, two iliac stents are needed As tested in our bench test with one proximal and two iliac stents It was found that the same conditions needed to dislodge

the stent graft with only one proximal stent, also dislodged this stent graft due to buckling of the fabric This is attributed to an ineffective radial force exerted by the proximal stent occurs which leads to stent graft migration A fully stented structure provides an adequate anchorage system Struts are a better alternative to a fully stented structure as these metal or polymeric rods can be placed on the outside of the graft between the proximal and iliac stents, thus excluding them from direct contact with the blood flow Two ∅0 4mm metal struts were tested in our bench test and it was found that the bifurcated stent graft could withstand a condition worse than that to be expected in the cardiovascular system This condition corresponded to a proximal pressure of nearly 23,000N/m^2 at 90rpm, which is in excess of the average blood pressure of 16,000N/m^2 and 20,000N/m^2 for older people When these values are substituted into the modified formulae for the bench test conditions a resultant force of nearly 8N was obtained For the same geometry of stent graft using typical pressure and flow relationships as found in the human vascular system the resultant force was calculated at 8 5N The difference are attributed to the use of *Gow and Taylors* equation in the theoretical calculations and the inability of using this equation for calculation of the bench test conditions since we did not know the proximal end pressure In neglecting this, the actual resultant force would have been greater due to the increase of the proximal end By using struts instead of a fully stented structure will give a lower wave velocity due to the reduced metal content As demonstrated by *Malina et al* hooks and barbs have distraction forces over 20N and provide a firmer fixation This force is in excess of resultant force of 12N as calculated for a 32mm diameter proximal end Hooks can provide a stable anchorage without the worry of further dilation of the artery Hooks and barbs can retain their displacement force even if the graft is undersized by 1 to 2mm The dangers of hooks and barbs that pierce the aortic wall is that they might penetrate to juxta-aortic structures, such as the duodenum and the renal vein and the long-term risks have not been assessed Placing additional hooks and barbs on each stent will increase the volume of the device and make them difficult to introduce through slim sheaths

For a successful endovascular procedure, accurate placement of the stent graft across the aneurysm sac had to be achieved. Since all the manipulations are controlled from a remote site by the use of guidewires and specially designed catheters, delivery system insertion must permit easy access through the vascular system. Possible buckling of the catheter and the consequent difficulty in controlling the catheter through the vascular system is due to the lateral pressures acting on the tip of the catheter. The lateral pressure is caused by the blood pressure and the kinetic energy of the blood. The contour of the surface at the catheter tip can have an effect on the total resultant force. We calculated the resultant axial force acting on the catheter tip for several surface options. This was done by summing the surface integral of the normal component of the scalar field (the scalar field represents the blood pressure of $16000N/m^2$) acting on a defined curved surface and the drag force acting on the catheter tip due to the impact of the blood. It is possible to apply the formulae for flow past immersed bodies to find the drag force since pulsatile flow in the aorta is turbulent and this gives a blunt velocity profile and therefore the effects of the boundary layer are negligible. As has been calculated, the resultant axial force acting on a tapered end with a rounded tip is 3 to 4 times lower than for any other surface option such as a rounded end in the form of a sphere or torus or either a flat faced catheter. For a normal blood pressure of $16000N/m^2$ the resultant force acting on the tapered tip is 3 to 4 times lower than the critical eulers load for buckling of a ∅0.8mm stainless steel guidewire. Therefore catheter tips should be as small, smooth and tapered as possible. A more flexible catheter material such as polyurethane or polyethylene can be used and this will give more flexibility and control around the vascular system. Unlike the other surface options in which a more stiffer catheter is needed to prevent buckling. These options could cause difficulty in guiding through the vascular system and could cause damage to the wall of the artery.

Miniaturisation of the bifurcated stent graft is an overall design consideration that is constantly been improved. For a safer delivery, the device when crimped has to be as small as possible. First the struts, proximal and distal stents are sewn onto the final unfolded bifurcated graft. Since we have shown that the actual folding method does not matter, the bifurcated shaped multifilament woven fabric can be easily squeezed or

wrapped any way onto the catheter It is then possible to crimp the Z-shaped Nitinol stent and fold the bifurcated graft with a proximal diameter of 32mm down into a sleeve of ∅8mm as we have demonstrated in chapter 7 For smaller aortas this crimped value will be smaller

The method of deployment must be simple in concept Accurate positioning and deployment of a unitary bifurcated stent graft is technically more demanding than the deployment of a modular device A snare catheter approach is preferred for placement of the bifurcated graft across the iliac bifurcation This uses the graft as a natural hinge This method is simple in concept and is a better alternative than the cross-femoral approach or any hinge type or attachment type mechanisms Since any complications such as jamming or buckling due to the distance you are from controlling the device The snare catheter approach could use the percutaneous needle puncture on the other iliac artery Once the bifurcated graft is in position removal of the proximal stent is a problem since a sleeve cannot be pulled down due to the position of both legs in the iliac arteries Since it was not possible to remove the sleeve upwards due to the frictional forces acting on the catheter tip, we tried a bow knot technique which is capable of releasing the proximal stent The bow knot can be pulled downwards and easily released This procedural method was tested in our bench test and worked successfully with accurate positioning of the bifurcated graft across the aneurysmal sac and accurate placement of the proximal stent as demonstrated in chapter 8

Endovascular aortic aneurysm repair has proved to be a less invasive way of treating aneurysms This is one of the great potentials associated with this procedure, as the risk of developing an aneurysm increases with age The proposed unitary bifurcated stent graft with its' accompanying delivery system as developed in this project has proved to be acceptable by the testing in our bench test Of course, for such a new technology, improvements to ones design is always sought after Material development and delivery methods are such areas for further development of these devices

Finally, I have appreciated how the interaction of engineering principals with medical problems can achieve products that is life saving

Chapter 10

References

10.0 References.

[1] www wcg org/churches/us/ny/buffalos/wegdanla htm

[2] Onhealth with WebMid Aneurysm – Introduction and Symptoms www onhealth com/ch1/resources/conditions/0,1014,201,00 htm July 1998

[3] Calligoro KD, Dougherty MJ & Hollier LH Diagnosis & Treatment of Aortic & Peripheral Arterial Aneurysms W B Sauders Co First edition 1999

[4] Hopkinson B, Yusuf W & Whitaker S Endovascular Surgery for Aortic Aneurysms W B Sauders Co First edition 1997

[5] Ernst CB The New England Journal of Medicine Vol 336, No 1 www nejm org/content/1997/0336/0001/0059 asp Jan 1997

[6] Vandar, Sherman & Luciano Human Physiology McGraw Hill, Inc Sixth edition 1996

[7] Fung YC Biomechanics-Circulation Springer-Verlag New York Inc Second edition 1996

[8] Nichols W & O'Rourke MF M^{c}Donald's Blood Flow in Arteries Edward Arnold Forth edition 1998

[9] Guyton AC Textbook of Medical Physiology Sauders Seventh edition 1986

[10] Rowan JO Physics & The Circulation Hilger in association with Hospital Physicistists' Association Medical Handbook, 9 1981

[11] Shigley JE & Uicker JR JJ Theory of Machines & Mechanisms McGraw-Hill Inc Second edition 1995

[12] Karassik, Krutzsch, Fraser & Messina Pump Handbook McGraw-Hill Inc Second edition 1985

[13] Wolfram S Mathematica Version 3 Cambridge University Press Third edition 1996

[14] Parametric Technology Corporation Pro/Engineer Part Modeling User's Guide Release 20

[15] Parametric Technology Corporation Pro/MFG & Pro/NC-Check User's Guide Release 18

[16] Uflacker R et al Abdominal Aortic Aneurysm Treatment Journal of Vascular & Interventional Radiology Vol 9, No 1, 51-60, Jan/Feb 1998

[17] www medicom com/world/pr-abstracts/pamler052098-abstracts htm

[18] NC State University
www4 ncsu edu/eos/info/bae/bae465_info/1995/dill/Stent html

[19] Marin L, Veith FJ & Levine BA Endovascular Stented Grafts for the Treatment of Vascular Diseases New York RG Landes 1995

[20] Adams A & Dondelinger RF Textbook of Metallic Stents 1997

[21] Pepine et al Coronary Artery Stents JACC Vol 28, No 3, Sep 1996

[22] phytis com/stent1 html

[23] link Springer-ny com/link/services/journals/00547/bibs/7n1p18 html

[25] Nitinol Devices & Components Applications
www nitinol com/4applications htm 13/05/99

[24] www Angiodynamics_com/stent stentfaq htm

[26] Andrews SM et al In Vitro Evaluation of Endovascular Stents to Assess Suitability for Endovascular Grafts European Journal of Vascular & Endovascular Surgery Vol9, Part4, 403-407, May, 1995

[27] Lambert AW et al Experimental Assessment of Proximal Stent Grafts European Journal of Vascular & Endovascular Surgery Vol17, Part1, 60-65 Jan 1999

[28] Malina et al Endovascular AAA Exclusion Journal of Endovascular Surgery Vol5, Part4, Nov 1998

[29] Lipscomb IP & Nokes LDM The Application of Shape Memory Alloys in Medicine Mechanical Engineering Publications 1996

[30] Hodgson DE Using Shape Memory Alloys Shape Memory Applications, Inc 1988

[31] Hodgson DE, Shape Memory Applications Inc Ming HWu, Memory Technologies & Biermann RJ, Harrison Alloys, Inc
www sma-inc com/SMAPaper html 17/08/98

[32] Shape Memory Applications Inc An Introduction to Shape Memory Alloys members it tripod de/SMArt/Introduction/Introduction html 18/06/99

[33] Shape Memory Applications Inc An Introduction to Shape Memory Alloys www sma-mems com/info htm 18/06/99

[34] Nitinol Devices & Components Technology www nitinol com/3tech htm 13/05/99

[35] me210abc standford edu/94-95/projects/Lockheed/Spring/8 html#HDR2

[36] Shape Memory Applications Inc Specifying NiTi Materials www sma-inc com/SpecifyingNiTi html 16/06/99

[37] Raudales JC Design of small Diameter Vascular Grafts for Arterial Replacement Department of Mechanical Engineering, Florida International University 08/17/99 www geocities com/TheTropics/Coast/9031/school/vascular_grafts htm

[38] Adanur S Wellington Sears Handbook of Industrial Textiles Technologic Publishing Company, Inc New edition 1995

[39] Jorgessen CS et al Physical & Mechanical Properties of ePTFE Stretch Vascular Grafts Eur J Vasc Endovasc Surg Vol15, Pages 416-422, 1998

[40] Corbman PB Textiles Fibre to Fabric Gregg. Sixth edition 1985

[41] Miller E Textiles Properties & behaviour in Clothing use Batsford First edition 1995

[42] Baker S Arterial Grafts 07/06/96 www bae ncsu edu/bae/courses/bae/1995_projects/bake/baker/sophie

[43] Salzmann DL et al Effects of Balloon dilation on ePTFE structural characteristics Journal of Biomedical Materials Research Vol15, 36 Part4, pages498- 507, Sept1997

[44] Palmaz F et al Physical Properties of PTFE Bypass Material after balloon dilation Journal of Vascular & Interventional Radiology Vol7, Part5, 657-663 Sept Oct 1996

[45] Rieu R et al In Vitro Study of a Physiological Type Flow in a bifurcated Vascular Prosthesis J Biomechanics Vol 24, No10, 923-933, 1991

[46] Wylie EB & Streeter VL Fluid Transients McGraw-Hill, Inc. 1978

[47] Fox JA Hydraulic Analysis of unsteady flow in pipe networks Ellis Horwood Series in Civil Engineering Macmillan 1977

[48] Parmakian J Waterhammer Analysis Dover Publications 1963

[49] White FM Fluid Mechanics McGraw Hill, Inc Fourth edition 1999

[50] Helal MA et al Hydraulic Simulation of Arterial Networks, which include Compliant and Rigid Bypass Grafts J Biomechanics Vol27, No3, 227-287, March 1994

[51] Morton WE & Hearle JWS Physical Properties of Textile Fibres Heinemann [for] the Textile Institute Second edition 1975

[52] Schneider PA Endovascular Skills Quality Medical Publishing, Inc 1998

[53] Stroud KA Further Engineering Mathematics McGraw-Hill, Inc Third edition 1996

[54] Kreyszig E Advanced Engineering Mathematics John Wiley & Sons, Inc Seventh edition 1993

[55] Benham PP, Crawford RJ & Armstrong CG Mechanics of Engineering Materials Harlow Longman Second edition 1996

[56] Hearn EJ Mechanics of Materials 2 Butterworth-Heinemann Third edition 1997

[57] Uflacker R et al Abdominal Aortic Aneurysm Treatment Preliminary Results with the Talent Stent-Graft System Journal of Vascular & Interventional Radiology Vol9, No1, Jan/Feb 1998

[58] Lieber B et al Alteration of Hemodynamics in Aneurysm Models by Stenting Influence of Stent Porosity Annals of Biomedical Engineering Vol 25, Part 3, 460-469, May-June 1997

Appendix A

```
<< NumericalMath`TrigFit

pressurepoints = {74 44, 73 62, 82 67, 97 02, 102 22, 106 2, 116 89, 122 8, 124 44,
  112, 104 89, 109, 103 33, 96, 93 33, 91, 86 67, 83, 82 27, 79, 77 78, 76, 73 33, 72}
```

```
{74 44, 73 62, 82 67, 97 02, 102 22, 106 2, 116 89, 122 8, 124 44, 112,
 104 89, 109, 103 33, 96, 93 33, 91, 86 67, 83, 82 27, 79, 77 78, 76, 73 33, 72}
```

```
period = 0 936,

bloodpressure = TrigFit[pressurepoints, 10, {t, period}]
```

```
93 3292 - 13 7413 Cos[6 7128 t] - 6 23376 Cos[13 4256 t] - 0 333545 Cos[20 1384 t] -
 0 07875 Cos[26 8512 t] - 1 82909 Cos[33 564 t] + 1 29167 Cos[40 2768 t] +
 0 515523 Cos[46 9896 t] + 0 789583 Cos[53 7024 t] + 0 703545 Cos[60 4152 t] -
 0 405408 Cos[67 128 t] + 16 4299 Sin[6 7128 t] - 2 11972 Sin[13 4256 t] -
 1 7538 Sin[20 1384 t] + 0 889841 Sin[26 8512 t] - 0 587946 Sin[33 564 t] -
 2 Sin[40 2768 t] + 0 879627 Sin[46 9896 t] - 0 713749 Sin[53 7024 t] +
 0 532864 Sin[60 4152 t] + 0 124725 Sin[67 128 t]
```

```
Plot[bloodpressure, {t, 0, 1}, AxesLabel -> {"seconds", "mmHg"}
    ]
```

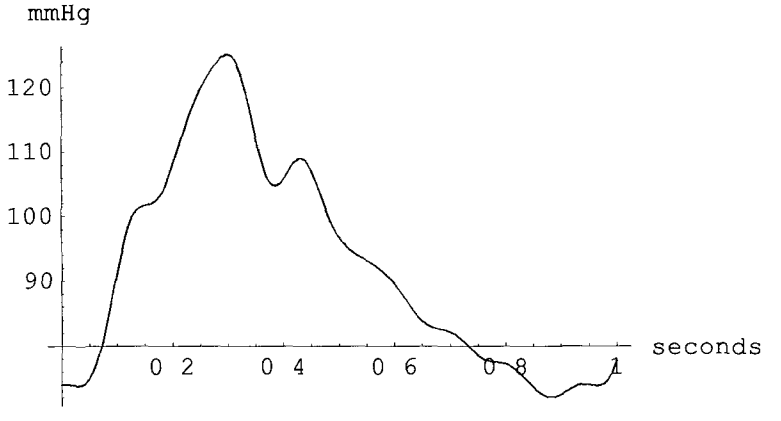


```
- Graphics -
```

```
flowratepoints = {0, -44 44, 0, 355 56, 551 11, 408 89, 332 44, 266 67,
  222 22, 0, -35, 53 33, 35 56, 0, 0, 0, 0, 0, 0, 0}
```

```
{0, -44 44, 0, 355 56, 551 11, 408 89, 332 44, 266 67, 222 22, 0, -35,
 53 33, 35 56, 0, 0, 0, 0, 0, 0, 0}
```

```
flowrate = TrigFit[flowratepoints, 10, {t, period}]
```

```
107 317 - 14 6712 Cos[6 7128 t] - 126 413 Cos[13 4256 t] - 20 4257 Cos[20 1384 t] -
 6 22739 Cos[26 8512 t] + 51 145 Cos[33 564 t] + 12 1241 Cos[40 2768 t] +
 7 97578 Cos[46 9896 t] - 7 61711 Cos[53 7024 t] - 6 52391 Cos[60 4152 t] +
 183 209 Sin[6 7128 t] + 4 07716 Sin[13 4256 t] - 63 7521 Sin[20 1384 t] -
 36 1477 Sin[26 8512 t] - 31 111 Sin[33 564 t] + 27 389 Sin[40 2768 t] +
 4 61055 Sin[46 9896 t] + 13 8758 Sin[53 7024 t] - 6 79499 Sin[60 4152 t]
```

```
Plot[flowrate, {t, 0, 1}, AxesLabel -> {"seconds", "cm^3/s"}]
```

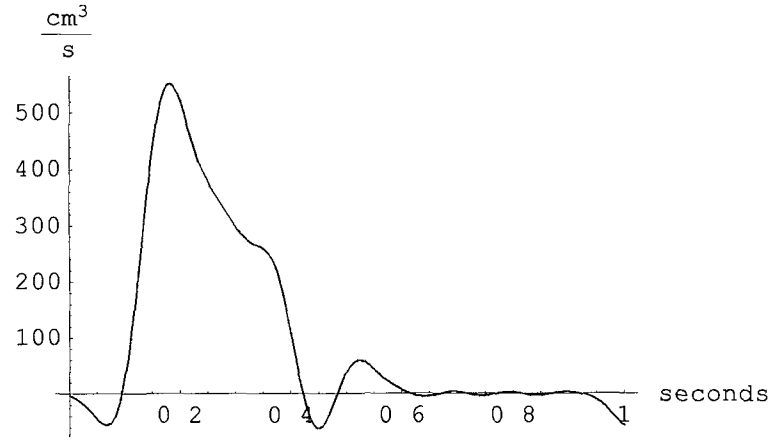

- Graphics -

```
pressureconvertion = 13 6 * 9 81,

bloodpressurepa = bloodpressure * pressureconvertion
```

```
133 416 (93 3292 - 13 7413 Cos[6 7128 t] - 6 23376 Cos[13 4256 t] -
   0 333545 Cos[20 1384 t] - 0 07875 Cos[26 8512 t] - 1 82909 Cos[33 564 t] +
   1 29167 Cos[40 2768 t] + 0 515523 Cos[46 9896 t] + 0 789583 Cos[53 7024 t] +
   0 703545 Cos[60 4152 t] - 0 405408 Cos[67 128 t] + 16 4299 Sin[6 7128 t] -
   2 11972 Sin[13 4256 t] - 1 7538 Sin[20 1384 t] + 0 889841 Sin[26 8512 t] -
   0 587946 Sin[33 564 t] - 2 Sin[40 2768 t] + 0 879627 Sin[46 9896 t] -
   0 713749 Sin[53 7024 t] + 0 532864 Sin[60 4152 t] + 0 124725 Sin[67 128 t])
```

```
Plot[bloodpressurepa, {t, 0, 1}, AxesLabel -> {"seconds", "N/m^2"}]
```

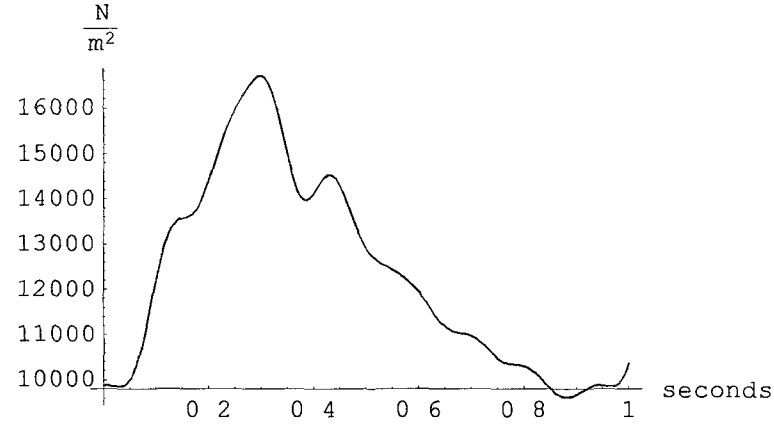

- Graphics -

Appendix B

Bench Test

Part No	Part Name	Material	Quantity
1	Feeder Tank	20L Plastic Tank	1
2	Collector Tank	5L Plastic Tank	1
3	Circulating Pump		1
4	Piston Pump		1
5	Silicon Artery		1
6	Thermostatic Temperature Controller		1
7	Pressure Valve	¾ inch	1
8	Plastic Tubing	1inch O D Length 400mm	1
9	Leak Collector	Plastic Tray 400mmX300mm X100mmhigh	1
10	Flexible Tubing	I D 14mm	12Ft
11	Transformer		1
12	Y piece	O D 20mm	1
13	Y piece	O D 16mm	1
14	Jubilee Clips	18 – 22 mm	7
15	Jubilee Clips	25 – 35 mm	2
16	Jubilee Clips	10 – 20 mm	4
17	Fittings		3

Piston Pump

Part No:	Part Name:	Material	Quantity
1	Cylinder	Aluminium	1
2	Plunger	Aluminium	1
3	Stuffing box	Aluminium	1
4	Top plate	Steel	1
5	Bottom plate	Steel	1
6	Top bushing	Phosphorus Bronze	1
7	Bottom bushing	Phosphorus Bronze	1
8	Hydraulic Seal	P T F E (Teflon) I D of 30mm	1
9	Bearing seal	Phosphorus Bronze	1
10	Support plate	Aluminium	1
11	Valve clamper	Aluminium	1
12	Crank shaft	Steel	1
13	Connecting rod	Forged or cast steel	1
14	Motor support	Steel	1
15	Base support	Steel	2
16	Arm	Steel	2
17	Threaded bar	M6 X 180mm long	4
18	One way valves	I D of 25mm	2
19	Motor	Wiper motor	1
20	Nuts	M6	14
21	Spring washers	I D 6mm	14
22	Nuts	M8	10
23	Washer	I D 8mm	10

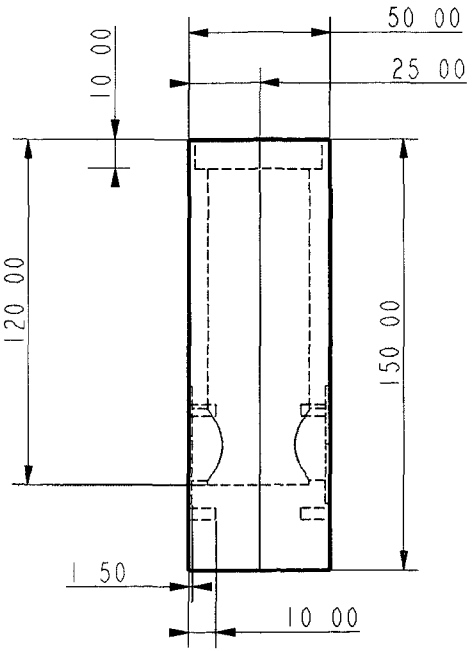

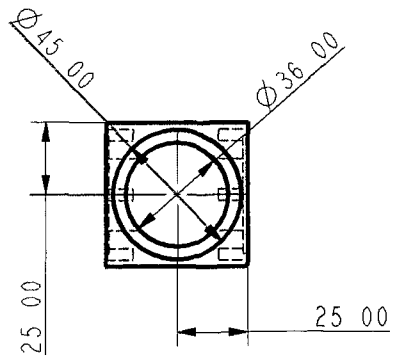

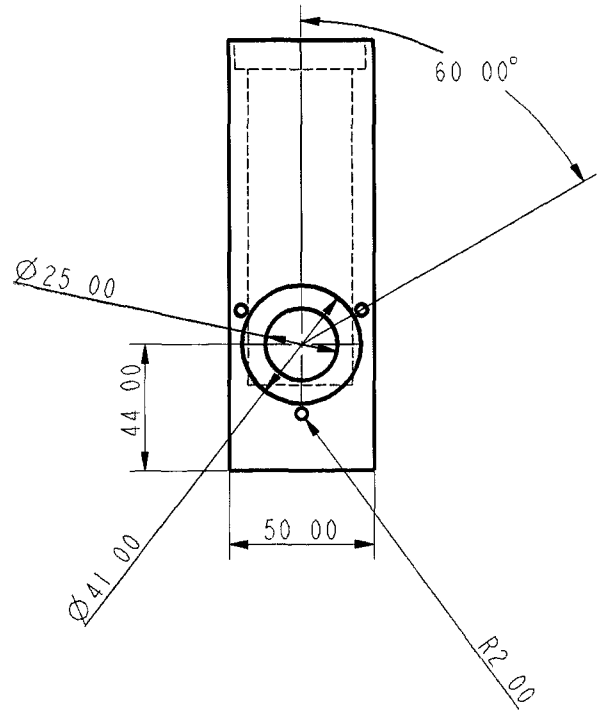

3 EQUI SPACED HOLES ON A P C D OF 48

	CYLINDER	PISTON PUMP	
		G M I T	ALL DIMENSIONS IN MM
		Liam Morris	PART NO 1

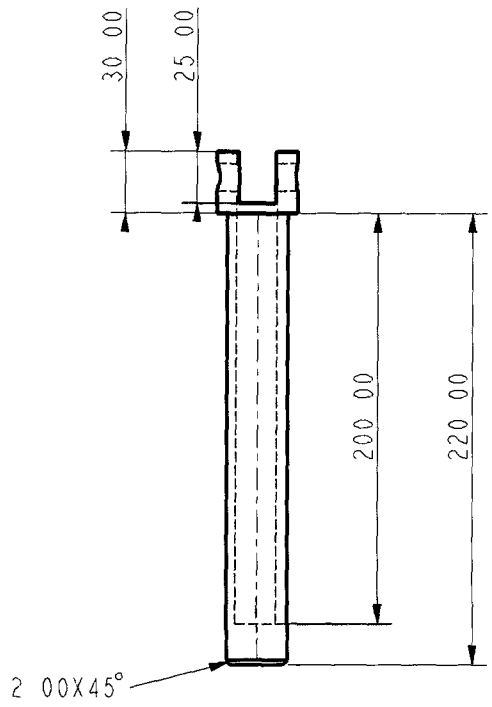

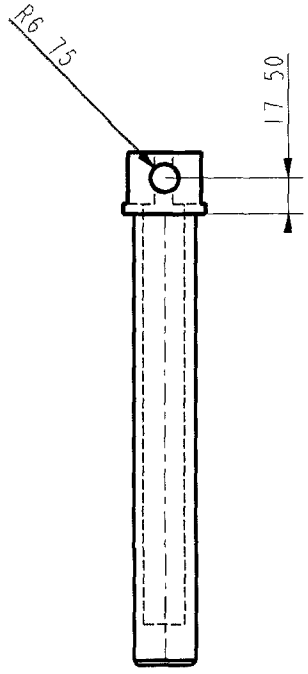

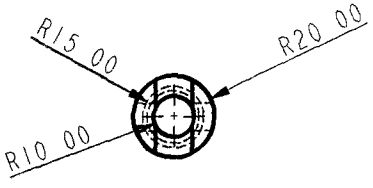

	PLUNGER	PISTON PUMP	
		G M I T	ALL DIMENSIONS IN MM
		Liam Morris	PART NO 2

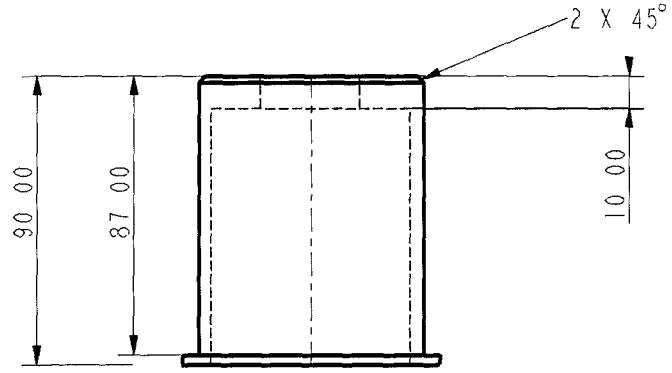

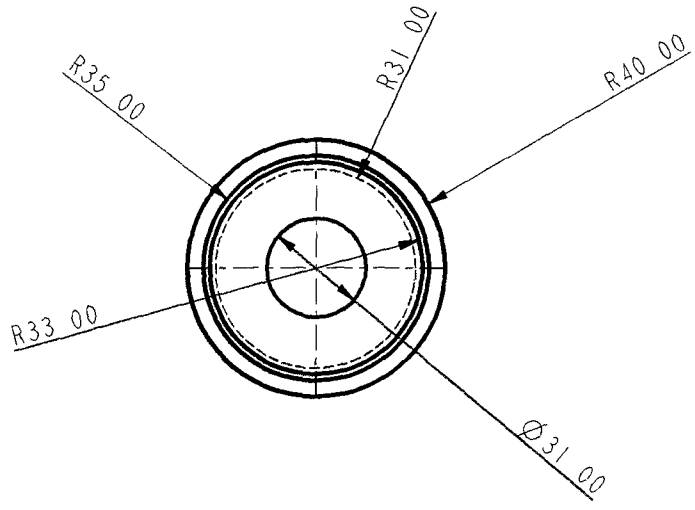

	STUFFING BOX	PISTON PUMP
		G M I T / ALL DIMENSIONS IN MM
		Liam Morris / PART NO 3

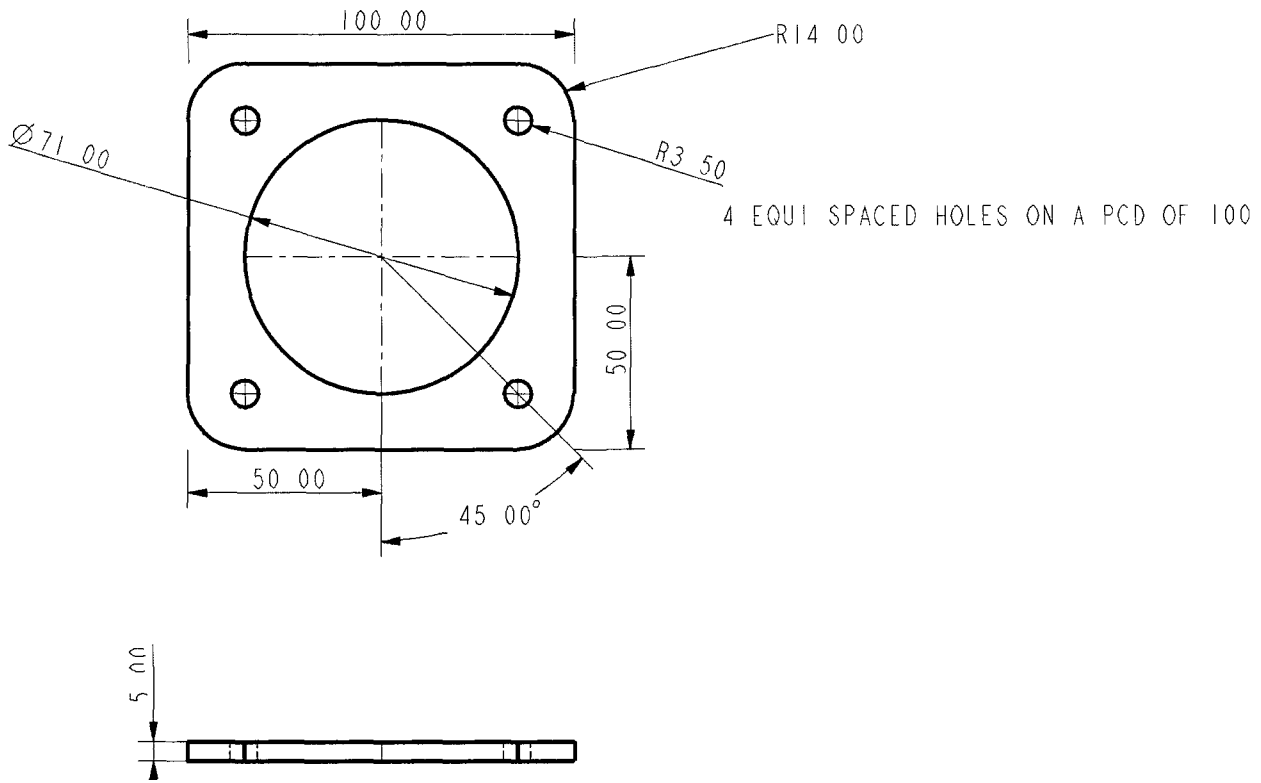

TOP PLATE	PISTON PUMP	
	G M I T	ALL DIMENSIONS IN MM
	Liam Morris	PART NO 4

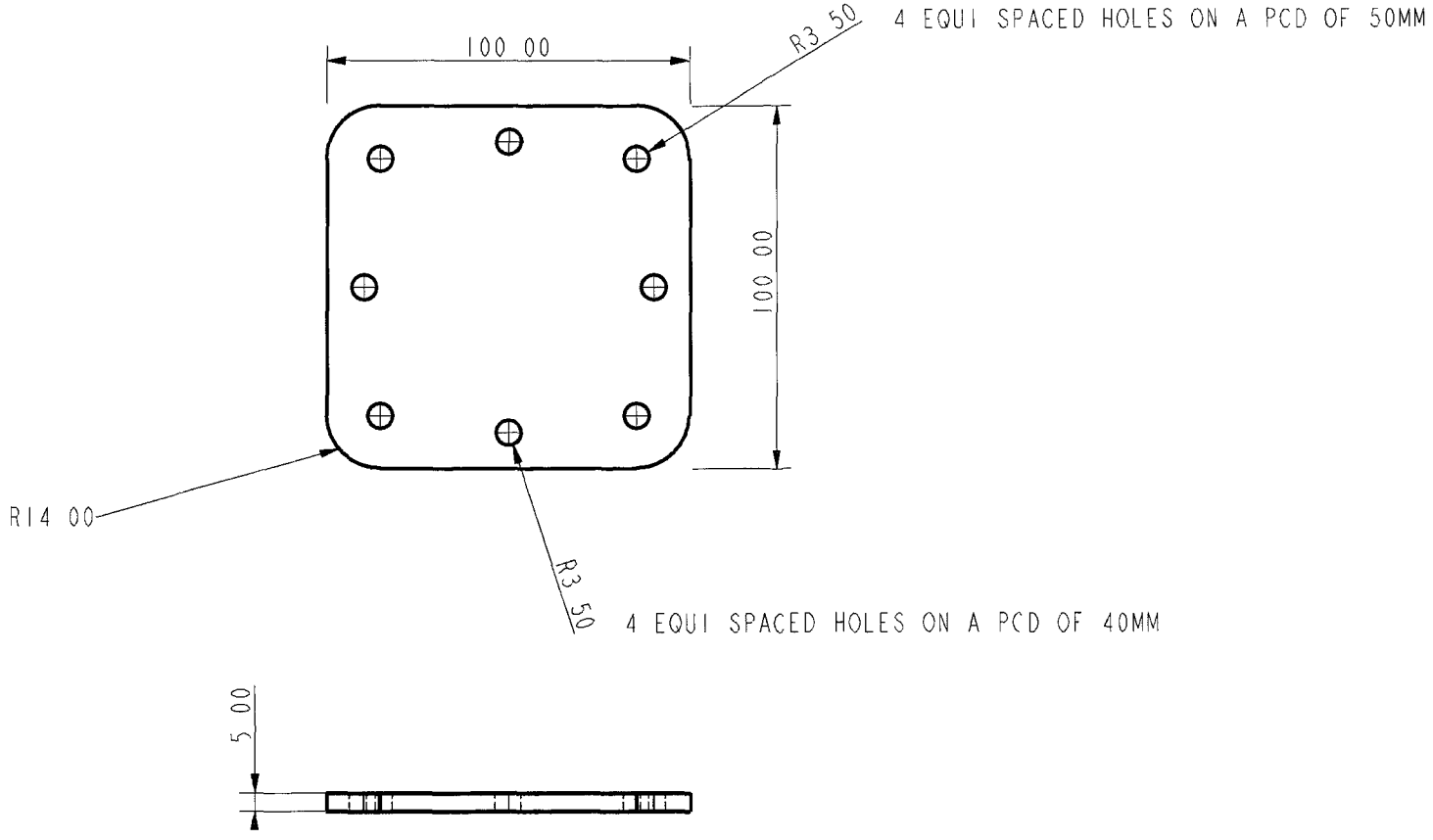

	BOTTOM PLATE	PISTON PUMP	
		G M I T	ALL DIMENSIONS IN MM
		Liam Morris	PART NO 5

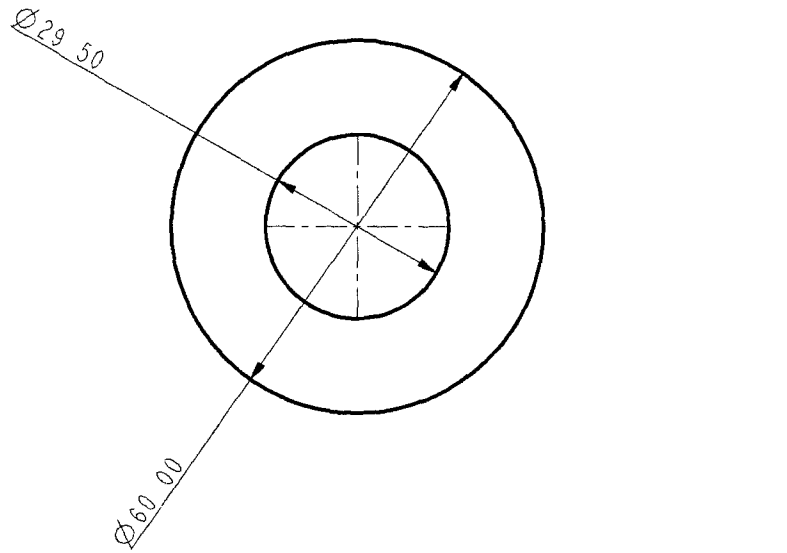

TOP BUSHING

PISTON PUMP

G M I T	ALL DIMENSIONS IN MM
Liam Morris	PART NO. 6

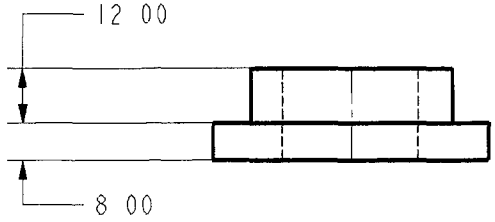

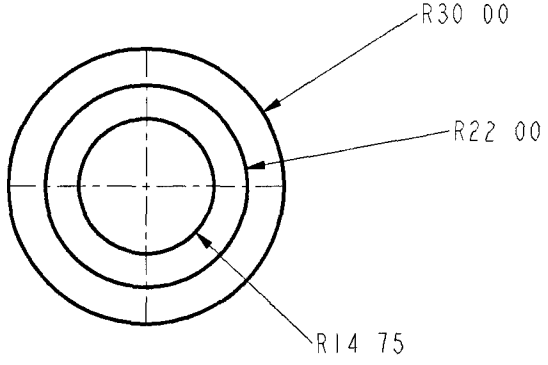

BOTTOM BUSHING

PISTON PUMP	
G M I T	ALL DIMENSIONS IN MM
Liam Morris	PART NO 7

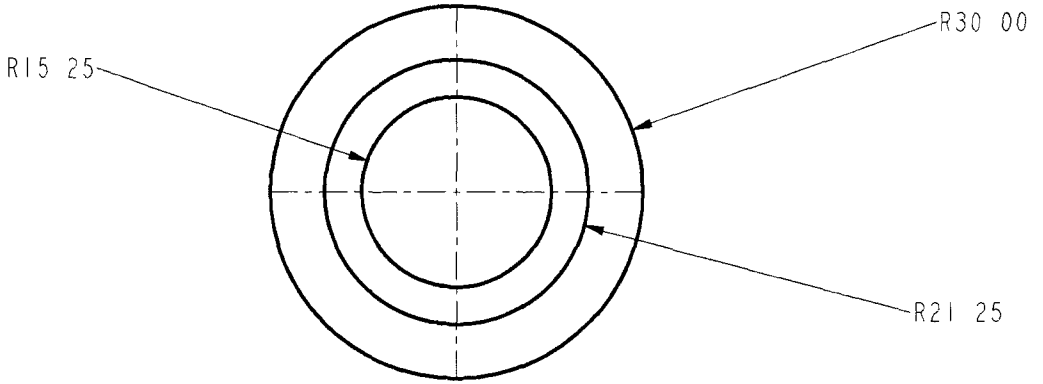

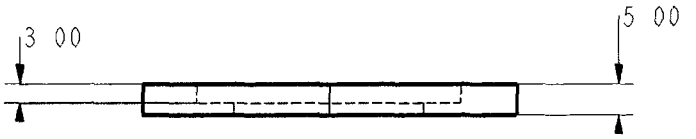

	BEARING SEAL	PISTON PUMP
		G M I T / ALL DIMENSIONS IN MM
		Liam Morris / PART NO 9

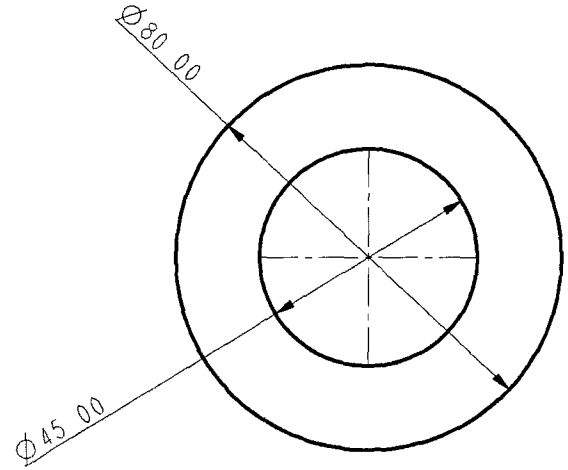

	SUPPORT PLATE	PISTON PUMP	
		G M I T	ALL DIMENSIONS IN MM
		Liam Morris	PART NO 10

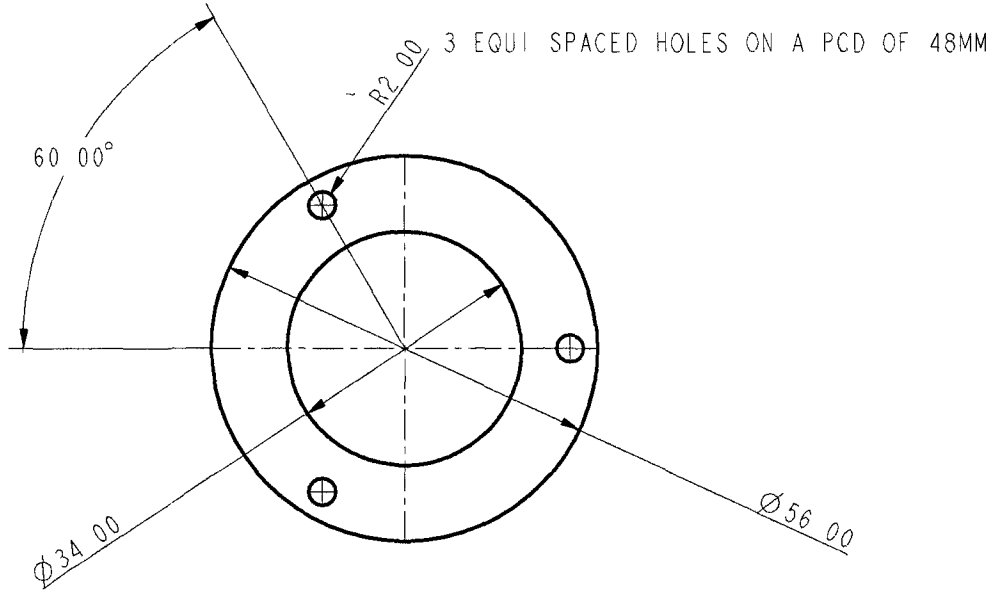

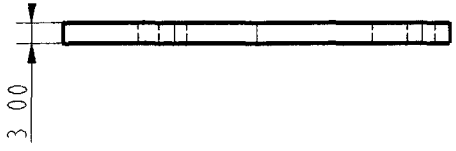

	VALVE CLAMPER	PISTON PUMP
		G M I T / ALL DIMENSIONS IN MM
		Liam Morris / PART NO 11

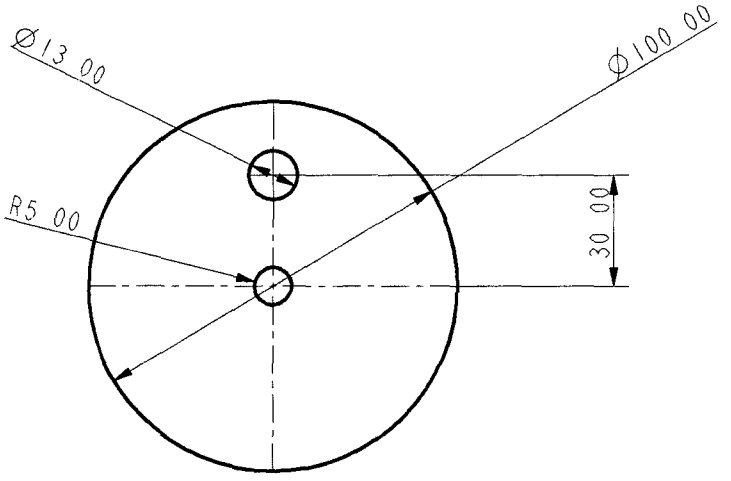

3MM THICKNESS

	CRANK SHAFT	PISTON PUMP
		G M I T / ALL DIMENSIONS IN MM
		Liam Morris / PART NO 12

MOTOR SUPPORT

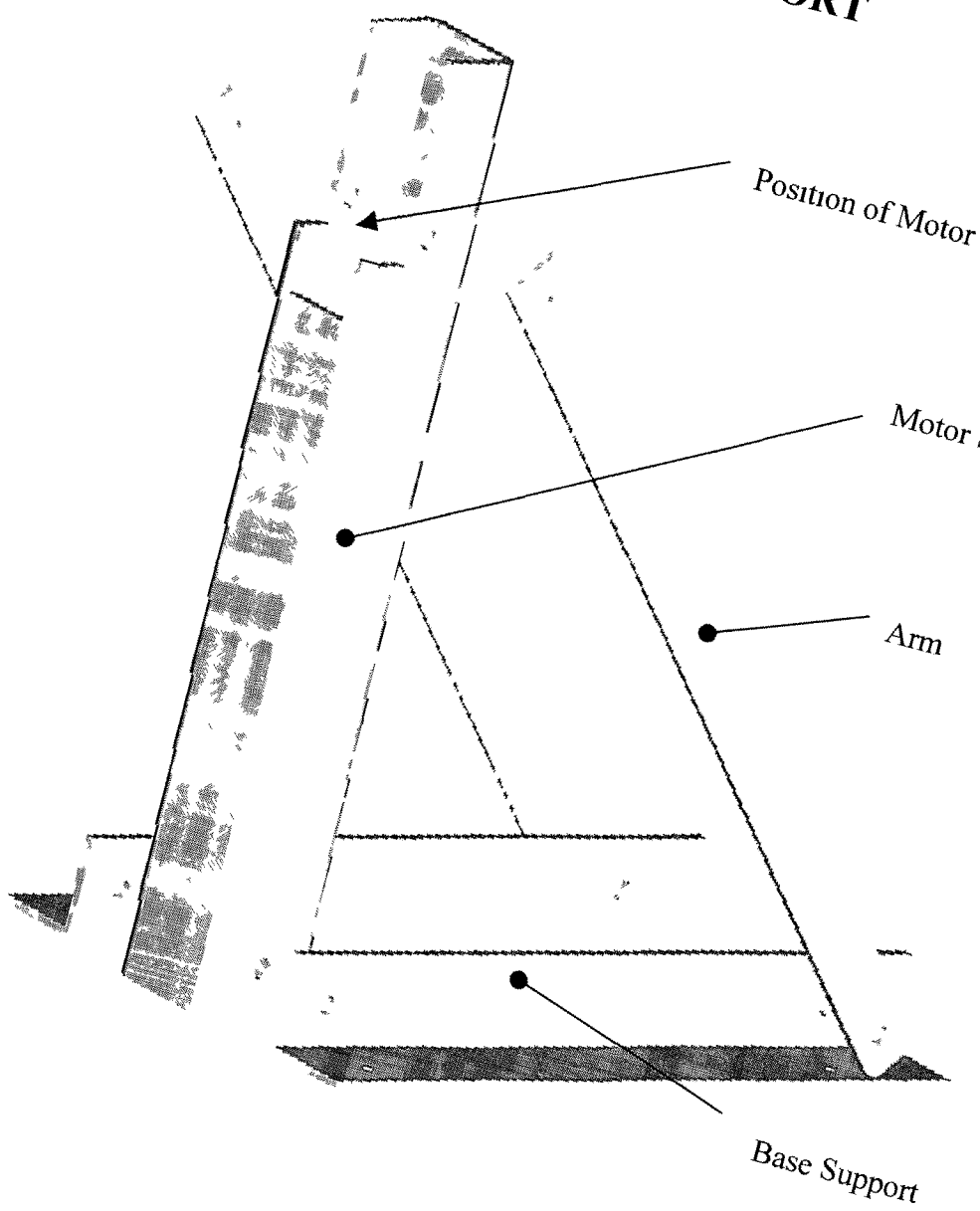

The motor, whose axle carries all the components of the power end, is hold in the right place by the use of a specially designed Motor Stand

To avoid vibrations of high amplitude, this stand was built using the principles of the trellis construction theory The main principle of this theory is that a triangular mesh, where the sides are made out of rigid rods, cannot get out of shape Thus, we followed this consideration and did an elementary static force analysis to find the best compromise for the dimension of the triangle The analysis is presented in the following lines

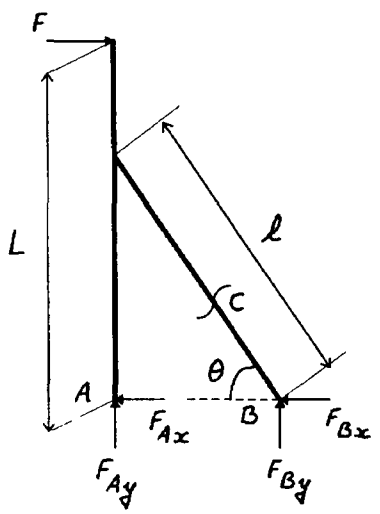

F = independent parameter

Given L = 380 mm

Unknown Which values of *l* and θ will minimise the reactions F_{Ax}, F_{Ay}, F_{Bx}, and F_{by}?

Analysis

$$\sum M_A = 0 \Rightarrow F \times L - F_{By} \times l \times \cos\theta = 0$$

$$\Leftrightarrow F_{By} = F \times \frac{L}{l \times \cos\theta} \qquad (1)$$

$$\sum F_y = 0 \Rightarrow F_{Ay} = -F_{By} = -F \times \frac{L}{l \times \cos\theta} \qquad (2)$$

$$\sum F_x = 0 \Rightarrow F_{Ax} + F_{Bx} = F \qquad (3)$$

Section C

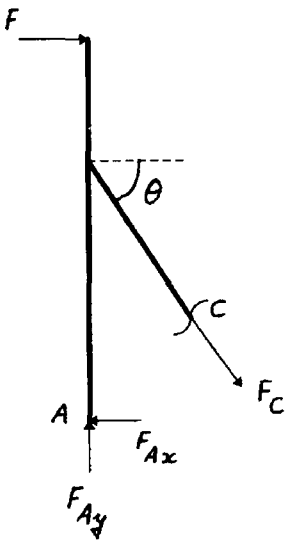

$$\sum M_A = 0 \Rightarrow F \times L + \left(F_C \times \cos\theta\right) \times \left(l \times \sin\theta\right) = 0$$

$$\Leftrightarrow F_C = -F \times \frac{L}{(l \times \sin\theta) \times \cos\theta} \qquad (4)$$

$$\sum F_x = 0 \Rightarrow F - F_{Ax} + F_C \times \cos\theta = 0$$

$$\Leftrightarrow F_{Ax} = F + F_C \times \cos\theta$$

$$\Leftrightarrow F_{Ax} = F - F \times \frac{L}{l \times \sin\theta}$$

$$\Leftrightarrow F_{Ax} = F \times \left(1 - \frac{L}{l \times \sin\theta}\right) \qquad (5)$$

$$(3)\&(5) \Rightarrow F_{Bx} = F - F_{Ax}$$

$$\Leftrightarrow F_{Bx} = F - \left(F - F \times \frac{L}{l \times \sin\theta}\right)$$

$$\Leftrightarrow F_{Bx} = F \times \frac{L}{l \times \sin\theta}$$

Conclusions :

1° We can notice that the length l is always at the denominator So, to reduce the dynamic constraints, its value must be as big as possible On the other hand, the rod BC cannot be too long because it is the most constrained part of the stand Consequently, a good compromise seems to be $l = L$

2° The results of the analysis also tell us that if the value for θ increases from θ to 90°, then the vertical constraints F_{iy} increase too but not the horizontal ones F_{ix} Therefore, the best compromise for the value of the angle θ is near 45° I chose 50° in order to reduce the bulk of the stand

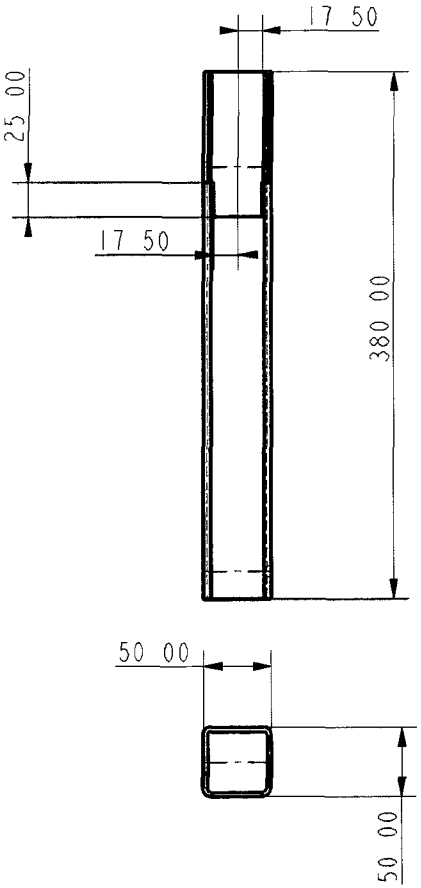

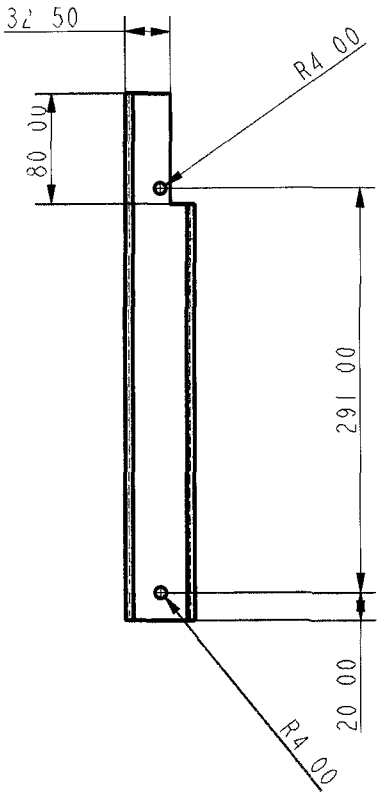

3MM THICKNESS
ALL FILLETS 2 5MM

MOTOR SUPPORT

PISTON PUMP	
G M I T	ALL DIMENSIONS IN MM
Liam Morris	PART NO 14

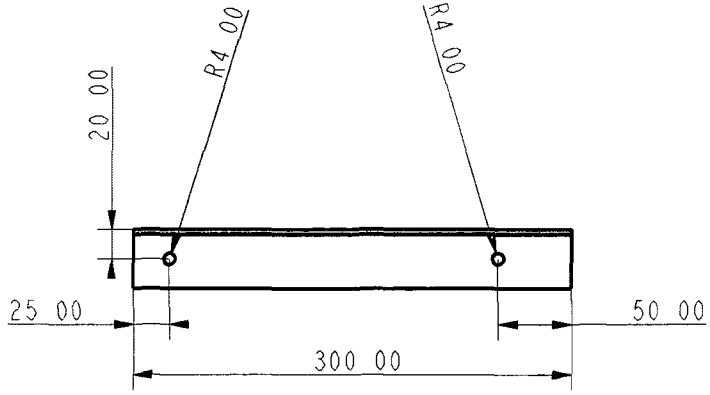

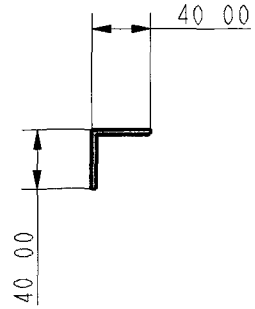

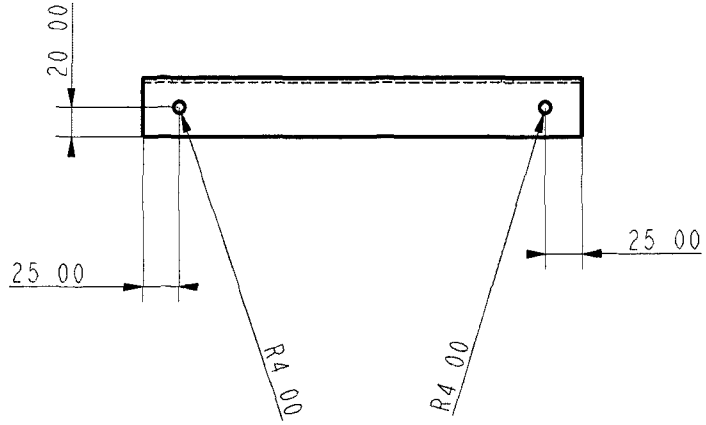

3MM THICKNESS

	BASE SUPPORT	PISTON PUMP
		G M I T / ALL DIMENSIONS IN MM
		Liam Morris / PART NO 15

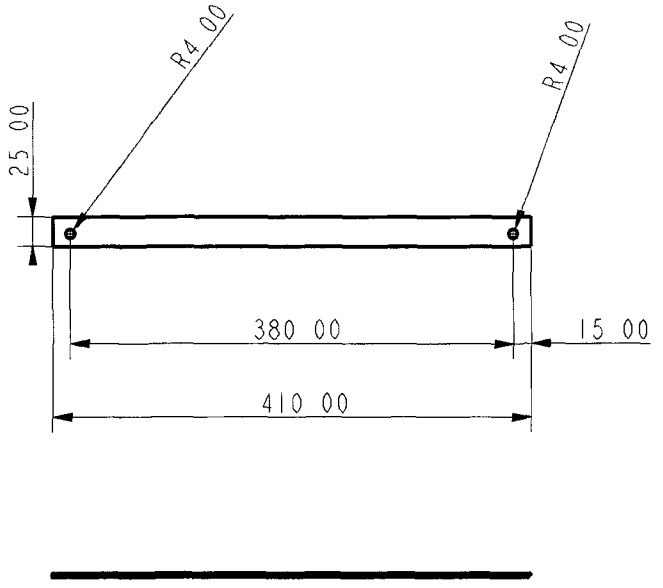

3MM THICKNESS

	ARM	PISTON PUMP	
		G M I T	ALL DIMENSIONS IN MM
		Liam Morris	PART NO 16

Female Cast.

Part No:	Part Name:	Material	Quantity
1	Female Cast	Aluminium	2
2	Threaded Bar	M8 Aluminium X 150mm long	3
3	Nuts	M8	6
4	Washers	I D 8mm	6

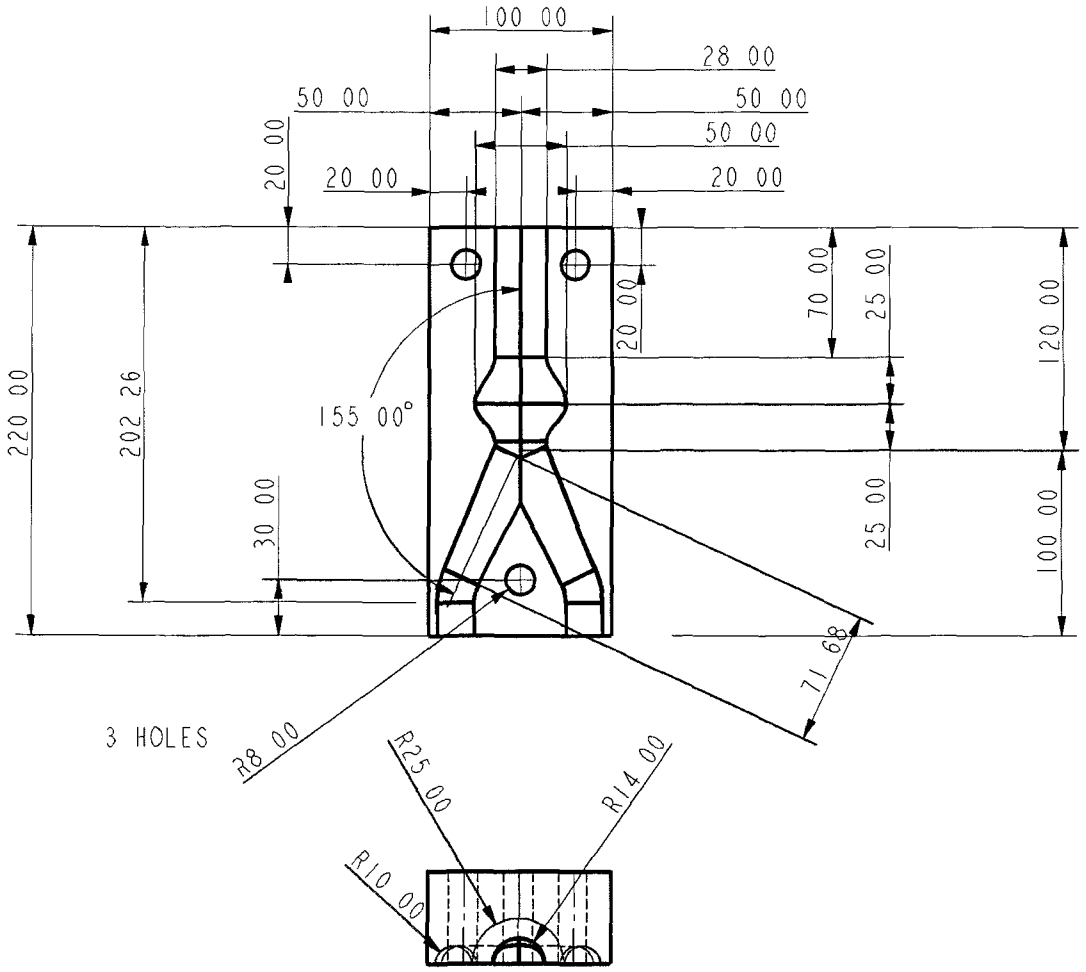

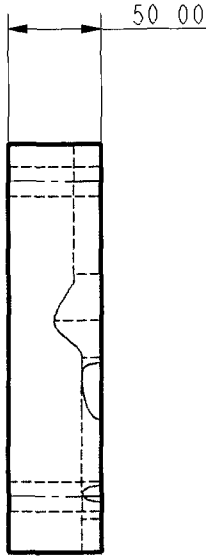

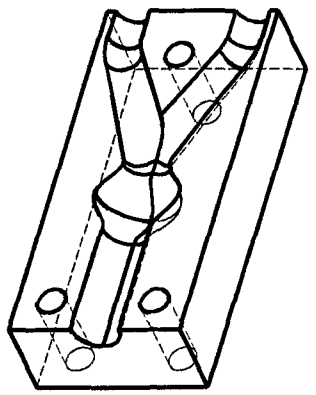

	FEMALE CAST	PISTON PUMP
		G M I T
		Liam Morris
		ALL DIMENSIONS IN MM
		PART NO 1

Appendix C

```
SetAttributes[r, Constant]
```

```
SetAttributes[l, Constant]
```

```
ramposition = r * Cos[θ] + l * (Sqrt[(1 - r^2/l^2 * Sin[θ]^2)])
```

$$30 \cos[\theta] + 100 \sqrt{1 - \frac{9 \sin[\theta]^2}{100}}$$

```
r = 30,
```

```
l = 100,
```

```
rpm = 80,
```

```
velocity = Dt[ramposition, t] /  Dt[θ, t] -> 2 π * rpm / 60
```

$$-80 \pi \sin[\theta] - \frac{24 \pi \cos[\theta] \sin[\theta]}{\sqrt{1 - \frac{9 \sin[\theta]^2}{100}}}$$

```
acceleration = Dt[velocity, t] /  {Dt[θ, t] -> 2 π * rpm / 60, Dt[θ, {t, 2}] -> 0}
```

$$-\frac{640}{3} \pi^2 \cos[\theta] - \frac{144 \pi^2 \cos[\theta]^2 \sin[\theta]^2}{25 \left(1 - \frac{9 \sin[\theta]^2}{100}\right)^{3/2}} - \frac{64 \pi^2 \cos[\theta]^2}{\sqrt{1 - \frac{9 \sin[\theta]^2}{100}}} + \frac{64 \pi^2 \sin[\theta]^2}{\sqrt{1 - \frac{9 \sin[\theta]^2}{100}}}$$

```
Plot[ramposition, {θ, 0, 4 π}, AxesLabel -> {"rads", "mm"}]
```

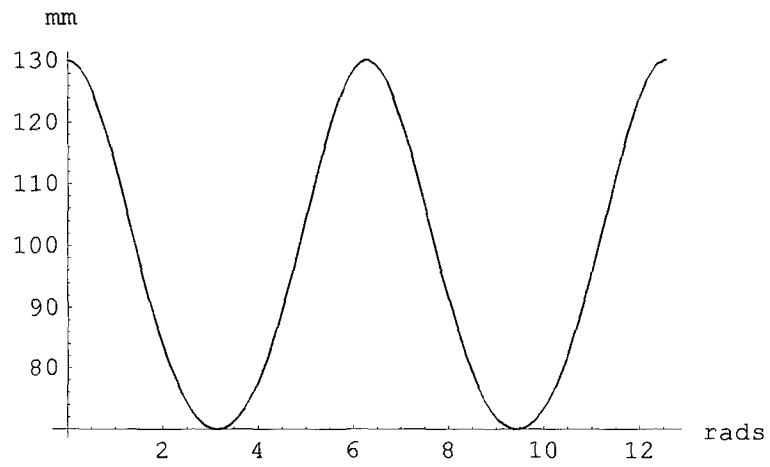

- Graphics -

```
Plot[velocity, {θ, 0, 4 π}, AxesLabel -> {"rads", "mm/s"}]
```

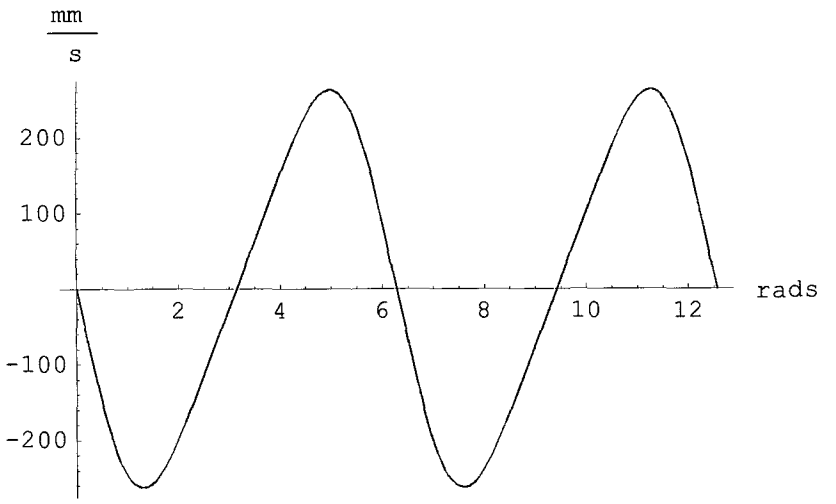


```
- Graphics -
```

```
Plot[acceleration, {θ, 0, 4 π}, AxesLabel -> {"rads", "mm/s^2"}]
```

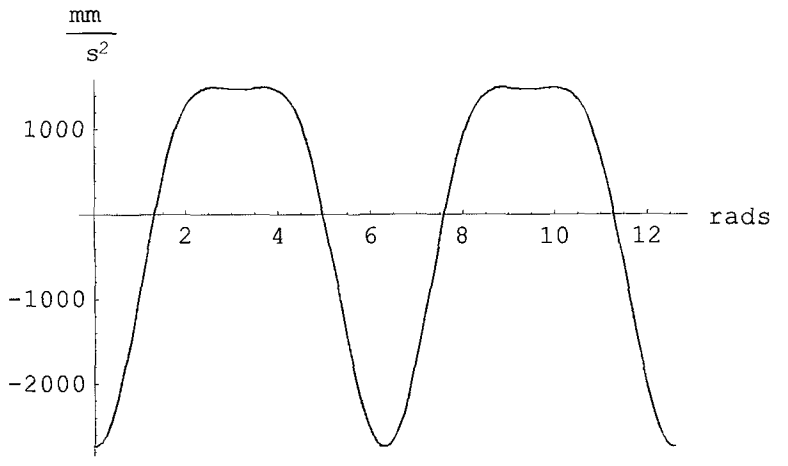


```
- Graphics -
```

```
dpump = 30,

daortic = 22,

velocityaortic = dpump^2 / daortic^2 * velocity / 10
```

$$\frac{45}{242}\left(-80\,\pi\,\text{Sin}[\theta] - \frac{24\,\pi\,\text{Cos}[\theta]\,\text{Sin}[\theta]}{\sqrt{1-\frac{9\,\text{Sin}[\theta]^2}{100}}}\right)$$

```
Plot[velocityaortic, {θ, 0, 4 * π}, AxesLabel -> {"rads", "cm/s"}]
```

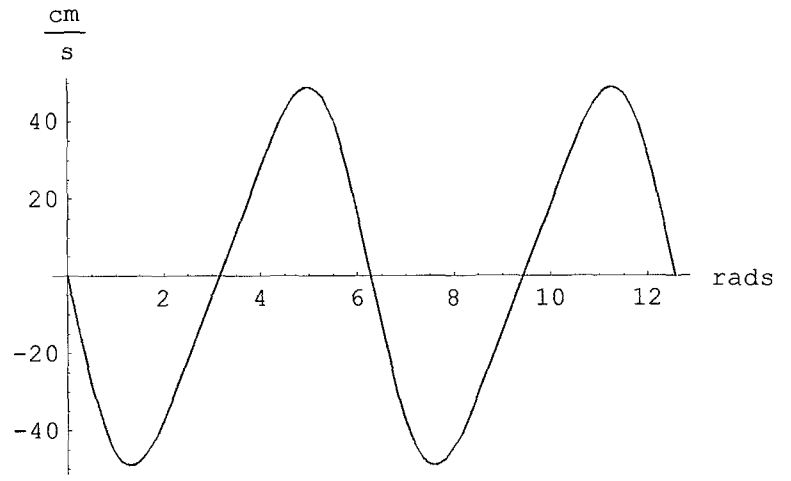


```
- Graphics -
```

Appendix D

Mechanical Properties of Selected Fibers.

Adapted from Adanur

Fiber	Tensile strength (MPa)	Breaking elongation (%) dry	wet	Elastic Recovery (%)	Youngs Modulus (MPa)	Density kg/m^3
Polyester						
Dacron® RT	345-683	24-42	24-42	76 at 3%	10512	1340
Dacron® HT	731-1158	12-25	12-25	88 at 3%	6307	1340
Fortel®	552-607	120-150	120-150		6704	1380
Trevira® HT	814-965	10-20	10-20	99 at 1%	9748	1380
Trevira® RT	228-290	130-145	130-145		6277	1380
Nylon						
Nylon 6 RT	503-690	17-45	20-47	98-100at 1-10%	1855	1140
Nylon 6 HT	703-862	16-20	19-33	99-100 at 2-8%	3851	1140
Nylon 6,6 RT	276-731	25-65	30-70	88 at 3%	5278	1140
Nylon 6,6 HT	593-924	15-28	18-32	89 at 3%	6515	1140
Fluorocarbons						
Gore-Tex®	586-793	5-20	5-20		13171	2000
Teflon®	97-138	40-62	40-62		1188	2100

RT = Regular Tenacity, HT = High Tenacity *Adapted from Adanur ref 38*

Mechanical Properties of Tested Fabrics

As Tested by the Instron Tensile Testing Machine.

No	Material	Yarn/No of fibres	Dir	Thickness (mm)	Initial Modulus MPa	Yield Stress MPa	% extension at yield
1	Polyester	Mono	Weft	1	852	26 7	04
2	Polyester	Mono	Warf	1	1060	18 6	022
3	Polyester	Multı/<25	Weft	28	84	6	131
4	Polyester	Multı/<25	Warf	28	175	14	077
5	Polyester	Multı/<30	Weft	25	120	5 6	048
6	Polyester	Multı/<30	Warf	25	144	8 2	063
7	Polyester	Multı/15	Weft	15	369	22	075
8	Polyester	Multı/15	Warf	15	390	24	072
9	Nylon	Multı/15	Weft	12	292	38	16
10	Nylon	Multı/15	Waft	12	342	58	195

Load Extension Curves for Tested Fabrics

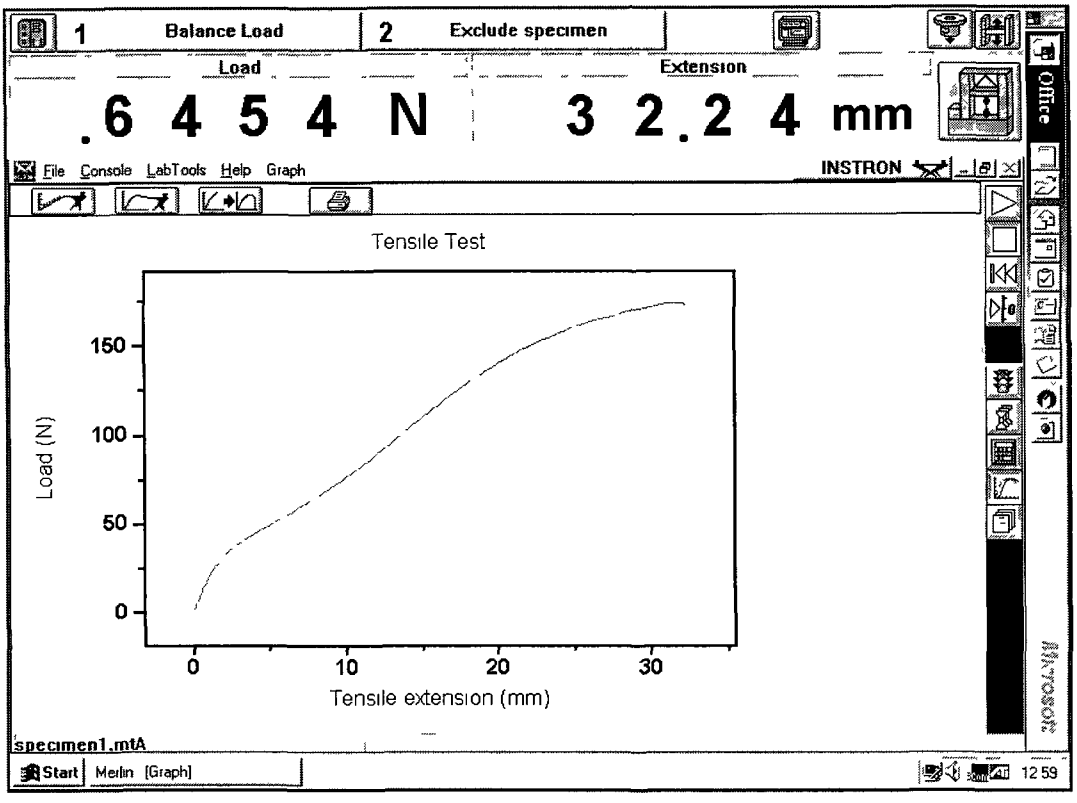

No 1: Polyester, Weft direction

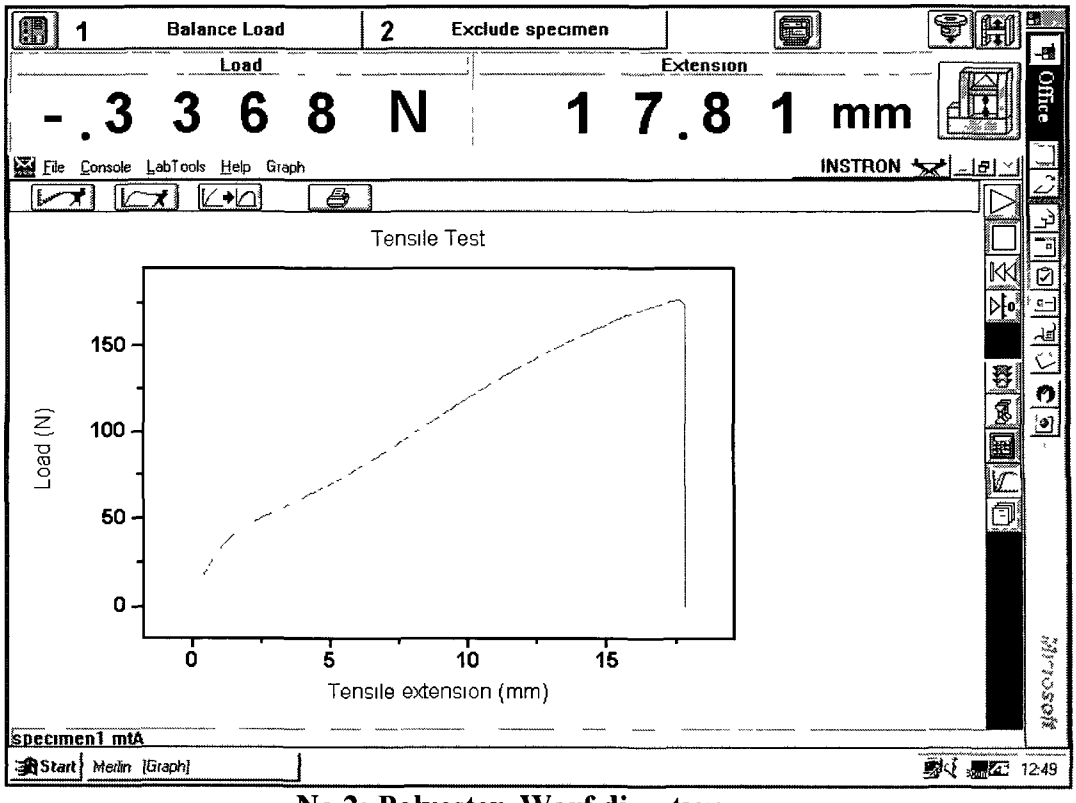

No 2: Polyester, Warf direction

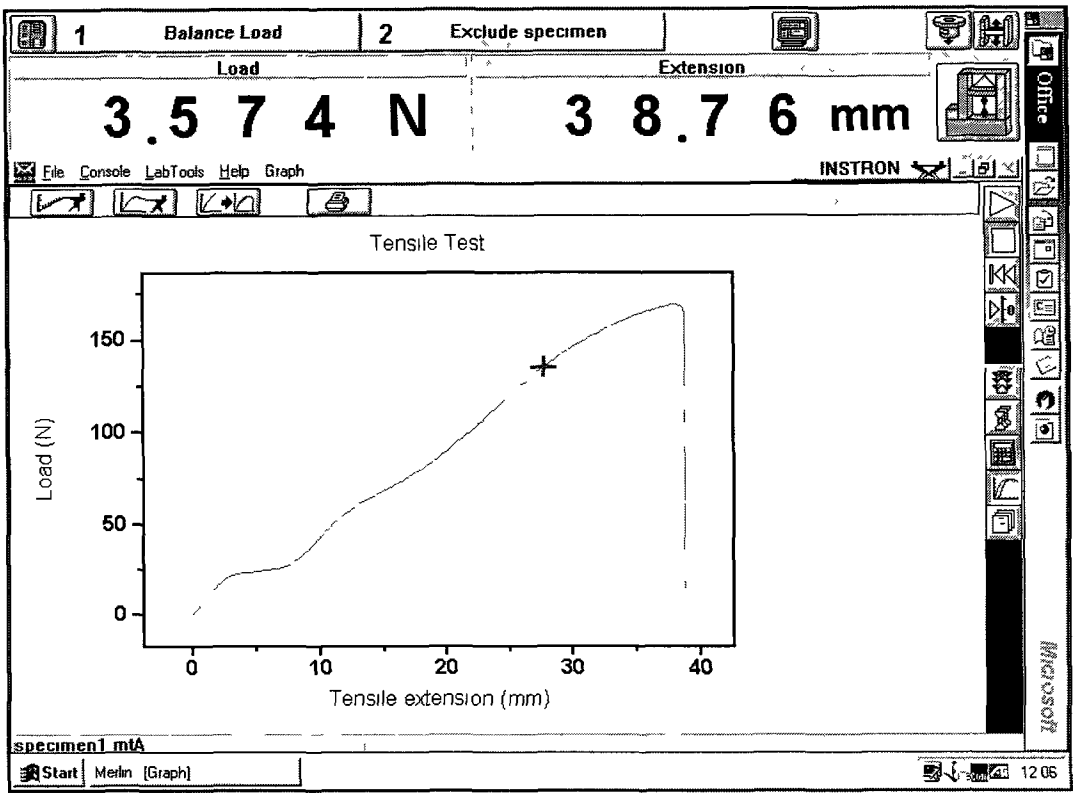

No 3: Polyester, Weft direction

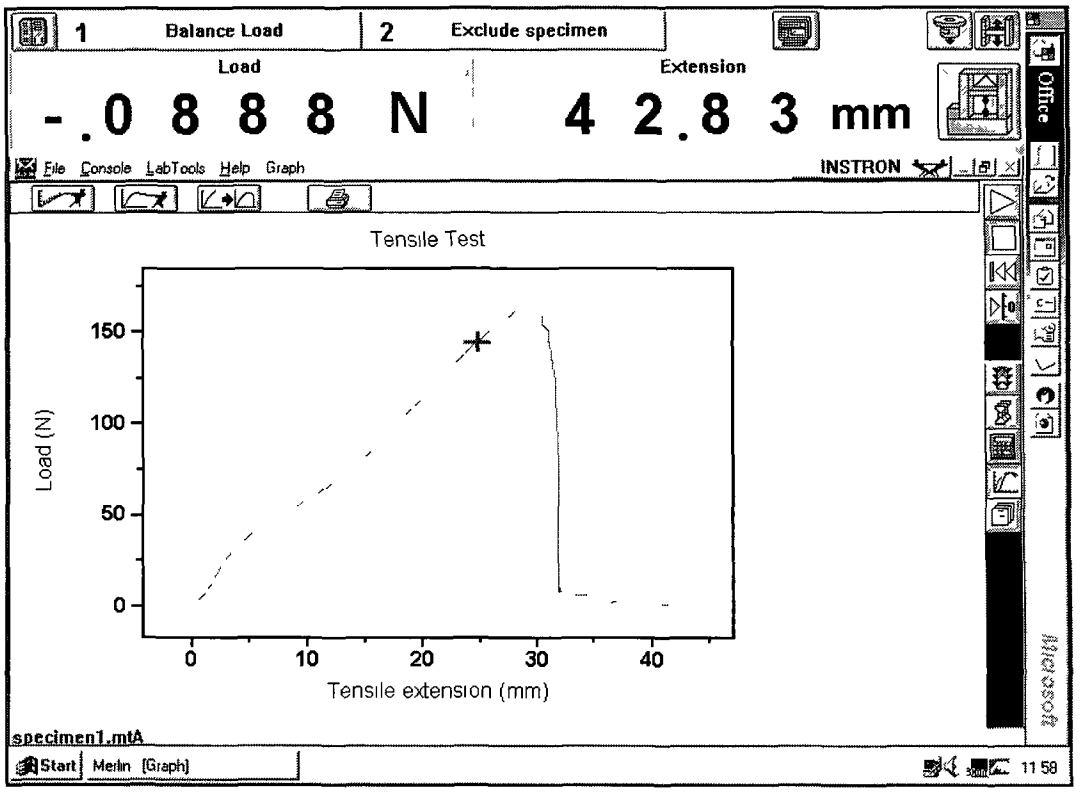

No 4: Polyester, Warf direction

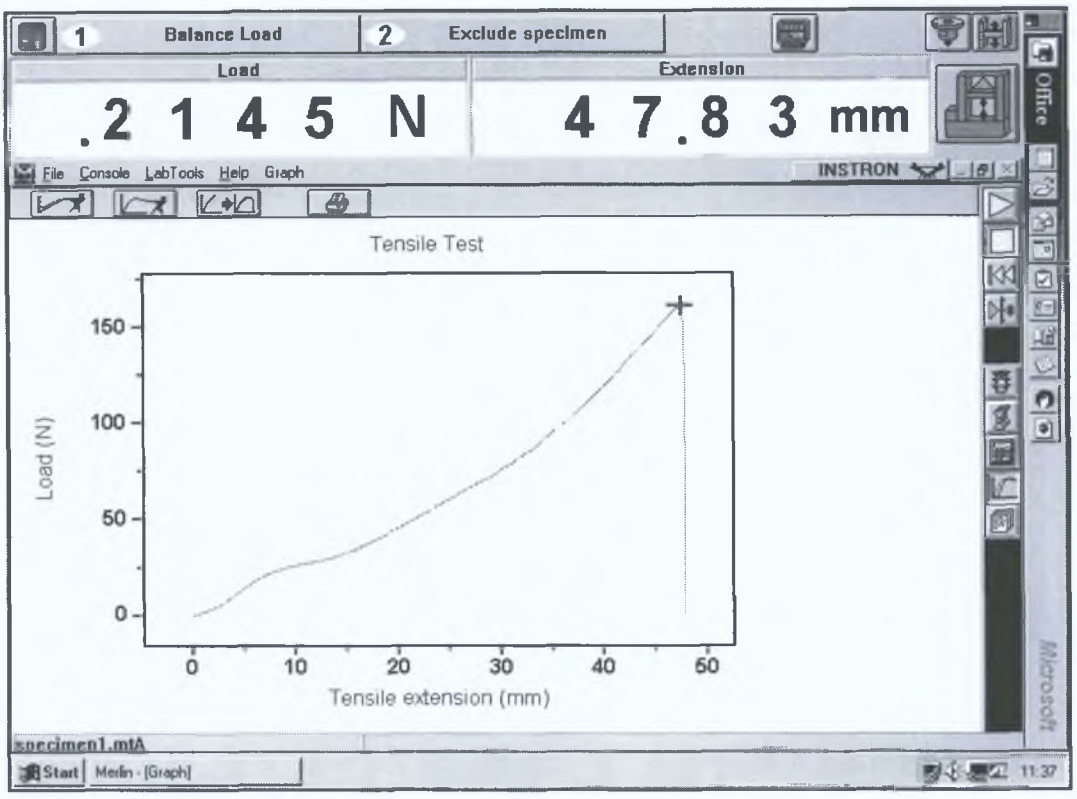

No 5: Polyester, Weft direction

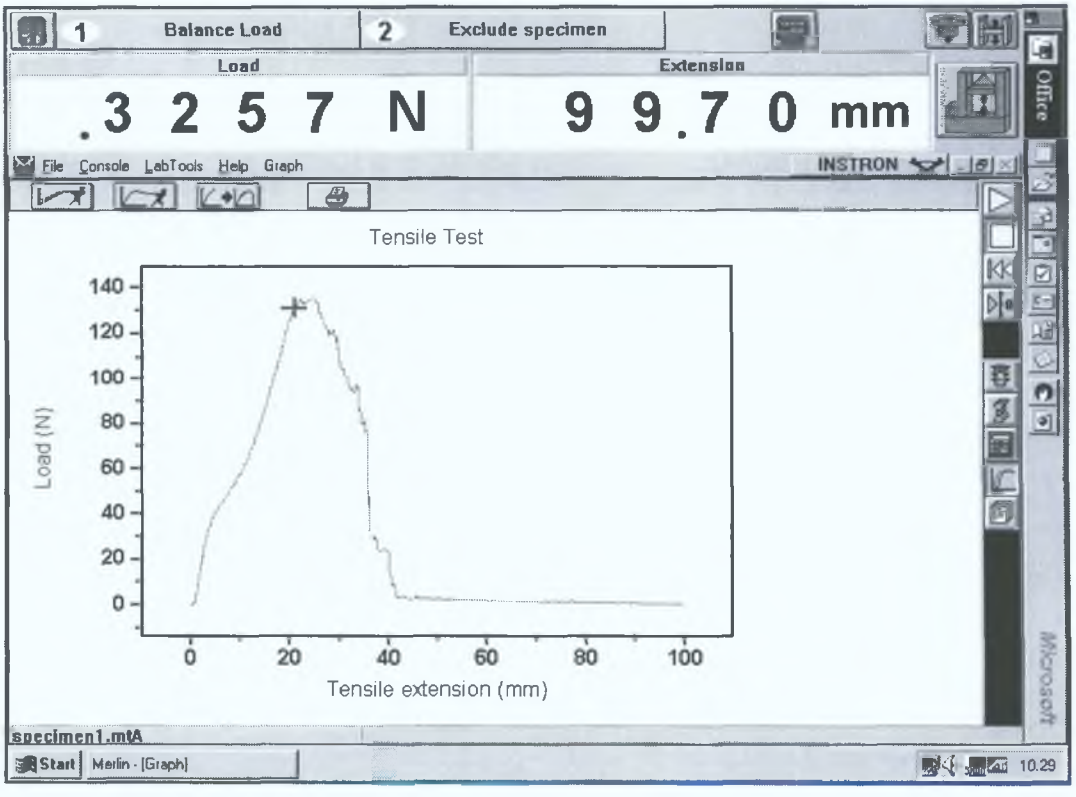

No 6: Polyester, Warf direction

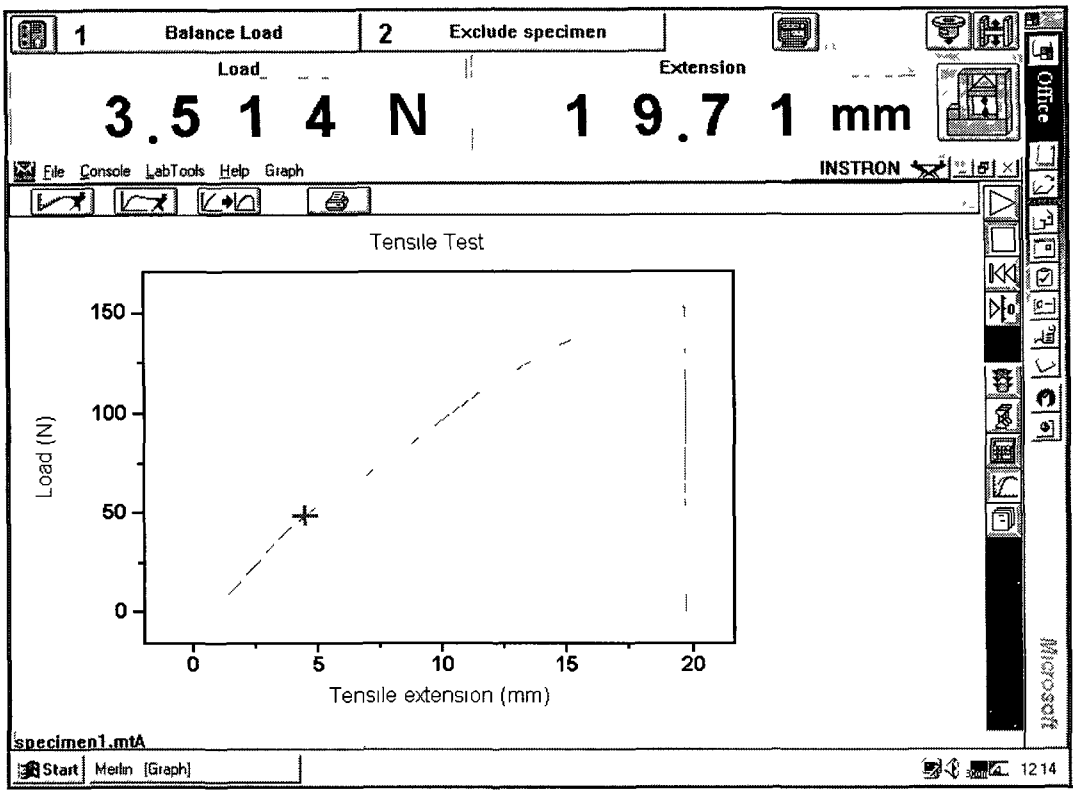

No 7: Polyester, Weft direction

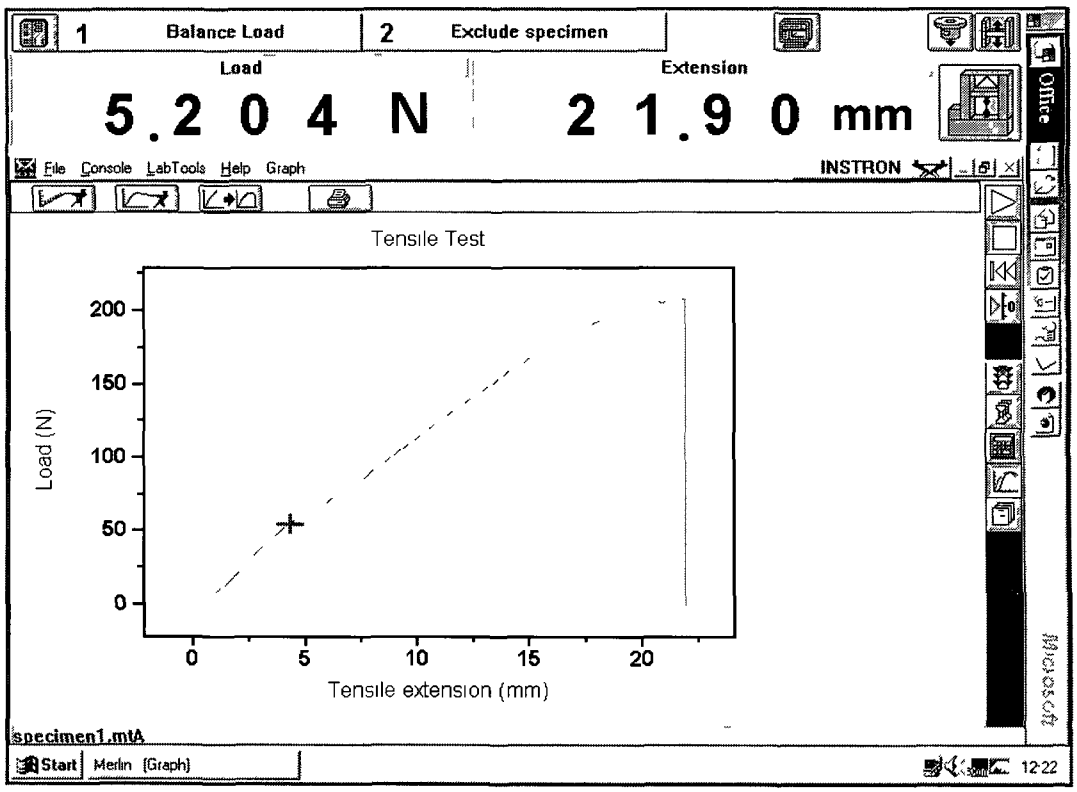

No 8: Polyester, Warf direction

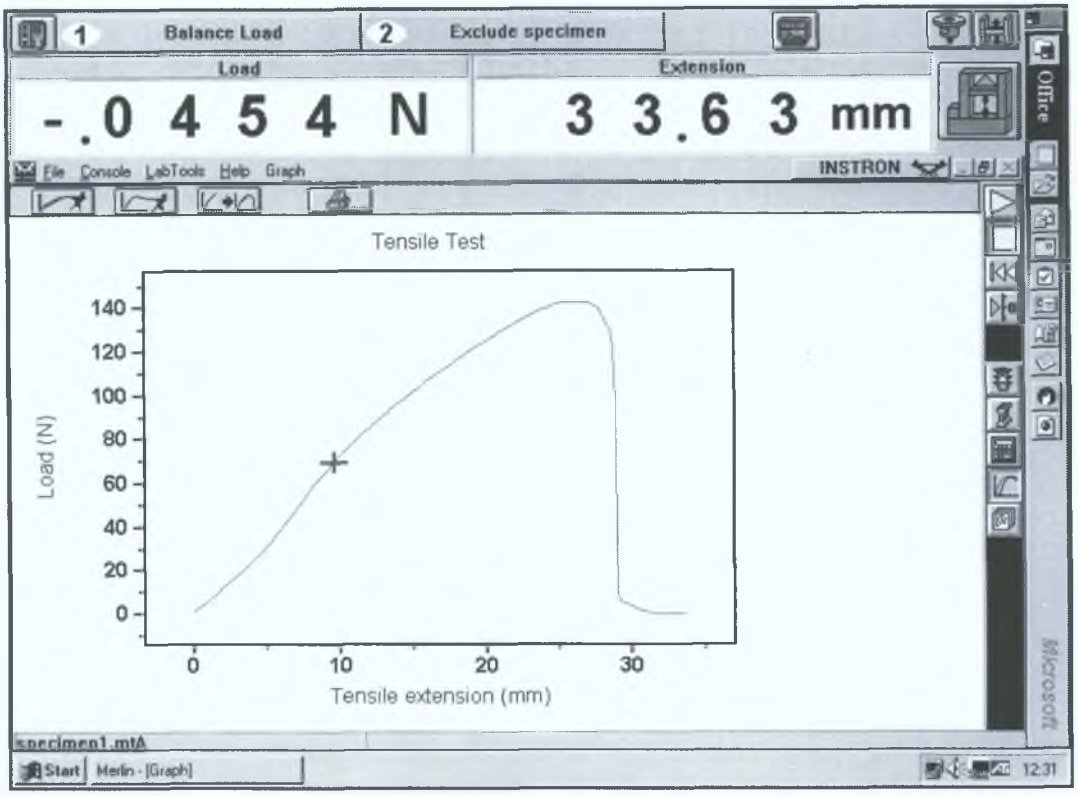

No 9: Nylon, Weft direction

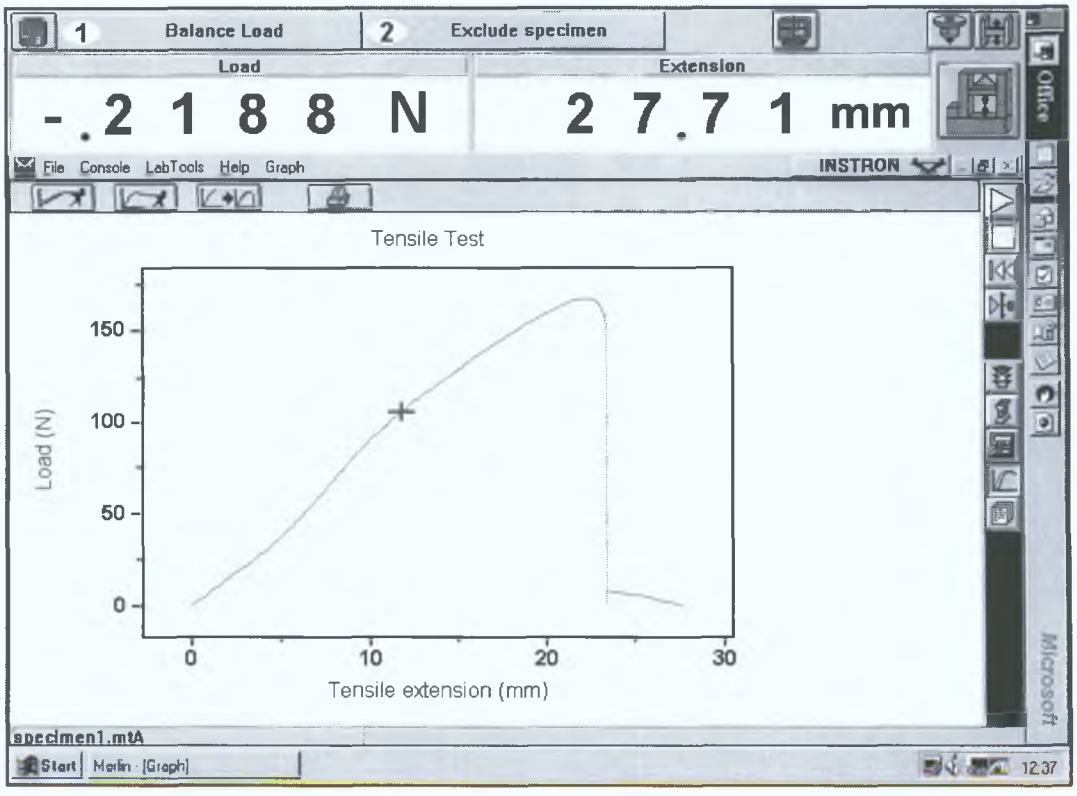

No 10: Nylon, Warf direction

Appendix E

Resultant Force on Bifurcated Graft Using Typical Pressure & Flow Relationships.

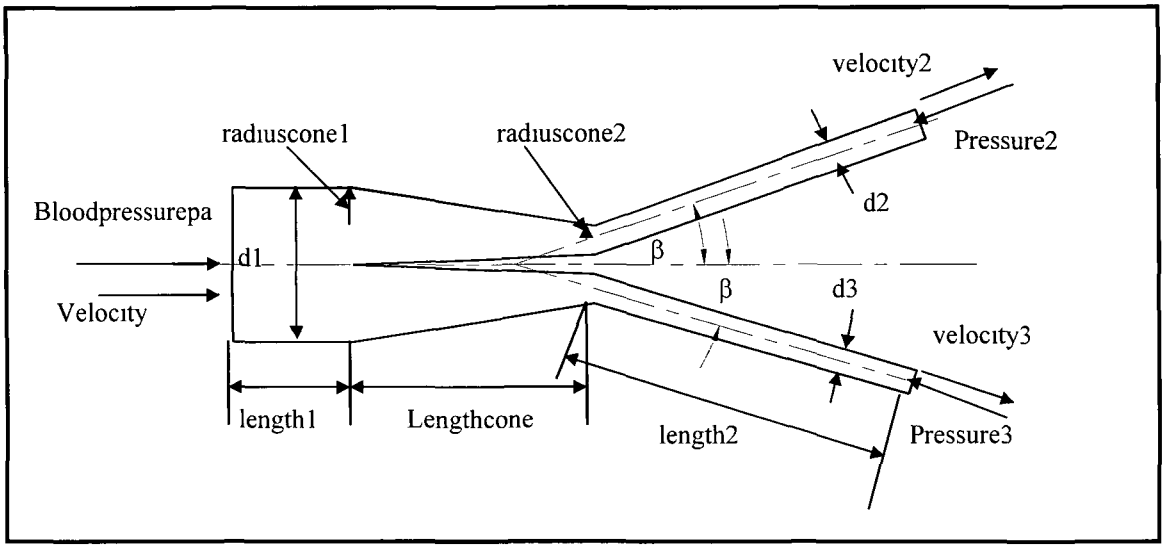

Where

d1 = Proximal diameter

Bloodpressurepa = Pressure of blood in pascals

Velocity = velocity of blood through proximal end

d3 = iliac leg diameter

velocity2 = velocity3 = velocity of blood through iliac legs

Pressure2 = Pressure3 = Pressure of blood at iliac legs in pascals

```
<< NumericalMath`TrigFit`

pressurepoints = {74.44, 82.67, 102.22, 116.89, 124.44, 104.89, 103.33,
  93.33, 86.67, 82.27, 77.78, 73.33};

period = 0.936;

bloodpressure = TrigFit[pressurepoints, 10, {t, period}];

flowratepoints = {0, -44.44, 0, 355.56, 551.11, 408.89, 332.44, 266.67,
  222.22, 0, -35, 53.33, 35.56, 0, 0, 0, 0, 0, 0, 0};

flowrate = TrigFit[flowratepoints, 10, {t, period}];

pressureconvertion = 13.6 * 9.81;

bloodpressurepa = bloodpressure * pressureconvertion;

d1 = {32 / 1000, 30 / 1000, 28 / 1000, 26 / 1000, 24 / 1000, 22 / 1000, 20 / 1000, 18 / 1000};

v = 0.5;

youngs = 7 * 10^5;

tartery = 1.1 / 1000;

Δrproximal = (2 * (1 - v^2) * (bloodpressurepa - 6200) * d1/2 * (1 - tartery/(d1/2))^2) /
  (youngs * (1 - (1 - tartery/(d1/2))^2));

area1 = π * (d1/2 + Δrproximal)^2;

flowconvertion = 10^-6 * .625;

velocity = flowrate * flowconvertion / area1;

length1 = 15 / 1000;

volume1 = length1 * area1;

ρ = 1065;

g = 9.81;

d2 = {16 / 1000, 15 / 1000, 14 / 1000, 13 / 1000, 12 / 1000, 11 / 1000, 10 / 1000, 9 / 1000};

area2 = d2^2 * π / 4;

length2 = 65 / 1000;

volume2 = area2 * length2;

radiuscone1 =
 {8 / 1000, 75 / 10000, 7 / 1000, 65 / 10000, 6 / 1000, 55 / 10000, 5 / 1000, 45 / 10000};

radiuscone2 = {113 / 10000, 106 / 10000, 10 / 1000, 9 / 1000, 85 / 10000,
  77 / 10000, 7 / 1000, 64 / 10000};
```

$$\text{lengthcone} = 30 / 1000,$$

$$\text{volumecone} = \text{Integrate}\left[\pi * \left(\text{radiuscone1} - (\text{radiuscone1} - \text{radiuscone2}) * \frac{x}{\text{lengthcone}}\right)\text{^}2, \{x, 0, \text{lengthcone}\}\right],$$

$$\text{totalvolumeproximal} = \text{volume1} + \Delta\text{rproximal} * \pi * \text{d1} * \text{length1},$$

$$\text{velocity2} = \frac{\text{area1}}{2 * \text{area2}} * \text{velocity} - \frac{\rho}{2} * \text{Dt}[\text{totalvolumeproximal}, t],$$

$$\text{areacone} = \pi * \left(\left(\text{radiuscone1} - (\text{radiuscone1} - \text{radiuscone2}) \frac{x}{\text{lengthcone}}\right)\text{^}2\right),$$

$$\text{velocitycone} = \text{Integrate}\left[\frac{\text{velocity2} * \text{area2}}{\text{areacone}}, \{x, 0, \text{lengthcone}\}\right],$$

$$\text{acceleration1} = \text{Dt}[\text{velocity}, t],$$

$$\text{acceleration2} = \text{Dt}[\text{velocity2}, t],$$

$$\text{accelerationcone} = \text{Dt}[\text{velocitycone}, t],$$

$$\text{fproximal} = 044,$$

$$\text{hfproximal} = \frac{\text{velocity}\text{^}2 * \text{fproximal} * \text{length1}}{2 * 9\ 81 * \text{d1}},$$

```
General  spelll
 Possible spelling error  new symbol name "hfproximal" is similar to existing symbol "fproximal"
```

$$\text{filiac} = 0\ 046,$$

$$\text{hfiliac} = \frac{\text{velocity2}\hat{}2 * \text{filiac} * \text{length2}}{2 * 9\ 81 * \text{d2}},$$

```
General  spell1
 Possible spelling error  new symbol name "hfiliac" is similar to existing symbol "filiac"
```

$$\text{kcone} = 0\ 02,$$

$$\text{hfcone} = \frac{\text{velocitycone}\hat{}2 * \text{kcone}}{2 * 9\ 81},$$

$$\text{pressure2} = \rho * g * \left(\frac{\text{bloodpressurepa}}{\rho * g} - \frac{\text{velocity2}^2}{2 * g} + \frac{\text{velocity}^2}{2 * g} - \frac{\text{length1} * \text{acceleration1}}{g} - \frac{\text{length2} * \text{acceleration2}}{g} - \frac{\text{accelerationcone} * \text{lengthcone}}{g} - \text{hfproximal} - \text{hfiliac} - \text{hfcone} \right),$$

$$\beta = \pi / 6,$$

$$\text{dtvelocitytotalvolumeproximal} = \text{Dt}[\text{velocity} * \text{totalvolumeproximal}, t],$$

$$\begin{aligned}\text{Forcexdirection} = {} & \text{bloodpressurepa} * \text{area1} - 2 * \text{pressure2} * \text{area2} * \text{Cos}[\beta] - \\ & \rho * \text{dtvelocitytotalvolumeproximal} - 2 * \rho * \text{accelerationcone} * \text{volumecone} - \\ & 2 * \rho * \text{acceleration2} * \text{volume2} * \text{Cos}[\beta] - 2 * \rho * \text{area2} * \text{velocity2}\hat{}2 * \text{Cos}[\beta] + \\ & \rho * \text{area1} * \text{velocity}^2 + \rho * \text{totalvolumeproximal} + 2 * \rho * \text{volume2} * \text{Cos}[\beta] + \\ & 2 * \rho * \text{volumecone},\end{aligned}$$

$$\text{force1} = \text{Forcexdirection}[[1]],$$

$$\text{force2} = \text{Forcexdirection}[[2]],$$

$$\text{force3} = \text{Forcexdirection}[[3]],$$

$$\text{force4} = \text{Forcexdirection}[[4]],$$

$$\text{force5} = \text{Forcexdirection}[[5]],$$

$$\text{force6} = \text{Forcexdirection}[[6]],$$

$$\text{force7} = \text{Forcexdirection}[[7]],$$

$$\text{force8} = \text{Forcexdirection}[[8]],$$

```
Plot[force1, {t, 0, 1}, AxesLabel -> {"seconds", "N"}]
```

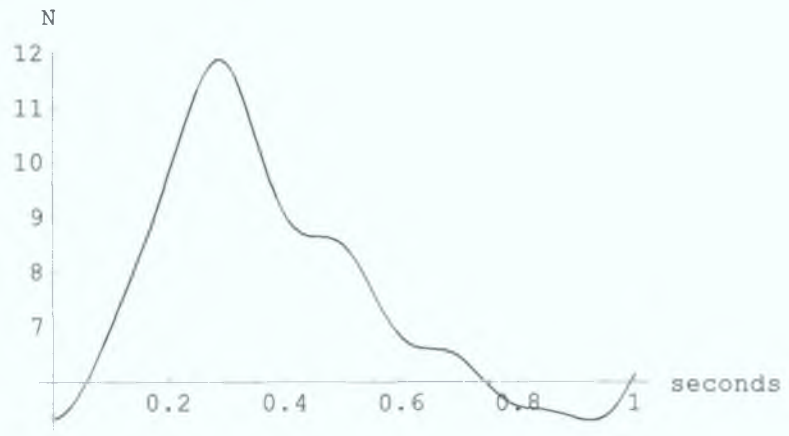

- Graphics -

```
Plot[force2, {t, 0, 1}, AxesLabel -> {"seconds", "N"}]
```

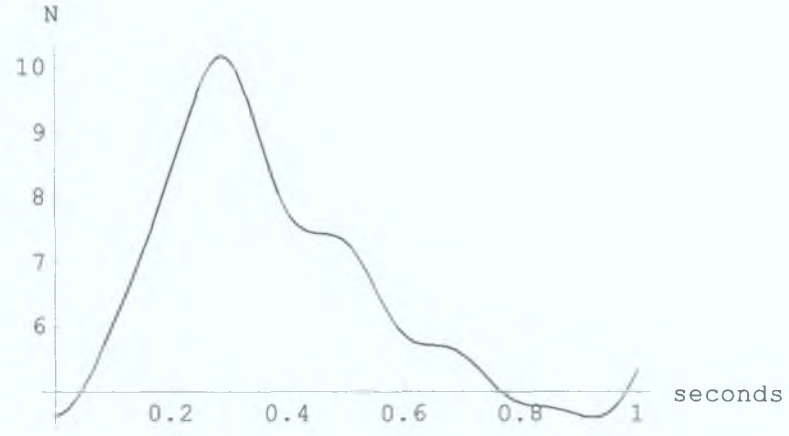

- Graphics -

```
Plot[force3, {t, 0, 1}, AxesLabel -> {"seconds", "N"}]
```

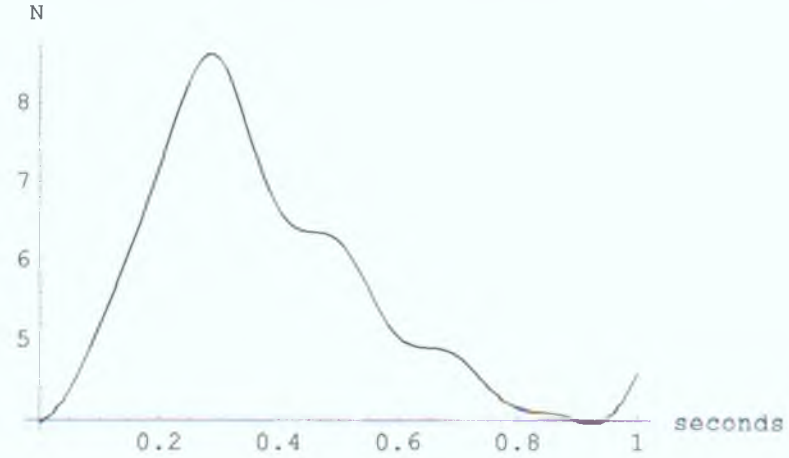

- Graphics -

```
Plot[force4, {t, 0, 1}, AxesLabel -> {"seconds", "N"}]
```

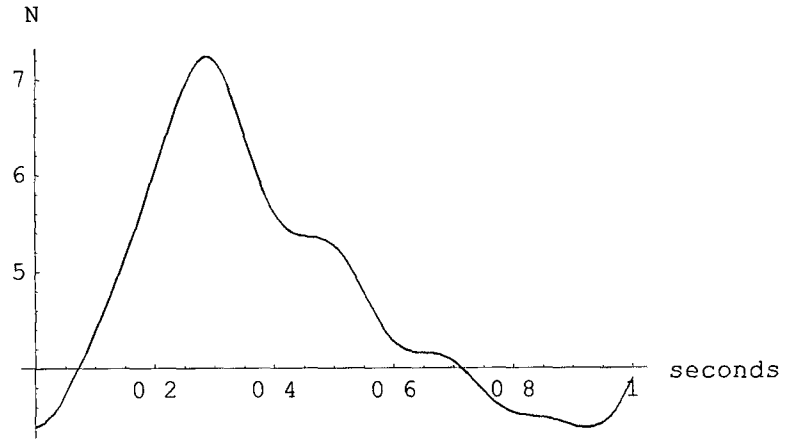

- Graphics -

```
Plot[force5, {t, 0, 1}, AxesLabel -> {"seconds", "N"}]
```

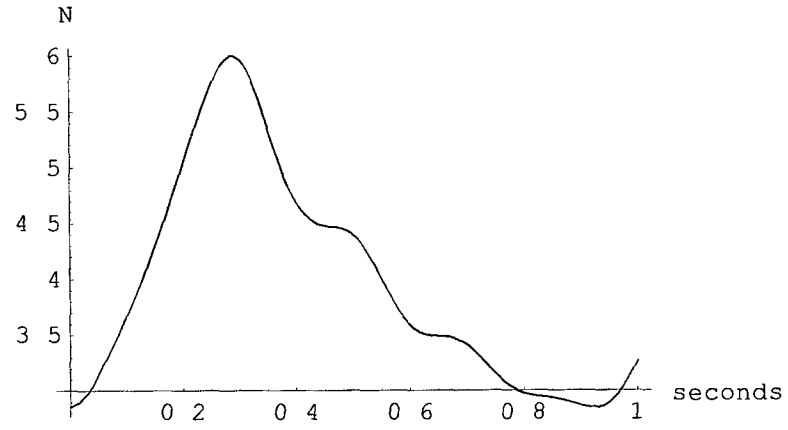

- Graphics -

```
Plot[force6, {t, 0, 1}, AxesLabel -> {"seconds", "N"}]
```

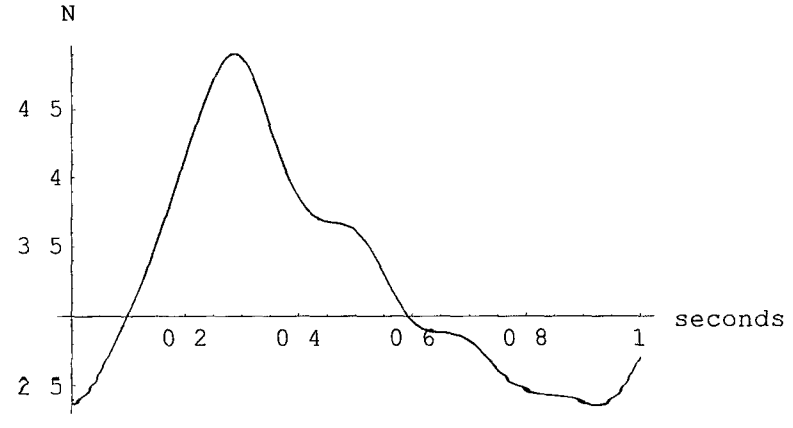

- Graphics -

```
Plot[force7, {t, 0, 1}, AxesLabel -> {"seconds", "N"}]
```

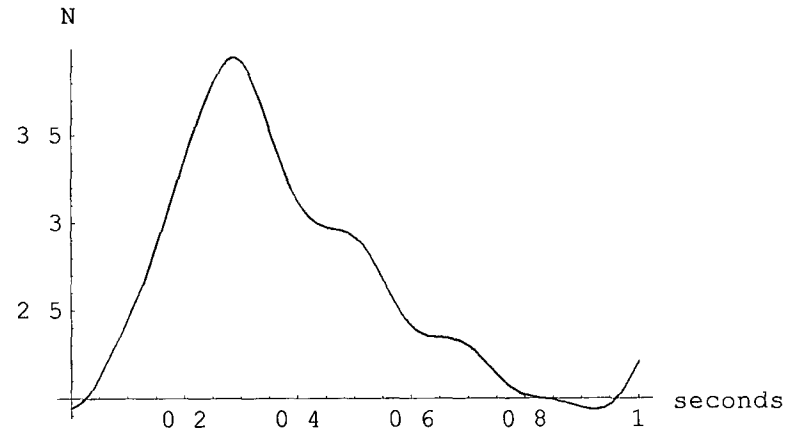


```
- Graphics -
```

```
Plot[force8, {t, 0, 1}, AxesLabel -> {"seconds", "N"}]
```

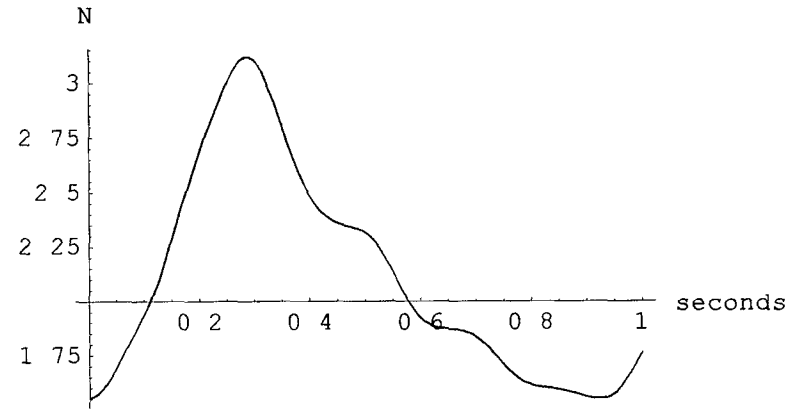


```
- Graphics -
```

Resultant Force Calculated for Conditions in Bench Test.

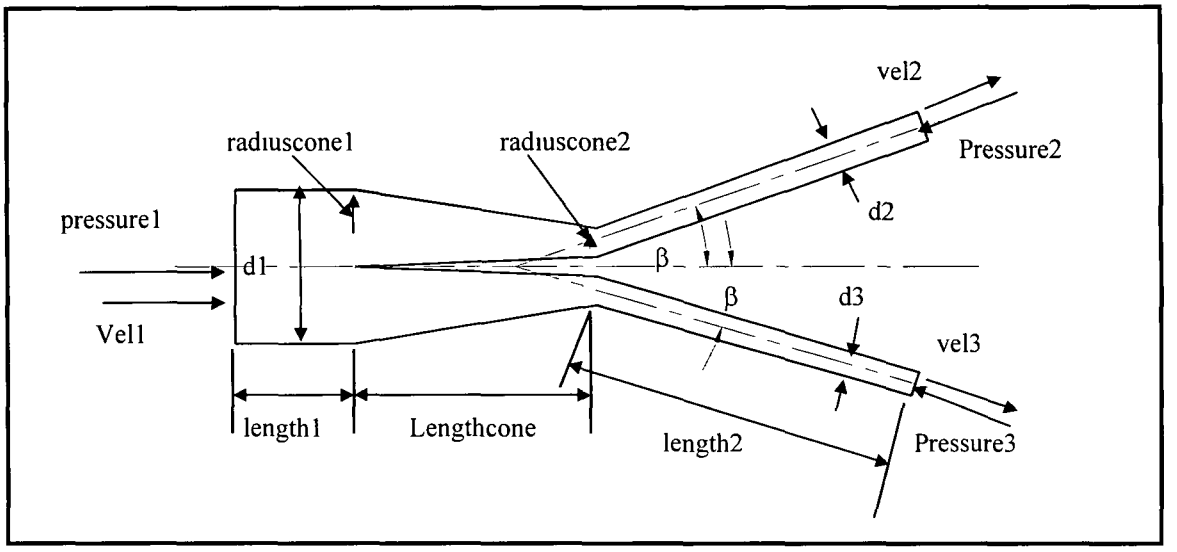

Where

d1 = Proximal diameter

pressure = Pressure of blood in pascals

Vel1 = velocity of blood through proximal end

d3 = iliac leg diameter

vel2 = vel3 = velocity of blood through iliac legs

Pressure2 = Pressure3 = Pressure of blood at iliac legs in pascals

Resultant Force Calculated for Conditions in Bench Test.

First Test:

One proximal stent holding graft against wall of mock silicon artery.

Bench Test Conditions for Migration of Bifurcated Graft:

Pulse Rate (RPM): 72

Pressure Valve Setting: 6,848N/m^2

```
SetAttributes[r, Constant]
```

```
SetAttributes[l, Constant]
```

$$\text{ramposition} = r\,\text{Cos}[\theta] + l\sqrt{1 - \frac{r^2\,\text{Sin}[\theta]^2}{l^2}},$$

$$r = \frac{30}{1000},$$

$$l = \frac{100}{1000},$$

$$\text{rpm} = 72,$$

$$\text{velocity} = \text{Dt}[\text{ramposition}, t] \;/\; \text{Dt}[\theta, t] \to \frac{2\,\pi\,\text{rpm}}{60},$$

$$\text{acceleration} = \text{Dt}[\text{velocity}, t] \;/\; \left\{\text{Dt}[\theta, t] \to \frac{2\,\pi\,\text{rpm}}{60}, \text{Dt}[\theta, \{t, 2\}] \to 0\right\},$$

$$d1 = \frac{28}{1000},$$

$$\text{area1} = \frac{d1^2\,\pi}{4},$$

$$\text{length1} = \frac{15}{1000},$$

$$\text{volume1} = \text{length1}\,\text{area1},$$

$$\rho = 1000,$$

$$g = 9\ 81,$$

$$d2 = \frac{14}{1000},$$

$$\text{area2} = \frac{d2^2\,\pi}{4},$$

$$\text{length2} = \frac{65}{1000},$$

$$\text{volume2} = \text{area2}\,\text{length2},$$

$$d3 = \frac{14}{1000},$$

$$\text{area3} = \frac{d3^2\,\pi}{4},$$

$$\text{length3} = \frac{65}{1000},$$

$$\text{volume3} = \text{length3}\,\text{area3},$$

$$\text{dpump} = \frac{30}{1000},$$

$$\text{areapump} = \frac{\text{dpump}^2\,\pi}{4},$$

$$\text{vel1} = \frac{\text{areapump velocity}}{\text{area1}},$$

```
Plot[vel1, {θ, 0, 4 * π}]
```

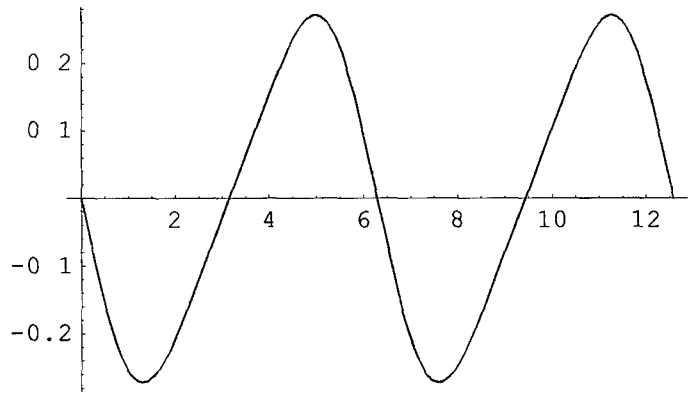


```
- Graphics -
```

$$\text{acc1} = \text{Dt[vel1, t]} \,/\, \text{Dt[}\theta\text{, t]} \to \frac{2\,\pi\,\text{rpm}}{60},$$

$$\text{vel2} = \frac{\text{area1 vel1}}{2\,\text{area2}},$$

$$\text{acc2} = \text{Dt[vel2, t]} \,/\, \text{Dt[}\theta\text{, t]} \to \frac{2\,\pi\,\text{rpm}}{60},$$

$$\text{vel3} = \frac{\text{area1 vel1}}{2\,\text{area3}},$$

```
Plot[vel3, {θ, 0, 2 * π}]
```

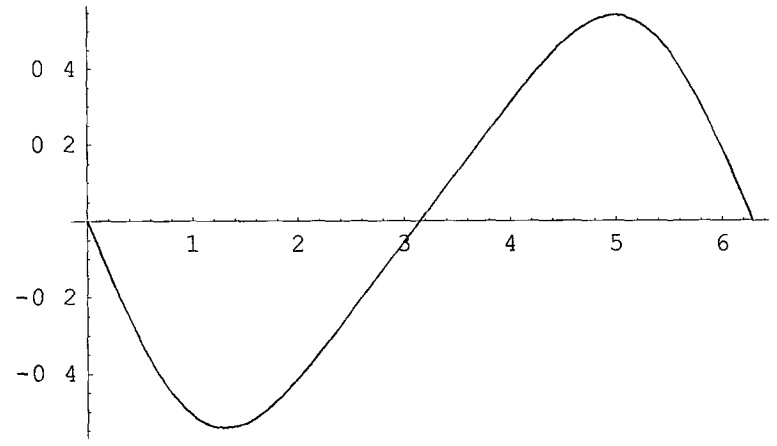


```
- Graphics -
```

$$\text{acc3} = \text{Dt}[\text{vel3}, t] \,/\, \text{Dt}[\theta, t] \to \frac{2\,\pi\,\text{rpm}}{60},$$

$$\text{radiuscon1} = \frac{10}{1000},$$

$$\text{radiuscon2} = \frac{7}{1000},$$

$$\text{lengthcon} = \frac{30}{1000},$$

$$\text{volumecon} = \frac{1}{3}\,\pi\,\text{lengthcon}\,(\text{radiuscon1}^2 + \text{radiuscon1}\,\text{radiuscon2} + \text{radiuscon2}^2),$$

$$\text{areacone} = \pi * \left(\text{radiuscon1} - \left(\frac{(\text{radiuscon1} - \text{radiuscon2})\,x}{\text{lengthcon}}\right)\right)^2,$$

$$\text{velocitycon} = \text{Integrate}\left[\frac{\text{vel2} * \text{area2}}{\text{areacone}},\ \{x, 0, \text{lengthcon}\}\right],$$

$$\text{accelerationcon} = \text{Dt}[\text{velocitycon}, t] \,/\, \text{Dt}[\theta, t] \to \frac{2\,\pi\,\text{rpm}}{60},$$

$$\text{pressure2} = 6848,$$

$$\text{pressure3} = 6848,$$

$$\text{pressure1} = \rho\,g\left(\frac{\text{pressure2}}{\rho\,g} + \frac{\text{vel2}^2}{2\,g} - \frac{\text{vel1}^2}{2\,g} + \frac{\text{length1}\,\text{acc1}}{g} + \frac{\text{length2}\,\text{acc2}}{g} + \frac{\text{accelerationcon} * \text{lengthcon}}{g}\right),$$

```
Plot[pressure1, {θ, 0, 4 π}, Frame -> True, FrameLabel -> {"rads", "N/m^2"}]
```

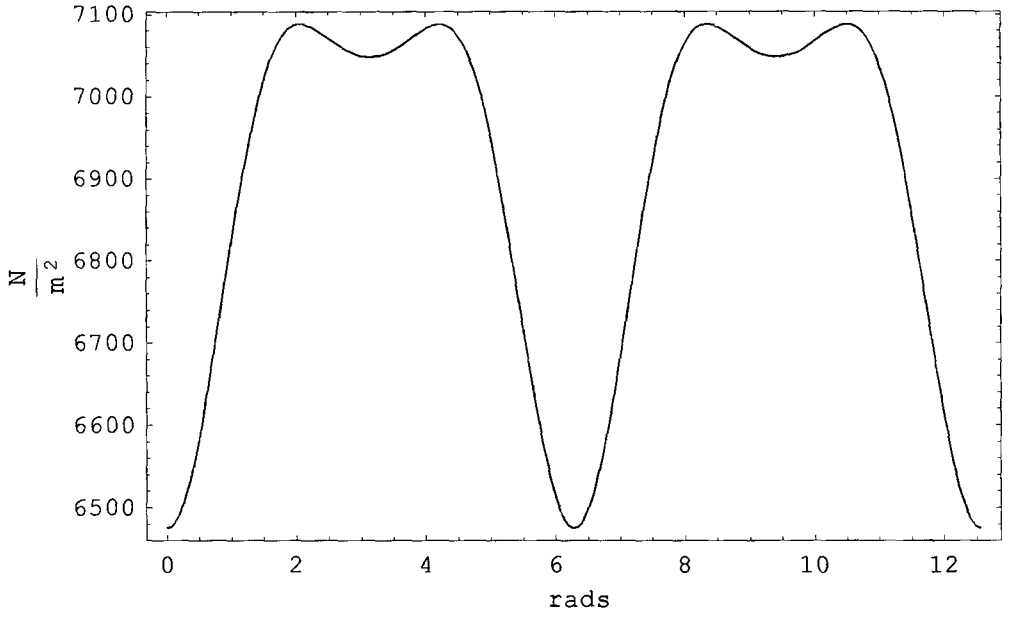

- Graphics -

$$\beta = \frac{2\,\pi\,30}{360},$$

```
Forcexdirection = pressure1 area1 - pressure2 area2 Cos[β] - pressure3 area3 Cos[β] -
  ρ acc1 volume1 - 2 ρ accelerationcon volumecon - ρ acc2 volume2 Cos[β] -
  ρ acc3 volume3 Cos[β] - ρ area2 vel2 vel2 Cos[β] + ρ area1 vel1^2,

Plot[Forcexdirection, {θ, 0, 4 π}, Frame -> True, FrameLabel -> {"rads", "N"}]
```

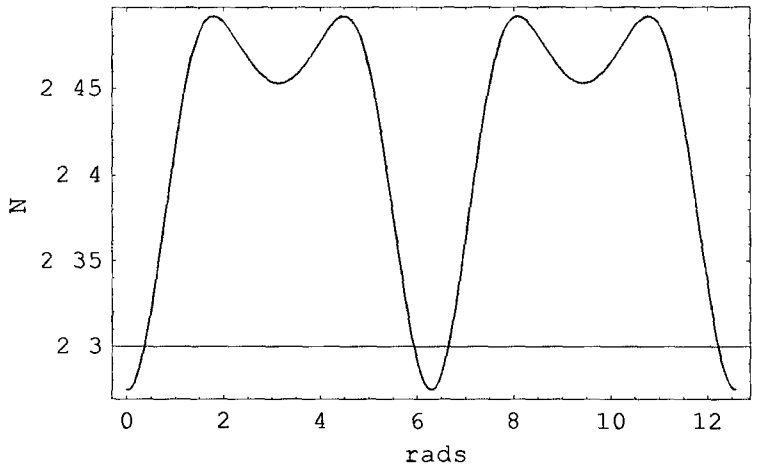

- Graphics -

Resultant Force Calculated for Conditions in Bench Test.

Second Test:

One proximal stent, two iliac stents & two struts.

Bench Test Conditions that Bifurcated Graft could withstand:

Pulse Rate (RPM): 90

Pressure Valve Setting: 22,173N/m^2

```
SetAttributes[r, Constant]
```

```
SetAttributes[l, Constant]
```

$$\text{ramposition} = r\,\text{Cos}[\theta] + l\sqrt{1 - \frac{r^2\,\text{Sin}[\theta]^2}{l^2}},$$

$$r = \frac{30}{1000},$$

$$l = \frac{100}{1000},$$

$$\text{rpm} = 90,$$

$$\text{velocity} = \text{Dt}[\text{ramposition}, t] \,/\, \text{Dt}[\theta, t] \to \frac{2\pi\,\text{rpm}}{60},$$

$$\text{acceleration} = \text{Dt}[\text{velocity}, t] \,/\, \left\{\text{Dt}[\theta, t] \to \frac{2\pi\,\text{rpm}}{60}, \text{Dt}[\theta, \{t, 2\}] \to 0\right\},$$

$$d1 = \frac{28}{1000},$$

$$\text{area1} = \frac{d1^2\,\pi}{4},$$

$$\text{length1} = \frac{15}{1000},$$

$$\text{volume1} = \text{length1}\,\text{area1},$$

$$\rho = 1000,$$

$$g = 9\ \ 81,$$

$$d2 = \frac{14}{1000},$$

$$\text{area2} = \frac{d2^2\,\pi}{4},$$

$$\text{length2} = \frac{65}{1000},$$

$$\text{volume2} = \text{area2}\,\text{length2},$$

$$d3 = \frac{14}{1000},$$

$$\text{area3} = \frac{d3^2\,\pi}{4},$$

$$\text{length3} = \frac{65}{1000},$$

$$\text{volume3} = \text{length3}\,\text{area3},$$

$$\text{dpump} = \frac{30}{1000},$$

$$\text{areapump} = \frac{\text{dpump}^2\,\pi}{4},$$

$$\text{vel1} = \frac{\text{areapump velocity}}{\text{area1}},$$

```
Plot[vel1, {θ, 0, 4 * π}]
```

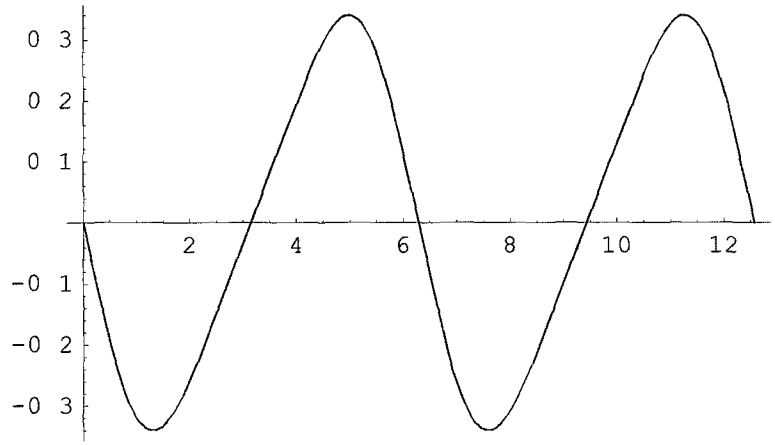


```
- Graphics -
```

$$\text{acc1} = \text{Dt[vel1, t]} \,/\, \text{Dt[}\theta\text{, t]} \to \frac{2\,\pi\,\text{rpm}}{60},$$

$$\text{vel2} = \frac{\text{area1 vel1}}{2\,\text{area2}},$$

$$\text{acc2} = \text{Dt[vel2, t]} \,/\, \text{Dt[}\theta\text{, t]} \to \frac{2\,\pi\,\text{rpm}}{60},$$

$$\text{vel3} = \frac{\text{area1 vel1}}{2\,\text{area3}},$$

```
Plot[vel3, {θ, 0, 2 * π}]
```

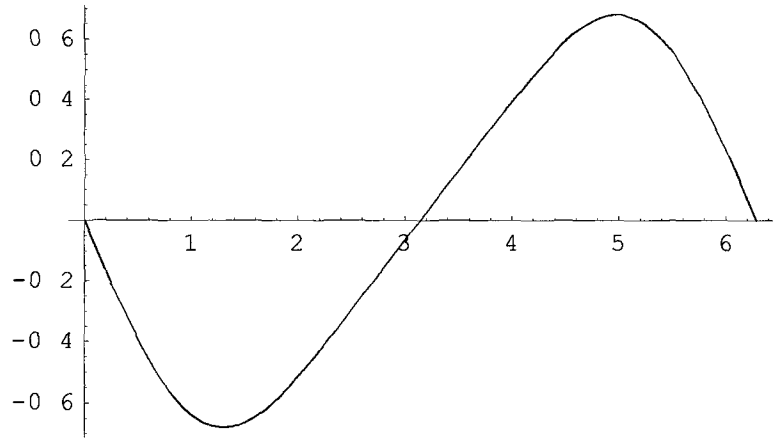


```
- Graphics -
```

$$\text{acc3} = \text{Dt[vel3, t]} \,/\, \text{Dt[}\theta\text{, t]} \to \frac{2\,\pi\,\text{rpm}}{60},$$

$$\text{radiuscon1} = \frac{10}{1000},$$

General spell1 Possible spelling error new symbol name "radiuscon1" is similar to existing symbol "radiuscone1"

$$\text{radiuscon2} = \frac{7}{1000},$$

General spell1 Possible spelling error new symbol name "radiuscon2" is similar to existing symbol "radiuscone2"

$$\text{lengthcon} = \frac{30}{1000},$$

General spell1
Possible spelling error new symbol name "lengthcon" is similar to existing symbol "lengthcone"

$$\text{volumecon} = \frac{1}{3}\,\pi\,\text{lengthcon}\,(\text{radiuscon1}^2 + \text{radiuscon1}\,\text{radiuscon2} + \text{radiuscon2}^2),$$

General spell1
Possible spelling error new symbol name "volumecon" is similar to existing symbol "volumecone"

$$\text{areacone} = \pi * \left(\text{radiuscon1} - \left(\frac{(\text{radiuscon1} - \text{radiuscon2})\,x}{\text{lengthcon}}\right)\right)^2,$$

$$\text{velocitycon} = \text{Integrate}\left[\frac{\text{vel2} * \text{area2}}{\text{areacone}},\ \{x,\ 0,\ \text{lengthcon}\}\right],$$

General spell1 Possible spelling error new symbol name "velocitycon" is similar to existing symbol "velocitycone"

$$\text{accelerationcon} = \text{Dt}[\text{velocitycon},\ t]\ /\ \text{Dt}[\theta,\ t] \to \frac{2\,\pi\,\text{rpm}}{60},$$

General spell1 Possible spelling error new symbol name "accelerationcon" is similar to existing symbol "accelerationcone"

$$\text{pressure2} = 22173,$$

$$\text{pressure3} = 22173,$$

$$\text{pressure1} = \rho\,g\left(\frac{\text{pressure2}}{\rho\,g} + \frac{\text{vel2}^2}{2\,g} - \frac{\text{vel1}^2}{2\,g} + \frac{\text{length1}\,\text{acc1}}{g} + \frac{\text{length2}\,\text{acc2}}{g} + \frac{\text{accelerationcon} * \text{lengthcon}}{g}\right),$$

```
Plot[pressure1, {θ, 0, 4 π}, Frame -> True, FrameLabel -> {"rads", "N/m^2"}]
```

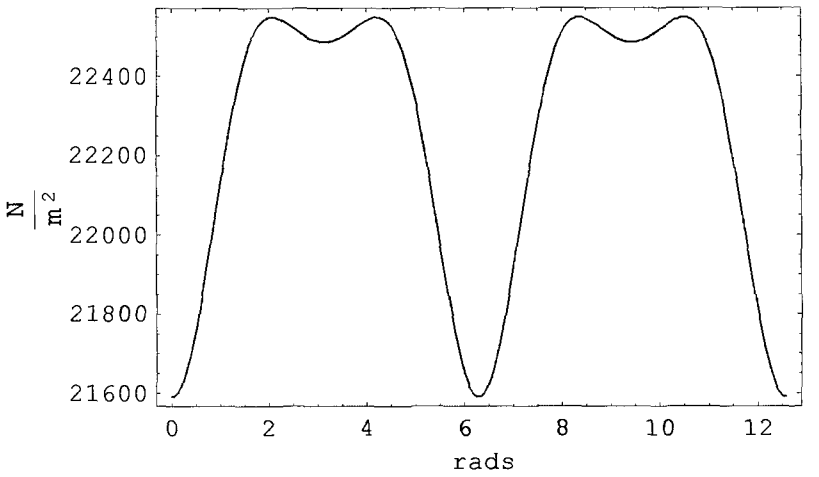

- Graphics -

$$\beta = \frac{2\,\pi\,30}{360},$$

```
Forcexdirection = pressure1 area1 - pressure2 area2 Cos[β] - pressure3 area3 Cos[β] -
  ρ acc1 volume1 - 2 ρ accelerationcon volumecon - ρ acc2 volume2 Cos[β] -
  ρ acc3 volume3 Cos[β] - ρ area2 vel2 vel2 Cos[β] + ρ area1 vel1^2,

Plot[Forcexdirection, {θ, 0, 4 π}, Frame -> True, FrameLabel -> {"rads", "N"}]
```

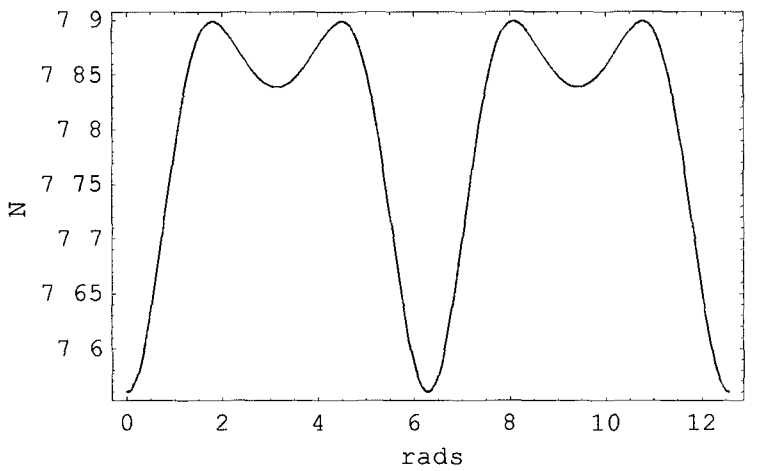

- Graphics -

Appendix F

Prosthesis Design

Part No:	Part Name:	Material	Quantity
1	Stent Holder	Steel	3 (for different size stents)
2	Bifurcated Graft	Woven Fabric – Polyester, Nylon or PTFE	1
3	Z-Stent	∅ 375mm round wire Shape Memory Alloy – super elastic effect	3

Note:

For the Z-Stent (procedure as followed in chapter 6, section 6 7), The outside diameter of the wound Z-Stent is usually 40% larger than the ∅A as shown for the stent holder

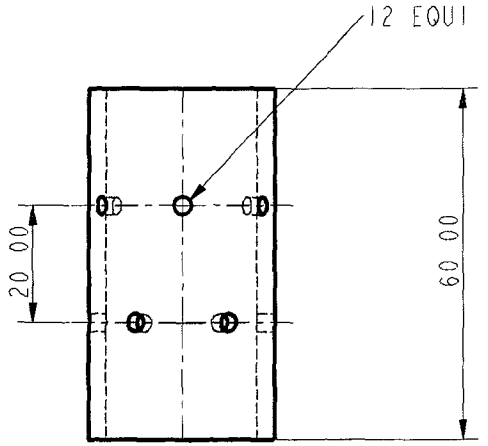

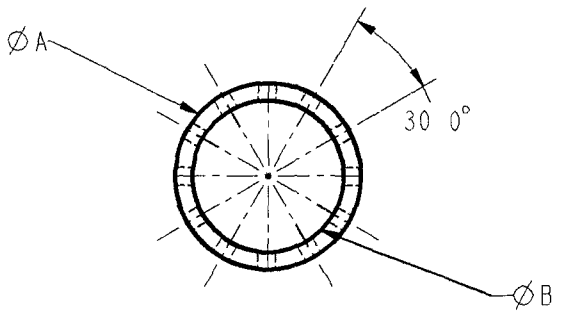

STENT TYPE	ØA	ØB
Stent 1	32	28
Stent 2	25	20
Stent 3	15	12

STENT HOLDER

Prosthesis Design

G M I T	ALL DIMENSTION IN MM
Liam Morris	PART NO 1

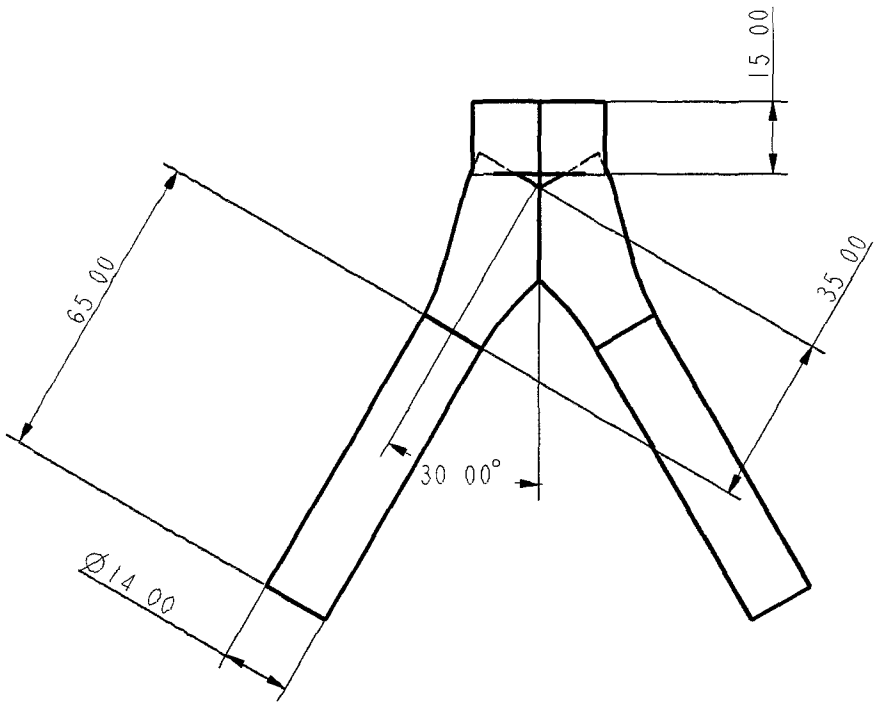

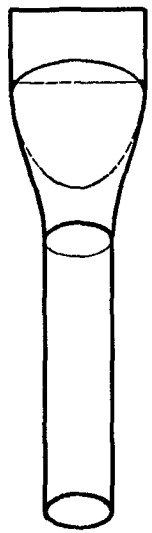

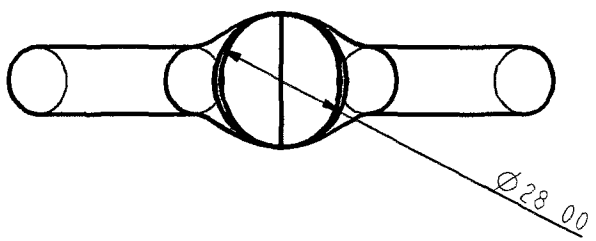

BIFURCATED GRAFT

PROSTHESIS DESIGN

G M I T	ALL DIMENSIONS IN MM
LIAM MORRIS	PART NO 2

Delivery System

Part No:	Part Name	Material	Quantity
1	Main Catheter	Polyurethane or Polyethylene	1
2	Floppy tip guidewire	∅0 9mm Stainless Steel	2
3	Sleeve	PTFE, Polyester or Nylon	1
4	Iliac Sleeve	PTFE, Polyester or Nylon	2
5	Snare Catheter	O D 4mm, I D 2mm length 400mm Polyurethane	1
6	Snare Loop	∅0 32 Monofilament fibre of length 1000mm	1
7	Bow Knot	Multifilament yarn	2

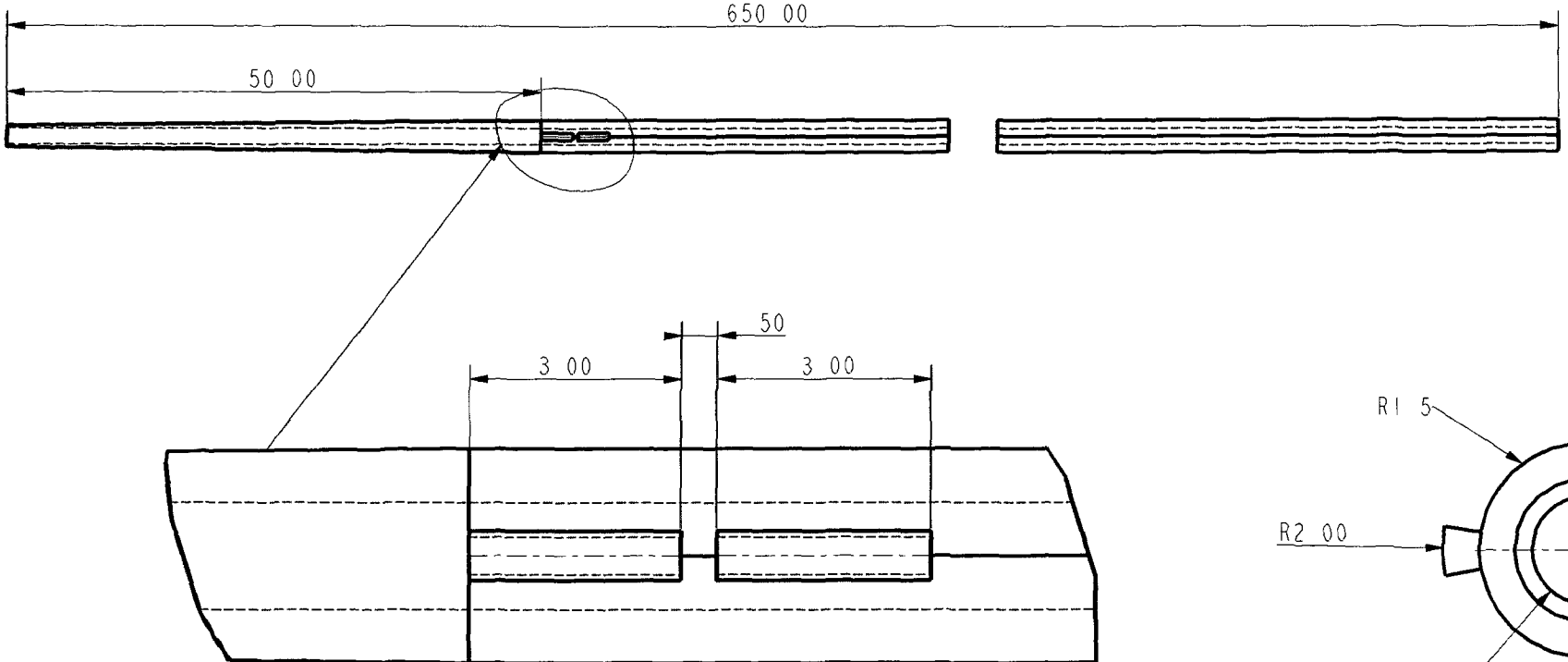

DETAILED VIEW OF STENT REMOVAL
SCALE 5 1

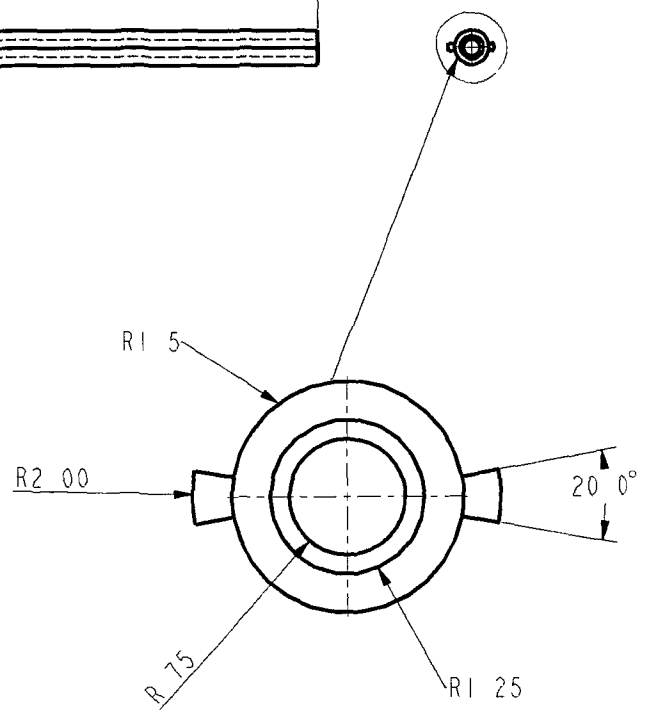

DETAILED VIEW OF END VIEW
SCALE 5 1

	MAIN CATHETER	DELIVERY SYSTEM
		G M I T / ALL DIMENSIONS IN MM
		LIAM MORRIS / PART NO 1

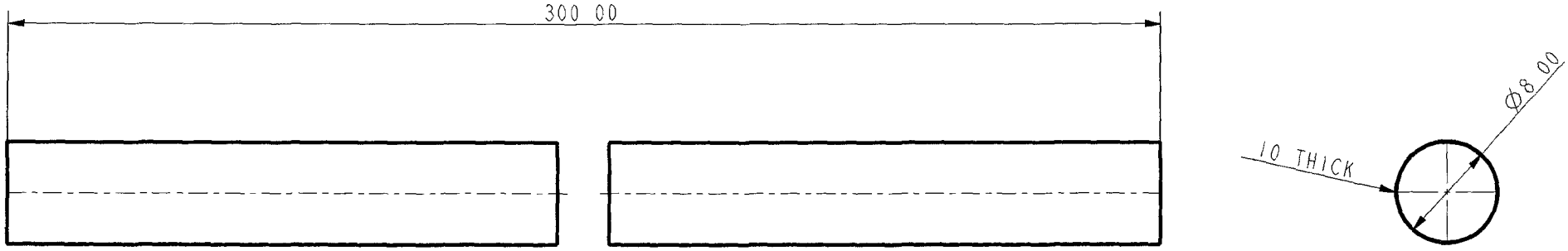

	SLEEVE	DELIVERY SYSTEM	
		G M I T	ALL DIMENSIONS IN MM
		LIAM MORRIS	PART NO 3

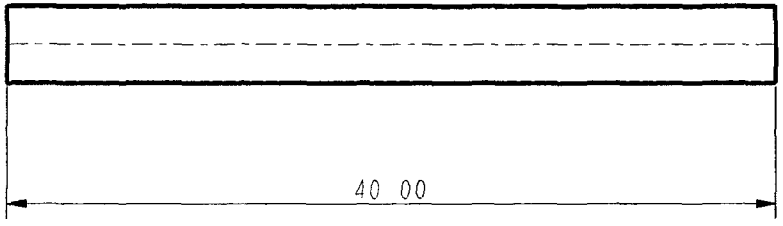

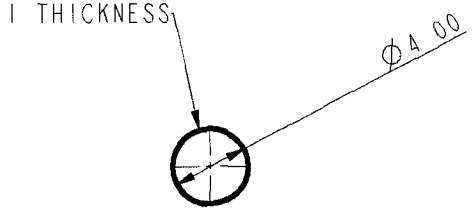

	ILIAC SLEEVE	DELIVERY SYSTEM	
		G M I T	ALL DIMENSIONS IN MM
		LIAM MORRIS	PART NO 4

Appendix G

- **Catheter Sphere Rounded End**

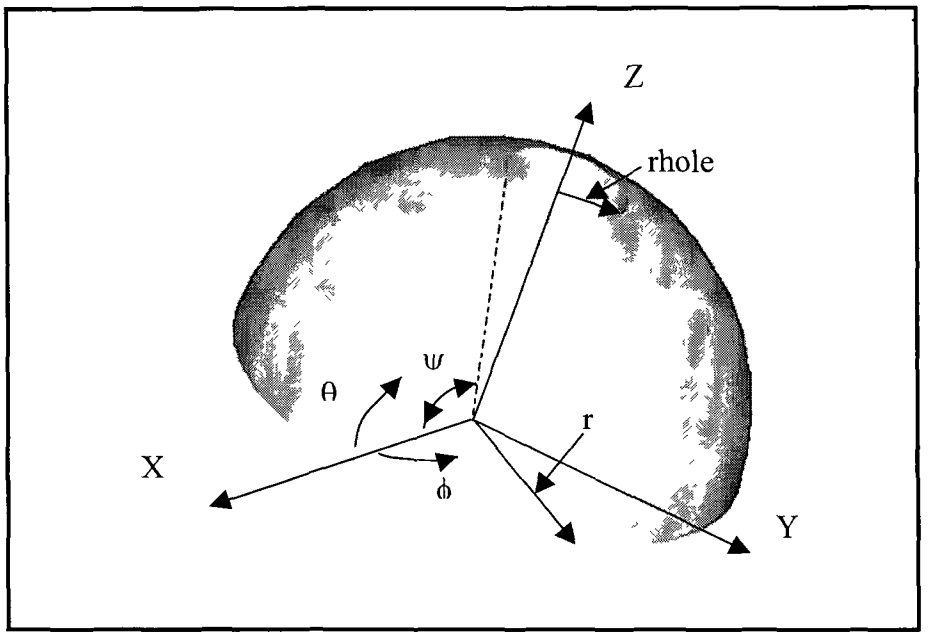

```
SetAttributes[r, Constant]

r = 15 / 10000,

P = {10000, 16000},

rhole = 75 / 100000,

β = ArcSin[rhole / r] // N
```

0 523599

$$\psi = \frac{\pi}{2} - \beta$$

1 0472

$$\text{ydirection} = \frac{P}{r} * \text{Integrate}[r^3 * \text{Cos}[\theta]^2 * \text{Sin}[\phi], \{\theta, 0, \psi\}, \{\phi, 0, 2 * \pi\}]$$

{0, 0}

$$\text{xdirection} = \frac{P}{r} * \text{Integrate}[r^3 * \text{Cos}[\theta]^2 * \text{Cos}[\phi], \{\theta, 0, \psi\}, \{\phi, 0, 2 * \pi\}]$$

{0, 0}

$$\text{zdirection} = \frac{P}{r} * \text{Integrate}[r^3 * \text{Sin}[\theta] * \text{Cos}[\theta], \{\theta, 0, \psi\}, \{\phi, 0, 2 * \pi\}]$$

{0 0530144, 0 084823}

- **Catheter Rounded End (Torus Shape)**

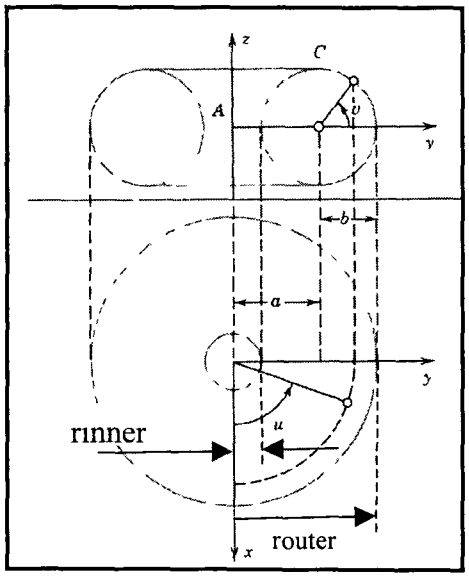

```
SetAttributes[a, Constant]

SetAttributes[b, Constant]

Clear[v]

P = {10000, 16000},

router = 15 / 10000,

rinner = 75 / 100000,

b = (router - rinner) / 2
```

$$\frac{3}{8000}$$

```
a = router - b
```

$$\frac{9}{8000}$$

```
zdirection = P * Integrate[b * (a + b * Cos[v]) * Sin[v], {u, 0, 2 * π}, {v, 0, π}]
```

General spell Possible spelling error new symbol name "zdirection" is similar to existing symbols {xdirection, ydirection}

$$\left\{\frac{27\,\pi}{1600}, \frac{27\,\pi}{1000}\right\}$$

- **Catheter Cone Sphere (Taper end with a Rounded end)**

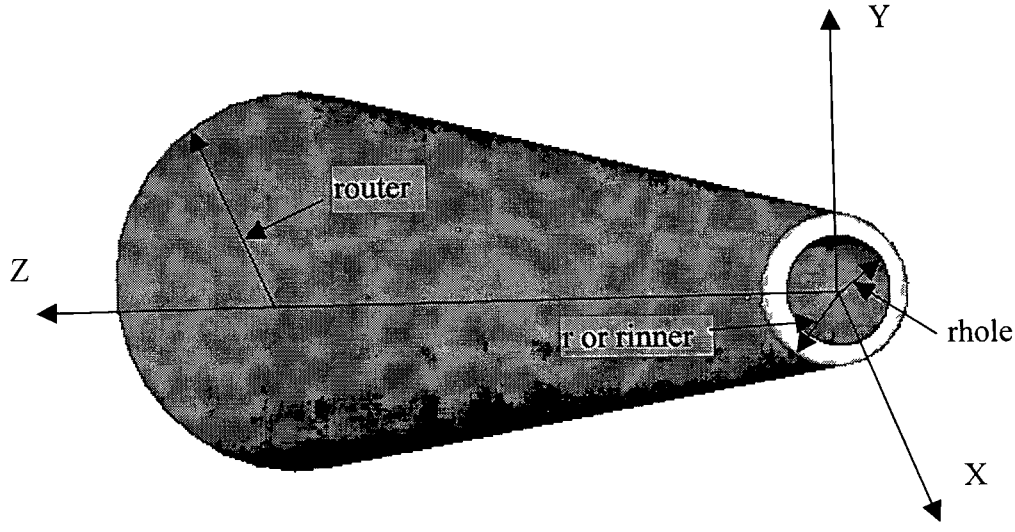

```
SetAttributes[v, Constant]
```

```
SetAttributes[v, Constant]
```

```
Clear[c, z1, z2]
```

```
bloodpressure = {10000, 16000},
```

```
router = 1 5,
```

```
rinner = 1,
```

```
Solve[{50 * c + c * z1 == router, c * z1 == rinner}]
```

```
{{z1 → 100 , c → 0 01}}
```

```
z1 = 100 / 1000
```

$$\frac{1}{10}$$

```
c =  01
```

```
0 01
```

$$z2 = \frac{\text{router}}{c * 1000}$$

```
0 15
```

```
x = u * Cos[v]
```

```
u Cos[v]
```

```
y = u * Sin[v]
```

```
u Sin[v]
```

```
z = c * u
```

```
0 01 u
```

```
zdirectioncone =
```

$$\text{bloodpressure} * \text{Integrate}\left[\frac{-c^2 * z}{\sqrt{x^2 + y^2 + c^4 * z^2}} * \left(u * \sqrt{c^2 + 1}\right), \{u, z2, z1\}, \{v, 0, 2 * \pi\}\right]$$

```
{0 000392719, 0 00062835}
```

```
ydirection =
```

$$\text{bloodpressure} * \text{Integrate}\left[\frac{2 * y}{\sqrt{x^2 + y^2 + c^4 * z^2}} * \left(u * \sqrt{c^2 + 1}\right), \{u, z2, z1\}, \{v, 0, 2 * \pi\}\right]$$

```
{0, 0}
```

```
xdirection =
 bloodpressure * Integrate[2 * x / Sqrt[x^2 + y^2 + c^4 * z^2] * (u * Sqrt[c^2 + 1]), {u, z2, z1}, {v, 0, 2 * π}]
```

```
General  spell1  Possible spelling error  new symbol name "xdirection" is similar
   to existing symbol "ydirection"
```

```
{0, 0}
```

```
SetAttributes[r, Constant]
```

```
r = 1 / 1000,
```

```
P = {10000, 16000},
```

```
rhole = 75 / 100000,
```

```
β = ArcSin[rhole / r] // N
```

```
0 848062
```

$$\psi = \frac{\pi}{2} - \beta$$

```
0 722734
```

$$\text{ydirection} = \frac{P}{r} * \text{Integrate}[r^3 * \text{Cos}[\theta]^2 * \text{Sin}[\phi], \{\theta, 0, \psi\}, \{\phi, 0, 2 * \pi\}]$$

```
{0, 0}
```

$$\text{xdirection} = \frac{P}{r} * \text{Integrate}[r^3 * \text{Cos}[\theta]^2 * \text{Cos}[\phi], \{\theta, 0, \psi\}, \{\phi, 0, 2 * \pi\}]$$

```
{0, 0}
```

$$\text{zdirectionsphere} = \frac{P}{r} * \text{Integrate}[r^3 * \text{Sin}[\theta] * \text{Cos}[\theta], \{\theta, 0, \psi\}, \{\phi, 0, 2 * \pi\}]$$

```
{0 0137445, 0 0219911}
```

```
totalforce = zdirectioncone + zdirectionsphere
```

```
{0 0141372, 0 0226195}
```

To Find Resultant Friction Force Due To Removal of Cap.

$$N_X = \int_0^{\pi} \frac{T_1 e^{\mu\theta} \mathrm{Cos}\left(\frac{\theta}{2}\right) d\theta}{\mu}$$

By Integration by parts

$$\int udv = uv - \int vdu$$

Let: $u = e^{\mu\theta}$ $\qquad dv = \mathrm{Cos}\left(\frac{\theta}{2}\right) d\theta$

$du = \mu e^{\mu\theta} d\theta$ $\qquad v = 2\,\mathrm{Sin}\left(\frac{\theta}{2}\right)$

$$\int \frac{T_1 e^{\mu\theta} \mathrm{Cos}\left(\frac{\theta}{2}\right) d\theta}{\mu} = \int udv = \frac{T_1}{\mu}\left(2e^{\mu\theta}\mathrm{Sin}\left(\frac{\theta}{2}\right) - \int 2\mathrm{Sin}\left(\frac{\theta}{2}\right)\mu e^{\mu\theta} d\theta\right)$$

$$\int \frac{T_1 e^{\mu\theta} \mathrm{Cos}\left(\frac{\theta}{2}\right) d\theta}{\mu} = \frac{T_1}{\mu}\left(2e^{\mu\theta}\mathrm{Sin}\left(\frac{\theta}{2}\right) - \left\{2\mu\left(-2e^{\mu\theta}\mathrm{Cos}\left(\frac{\theta}{2}\right) + \int 2\mu\mathrm{Cos}\left(\frac{\theta}{2}\right) e^{\mu\theta} d\theta\right)\right\}\right)$$

$$\int \frac{T_1 e^{\mu\theta} \mathrm{Cos}\left(\frac{\theta}{2}\right) d\theta}{\mu} = \frac{2T_1}{\mu} e^{\mu\theta}\mathrm{Sin}\left(\frac{\theta}{2}\right) + 4T_1 e^{\mu\theta}\mathrm{Cos}\left(\frac{\theta}{2}\right) - 4\mu^2 \frac{T_1}{\mu}\int \mathrm{Cos}\left(\frac{\theta}{2}\right) e^{\mu\theta} d\theta$$

Now let I = $\int \frac{T_1 e^{\mu\theta} \mathrm{Cos}\left(\frac{\theta}{2}\right) d\theta}{\mu}$

$$I = \frac{2T_1}{\mu} e^{\mu\theta}\mathrm{Sin}\left(\frac{\theta}{2}\right) + 4T_1 e^{\mu\theta}\mathrm{Cos}\left(\frac{\theta}{2}\right) - 4\mu^2 I$$

$$I + 4\mu^2 I = \frac{2T_1}{\mu} e^{\mu\theta}\mathrm{Sin}\left(\frac{\theta}{2}\right) + 4T_1 e^{\mu\theta}\mathrm{Cos}\left(\frac{\theta}{2}\right)$$

$$I(1 + 4\mu^2) = 2T_1 e^{\mu\theta}\left(\frac{\mathrm{Sin}\left(\frac{\theta}{2}\right)}{\mu} + 2\mathrm{Cos}\left(\frac{\theta}{2}\right)\right)$$

$$I = \frac{2T_1 e^{\mu\theta}}{1+4\mu^2}\left(\frac{\mathrm{Sin}\left(\frac{\theta}{2}\right)}{\mu} + 2\mathrm{Cos}\left(\frac{\theta}{2}\right)\right)$$

Between the limits 0 and π

$$I = \left[\frac{2T_1 e^{\mu\theta}}{1+4\mu^2}\left(\frac{\mathrm{Sin}\left(\frac{\theta}{2}\right)}{\mu} + 2\mathrm{Cos}\left(\frac{\theta}{2}\right)\right)\right]_0^{\pi}$$

Let the coefficient of friction $\mu = 0.2$

$$I = \left(\frac{2T_1}{1\,04}(1\,87)\left(\frac{1}{0\,2} + 2(0)\right) - \left(\frac{2T_1}{1\,04}(1)(0+2(1))\right)\right)$$

$I = 17\,98T_1 - 3\,85T_1 =$ ***14.13*** T_1